Journal of Immunology Research

Peptide-Based Immunotherapeutics and Vaccines 2015

Guest Editors: Pedro Reche, Darren R. Flower, Masha Fridkis-Hareli, and Yoshihiko Hoshino

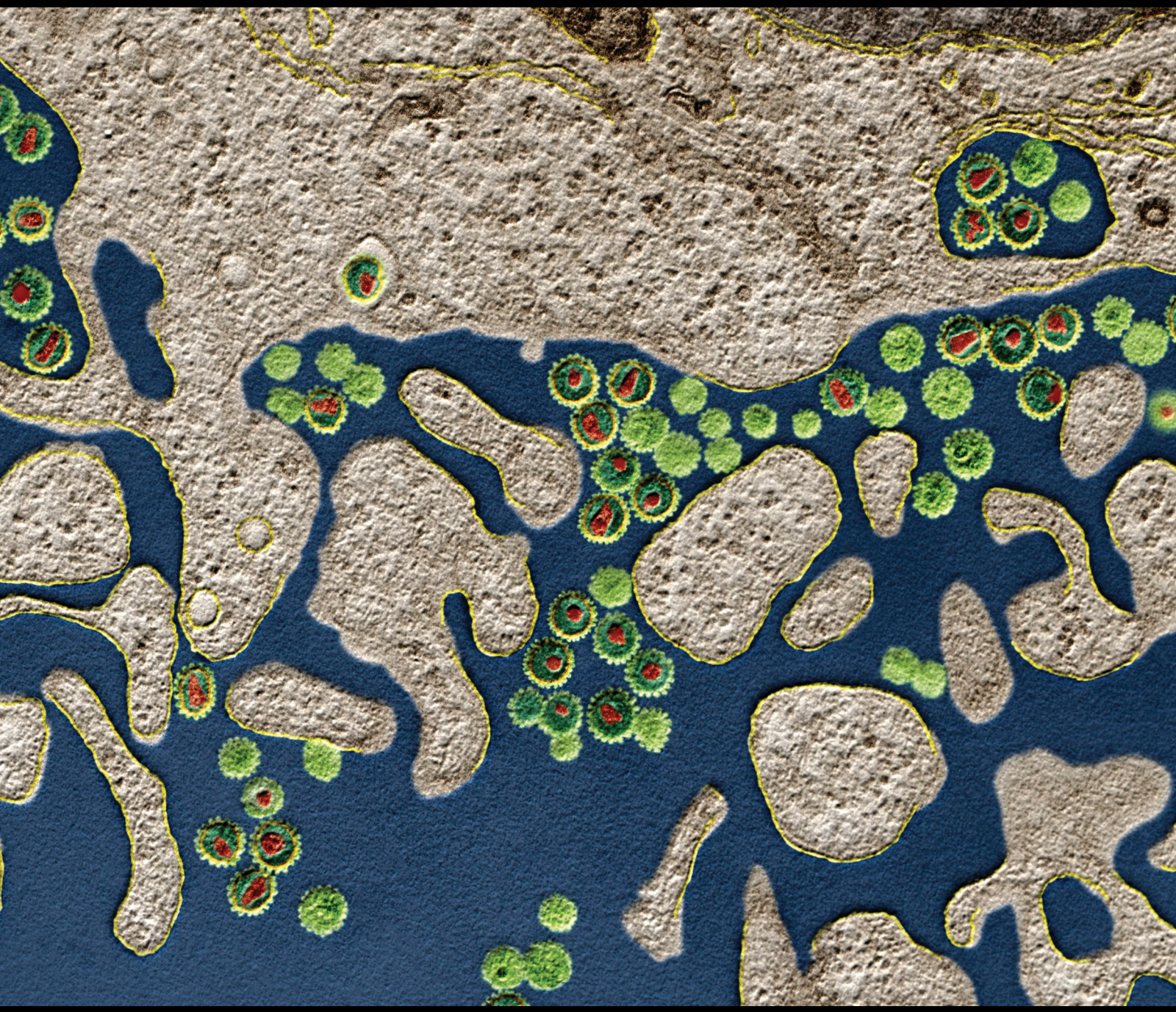

Peptide-Based Immunotherapeutics and Vaccines 2015

Journal of Immunology Research

Peptide-Based Immunotherapeutics and Vaccines 2015

Guest Editors: Pedro Reche, Darren R. Flower, Masha Fridkis-Hareli, and Yoshihiko Hoshino

Editorial Board

Contents

Hindawi Publishing Corporation
Journal of Immunology Research
Volume 2015, Article ID 349049, 2 pages
http://dx.doi.org/10.1155/2015/349049

Editorial

Peptide-Based Immunotherapeutics and Vaccines 2015

Pedro Reche,[1] Darren R. Flower,[2] Masha Fridkis-Hareli,[3] and Yoshihiko Hoshino[4]

[1]*Department of Microbiology-I/Immunology, Facultad de Medicina, Universidad Complutense, 28040 Madrid, Spain*
[2]*School of Life and Health Sciences, Aston University, Birmingham B4 7ET, UK*
[3]*ATR, LLC, Worcester, MA 01606, USA*
[4]*Department of Mycobacteriology, National Institute of Infectious Diseases, Higashi-Murayama, Tokyo 189-0002, Japan*

Correspondence should be addressed to Pedro Reche; parecheg@med.ucm.es

Received 18 October 2015; Accepted 18 October 2015

Vaccination produces profound and long lasting modifications in the adaptive immune system comprising T and B cells. Vaccines are curative not mere palliative remedies and thus vaccination is the most efficient method to prevent and to lesser extent treat infectious diseases, cancer, and allergy conditions. Currently, there is an increasing interest in developing vaccines based on synthetic peptides encompassing B and T cell epitopes that precisely trigger a protective immune response. Because they are synthetic, peptide vaccines are intrinsically safer than alternative vaccine formulations. Moreover, peptide-based vaccines will allow focusing solely on relevant epitopes, avoiding those that lead to nonprotective responses, immune evasion, or unwanted side effects, such as autoimmunity. However, developing a successful peptide-based vaccine requires addressing a number of significant difficulties, such as overcoming the low intrinsic immunogenicity of individual peptides. In this special issue on peptide-based vaccines, we have incorporated 9 original articles and two reviews that deal with and examine various aspects of peptide-based vaccine design.

The review by H. Kimura et al. offers new insights into the function of the immunoproteasome in immune and nonimmune cells. Cleavage of intracellular proteins by immunoproteasome is a key step on the MHC class I antigen presentation pathway and this review highlights the relevance of understanding immunoproteasome function for developing peptide-based vaccines and novel pharmacological treatments. The second review by Y.-F. Xiao et al. offers an outstanding analysis on peptide-based treatments for cancer. The authors divide peptide-based cancer treatments into three types, peptide-alone therapy, peptide vaccines, and peptide-conjugated nanomaterials, describing new advances in using peptides to treat lung, pancreatic, prostate, and gastric cancers. Moreover, the authors masterly collect evidence on how peptides represent ideal tumor immunotherapeutics as one can specifically target tumor cells with little toxicity and efficient immunoreaction.

The original articles incorporated in this issue consist of cutting-edge computational and experimental reports that are relevant for the design of peptide-based vaccines. Within the *in silico* manuscripts, we include a work by D. Kanduc et al. in which the authors compared the proteome of poliovirus with that of humans and found unique poliovirus peptide sequences that could be basis for developing a specific/universal vaccine, with no cross-reactions with human proteins. As an additional advantage, the authors argue that a peptide-based vaccine instead of current antipolio DNA vaccines would eliminate the rare postpoliomyelitis cases and other disabling symptoms that may appear following vaccination. Computer-assisted design of peptide-based vaccines often relies on more complex predictive models to select peptide fragments within antigens containing T and B cell epitopes. Generation of predictive models requires the assembling of categorized datasets for training the models. Dataset assembly is labor intense and time consuming. S. C. Pro et al. have masterly addressed the problem, devising a method to automate the generation of validated specific epitope sets from the IEDB database (http://www.iedb.org/). The availability of the disease-specific sequence data enables the use of predictive tools that reveal entire epitomes thus facilitating the development of epitope-based vaccines. However, in large and complex pathogens the potential T cell epitome can be so sizeable that it will challenge experimental validation. To address this problem M. Molero-Abraham

et al. report a method and resource, EPIPOX, that allows downsizing the relevant T cell epitome for variola virus according to conservation criteria and antigen features such as expression and localization.

The experimental articles contained in the issue have a wide scope and include a phase II clinical trial by S. Yutani et al. The study is based on a personalized peptide vaccination with both a hepatitis C virus- (HCV-) derived peptide and peptides from tumor-associated antigens (TAA) for the treatment of HCV-positive advanced hepatocellular carcinoma patients. The authors show that the peptide-based vaccine (PPV) was safe and elicited HCV specific CTL responses as well as peptide-specific IgG1 responses to both the viral peptides and TAA-derived peptides supporting further clinical study of PPV. Identification of the antigens that are targeted by the immune system and characterizing the type of response are clearly a step forward towards designing a useful peptide-based vaccine. In this context, M. Niki et al. present an evaluation of humoral immunity to *Mycobacterium tuberculosis*- (TB-) specific antigens concluding that the induction of antigen-specific humoral immunity, especially for IgA response, is relevant for TB protection. Similarly, A. N. Kamali et al. show that *Plasmodium* antigens isolated by antibody affinity of sera from malaria-self-resistant ICR mice are capable of delaying infection when inoculated into BALB/c mice. Thereby, the authors conclude that immunoaffinity purified antigens using IgGs from protected individuals can be relevant for developing multiantigen blood-stage malaria vaccines. Vaccine development and optimization require finding appropriated animal models for testing. In this issue, I. Sominskaya et al. show that rabbits are suitable animal models to test the immunogenicity of core peptides from hepatitis C virus, promoting the use of rabbit models for preclinical trials of HCV vaccines.

Peptides exhibit little immunogenicity and thereby it is key to devise means of increasing their immunogenicity for vaccine design purposes. In this issue, A. Yano et al. show that combining amyloid beta (Aβ) peptides with toxoid (DT) enhanced the immunogenicity of the peptide on cynomolgus monkeys and guinea pigs that were first immunized with conventional diphtheria-tetanus. Moreover, the peptide vaccine induced anti-Aβ antibodies in cynomolgus monkeys and guinea pigs without chemical adjuvants, and excessive immune responses were not observed. Peptides can also have immunomodulatory properties as shown in the article by J.-P. Vernot et al., in which the authors show that it is possible to modulate p56Lck in T cells by a chimeric peptide comprising two functionally different motifs of Tip from *Herpesvirus saimiri*.

In conclusion, this special issue surveyed many aspects of peptide-based vaccines and we hope readers will find it both interesting and inspiring. It certainly has been a pleasure for us to select the work presented in this issue.

Pedro Reche
Darren R. Flower
Masha Fridkis-Hareli
Yoshihiko Hoshino

Hindawi Publishing Corporation
Journal of Immunology Research
Volume 2015, Article ID 762426, 12 pages
http://dx.doi.org/10.1155/2015/762426

Research Article

Comparative Immunogenicity in Rabbits of the Polypeptides Encoded by the 5′ Terminus of Hepatitis C Virus RNA

Irina Sominskaya,[1] Juris Jansons,[1] Anastasija Dovbenko,[1] Natalia Petrakova,[2] Ilva Lieknina,[1] Marija Mihailova,[1] Oleg Latyshev,[2] Olesja Eliseeva,[2] Irina Stahovska,[1] Inara Akopjana,[1] Ivars Petrovskis,[1] and Maria Isaguliants[2,3,4]

[1]*Latvian Biomedical Research and Study Center, Ratsupites Street 1, Riga LV-1067, Latvia*
[2]*N. F. Gamaleja Research Center of Epidemiology and Microbiology, Gamaleja Street 18, Moscow 123098, Russia*
[3]*Department of Microbiology, Tumor and Cell Biology, Karolinska Institutet, Nobels Väg 16, 17177 Stockholm, Sweden*
[4]*Riga Stradins University, Dzirciema Street 16, Riga LV-1007, Latvia*

Correspondence should be addressed to Maria Isaguliants; maria.issagouliantis@ki.se

Received 22 July 2015; Accepted 29 September 2015

Academic Editor: Masha Fridkis-Hareli

Recent studies on the primate protection from HCV infection stressed the importance of immune response against structural viral proteins. Strong immune response against nucleocapsid (core) protein was difficult to achieve, requesting further experimentation in large animals. Here, we analyzed the immunogenicity of core aa 1–173, 1–152, and 147–191 and of its main alternative reading frame product F-protein in rabbits. Core aa 147–191 was synthesized; other polypeptides were obtained by expression in *E. coli*. Rabbits were immunized by polypeptide primes followed by multiple boosts and screened for specific anti-protein and anti-peptide antibodies. Antibody titers to core aa 147–191 reached 10^5; core aa 1–152, 5×10^5; core aa 1–173 and F-protein, 10^6. Strong immunogenicity of the last two proteins indicated that they may compete for the induction of immune response. The C-terminally truncated core was also weakly immunogenic on the T-cell level. To enhance core-specific cellular response, we immunized rabbits with the core aa 1–152 gene forbidding F-protein formation. Repeated DNA immunization induced a weak antibody and sustained proliferative response of broad specificity confirming a gain of cellular immunogenicity. Epitopes recognized in rabbits overlapped those in HCV infection. Our data promotes the use of rabbits for the immunogenicity tests of prototype HCV vaccines.

1. Introduction

Nucleocapsid (core) protein of hepatitis C virus (HCV) is the most conserved HCV antigen capable of inducing strong broadly cross-reactive responses, and therefore an attractive component of a genotype-non-restricted HCV vaccine. As such, it has been included in a number of HCV vaccine candidates including ones reaching primate trials [1]. The responses observed were described as limited. In immunizations, HCV core demonstrated features of a weak immunogen capable of inducing mainly CTL and low or no CD4+ T-cell responses with moderate IFN-gamma, weak IL-2 production, and no antibodies [2, 3]. In primate trials, HCV core induced stable low-level T-cell response of CD4+ and CD8+ T-cells manifested by IFN-gamma, but no IL-2 or IL-4 responses, weak T-cell proliferation, and low titer of core-specific antibodies [4–8]. Attempts to achieve a more efficient anticore immune response met with difficulties [9–11] even when using viral vectors [12].

Interestingly, in natural infection HCV core acts as a strong humoral immunogen inducing an early potent antibody production, but limited cellular response. Furthermore, in patients developing chronic infection, antibody response to HCV core protein continues to expand, whereas the cellular responses shrink [13]. This scenario points at a limited (low to no) protective potential of core-specific humoral

responses. At the same time, in primate trials, the responses to structural HCV proteins including core were shown to significantly correlate with primate protection against HCV challenge (whereas no protection was rendered by immunizations with nonstructural proteins) [1]. This indicates a potential positive input of anticore response (moderate as it was) on the observed protection effects, emphasizing the necessity to achieve an effective core-specific cellular response. Achieving stronger core-specific responses required the addition of recombinant HCV core protein or core-derived peptides [9, 14], involvement of the Th2-tilting carriers as HBcAg [15], or coadministration of cytokines such as IL-2, IL-4, or granulocyte-macrophage CSF [16], altogether pointing at the necessity of a shift towards the Th2-type T-helper cell response. Interestingly, these particular responses (of CD4+ T-cells) are involved in the spontaneous clearance of HCV infection, contrary to the CTL response reported to be stunned and ineffective [13, 17].

The reasons for a deficiency of such response in natural infection are not yet fully understood. Several explanations can be named, firstly, the well-known immunomodulating properties of HCV core protein [18–20]. The other reason could be the abundance of HCV core as an antigen. The core antigen quantity correlates with the virus load and can reach high levels in chronic HCV infection [21, 22], whereas the induction of potent cellular response appears to rely on the low immunogen doses [23]. An interference was also implied by the proteins translated from the HCV alternative reading frames (ARFs) [24, 25]. Most of the core gene products appear to be contaminated with the proteins translated from the HCV alternative reading frames (ARFPs) [24, 25]. The difference in anti-F response between chronic and self-limiting infection, the cross-reactivity irrespective of genotype, and the correlation of anti-F response to the response against other structural and nonstructural HCV antigens pointed at the immune response to F-protein as an integral part of the natural HCV infection [26]. As in case of HCV core, strong antibody response to F-protein correlates with the chronical course of HCV infection [27]. Kong et al. showed recently that presence of anti-F-specific antibodies negatively correlates with HCV RNA viral load suggesting that F-protein may participate in viral clearance [28]. However, other results suggest the potential involvement of F-protein (as of core antigen) in increasing the frequency of CD4+CD25+FoxP3+ T-cell-like population and IL-10-producing CD4+CD25+ T-cells [24] and biased cytokine responses (significantly decreased IFN-γ and/or IL-2 and significantly increased IL-4 and/or IL-5 levels) [25] predisposing to persistent HCV infection. ARFPs may induce some of the negative effects ascribed to HCV core [29] and also sidetrack the immune response away from HCV core. The true role of anti-ARFP responses in resistance to viral infection or vaccine protection is yet unknown.

In this work we aimed to directly compare immunogenicity of protein products encoded by 5′ end of HCV RNA in comparatively large animals, namely, in rabbits, which have numerous advantages over mice and are regularly used prior to testing vaccines in primates. Specifically, we compared immunogenicity of the main form of HCV core, core aa 1–173, its shorter form core aa 1–152, the C-terminal core aa 147–191, and F-protein as an ARFP form with the longest unique protein domain. All polypeptides generated extremely potent humoral response resembling that in chronic HCV infection. At the same time, a synthetic gene for the C-terminally truncated HCV core forbidding F-protein synthesis generated a sustained T-cell and only low antibody response indicating a clear shift towards cellular immunity deemed essential for an effective HCV vaccine.

2. Materials and Methods

2.1. E. coli Strains. E. coli strain DH5α [F$^-$ *gyrA96* (Nal^r) *recA1 relA1 endA1 thi-1 hsdR17* ($r_k^- m_k^+$) *glnV44 deoR* Δ*(laczya-argF) U169* [Φ80dΔ*(lacZ)M15*] was used for genetic manipulations and *E. coli* strains JM109 [F′ *traD36 proA*$^+$*B*$^+$ *lacI*^{q} Δ*(lacZ)M15/*Δ*(lac-proAB) glnV44* e14$^-$ (McrA$^-$) *gyrA96* (Nal^r) *recA1 relA1 endA1 thi-1 hsdR17* ($r_k^- m_k^+$)] and BL21(DE3) [F$^-$ *ompT dcm lon hsdS* ($r_B^- m_B^-$) *gal λ(DE3)*] were used for expression.

2.2. Plasmids for Expression of HCV Core. Fragment corresponding to HCV core 1–173 aa was obtained by polymerase chain reaction (PCR) using cDNA of HCV AD78 isolate genotype 1b (GenBank accession number AJ132996 [30]) as a template and two primers: forward 5′-GATCCATGGGCACGAATCCTAAACCTCA contained NcoI site and reverse 5′-GTGATGAGATCTAGAGCAACCGGGCAGATTCCCTGTTGCA contained BglII site. Second codon AGC from AJ132996 was substituted for GGC and thus gave us S to G substitution. NcoI/BglII PCR fragment was ligated into NcoI/BglII pQE-60 plasmid (Qiagen). The resulting plasmid was named pQE/core 173 (GenBank accession number KT824963).

Amplification of the DNA fragment corresponding to 1–10 aa of core and in +1 frame of the core from aa 11 to aa 143 and two additional aa (LE) was performed by PCR using 5′-GAGCATATGAGCACGAATCCTAAACCTCAAAGAAAACCAAACGTA as forward primer and 5′-GTGGTGCTCGAGTGGTGGCGCCGACGAGCGGA as reverse primer; harboring NdeI and XhoI restriction sites, respectively, was done from plasmid bearing HCV core fragment corresponding to 1–191 aa of HCV 1b isolate 274933RU (GenBank accession #AF176573 [31]). After amplification and treatment with restriction endonucleases NdeI and XhoI fragment was ligated into NdeI/XhoI pET22b(+). pET22b(+) plasmid contains T7 promoter and 6xHis-tag coding sequence at 3′ end of the cloned DNA fragment. The resulting plasmid was named pET22/ARFP.

2.3. Sources of HCV-Derived Peptides. Polypeptide representing aa 147–191 of HCV core VARALAHGVRVLEDGVNYATGNLPGCSFSIFLLALLSCLTIPASA (core 147–191) was purchased from GL Biochem (Shanghai, China) and was at least 70% pure by HPLC.

HCV core-derived synthetic peptides used in analysis of immune response were purchased from GL Biochem (Shanghai, China) or kindly provided by Mati Sällberg (Karolinska Institutet, Sweden); and F-protein-derived peptides were purchased from Peptron (South Korea). Peptides were purified

Table 1: A panel of overlapping peptides derived from HCV core and F-protein used in the tests of humoral and cellular immune response. First and last amino acid position are given according to HCV AD78 isolate genotype 1b (GenBank accession number AJ132996 [30, 36]).

Protein	Amino acid positions	Amino acid sequence
HCV core	1–35	MSTNPKPQRKTKRNTNRRPQDVKFPGGGQIVGGVY
	21–55	DVKFPGGGQIVGGGVYLLPRRGPRLGVRATRKTSER
	41–75	GPRLGVRATRKTSERSQPRGRRQPIPKARRPEGRT
	61–95	RRQPIPKARRPEGRTWAQPGYPWPLYGNEGMGWAG
	81–115	YPWPLYGNEGMGWAGWLLSPRGSRPSWGPNDPRRR
	101–135	RGSRPSWGPNDPRRRSRNLGKVIDTLTCGFADLMG
	121–155	KVIDTLTCGFADLMGYIPLVGAPLGGAARALAHGV
	161–195	GVNYATGNLPGCSFSILLALLSCLTTIPASAYEVR
	1–18	MSTIPKPQRKTKRNTNRR
	13–33	RNTNRRPQDVKFPGGGQIVGG
	34–42	VYLLPRRGP
	67–81	KARRPEGRTWAQPGY
	129–145	GFADLMGYIPLVGAPLG
	141–160	GAPLGGAARALAHGVRVLED
F-protein	30–49	SLAEFTCCRAGAPGWACARL
	45–64	ACARLGRLPSGRNLVEGDNL
	60–79	EGDNLSPRLAIPRAGPGLSL
	75–94	PGLSLGTLGPSMAMRAWGGQ
	90–109	AWGGQDGSCHPVALGLVGAP

by HPLC to 70% purity. The list of synthetic peptides used is given in Table 1.

2.4. Sources of HCV Polyproteins. Expression of HCV core aa 1–152 (core 1–152) and core aa 1–173 (core 1–173) was carried out in the *E. coli* strain JM109 as was described earlier in [32] and [33], respectively.

F-protein was expressed in *E. coli* BL21(DE3) transformed with pET22/ARFP. Transformed bacterial cells were grown at 37°C in 2x TY medium (16 g/L bacto-peptone (Difco), 10 g/L yeast extract (Difco), and 5 g/L NaCl), supplemented with 100 μg/mL ampicillin, to an OD 540 of 0.8–1.0, and protein expression was induced with 0.2 mM IPTG. Induction was continued for 4 h at 37°C; after that cells were sedimented by low-speed centrifugation (10 min at 4,000 ×g) and frozen at −20°C. Frozen biomass was thawed and suspended in 10 volumes of 8 M urea containing 100 mM Tris-HCl, pH 8.0, and ultrasonicated with ten 60 s ultrasound pulses of 22 kHz. After ultrasonication incubation on ice was continued for 60 min. After clarification (30 min at 10000 ×g), supernatant was collected and dithiothreitol (DTT) was added to 100 mM and incubation was continued overnight by shaking on rotary shaker at 4°C. After repeated clarification (30 min at 10000 ×g) before loading onto immobilized-metal affinity chromatography (IMAC) Ni-superflow agarose (Qiagen, Hilde, Germany), buffer exchange was performed with Sephadex G-25 column to replace 100 mM DTT with 5 mM β-mercaptoethanol (β-ME). The recombinant protein was purified by IMAC under denaturing conditions (8 M urea, 5 mM β-ME, 100 mM Tris-HCl, and pH 8.0) according to the manufacturer's instructions. F-protein containing fractions were pooled, and purified protein was diluted to final concentration of 0.5 mg/mL. The proteins were subsequently dialyzed two times (overnight and for 4 to 6 h) using refolding buffer I (2 M urea, 100 mM PB (Na_2HPO_4: 94.7 mM; NaH_2PO_4: 5.3 mM), pH 8.0, 0.5 M arginine, 5 mM glutathione reduced [GSH], and 0.5 mM glutathione oxidized [GSSG]) and refolding buffer II (100 mM PB, pH 8.0, 0.5 M arginine, 5 mM GSH, and 0.5 mM GSSG) and then PBS with 10% glycerin. Soluble proteins were concentrated using Amicon Ultra-15 10 K centrifugal filter device 10,000 MWCO (Millipore, Ireland). Its purity according to Coomassie blue staining of the SDS-PAGE gel was 95%.

2.5. SDS-PAGE and Western Blot Analysis. The purified proteins were analyzed on 15% SDS-PAGE by standard procedures (under denaturing conditions). Proteins were transferred to nitrocellulose membrane (Thermo Scientific). After blocking, the membranes were probed with rabbit antibodies specific to HCV core [34] or anti-core 1–173 or F-protein antibodies obtained here (see Section 2.6) diluted 1 : 10000, followed by a protein A horseradish peroxidase-conjugated antibody diluted 1 : 1000. Detection was performed with the DAB Substrate Kit (Thermo Scientific) according to the manufacturer's protocol.

2.6. Immunization of Rabbits. All animal experiments were performed in accordance with the Russian Federation law and were approved by the institutional ethical committee for animal experiments. Moscow strain of Chinchilla grey rabbits (female, 2-month-old, 1.5 to 1.8 kg) was obtained from the laboratory animal breeders "Manikhino"

(settlement Manikhino, Ivanovskoe, Moscow region, Russia) or "Krolinfo" (Orekhovo-Zuevo, Moscow region, Russia, http://krolinfo.umi.ru). The animals were maintained at 20 to 22°C and a relative humidity of 50% ± 10% on a 12 h light/dark cycle, fed with commercial rodent chow and herbal vitamin flour ("Krosha" and "Meadow grass," both from Zoomir, Russia), and provided with tap water *ad libitum*. The treatment of animals was in accordance with regulations outlined in the USDA Animal Welfare Act and the conditions specified in the guide for care and use of laboratory animals [35].

In protein immunizations, groups of two Chinchilla rabbits were immunized with injections of recombinant core 147–191 (numbers 87, 88), core 1–152 (89/4, 90/5), F-protein (91, 92), and core 1–173 (93, 94) or mock-immunized with PBS (95, 96). At week 0 animals were administered 100 μg of the respective polypeptides in 400 μL PBS mixed (1 : 1 v/v) with the complete Freund Adjuvant (CFA) and a week later (week 1) with 100 μg of the respective polypeptides in 400 μL PBS mixed (1 : 1 v/v) with the incomplete Freund Adjuvant (IFA). Injections were done subcutaneously at four sites along the back. Animals were boosted three times with one-month intervals by the intravenous injections of 50 μg of polypeptides in 200 μL PBS mixed with IFA (1 : 1 v/v). Control animals (95, 96) received the adjuvants mixed with PBS. Rabbits were bled from the ear vein two weeks after each immunization. Sera were prepared and stored at −20°C until further analysis. A portion of blood was collected in the heparinized Vacutainer tubes, and peripheral mononuclear cells (PBMCs) were isolated by Ficoll Paque gradient centrifugation.

DNA immunizations were performed with pUC8-based plasmid encoding core aa 1–152 [36] under the control of CMV promoter and HPV16 polyA [37] (DNAcore152). For this, four rabbits (nn 98, 99, 101, and 102) were injected with 90 μg DNAcore152 in 400 μL water intramuscularly in tibialis anterior on weeks 1 and 2. Two rabbits (101, 102) were further boosted with 90 μg DNAcore152 in 400 μL on weeks 5 (boost 1), 18 (2), 37 (3), and 54 (4). Control rabbits (43, 44) were immunized with empty pCMV vector [37] administered repeatedly along the same scheme. Rabbits were bled at weeks 0, 3, 4, 8, 20, 36, 38, 41, 54, 56, and 57. Sera and PBMC samples were prepared and treated as described above for the protein immunization.

2.7. Antibody Assays. Sera were assessed for the levels of antibodies against HCV core-derived polypeptides and F-protein.

Core-derived peptides (Table 1) and core 147–191 were coated onto 96-well MaxiSorp plates and core polypeptides on the 96-well PolySorp plates (both from Nunc, Denmark). Coating was done overnight at 4°C in 50 mM carbonate buffer, pH 9.6, at antigen concentration of 10 μg/mL. After blocking with PBS containing 1% BSA for 1 h at 37°C, serial dilutions of rabbit sera were applied on the plates and incubated for an additional hour at 37°C. Incubation was followed by three washings with PBS containing 0.05% Tween-20. Afterwards, plates were incubated for 1 h at 37°C with the protein A horseradish peroxidase-conjugated antibody (Sigma, USA) diluted 1 : 20000. Following three washes with PBS containing 0.05% Tween-20, the substrate OPD (Sigma, USA) was added, incubated at room temperature for 15 min in the dark, and stopped with 1 N H_2SO_4. Plates were read on an automatic reader (Multiscan, Sweden) at a dual length of 492 versus 630 nm. Immune serum was considered positive for anti-core antibodies whenever a specific OD value exceeded, by at least twofold, the signals generated by preimmune serum reacting with core-derived antigen and by immune serum reacting with BSA-coated wells.

2.8. PBMC Proliferation Assay. Peripheral mononuclear cells (PBMCs) were isolated by Ficoll Paque gradient centrifugation of blood which was collected in heparinized Vacutainer tubes. PBMCs were subjected to *in vitro* stimulation with core-derived synthetic peptides (Table 1) using the procedure described by us earlier [38]. In brief, T-cell proliferation assay was performed in triplicate with RPMI containing HCV core-derived peptides, all at 1 mcg/well; phytohemagglutinin (PHA; 10 mcg/well) was used as positive and RPMI alone and control peptide representing aa 605–613 of gp41 of HIV-1 were used as negative controls. Data were expressed as stimulation indices (SI) defined as the ratio of a mean value of [3H]-thymidine incorporation in the antigen-stimulated cultures to a mean value of radioactivity incorporation in medium containing negative control peptide from gp41 or RPMI, the highest of the values selected. SI values of 2.0 and above were considered positive. Data sets were discarded if SI by PHA was lower than 2.

2.9. Statistical Analysis. Statistical analysis was by paired Student's t-test, one-way ANOVA with pairwise comparisons, and two-way ANOVA with pairwise comparisons. $P < 0.05$ was considered significant. Analyses were performed using STATISTICA AXA 10.0.

3. Results and Discussion

3.1. Design and Expression of Proteins Encoded by the 5′ Terminus of HCV Genomic RNA. The full-length HCV core 1–191 is unstable and is quickly processed to a more stable shorter core aa 1–173 (core 1–173) [39]. We have chosen the latter as the immunogen and designed a recombinant core 1–173 of HCV 1b basing it on the isolate AD78P1 [30] with modifications that aimed to improve the prokaryotic expression (GenBank accession #KT824963). HCV core 1–173 is further degraded to the shorter forms, of which only core aa 1–152 (core 1–152) is readily detectable [40] motivating its choice as a second immunogen for the comparative immunogenicity studies. The expression of HCV core aa 1–152 variant was described by us earlier [32]. The panel of immunogens was complemented by the C-terminal fragment of HCV core aa 147–191 represented by a synthetic peptide (core 147–191).

The 5′ terminus of HCV RNA encodes also the proteins from the alternative reading frame (ARF). ARF of HCV lacks an in-frame AUG start codon; its expression involves unusual translation-level events involving ribosomal frameshifting [41]. ARF encoded proteins (ARFPs) are synthesized through

multiple events and sites such as codons (in phase +1) 26, 42, 85/87, and 144 yielding different ARFP forms including double frameshifts [42–45]. Of those, the main most stable form is F-protein, whereas the rest are comparatively short and proteolytically unstable [46]. The frameshift leading to the production of ARFP/F is remarkable: it leads to the shutdown of the main ORF for at least one round of translation and occurs so frequently that it causes the ribosome to translate +1 reading frame approximately 30% of the time [47, 48]. This points at the abundance of F-protein and its significance as a target of HCV-specific immune response. We have chosen this longest and most stable ARFP form for the immunogenicity study in rabbits, to compare its immunogenic performance to that of the "classical" product of translation of the 5-terminus of HCV RNA. For this, we designed a recombinant protein containing the N-terminal 10 amino acids of HCV core and aa 11 to 143 belonging to F-protein of HCV 1b variant [31]. Only the first ten amino acids of HCV core were retained as they were shown to stabilize F-protein and support its correct folding [49]. One of the major antigenic sites of the core protein has been located away from the very N-terminus of HCV core (amino acids 9–16 [50]). Hence, we expected that sharing of the first ten amino acids will not interfere with the development of F-specific immune response.

Core 1–173 and F-protein were expressed in *E. coli* with high yields (2–5 mg/L) and purified by His-tag chromatography. Coomassie staining of PAAG containing protein-rich fractions demonstrated the presence of proteins of expected molecular mass of 19 kDa for HCV core 1–173 (lanes 4–6) and of 16 kDa for F-protein (lanes 7–9) (Figure 1), in conformity with the observed products of translation of ARFs of HCV genotypes 1a, 1b, 1c, 2, and 3 [27, 51–55]. Proteins were of over 95% purity (Figure 1).

3.2. Polypeptides Derived from the 5′ Terminus of HCV RNA Induce Potent Antibody Response in Rabbits. Rabbits were immunized by the repeated injections of the polypeptides representing core aa 1–173 (core 173), core aa 1–152 (core 1–152), core aa 147–191 (core 147–191), and F-protein. All polypeptides were highly immunogenic on the humoral level; maximum antibody titers after completion of immunization cycle reached 10^6 and the titer of antibodies to aa 147–191 reached over 10^5 (Figure 2(a)). The strongest antibody response was achieved after immunization with HCV core 1–173 and F-protein (Figures 2(a) and 2(b)). HCV core 1–152 devoid of C-terminus generated a weaker antibody response with the maximum titer of 5×10^5 despite an identical immunization scheme and almost identical antigen structure of the proteins (except for the lack of C-terminus) (Figures 2(a) and 2(b)). A 44-amino-acid long core 147–191, although used in immunization without carriers (which normally ensure strong antibody response against the synthetic peptides), induced a strong specific immune response with the titers reaching 10^5 and the same kinetics of the antibody response as the longer polypeptides (Figures 3(a) and 3(b)). No anti-HCV core or anti-F-protein antibodies were detected in control rabbits 95, 96 receiving adjuvant alone (data not shown).

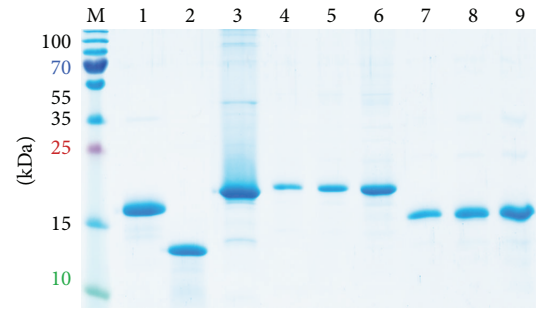

Figure 1: Expression of structural proteins encoded by the 5′ terminus of HCV RNA, HCV core aa 1–173 (lanes 4–6) and F-protein (lanes 7–9). *E. coli* were transformed with plasmids expressing core 1–173 and F-protein; cell lysates were resolved by 15% SDS-PAGE; gel was stained with Coomassie brilliant blue. HCV core 1–173 (0.5, 1, and 2.5 μg per well, lanes 4–6) and F-protein (0.5, 1, and 2.5 μg per well, lanes 7–9), respectively. Controls: His-tagged outer surface protein BB0689 of *B. burgdorferi* (2.5 μg, lane 1), lysozyme (2.5 μg, lane 2); HBcAg (2.5 μg, lane 3); PageRuler Plus Prestained Protein Ladder (Thermo Scientific, lane M). Position of molecular mass markers is given on the left.

Sera raised against F-protein, core 1–152, and core 1–173 specifically recognized the respective recombinant proteins in Western blotting (Figures 2(c) and 2(d) and data not shown). Core 1–173 and F-protein specific sera demonstrated also a weak cross-reactivity (Figures 2(c) and 2(d) and Supplementary Figure S1 in Supplementary Material available online at http://dx.doi.org/10.1155/2015/762426). The latter can be attributed to the presence in both proteins of 6xHis-tag. Indeed, we showed rabbits to develop antibodies against anti-His-tag in titer of 10^4 to 5×10^4 (Figure 2(a)).

We have used a panel of synthetic peptides (Table 1) to map the B-cell epitopes of HCV core and F-protein recognized in rabbits. In HCV core aa 1–173, nine epitopes were identified which were distributed throughout the protein with the dominant region located at N-terminus of the protein (Figure 3(a)). The sera of core 1–152 immunized rabbits recognized only the immunodominant epitope at aa 1–35 (titer 5.5×10^4, Figure 3(a)). Similar analysis was performed for the epitopes of F-protein (Figure 3(b)). B-cell epitopes of F-protein recognized in rabbits were localized at aa 30–49, 45–64, 60–79, and 90–109 (Figure 3(b)). The titer of antibodies against linear epitopes of F-protein was on the average 10-fold lower than against the linear epitopes of HCV core indirectly indicating a dominance of the HCV core-specific immune response over that against F-protein, at least in the rabbit model. The analysis of B-cell reactivity against HCV core and F-protein in rabbits uncovered similarity to the B-cell responses observed in HCV infection [27, 50, 54, 56–59]. Most of these epitopes were also shown to be recognized in mice [60, 61]. This reveals a promiscuous character of HCV core and F-specific B-cell response. Our findings also indicate that the recombinant F-protein obtained here is immunologically identical to the one formed after translation of viral RNA in infection and can be utilized in the diagnostic and possibly vaccine studies.

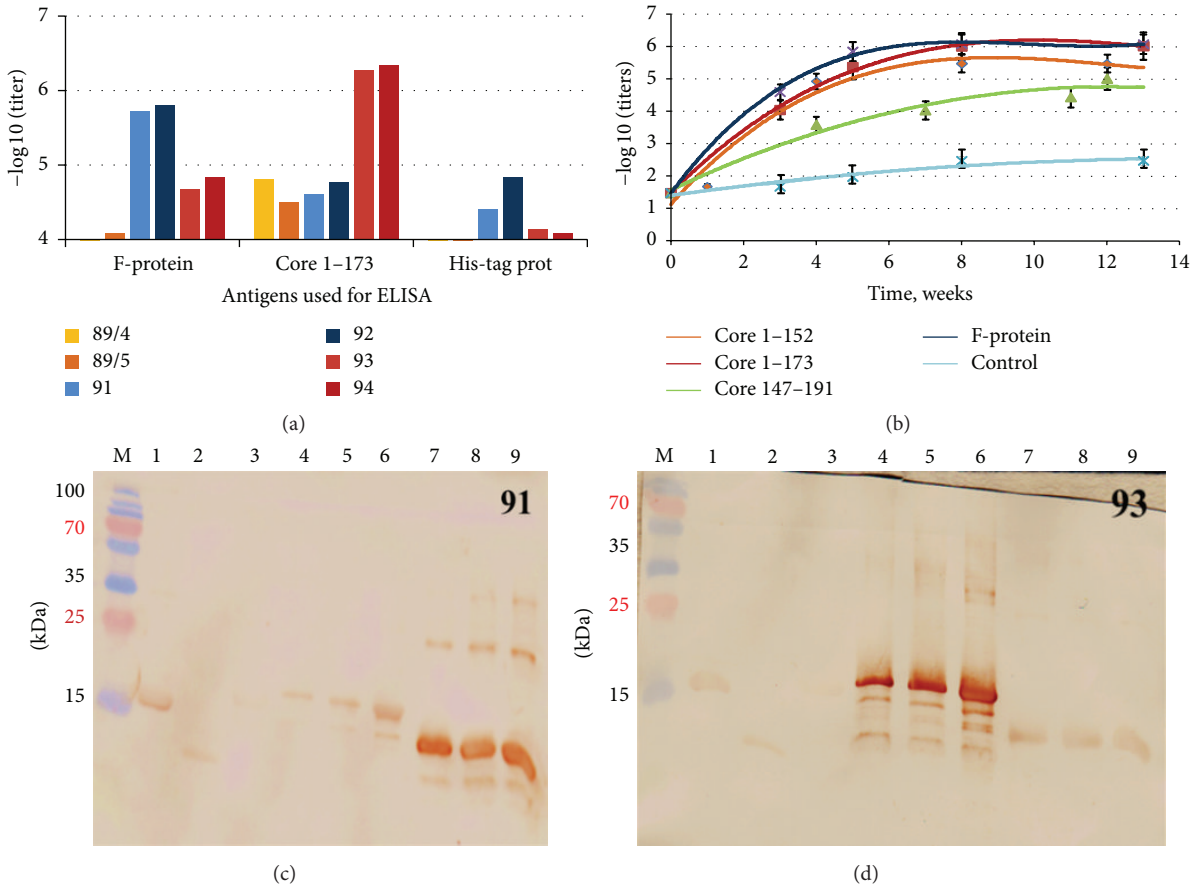

Figure 2: Antibody responses raised after immunization of rabbits with polypeptides encoded by the 5′ terminus of HCV genomic RNA. Maximum titer of antibodies against the immunogens (a); kinetics of the development of specific antibody response; controls represent rabbits mock-immunized with adjuvant alone; serum reactivity was tested by ELISA on plates coated with core 1–173 and F-protein (b); reactivity in Western blotting of hyperimmune sera raised against F-protein (serum of rabbit 91, (c)) and HCV core 1–173 (serum of rabbit 93, (d)). Western blotting was done with hyperimmune sera of rabbits collected by the end of immunization and diluted $1:10^4$. Lanes in panels (c and d) represent outer surface protein BB0689 of *B. burgdorferi* carrying 6xHis-tag (2.5 μg, lane 1), lysozyme (2.5 μg, lane 2), HBcAg (2.5 μg, lane 3), core 1–173 (0.5, 1, and 2.5 μg, lanes 4–6, resp.), and F-protein (0.5, 1, and 2.5 μg, lanes 7–9, resp.). PageRuler Plus Prestained Protein Ladder (Thermo Scientific, lane M). Position of molecular mass markers is given on the left.

We have further characterized the nature of cross-reactivity between anti-HCV core and anti-F-protein sera seen in Western blotting (Figures 2(c) and 2(d)). The cross-reactivity of anti-HCV core 1–173 and anti-F-protein sera amounted to 10% of the total reactivity of both HCV core and F-protein immunized rabbits (Supplementary Figure S1). Immunization with HCV core 1–173 did not induce any antibodies reacting with F-protein-derived peptides. Immunization with F-protein did not induce an immune response reacting to core peptides except for the region aa 61–95 (Figure 3(a)). Analysis of the sequences of HCV core 1–173 and F-protein did not reveal any amino acid homologies, indicating that cross-reacting anti-F-protein antibodies might have recognized not a linear but a conformational epitope at aa 61–95 which could be reproduced by the synthetic peptide. Indeed, preblocking with the peptide encompassing aa 61–95 had no effect on the cross-reactivity of anti-F-protein sera with core 1–173 in Western blotting (i.e., anti-F-protein antibodies reacting to the peptide core aa 61–95 in ELISA were unable to recognize this sequence in the context of the denatured core 1–173; data not shown). Importantly, although 10 amino acids overlap between HCV core 1–173 and F-protein at N-terminus, anti-F-protein sera did not recognize synthetic peptide representing aa 1–35 of HCV core (Figure 3(b)). Altogether, this indicated that the cross-reactivity was apparently due to the immune recognition of His-tag.

Thus, all polypeptides derived from the 5′ terminus of HCV genomic RNA were found to be extremely immunogenic on the antibody level. Furthermore, we have demonstrated a similarly strong immunogenicity of the HCV core and F-proteins. Albeit no function has yet been attributed to F-protein (or other products of ARFPs), it represents a target of immune response equal in potency to HCV core [26, 54, 62]. Supposedly nonfunctional but abundant ARFPs may induce a decoy response leading to the immune system away from addressing "the meaningful" viral proteins; its high immunogenicity in rabbits confirms a possibility of their

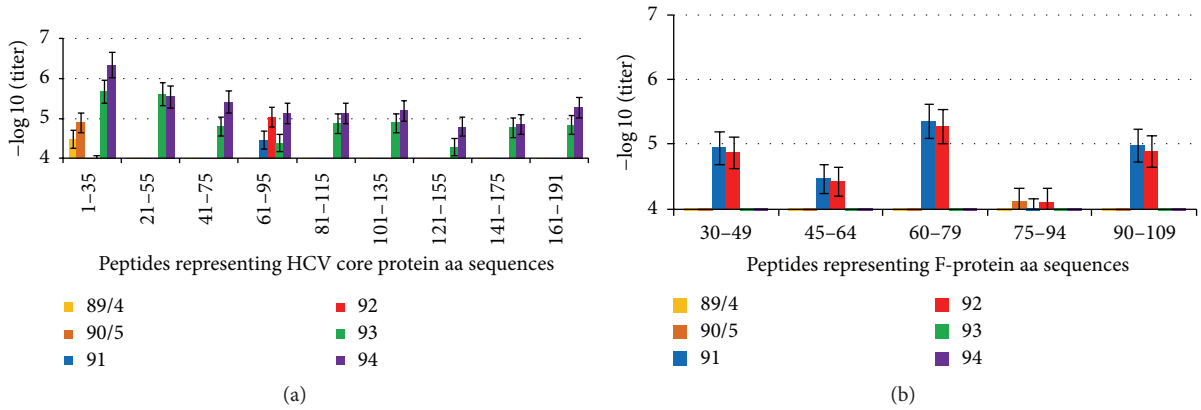

Figure 3: Fine epitope mapping of antibody response to linear epitopes of HCV core (a) and F-protein (b) recognized by rabbits immunized with HCV core aa 1–173 (nn 93, 94), HCV core 1–152 (89/4, 90/5), and F-protein (91, 92). Graphs demonstrate the highest antibody titers reached throughout immunization and represent the result of two to three independent ELISA runs. Unspecific antipeptide reactivity in control rabbits receiving adjuvant alone was below 5×10^2.

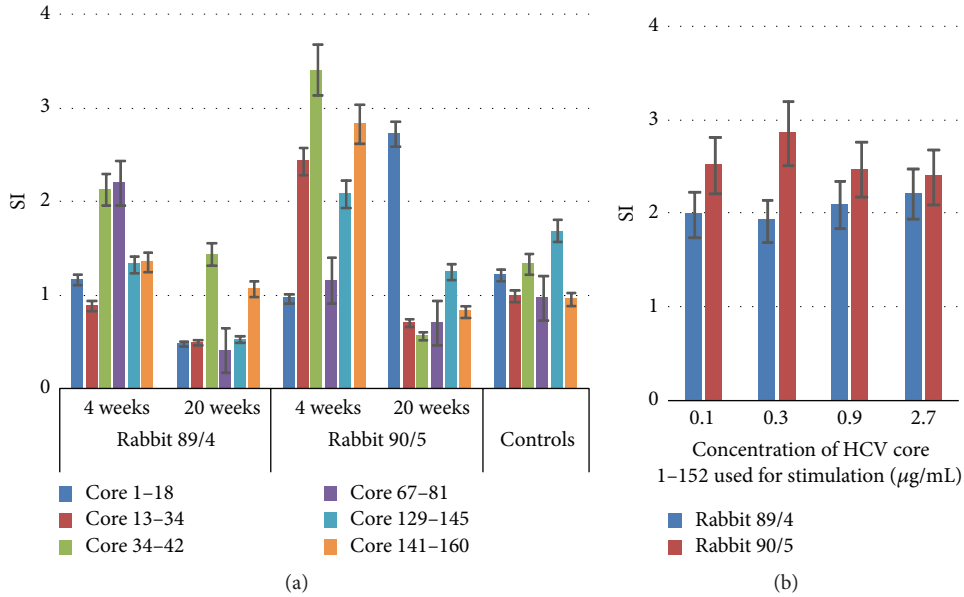

Figure 4: Proliferative response to HCV core in rabbits immunized with HCV core 1–152 visualized as stimulation indexes (SI). Stimulation of PBMCs of rabbits 89/4 and 90/5 with synthetic peptides derived from core 1–152 two weeks after prime (week 4) and two weeks after the last boost (week 20); controls are naïve rabbits ($n = 3$) and rabbits were immunized with irrelevant protein antigens ($n = 4$) (a); low or no dependence of T-cell stimulation on the concentration of HCV core 1–152 used in proliferation test in the test done prime (week 4) (b). All antigen stimulation tests were performed in triplicate. Test results were discarded if radioactivity incorporation values demonstrated by mitogen PHA were below 1000 counts per minute and if stimulation indexes in response to PHA were below 2.

competition in the induction of antiviral immune response. This would fall in line with the recent model of Skums et al. which suggests antigenic cooperation in HCV infection, with immune responses against one antigen variant creating protective immune environment for other variants [63].

Since F-protein has not yet been ascribed any function in the virus, while functions of HCV core are well known and essential, we concentrated our further immunogenicity studies on the cellular immune response against HCV core. Peripheral blood mononuclear cells (PBMCs) of rabbits immunized with HCV core 1–152 and core 1–173 were collected prior to and after each boost and subjected to stimulation with HCV core-derived peptides. Weak infrequent T-cell responses with stimulation indexes (SI) exceeding 2 were repeatedly observed only in rabbits immunized with HCV core 1–152, but not in the naïve or adjuvant or core 1–173-immunized animals (Figure 4, data not shown). Proliferative response of rabbit PBMCs was observed after two priming HCV core 1–152 immunizations (week 4) and was not boosted except for a single response to the epitope at the HCV core N-terminus observed in the rabbit 90/5 at week 20 (Figure 4(a)). Stimulation of the hyperimmune rabbit

PBMCs with recombinant HCV core 1–152 induced a weak proliferative response independent of antigen concentration (Figure 4(b)).

Analysis of HCV core-specific humoral and cellular responses revealed that the C-terminally truncated HCV core form had somewhat weaker humoral immunogenicity than HCV core aa 1–173: antibodies were two to three times lower in titer and of restricted specificity targeting mainly the N-terminus of the protein (Figures 2 and 3). At the same time, only core 1–152 was able to induce a specific T-cell response, albeit of a very low level. Apparently, the truncation of the C-terminus led to a partial loss of B-cell immunogenicity (in terms of both breadth and potency) and at the same time the induction of the T-cell arm of immune response. We have recently shown that HCV core devoid of the N-terminus upregulated the transcription of a ROS-generating enzyme cytochrome P450 2E1 [64]. Furthermore, the same fragment induced the expression of endoplasmic reticulum oxidoreductin 1α. The latter triggers the efflux of Ca^{2+} ions from ER to mitochondria via mitochondrial Ca^{2+} uniporter, leading to the generation of superoxide anions and possibly also H_2O_2 [64]. ROS have a physiological role in signaling extending to every cell type involved in the induction of immune response; ROS were the first molecules found to suppress the T-cell function [65]. As with any signaling mechanism, ROS can become cytotoxic if the signal is too strong and/or too prolonged. ROS help to mediate T-cell activation; however, T-cell activation also depends on the capacity of accessory cells to maintain sufficient level of glutathione and is compromised by the oxidative stress [66]. Furthermore, excessive amounts of ROS can oxidize the protein kinases and phosphatases that regulate critical cell signals and distort the activation of signaling pathways including regulation of the lymphocyte functions [67]. Immunosuppressive effects of ROS may also be due to the fact that Tregs cells are more resistant to ROS than the effector T-cells and pertain their downregulating activity when the effector T-cells fail [66]. An excessive oxidative stress may thus be detrimental for the normal T-cell functions. This would explain the observed deleterious role of the high HCV core protein "doses" for the specific T-cell immunity in a mouse model [9]. For humoral response, on the contrary, ROS appear to contribute to Th1/Th2/Th17 cell fate decisions during T-lymphocyte activation and enhance immunoglobulin production by B-lymphocytes [68]. Our data indicates that (as in HCV infection) high levels of HCV core support the strong multiepitopic B-cell, but low or no T-cell response, and point at the role of certain core domains, specifically at the C-terminus, in tilting the response towards the humoral one. Involvement in ROS induction may explain an unexpectedly strong humoral immunogenicity in rabbits of a peptide covering aa 147–191 derived from the ROS-inducing core fragment.

3.3. Immunogenicity in Rabbits of DNA Encoding Core aa 1–152. High levels of circulating HCV core antigen in HCV infection would induce high levels of ROS and promote strong humoral response but little immunity on the T-cell level, a scenario of immune response in the chronic HCV infection, whereas the immune success and viral clearance coincide with a weak or no antibody response [69] and potent cellular immunity manifested mainly CD4+ T-cells [13, 17]. To strengthen the cellular immune response component, one would need to both decrease the immunogen dose and delete the ROS-inducing/B-cell activating signals.

To evade both the potential pitfalls as immune suppression induced by an excess of ROS and the immune competition from the ARF products, we exploited a synthetic gene encoding HCV core devoid of the C-terminus (DNAcore152) with a forbidden frameshift (not supporting F-protein formation [36]). Rabbits were immunized with DNAcore152 by two closely spaced priming injections (double prime, four rabbits), in two rabbits followed by a series of boosts performed first with one-month and then with four-month intervals. The latter scheme was applied in view of earlier experiments in chimpanzees which demonstrated gradual increase if there were proliferative responses to HCV core after repeated boosts performed under long period of time [4]. Contrary to the HCV core 1–152 immunized rabbits, rabbits receiving injections of DNAcore152 exhibited low but consistent proliferative response to both HCV core and core-derived peptides (Figure 5(a)), boosted by the booster DNA injections (Figure 5(b); Supplementary Figure S2). Rabbits immunized with repeated injections of DNAcore152 developed also a low-level humoral response to HCV core, weakly boosted after the repeated gene administrations (Figure 5(c)). No anticore responses were registered in rabbits mock-immunized with empty vector DNA (data not shown).

Immunization with DNA encoding HCV core devoid of the 39 amino acids on the C-terminus allowed shifting the immune response to almost exclusively Th1 type as manifested by weak but consistent core-specific proliferative responses of PBMCs and low level of anti-core antibody production resembling the profiles observed in the primate trials of the multicomponent immunogens including diverse forms of HCV core (DNA, recombinant virus, protein) [4–6]. These results fall in line with our earlier observations made in the DNA-immunized mice; namely, the induction of cellular response to HCV core does not require high levels of HCV core protein (low amounts provided by cells *in vivo* transfected at immunization sites appear to be sufficient). Furthermore, we could show that truncation, at least partial, of the ROS-inducing core domain may rescue cellular response. Additional positive input was possibly made by forbidding the formation of F-protein. The actual role of immune competition from the F-protein is currently being assessed in a series of mouse immunizations.

Again, as in the case of protein immunizations, the specificity of B- and T-cell response to HCV core-derived peptides in DNA-immunized rabbits resembled that observed in the HCV infection [70]. Core-specific T-cell responses were persistent and boostable, resembling responses observed in the self-limiting rather than chronic HCV infection which is characterized by a gradual loss of the specific T-cell response [17, 71].

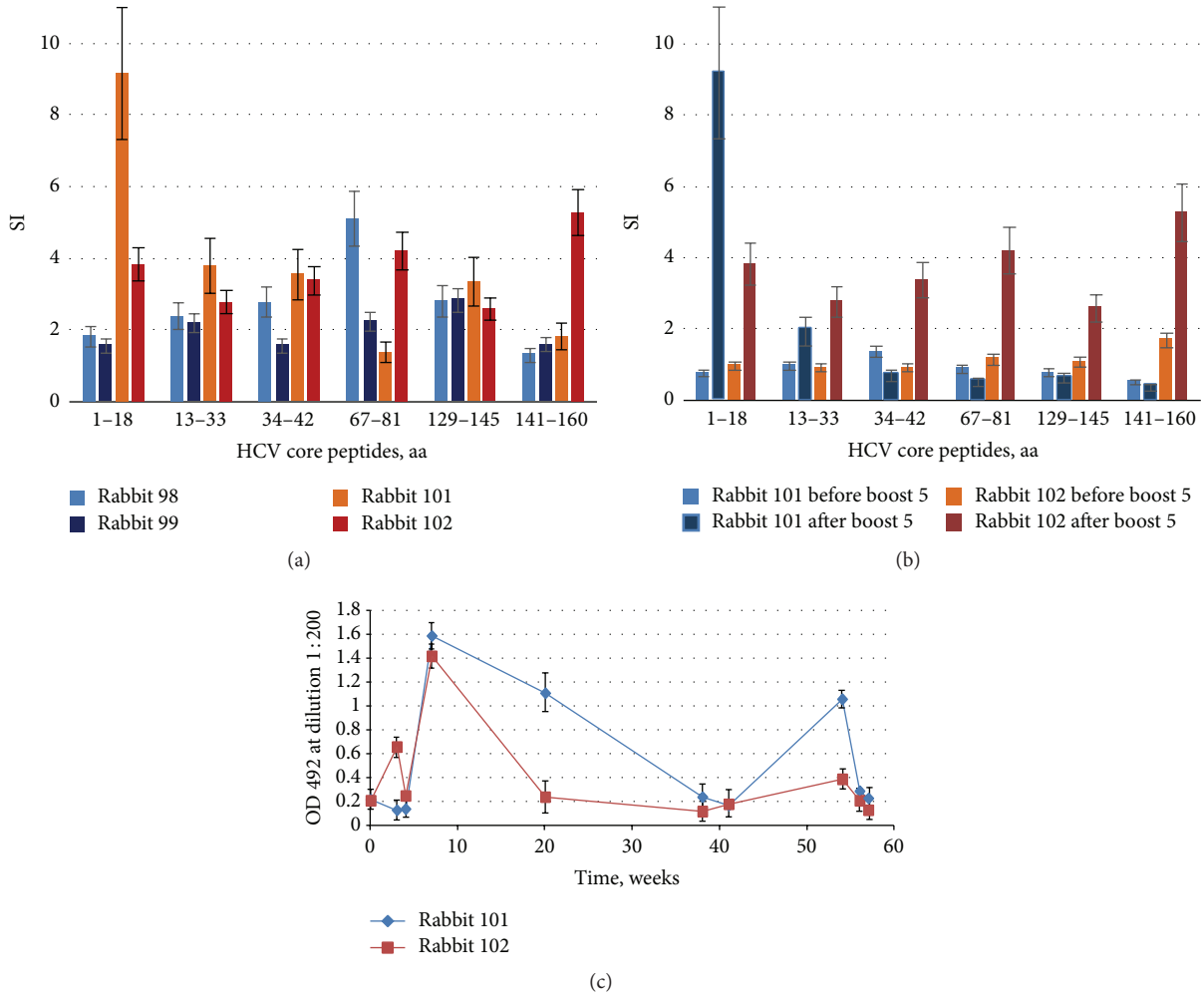

Figure 5: Anti-HCV core immune response induced by single and repeated immunizations with synthetic gene encoding core aa 1–152 (DNAcore152). Rabbits were regularly bled; PBMCs were isolated and subjected to stimulation with HCV core-derived peptides and recombinant HCV core aa 1–152. Stimulation indexes (SI) observed after double priming (week 4) (a); boosting of T-cell response in rabbits receiving multiple injections of DNAcore152 illustrated by stimulation indexes exhibited by PBMCs of rabbits 101 and 102 before and after boost 5 at weeks 54 and 56, respectively (b); dynamics of antibody response to HCV core aa 1–152 in rabbits receiving repeated injections of DNAcore152 (c). All antigen stimulation tests were performed in triplicate; SI values represent an average with standard deviation. Test results were discarded if radioactivity incorporation values demonstrated by mitogen PHA were below 1000 counts per minute and if stimulation indexes in response to PHA were below 2. HCV core-specific antibodies response represent an average optical density exhibited by sera of each of the rabbits collected at given time points in two ELISA runs with standard deviations. OD of sera of rabbits immunized with empty vector DNA collected at the same time points did not exceed the optical density of 0.3 (data not shown).

4. Conclusions

In primate trials, the responses to the structural HCV proteins including the nucleocapsid (core) were shown to significantly correlate to the protection against HCV challenge [1] implying an input of anticore response on the observed protection effects. This emphasizes the necessity of the experiments aimed at achieving an effective core-specific cellular response in larger animals than mice. Rabbits are widely used in the toxicity and safety testing of medical devices, drugs, and vaccines because of both genetic heterogeneity and possibility of the longitudinal follow-up experiments. Here, we used the rabbit model to evaluate the immunogenicity of polypeptides encoded by the 5′ terminus of HCV RNA. By polypeptide immunization, we have induced in rabbits a strong humoral immune response to an abundant HCV core form aa 1–173 and the most stable ARFP form, F-protein. Immunization with HCV core aa 1–173 led to a B-cell response of broad specificity targeting multiple linear epitopes. The C-terminally truncated core 1–152 induced a weaker antibody response directed only against the N-terminus of the protein implicating the role of the C-terminus in promoting humoral immunogenicity. Delivery of the C-terminally truncated HCV core by DNA immunization with a plasmid forbidding frameshift led to the induction of weak but sustained T-cell response to multiple epitopes within the protein. Both B- and

T-cell responses observed in rabbits mimicked that in HCV infection which indicates the promiscuity of major epitopes localized in the polyproteins encoded by the 5′-terminus of HCV genomic RNA. These are promising findings which allow a step forward in the development of the HCV core based prototype HCV vaccines, as the previous data indicated that although HCV core is the main target of an immune response in the infected individuals [72], it is not so immunogenic in the larger species as humans [73] and could even suppress the immune response [14], also heterologous [74]. The immunogenicity of DNA representing the 5′ terminus of HCV RNA and of the polyproteins encoded therein and the promiscuity of the observed responses promote the use of rabbit model for the preclinical trials of HCV vaccines, although other adjuvants would be needed to comply with the requests to vaccine formulations. These considerations may be important in further development and testing of HCV vaccines based on the structural viral proteins.

Conflict of Interests

The authors declare that there is no conflict of interests regarding the publication of this paper.

Acknowledgments

This research was funded by grant from the Research Council of Latvia no. 532/2012 and grant from the Russian Fund for Basic Research no. 13-04-0152313. Networking between the partners was supported by the Thematic Partnership Grant of the Swedish Institute no. 09272_2013. Maria Isaguliants was in part supported by the EU BALTINFECT project contract no. 316275. Recombinant *B. burgdorferi* outer surface protein BB0689 with 6xHis-tag was a generous gift of Dr. Kaspars Tars.

References

[1] H. Dahari, S. M. Feinstone, and M. E. Major, "Meta-analysis of hepatitis C virus vaccine efficacy in chimpanzees indicates an importance for structural proteins," *Gastroenterology*, vol. 139, no. 3, pp. 965–974, 2010.

[2] P. Fietta and G. Delsante, "The effector T helper cell triade," *Rivista di Biologia*, vol. 102, no. 1, pp. 61–74, 2009.

[3] N. Zhang and M. J. Bevan, "$CD8^+$ T cells: foot soldiers of the immune system," *Immunity*, vol. 35, no. 2, pp. 161–168, 2011.

[4] G. A. Elmowalid, M. Qiao, S.-H. Jeong et al., "Immunization with hepatitis C virus-like particles results in control of hepatitis C virus infection in chimpanzees," *Proceedings of the National Academy of Sciences of the United States of America*, vol. 104, no. 20, pp. 8427–8432, 2007.

[5] C. Rollier, E. Depla, J. A. R. Drexhage et al., "Control of heterologous hepatitis C virus infection in chimpanzees is associated with the quality of vaccine-induced peripheral T-helper immune response," *Journal of Virology*, vol. 78, no. 1, pp. 187–196, 2004.

[6] C. S. Rollier, G. Paranhos-Baccala, E. J. Verschoor et al., "Vaccine-induced early control of hepatitis C virus infection in chimpanzees fails to impact on hepatic PD-1 and chronicity," *Hepatology*, vol. 45, no. 3, pp. 602–613, 2007.

[7] J.-W. Youn, S.-H. Park, D. Lavillette et al., "Sustained E2 antibody response correlates with reduced peak viremia after hepatitis C virus infection in the chimpanzee," *Hepatology*, vol. 42, no. 6, pp. 1429–1436, 2005.

[8] J.-W. Youn, Y.-W. Hu, N. Tricoche et al., "Evidence for protection against chronic hepatitis C virus infection in chimpanzees by immunization with replicating recombinant vaccinia virus," *Journal of Virology*, vol. 82, no. 21, pp. 10896–10905, 2008.

[9] E. Alekseeva, I. Sominskaya, D. Skrastina et al., "Enhancement of the expression of HCV core gene does not enhance core-specific immune response in DNA immunization: advantages of the heterologous DNA prime, protein boost immunization regimen," *Genetic Vaccines and Therapy*, vol. 7, article 7, 2009.

[10] J. Satoi, K. Murata, M. Lechmann et al., "Genetic immunization of wild-type and hepatitis C virus transgenic mice reveals a hierarchy of cellular immune response and tolerance induction against hepatitis C virus structural proteins," *Journal of Virology*, vol. 75, no. 24, pp. 12121–12127, 2001.

[11] O. Vidalin, M. Muslmani, C. Estienne, H. Echchakir, and A. M. Abina, "In vivo target validation using gene invalidation, RNA interference and protein functional knockout models: it is the time to combine," *Current Opinion in Pharmacology*, vol. 9, no. 5, pp. 669–676, 2009.

[12] O. Vidalin, A. Fournillier, N. Renard et al., "Use of conventional or replicating nucleic acid-based vaccines and recombinant semliki forest virus-derived particles for the induction of immune responses against hepatitis C virus core and E2 antigens," *Virology*, vol. 276, no. 2, pp. 259–270, 2000.

[13] B. Rehermann, "Hepatitis C virus versus innate and adaptive immune responses: a tale of coevolution and coexistence," *The Journal of Clinical Investigation*, vol. 119, no. 7, pp. 1745–1754, 2009.

[14] G.-J. Hu, R. Y.-H. Wang, D.-S. Han, H. J. Alter, and J. W.-K. Shih, "Characterization of the humoral and cellular immune responses against hepatitis C virus core induced by DNA-based immunization," *Vaccine*, vol. 17, no. 23-24, pp. 3160–3170, 1999.

[15] M. Geissler, K. Tokushige, T. Wakita, V. R. Zurawski Jr., and J. R. Wands, "Differential cellular and humoral immune responses to HCV core and HBV envelope proteins after genetic immunizations using chimeric constructs," *Vaccine*, vol. 16, no. 8, pp. 857–867, 1998.

[16] M. Geissler, A. Gesien, K. Tokushige, and J. R. Wands, "Enhancement of cellular and humoral immune responses to hepatitis C virus core protein using DNA-based vaccines augmented with cytokine-expressing plasmids," *Journal of Immunology*, vol. 158, no. 3, pp. 1231–1237, 1997.

[17] S.-H. Park and B. Rehermann, "Immune responses to HCV and other hepatitis viruses," *Immunity*, vol. 40, no. 1, pp. 13–24, 2014.

[18] J. G. Bode, E. D. Brenndörfer, and D. Häussinger, "Hepatitis C virus (HCV) employs multiple strategies to subvert the host innate antiviral response," *Biological Chemistry*, vol. 389, no. 10, pp. 1283–1298, 2008.

[19] K. Hiroishi, T. Ito, and M. Imawari, "Immune responses in hepatitis C virus infection and mechanisms of hepatitis C virus persistence," *Journal of Gastroenterology and Hepatology*, vol. 23, no. 10, pp. 1473–1482, 2008.

[20] Z. Q. Yao, E. King, D. Prayther, D. Yin, and J. Moorman, "T cell dysfunction by hepatitis C virus core protein involves PD-1/PDL-1 signaling," *Viral Immunology*, vol. 20, no. 2, pp. 276–287, 2007.

[21] G. J. Dawson, "The potential role of HCV core antigen testing in diagnosing HCV infection," *Antiviral Therapy*, vol. 17, no. 7, pp. 1431–1435, 2012.

[22] H. L. Tillmann, "Hepatitis C virus core antigen testing: role in diagnosis, disease monitoring and treatment," *World Journal of Gastroenterology*, vol. 20, no. 22, pp. 6701–6706, 2014.

[23] C. J. Kroger and M. A. Alexander-Miller, "Dose-dependent modulation of CD8 and functional avidity as a result of peptide encounter," *Immunology*, vol. 122, no. 2, pp. 167–178, 2007.

[24] T. Hashempour, T. Bamdad, A. Bergamini et al., "F protein increases CD4+CD25+ T cell population in patients with chronic hepatitis C," *Pathogens and Disease*, vol. 73, no. 4, 2015.

[25] M. Yue, X. Deng, X. Zhai et al., "Th1 and Th2 cytokine profiles induced by hepatitis C virus F protein in peripheral blood mononuclear cells from chronic hepatitis C patients," *Immunology Letters*, vol. 152, no. 2, pp. 89–95, 2013.

[26] W. C.-M. Chuang and J.-P. Allain, "Differential reactivity of putative genotype 2 hepatitis C virus F protein between chronic and recovered infections," *Journal of General Virology*, vol. 89, no. 8, pp. 1890–1900, 2008.

[27] F. Komurian-Pradel, A. Rajoharison, J.-L. Berland et al., "Antigenic relevance of F protein in chronic hepatitis C virus infection," *Hepatology*, vol. 40, no. 4, pp. 900–909, 2004.

[28] J. Kong, X. Deng, Z. Wang, J. Yang, Y. Zhang, and J. Yu, "Hepatitis C virus F protein: a double-edged sword in the potential contribution of chronic inflammation to carcinogenesis," *Molecular Medicine Reports*, vol. 2, no. 3, pp. 461–469, 2009.

[29] A. D. Branch, D. D. Stump, J. A. Gutierrez, F. Eng, and J. L. Walewski, "The hepatitis C virus alternate reading frame (ARF) and its family of novel products: the alternate reading frame protein/F-protein, the double-frameshift protein, and others," *Seminars in Liver Disease*, vol. 25, no. 1, pp. 105–117, 2005.

[30] K. Rispeter, M. Lu, S. Lechner, A. Zibert, and M. Roggendorf, "Cloning and characterization of a complete open reading frame of the hepatitis C virus genome in only two cDNA fragments," *Journal of General Virology*, vol. 78, part 11, pp. 2751–2759, 1997.

[31] V. V. Mokhonov, D. V. Novikov, E. I. Samokhvalov et al., "Genome analysis of hepatitis C virus strain 274933RU isolated in Russian Federation," *Voprosy Virusologii*, vol. 47, no. 1, pp. 9–12, 2002.

[32] N. V. Petrakova, T. I. Kalinina, I. Khudiakov, E. V. Gazina, and V. D. Smirnov, "Preparation and purification of a polypeptide containing antigenic determinants of hepatitis C core protein," *Voprosy Virusologii*, vol. 42, no. 5, pp. 208–212, 1997.

[33] M. Mihailova, M. Fiedler, M. Boos et al., "Preparation of hepatitis C virus structural and non-structural protein fragments and studies of their immunogenicity," *Protein Expression and Purification*, vol. 50, no. 1, pp. 43–48, 2006.

[34] M. G. Isaguliants, K. Iakimtchouk, N. V. Petrakova et al., "Gene immunization may induce secondary antibodies reacting with DNA," *Vaccine*, vol. 22, no. 11-12, pp. 1576–1585, 2004.

[35] National Research Council (US) Committee for the Update of the Guide for the Care and Use of Laboratory Animals, *Guide for the Care and Use of Laboratory Animals*, National Academies Press, Washington, DC, USA, 8th edition, 2011.

[36] Y. E. Khudyakov, H. A. Fields, M. O. Favorov, N. S. Khudyakova, M.-T. Bonafonte, and B. Holloway, "Synthetic gene for the hepatitis C virus nucleocapsid protein," *Nucleic Acids Research*, vol. 21, no. 11, pp. 2747–2754, 1993.

[37] B. Wahren, J. Hinkula, E. Ljungdahl Stahle, C. A. K. Borrebaeck, S. Schwartz, and H. Wigzell, "Nucleic acid vaccination with HIV regulatory genes," *Annals of the New York Academy of Sciences*, vol. 772, pp. 278–281, 1995.

[38] M. G. Isaguliants, S. Nordlund, M. Sallberg et al., "HIV-1 epitopes exposed by hybrid hepatitis B core particles affect proliferation of peripheral blood mononuclear cells from HIV-1 positive donors," *Immunology Letters*, vol. 52, no. 1, pp. 37–44, 1996.

[39] K. Yasui, T. Wakita, K. Tsukiyama-Kohara et al., "The native form and maturation process of hepatitis C virus core protein," *Journal of Virology*, vol. 72, no. 7, pp. 6048–6055, 1998.

[40] R. Suzuki, K. Tamura, J. Li et al., "Ubiquitin-mediated degradation of hepatitis C virus core protein is regulated by processing at its carboxyl terminus," *Virology*, vol. 280, no. 2, pp. 301–309, 2001.

[41] N. Vassilaki and P. Mavromara, "The HCV ARFP/F/Core+1 protein: production and functional analysis of an unconventional viral product," *IUBMB Life*, vol. 61, no. 7, pp. 739–752, 2009.

[42] M. Baril and L. Brakier-Gingras, "Translation of the F protein of hepatitis C virus is initiated at a non-AUG codon in a +1 reading frame relative to the polyprotein," *Nucleic Acids Research*, vol. 33, no. 5, pp. 1474–1486, 2005.

[43] S. Boulant, M. Becchi, F. Penin, and J.-P. Lavergne, "Unusual multiple recoding events leading to alternative forms of hepatitis C virus core protein from genotype 1b," *The Journal of Biological Chemistry*, vol. 278, no. 46, pp. 45785–45792, 2003.

[44] A. Boumlic, Y. Nominé, S. Charbonnier et al., "Prevalence of intrinsic disorder in the hepatitis C virus ARFP/Core+1/S protein," *FEBS Journal*, vol. 277, no. 3, pp. 774–789, 2010.

[45] N. Vassilaki and P. Mavromara, "Two alternative translation mechanisms are responsible for the expression of the HCV ARFP/F/core+1 coding open reading frame," *The Journal of Biological Chemistry*, vol. 278, no. 42, pp. 40503–40513, 2003.

[46] H.-C. Li, H.-C. Ma, C.-H. Yang, and S.-Y. Lo, "Production and pathogenicity of hepatitis C virus core gene products," *World Journal of Gastroenterology*, vol. 20, no. 23, pp. 7104–7122, 2014.

[47] A. Varaklioti, N. Vassilaki, U. Georgopoulou, and P. Mavromara, "Alternate translation occurs within the core coding region of the hepatitis C viral genome," *Journal of Biological Chemistry*, vol. 277, no. 20, pp. 17713–17721, 2002.

[48] Z. Xu, J. Choi, T. S. B. Yen et al., "Synthesis of a novel hepatitis C virus protein by ribosomal frameshift," *The EMBO Journal*, vol. 20, no. 14, pp. 3840–3848, 2001.

[49] V. Barban, S. Fraysse-Corgier, G. Paranhos-Baccala et al., "Identification of a human epitope in hepatitis C virus (HCV) core protein using a molecularly cloned antibody repertoire from a non-symptomatic, anti-HCV-positive patient," *Journal of General Virology*, vol. 81, no. 2, pp. 461–469, 2000.

[50] M. Sällberg, U. Rudén, B. Wahren, and L. O. Magnius, "Immune response to a single peptide containing an immunodominant region of hepatitis C virus core protein: the isotypes and the recognition site," *Immunology Letters*, vol. 33, no. 1, pp. 27–33, 1992.

[51] F. Baghbani-arani, F. Roohvand, M. R. Aghasadeghi et al., "Expression and characterization of *Escherichia coli* derived hepatitis C virus ARFP/F protein," *Journal of Molekuliarnaia Biologiia*, vol. 46, no. 2, pp. 251–259, 2012.

[52] C. Bain, P. Parroche, J. P. Lavergne et al., "Memory T-cell-mediated immune responses specific to an alternative core protein in hepatitis C virus infection," *Journal of Virology*, vol. 78, no. 19, pp. 10460–10469, 2004.

[53] D.-Y. Gao, X.-X. Zhang, G. Hou et al., "Assessment of specific antibodies to F protein in serum samples from Chinese hepatitis C patients treated with interferon plus ribavarin," *Journal of Clinical Microbiology*, vol. 46, no. 11, pp. 3746–3751, 2008.

[54] H. Qureshi, R. Qazi, S. Hamid, and S. A. Qureshi, "Identification of immunogenic regions within the alternative reading frame protein of hepatitis C virus (genotype 3)," *European Journal of Clinical Microbiology and Infectious Diseases*, vol. 30, no. 9, pp. 1075–1083, 2011.

[55] K. M. Shesheer, R. K. Venkateswara, H. C. Mohammed, and V. D. Reddy, "Expression of alternate reading frame protein (F1) of hepatitis C virus in *Escherichia coli* and detection of antibodies for F1 in Indian patients," *Infection, Genetics and Evolution*, vol. 8, no. 3, pp. 374–377, 2008.

[56] M. U. Mondelli, A. Cerino, F. Bono et al., "Hepatitis C virus (HCV) core serotypes in chronic HCV infection," *Journal of Clinical Microbiology*, vol. 32, no. 10, pp. 2523–2527, 1994.

[57] F. H. Pujol, Y. E. Khudyakov, M. Devesa et al., "Characterization of the antibody reactivity to synthetic peptides from different parts of the hepatitis C virus genome," *Viral Immunology*, vol. 9, no. 2, pp. 89–96, 1996.

[58] K. Siemoneit, M. da Silva Cardoso, A. Wölpl et al., "Isotype-specific immune response to a single hepatitis C virus core epitope defined by a human monoclonal antibody: diagnostic value and correlation to PCR," *Annals of Hematology*, vol. 69, no. 3, pp. 129–133, 1994.

[59] J. L. Walewski, T. R. Keller, D. D. Stump, and A. D. Branch, "Evidence for a new hepatitis C virus antigen encoded in an overlapping reading frame," *RNA*, vol. 7, no. 5, pp. 710–721, 2001.

[60] I. Harase, T. Moriyama, T. Kaneko et al., "Immune response to hepatitis C virus core protein in mice," *Immunology and Cell Biology*, vol. 73, no. 4, pp. 346–352, 1995.

[61] K. Kakimi, K. Kuribayashi, M. Iwashiro et al., "Hepatitis C virus core region: helper T cell epitopes recognized by BALB/c and C57BL/6 mice," *Journal of General Virology*, vol. 76, no. 5, pp. 1205–1214, 1995.

[62] M. G. Shehat, M. Bahey-El-Din, M. A. Kassem, F. A. Farghaly, M. H. Abdul-Rahman, and N. H. Fanaki, "Recombinant expression of the alternate reading frame protein (ARFP) of hepatitis C virus genotype 4a (HCV-4a) and detection of ARFP and anti-ARFP antibodies in HCV-infected patients," *Archives of Virology*, vol. 160, no. 8, pp. 1939–1952, 2015.

[63] P. Skums, L. Bunimovich, and Y. Khudyakov, "Antigenic cooperation among intrahost HCV variants organized into a complex network of cross-immunoreactivity," *Proceedings of the National Academy of Sciences of the United States of America*, vol. 112, no. 21, pp. 6653–6658, 2015.

[64] A. V. Ivanov, O. A. Smirnova, I. Y. Petrushanko et al., "HCV core protein uses multiple mechanisms to induce oxidative stress in human hepatoma huh7 cells," *Viruses*, vol. 7, no. 6, pp. 2745–2770, 2015.

[65] R. I. Fisher and F. Bostick-Bruton, "Depressed T cell proliferative responses in Hodgkin's disease: role of monocyte-mediated suppression via prostaglandins and hydrogen peroxide," *Journal of Immunology*, vol. 129, no. 4, pp. 1770–1774, 1982.

[66] C. Nathan and A. Cunningham-Bussel, "Beyond oxidative stress: an immunologist's guide to reactive oxygen species," *Nature Reviews Immunology*, vol. 13, no. 5, pp. 349–361, 2013.

[67] Y. Yang, A. V. Bazhin, J. Werner, and S. Karakhanova, "Reactive oxygen species in the immune system," *International Reviews of Immunology*, vol. 32, no. 3, pp. 249–270, 2013.

[68] J. Cachat, C. Deffert, S. Hugues, and K. Krause, "Phagocyte NADPH oxidase and specific immunity," *Clinical Science*, vol. 128, no. 10, pp. 635–648, 2015.

[69] S. Reiche, C. Nestler, M. Sieg et al., "Hepatitis C virus (HCV)-specific memory B-cell responses in transiently and chronically infected HIV positive individuals," *Journal of Clinical Virology*, vol. 59, no. 4, pp. 218–222, 2014.

[70] S. Ward, G. Lauer, R. Isba, B. Walker, and P. Klenerman, "Cellular immune responses against hepatitis C virus: the evidence base 2002," *Clinical and Experimental Immunology*, vol. 128, no. 2, pp. 195–203, 2002.

[71] M. A. A. Claassen, H. L. A. Janssena, and A. Boonstra, "Role of T cell immunity in hepatitis C virus infections," *Current Opinion in Virology*, vol. 3, no. 4, pp. 461–467, 2013.

[72] M. Sillanpää, K. Melén, P. Porkka et al., "Hepatitis C virus core, NS3, NS4B and NS5A are the major immunogenic proteins in humoral immunity in chronic HCV infection," *Virology Journal*, vol. 6, article 84, 2009.

[73] L. Alvarez-Lajonchere, N. H. Shoukry, B. Grá et al., "Immunogenicity of CIGB-230, a therapeutic DNA vaccine preparation, in HCV-chronically infected individuals in a Phase i clinical trial," *Journal of Viral Hepatitis*, vol. 16, no. 3, pp. 156–167, 2009.

[74] M. Lechmann and T. J. Liang, "Vaccine development for hepatitis C," *Seminars in Liver Disease*, vol. 20, no. 2, pp. 211–226, 2000.

[75] W. Zhu, C. Wu, W. Deng et al., "Inhibition of the HCV core protein on the immune response to HBV surface antigen and on HBV gene expression and replication in vivo," *PLoS ONE*, vol. 7, no. 9, Article ID e45146, 2012.

Hindawi Publishing Corporation
Journal of Immunology Research
Volume 2015, Article ID 738020, 11 pages
http://dx.doi.org/10.1155/2015/738020

Research Article

EPIPOX: Immunoinformatic Characterization of the Shared T-Cell Epitome between Variola Virus and Related Pathogenic Orthopoxviruses

Magdalena Molero-Abraham,[1] John-Paul Glutting,[1] Darren R. Flower,[2] Esther M. Lafuente,[1] and Pedro A. Reche[1]

[1]*School of Medicine, Unit of Immunology, Complutense University of Madrid, Pza. Ramón y Cajal, s/n, 28040 Madrid, Spain*
[2]*School of Life and Health Sciences, University of Aston, Aston Triangle, Birmingham B4 7ET, UK*

Correspondence should be addressed to Pedro A. Reche; parecheg@med.ucm.es

Received 26 June 2015; Revised 8 September 2015; Accepted 1 October 2015

Academic Editor: Jacek Tabarkiewicz

Concerns that variola viruses might be used as bioweapons have renewed the interest in developing new and safer smallpox vaccines. Variola virus genomes are now widely available, allowing computational characterization of the entire T-cell epitome and the use of such information to develop safe and yet effective vaccines. To this end, we identified 124 proteins shared between various species of pathogenic orthopoxviruses including variola minor and major, monkeypox, cowpox, and vaccinia viruses, and we targeted them for T-cell epitope prediction. We recognized 8,106, and 8,483 unique class I and class II MHC-restricted T-cell epitopes that are shared by all mentioned orthopoxviruses. Subsequently, we developed an immunological resource, EPIPOX, upon the predicted T-cell epitome. EPIPOX is freely available online and it has been designed to facilitate reverse vaccinology. Thus, EPIPOX includes key epitope-focused protein annotations: time point expression, presence of leader and transmembrane signals, and known location on outer membrane structures of the infective viruses. These features can be used to select specific T-cell epitopes suitable for experimental validation restricted by single MHC alleles, as combinations thereof, or by MHC supertypes.

1. Introduction

Smallpox was a devastating contagious disease that ravaged humankind for millennia, wiping out entire civilizations [1]. The disease was caused by two types of variola virus (VARV), major and minor, which differed greatly in their average mortality rates: 30% versus 1%, respectively. VARV major was the most prevalent form [2, 3]. Systematic vaccination against smallpox began in the early 19th century but the disease lingered until the World Health Organization (WHO) initiated worldwide vaccination campaigns in 1967. The last case was reported in Somalia in 1977 and in May 1980 the WHO declared that smallpox had been eradicated, ceasing vaccination [1, 2]. Eradication was facilitated because there are no animal reservoirs for the virus, as it only infects humans [4].

VARV belongs to the *Orthopox* genus of the *Poxviridae* family, consisting of large double-stranded DNA viruses that replicate in the cytoplasm of infected cells [5, 6]. Poxviruses are large and complex with ~250 genes and a multistage life cycle, producing different infective forms including intracellular mature virions (IMV) and extracellular enveloped virus (EEV) [5, 6]. Humans can be infected by several poxviruses; the closest to VARV that are also pathogenic to humans are vaccinia (VACV), cowpox (CPXV), and monkeypox (MPXV) viruses [7, 8]. The primary reservoir of MPXV is rodents [9], while CPXV has the broadest animal reservoir range of all poxvirus, including cats, dogs, elephants, and rodents [10]. Historically, VAVC has been considered to emerge after repeated passages from an ancestral CPXV [11]. However, phylogenetic studies question that view and there are some speculations that VACV could be a horsepox virus (HPXV) [12]; yet both, the host and origin of VACV, remain unknown [13]. VACV and CPXV infections in humans are generally mild and self-limiting and can induce cross-protective

immunity [14]. The observation that CPXV sufferers did not get smallpox led Edward Jenner in 1798 to introduce a method of vaccination through scarifications with *Variolae Vaccinae*, Latin, for CPXV [15]. Immunization with CPXV was eventually displaced by VACV vaccine, which was used subsequently for global smallpox vaccination [12].

As smallpox was eradicated and vaccination ceased, the global population has become increasingly susceptible to both smallpox and zoonosis by orthopoxviruses [8, 9]. People under 30 have no immunity against these viruses and VACV-induced immunity is waning in those that were vaccinated [16]. Despite recommendations by the WHO, stockpiles of smallpox virus had never been destroyed and there are concerns that unregistered stocks could be used as a weapon of bioterrorism [17]. Several features make smallpox a major terrorist threat. It replicates easily, is aerosolizable, and is highly contagious before, during, and after disease onset. Moreover, smallpox is lethal and disfiguring and has already been used as a biological weapon in North America during the French and Indian Wars [18]. Thus, there is renewed interest in the development of vaccines against smallpox, particularly safer ones, since immunization with VACV can result in serious adverse events and it is considered risky in immunocompromised or immune-suppressed individuals [19].

Immune protection against orthopoxviruses requires both B and T cells [20] but the relevance of T cells is paramount. CD8 T cells are required to eliminate infected cells, while help by CD4 T cells is essential to elicit effective humoral responses [21]. Thus, people with dysfunctional humoral responses (e.g., agammaglobulinemia) can be vaccinated with VACV, while those with loss of T cells cannot as they can suffer severe disease [22]. T-cell immune responses are triggered by the recognition of foreign peptides bound to cell surface-expressed major histocompatibility complex (MHC) molecules, also known as human leukocyte antigens, HLA, in humans. CD4 T cells recognize peptides presented by MHC class II (MHC II) molecules while CD8 T cells recognize peptides presented by MHC class I (MHC I) molecules.

Advances in both immunology and genomic analysis offer new possibilities for eliciting immune protection without the requirement for live-virus vaccination and attendant complications. The identification of HLA class I and class II restricted T-cell epitopes (CD8 and CD4 T-cell epitopes, resp.) from poxviruses may allow us to develop safe and yet immunogenic peptide-based vaccines. Here, we describe the identification of protein antigens that are shared between several pathogenic orthopoxviruses, including VARV, MPXV, CPXV, and VACV, and T-cell epitopes that are identical in all selected proteins. This information was used to create a freely accessible web resource, EPIPOX: URL http://imed.med.ucm.es/epipox/, intended to facilitate the design of epitope-based vaccines against orthopoxviruses.

2. Materials and Methods

2.1. Orthopoxvirus Sequences and Experimentally Defined T-Cell Epitopes. In this study, we used the entire proteomes of 8 orthopoxviruses: VARV major, strain Bangladesh-1975, GenBank Accession: GB: L22579; VARV major, strain India-1967, GB: NC_00161; Variola major minor, strain Garcia-1966, GB: Y16780; Monkeypox virus, strain Zaire-96-I-16, GB: NC_003310; Cowpox virus strain, strain Brighton Red, GB: AF482758, Vaccinia virus, strain Copenhagen, GB: M35027; Vaccinia virus, strain Tian Tan, GB: AF095689; Vaccinia virus, strain Ankara, GB: U94848. The proteomes were obtained from the various translation features of the relevant GenBank genomic records using BIOPERL [23] (Table 1).

Table 1: Orthopoxviruses used in this study.

Virus	Strain	ACC	Genes
VARV major	Bangladesh-1975	L22579	189
VARV major	India-1967	NC_00161	197
VARV minor	Garcia-1966	Y16780	206
MPXV	Zaire-96-I-16	NC_003310	191
CPXV	Brighton Red	AF482758	218
VACV	Copenhagen	M35027	262
VACV	Tian Tan	AF095689	243
VACV	Ankara*	U94848	157

*Modified strain that has lost the ability to replicate; VARV: variola virus; MPXV: monkeypox virus; CPXV: cowpox virus; VACV: vaccinia virus.

We also used experimentally defined poxvirus-specific HLA I and HLA II-restricted T-cell epitopes that were retrieved from the IEDB [24] and EPIMHC [25] databases. We only considered unique T-cell epitope sequences with a size of 9 amino acids that were reported to be identified in humans infected with orthopoxviruses or who were vaccinated. We provide a list of experimentally defined T-cell epitopes as supplementary material in Additional File S1 in Supplementary Material available online at http://dx.doi.org/10.1155/2015/738020.

2.2. Protein Sequence Analyses and Annotations. We took VARV major, strain Bangladesh-1975, as the reference for subsequent sequence analyses. We identified proteins with leader signals using SIGNALP [26] and transmembrane regions using TMHMM [27]. We identified protein orthologs using BLAST [27]. Briefly, we first BLAST the reference proteins against formatted databases of each of the remaining orthopoxvirus proteomes. We performed BLAST searches with default settings and considered only the description of the first hit and the corresponding alignment. Subsequently, we selected those protein searches that gave hits in each of the proteomes with identities greater than 60% and identified the corresponding orthologs. We used BIOPERL to parse BLAST hits [23].

Information on the temporal expression of VACV genes was kindly provided by Dr. Lefkowitz from the Poxvirus Bioinformatics Resource Center [28]. The information consisted on annotations identifying those genes that are expressed early (E), intermediate (I), and late (L) during the life cycle of VACV. This information is provided as supplementary material in Additional File S2. In addition, we identified, from the data provided by Dr. Lefkowitz, gene products associated with the outer membranes of VACV IMV

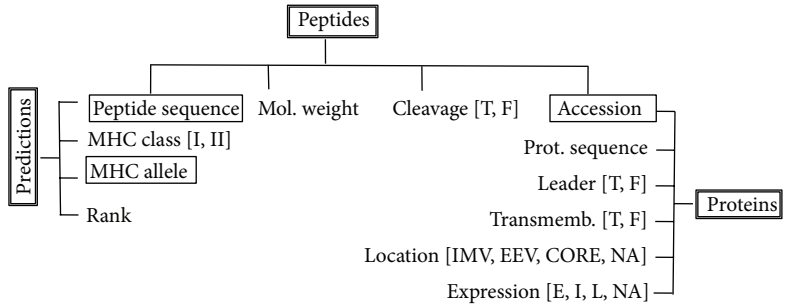

Figure 1: EPIPOX database structure. EPIPOX is a relational database consisting of three main tables: *peptides*, *predictions*, and *proteins*. Table names are boxed with double lines. For each table, we show their fields and boxed with single lines the fields that work as table keys. For fields taking discrete nominal values, we show them between square brackets.

and EEV infective forms, as well as those proteins that are part of the VACV virion or CORE. This information is also included as supplementary material in Additional File S2. Protein annotations obtained for VACV were transferred to protein orthologs.

2.3. Prediction of T-Cell Epitopes. We predicted MHC I and MHC II peptide binding to anticipate potential CD8 and CD4 T-cell epitopes, respectively. Specifically, we predicted peptide-MHC binding from VARV Bangladesh proteins that are shared between all selected orthopoxviruses using 32 HLA I- and 33 HLA II-allele specific position-specific scoring matrices (PSSMs) [29–31]. For a given protein, we considered the top 2% and 4% of scoring peptides to constitute HLA I- and HLA II-binding peptides, respectively. We only predicted binding for peptides of nine residues; most HLA I-restricted peptides are 9 residues in length and while HLA II-restricted peptides vary in length (9–22 amino acids) they have a core of 9 residues that anchor the peptide in the binding groove of HLA II molecules [30, 32]. We also used N-gram language models to identify whether peptides can be generated from the source antigen by proteasomal cleavage [33]. This information is only relevant to HLA I-binding peptides, since most peptides presented by MHC I are derived from antigens degraded by the proteasome [34].

2.4. Database Building and Web Server Implementation. Predicted T-cell epitopes and obtained protein annotations were incorporated into a POSTGRES relational database. The database consists of 3 tables (*peptides*, *predictions*, and *proteins*) that are linked through unique keys (Figure 1). Briefly, table *predictions* contains peptide sequences and their MHC restriction elements; table *peptides* includes the peptide molecular weight, its protein accession number, and whether the peptide is cleaved by the proteasome; and table *proteins* contains gene product information including temporal expression (E: early, I: intermediate, and L:late), location in the virus (IMV, EEV, and CORE), and the existence of leader and transmembrane regions. We also developed a web front end or GUI to allow ready access to EPIPOX. Behind the interface is a Python script that handles database queries through underlying SQL. The EPIPOX resource is implemented on an Apache Web server under the Mac OSX operating system.

3. Results and Discussion

3.1. Epitope-Vaccine Design against Orthopoxviruses. T-cell adaptive immunity is required for clearance of poxviruses during infection and/or vaccination and can also contribute to protective immunity from subsequent exposures [35, 36]. Moreover, peptides corresponding to VACV-specific CD8 T-cell epitopes can confer protection to mice subjected to lethal VACV challenges [37]. Fueled by the need to develop safer smallpox vaccines, such knowledge has led to the recent identification of many VACV-specific T-cell epitopes [37, 38]. These T-cell epitopes are deposited haphazardly in various specialized databases, including IEDB [24], EPIMHC [25], TEPIDAS [39], and AntiJen [40]. Of relevance for epitope-vaccine design, CD8 T-cells target primarily early and nonstructural gene products [41, 42]. CD4 T cells target late and the most abundant genes products (IMV and EEV membrane proteins and CORE proteins), as do antibodies [42, 43]. While some of the identified VAVC-specific T-cell epitopes are conserved in VARV a rational approach to identifying all potential T-cell epitopes eliciting cross-protective immunity is still required.

3.2. Shared Orthopoxvirus Proteins for Cross-Protective Immunity. Nearly all orthopoxviruses can protect against challenge with another orthopoxvirus [14]. This exquisite cross-protective immunity is likely a result of direct antigenic similarity between poxviruses. Therefore, prior to defining potential T-cell epitopes we identified shared antigens between pathogenic orthopoxviruses. Identification of shared antigens is also relevant to reducing the experimental burden associated with T-cell identification. Human pathogen orthopoxviruses have large genomes encompassing over 180 open reading frames (ORF) with the exception of VACV Ankara strain, which has only 157 genes and lacks the ability to replicate [44] (Table 1). Using VARV major, strain Bangladesh-1975, as a reference, we identified 124 ORFs that are shared between 8 different complete genomes from several orthopoxviruses, including VARV minor, CPXV, MPXV, and several VACV strains (Additional File S3). Despite the

Table 2: Orthopoxvirus proteins contributing to cross-protective immunity.

VACC: GI|ORF	VARV: GI|ORF	MPXV: GI|ORF	CPXV: GI|ORF	LOC[1]/EXP[2]/TM[3]/LD[4]
335424|L1R	438991|M1R	17974993|M1R	20153082|V099	IMV/late/yes/no
335455|D8L	439016|F8L	17975018|E8L	20153106|V119	IMV/late/yes/no
335500|A27L	439052|A31L	17975052|A29L	20153143|V156	IMV/late/no/no
335508|A33R	439057|A36R	17975058|A35R	20153149|V162	EEV/early/yes/no
335549|B5R	439084|B6R	17975080|B6R	20153177|V190	EEV/#/yes/yes
335438|H3L	439004|I3L	17975006|H3L	20153094|V107	IMV/late/yes/no
335477|A10L	439032|A11L	17975034|A11L	20153122|V135	CORE/#/no/no
335341|C7L	438926|D11L	17974926|D10L	20153015|V028	U/early/no/no

Table shows GenBank identification numbers (GI) and open reading frame names (ORF) for VACC (strain Copenhagen), VARV (strain Bangladesh-1975), MPXV (strain Zaire-96-I-16), and CPXV (strain Brighton Red). [1]LOC: location, [2]EXP: temporal expression, [3]TM: transmembrane, and [4]LD: leader signal. NS: nonstructural gene. #: information not available. U: unknown. List of proteins was obtained from [45]. Annotations 1, 2, 3, and 4 obtained as indicated elsewhere in Section 2.

criterion for selection being 60% identity, all 124 selected proteins have an average identity ≥ 85% as shown in Additional File S3. These proteins are prime candidates to induce cross-protective immunity although they need to be targeted by the immune system. Interestingly, within the selected proteins there are 8 known immunogens that conferred >60% protection to VACV in animal models (Table 2) [45]. Six of these immunogens are IMV or EEV proteins carrying transmembrane regions and/or are being late gene products. Interestingly, among the selected 124 proteins we found 26 additional proteins with transmembrane regions that could also be prime vaccine subunits candidates (Table 3). Some of these proteins also have leader signal sequences (Table 3). Viral proteins with leader sequences follow the cell secretory pathway and are thus also important targets to consider for vaccine design [46, 47].

3.3. T-Cell Epitome from Pathogenic Orthopoxvirus Proteins. We targeted the shared orthopoxvirus proteins for T-cell epitopes prediction using 32 and 33 HLA I- and HLA II-specific profile matrices (details in Material and Methods). The alleles targeted for peptide binding prediction are shown in Additional File S4. We selected these alleles because there are experimental peptide-binding data for them, which is required to make accurate peptide-MHC binding predictors [48]. Incidentally, these HLA alleles are frequently expressed in the general population and targeting them for epitope prediction permits the development of epitope-based vaccines covering the entire population. These HLA allelic variants can have overlapping peptide-binding repertoires and can be clustered accordingly in supertypes [49, 50]. Selecting promiscuous peptide-binders to multiple HLA molecules facilitates the development of vaccines with a minimum number of peptides [49–51].

We predicted a total of 18726 HLA I-restricted and 32722 HLA II-restricted orthopoxvirus specific T-cell epitopes, all being identical between all orthopoxviruses considered in this study. In Additional File S4 we provide numbers of T-cell epitopes predicted by each HLA-specific profile used in this study. We predicted more CD4 than CD8 T-cell epitopes because we used a more permissive peptide-binding threshold for MHC II molecules (4% of top scoring peptides) than for MHC I molecules (2% of top scoring peptides) since peptide-binding prediction to MHC II molecules is considerably less accurate than to MHC I molecules [46]. Interestingly, we identified only 8106 unique HLA I-restricted T-cell epitope sequences and a few more (8483) unique HLA II-restricted T-cell epitope sequences. Therefore, there is a considerable overlap between the peptide binding repertoires of HLA molecules, which is larger for HLA II molecules than for HLA I molecules. HLA I-restricted peptides bound on average to 2.3 distinct HLA I molecules, while HLA II-restricted peptides bound on average to 3.8 distinct HLA II molecules. This is due to the fact that peptide-binding to MHC II molecules is more degenerate than to MHC I molecules [29, 30]. In Additional File S5, we provide all distinct predicted peptides with the HLA molecules that they were predicted to bind. Interestingly, there is also some overlap between HLA I- and HLA II-restricted peptides. In particular, we find that there are 2452 peptides that are predicted to be restricted by both HLA I and HLA II molecules. Thus, in total the predicted T-cell epitome consisted of just 14137 unique sequences among all predicted T-cell epitopes.

We compared the predicted T-cell epitome with experimentally defined poxvirus-specific HLA-restricted T-cell epitopes deposited in the IEDB [24] and EPIMHC [25]. We retrieved 170 HLA I and 9 HLA II-restricted T-cell epitopes meeting our criteria (see Additional File S1) but we only considered for comparison 85 HLA I- and 8 HLA II-restricted T-cell epitopes that we identified here to be conserved in all orthopoxviruses considered in this study. Of those, 72 HLA I- and 6 HLA II-restricted T-cell epitopes were found within our predicted T-cell epitome. Moreover, we predicted the experimentally verified restriction element in > 80%. The experimentally determined and shared epitopes that were not predicted (a minority) either are restricted by noncovered alleles or were simply not predicted. In Table 4, we summarize the data showing the verified and predicted HLA restriction elements. In sum, we readily predicted most of the experimentally verified T-cell epitopes. Considering that on average 10% of predicted T-cell epitopes can be experimentally verified [52], we shall expect that there are many more valid T-cell epitopes remaining to be validated within the T-cell epitome predicted in this study.

Table 3: Shared orthopoxvirus proteins with transmembrane and/or leader sequences.

VARV GI|ORF	MPXV GI|ORF	CPXV GI|ORF	VACV GI|ORF	IDEN[1] (%)	TM[2]	LEAD[3]	EXP[4]	LOCATION[5]
GI:439084|B6R	GI:17975080|B6R	GI:20153177|V190	GI:335549|B5R	93.1	Yes	Yes	L	EEV membrane*
GI:439016|F8L	GI:17975018|E8L	GI:20153106|V119	GI:335455|D8L	94.7	Yes	No	L	IMV membrane*
GI:438990|H9R	GI:17974992|G10R	GI:20153081|V094	GI:335423|G9R	98.1	Yes	No	L	U
GI:438919|D4R	GI:17974919|D3R	GI:20153007|V020	GI:335333|C11R	88.8	Yes	Yes	U	U
GI:439085|B7R	GI:17975081|B7R	GI:20153178|V191	GI:335550|B6R	93.1	Yes	No	U	U
GI:439035|A14L	GI:17975037|A14L	GI:20153125|V138	GI:335483|A13L	88.6	Yes	No	L	IMV membrane
GI:438946|C8L	GI:17974949|C10L	GI:20153036|V049	GI:335366|F4L	97.6	Yes	No	E	U
GI:438977|K5L	GI:17974979|I5L	GI:20153068|V081	GI:335409|I5L	94.9	Yes	No	L	IMV membrane
GI:438967|E8R	GI:17974969|F7R	GI:20153058|V071	GI:335395|E8R	97.4	Yes	No	L	U
GI:439004|I3L	GI:17975006|H3L	GI:20153094|V107	GI:335438|H3L	95.8	Yes	No	L	IMV membrane*
GI:439014|F6R	GI:17975016|E6R	GI:20153104|V117	GI:335453|D6R	99.0	Yes	No	L	U
GI:439003|I2R	GI:17975005|H2R	GI:20153093|V106	GI:335437|H2R	99.2	Yes	No	L	U
GI:439056|A35L	GI:17975057|A34L	GI:20153148|V161	GI:335506|A32L	98.1	Yes	No	L	U
GI:439000|L5L	GI:17975002|L5L	GI:20153090|V103	GI:335433|J5L	98.1	Yes	No	L	U
GI:439058|A37R	GI:17975059|A36R	GI:20153150|V163	GI:335509|A34R	98.1	Yes	No	L	EEV membrane
GI:438991|M1R	GI:17974993|M1R	GI:20153082|V095	GI:335424|L1R	99.2	Yes	No	L	IMV membrane*
GI:439057|A36R	GI:17975058|A35R	GI:20153149|V162	GI:335508|A33R	93.0	Yes	No	E	EEV membrane*
GI:438951|C13L	GI:17974954|C15L	GI:20153041|V054	GI:335373|F9L	97.5	Yes	No	L	U
GI:439038|A17L	GI:17975040|A17L	GI:20153129|V142	GI:335486|A16L	97.0	Yes	No	L	U
GI:438974|K2L	GI:17974976|I2L	GI:20153065|V078	GI:335405|I2L	99.3	Yes	No	L	U
GI:439008|I7R	GI:17975010|H7R	GI:20153098|V111	GI:335442|H7R	95.2	Yes	No	L	U
GI:438982|H3L	GI:17974984|G2L	GI:20153073|V086	GI:335414|G3L	95.8	Yes	No	L	U
GI:439042|A22L	GI:17975044|A21L	GI:20153134|V147	GI:335490|A21L	96.9	Yes	No	U	U
GI:439059|A38R	GI:17975061|A38R	GI:20153152|V165	GI:335512|A36R	92.3	Yes	No	E, L	EEV membrane
GI:439031|A10L	GI:17975033|A10L	GI:20153121|V134	GI:335476|A9L	89.0	Yes	Yes	E, L	U
GI:439033|A12R	GI:17975035|A12R	GI:20153123|V136	GI:335481|A11R	98.5	Yes	No	L	U
GI:439036|A15L	GI:17975038|A15L	GI:20153126|V139	GI:335484|A14L	97.8	Yes	No	L	IMV membrane
GI:439067|A46R	GI:17975066|A43R	GI:20153159|V172	GI:335522|A43R	92.3	Yes	Yes	U	U
GI:439039|A18L	GI:17975041|A18L	GI:20153130|V143	GI:335487|A17L	98.0	Yes	No	L	IMV membrane
GI:439077|J7R	GI:17975076|B2R	GI:20153172|V185	GI:335539|A56R	82.1	Yes	Yes	E, L	EEV membrane
GI:439062|A41L	GI:17975063|A40L	GI:20153155|V168	GI:335516|A38L	94.7	Yes	Yes	U	U

Table shows GenBank identification numbers (GI) and open reading frame names (ORF) for VARV: strain Bangladesh-1975, MPXV: strain Zaire-96-I-16, CPXV: strain Brighton Red, and VACV: strain Copenhagen. [1]IDEN: average identity between the selected proteins. [2]TM: transmembrane. [3]LEAD: leader signal. [4]EXP: temporal expression (E: early, I: intermediate, and L: late). [5]LOCATION: location. *Proteins known to induce protective immunity (see Table 2). Annotations were obtained as indicated elsewhere in Section 2. U: information not found.

3.4. EPIPOX Database and Web Server. We developed a relational database based upon the predicted T-cell epitome and a web-based resource to facilitate online access and to query the database. We named this resource EPIPOX and made it available for free public use (URL: http://imed.med.ucm.es/epipox/). EPIPOX is a *de facto* analysis pipeline of viral T-cell epitomes. The content of the EPIPOX database is organized in three tables (*peptides*, *predictions*, and *proteins*) (Figure 1). The table *predictions* contains all predicted T-cell epitopes, consisting of 18726 HLA I- and 32722 HLA II-restricted peptides, each identified by its sequence and restriction element. Peptide sequences in this table are not unique as each peptide can bind to numerous HLA I molecules. Peptide sequences are, however, unique in the table *peptides*. This table contains 14137 sequences comprising the whole predicted epitome regardless of the restriction elements. Antigen annotations in EPIPOX are found within the table *proteins* (Figure 1). We only included annotations that are relevant to epitope vaccine design, such as temporal expression of gene products and location in relevant structures of the virus such as the EEV and IVM membranes and CORE. Early expressed proteins and highly expressed proteins are generally thought to be more immunogenic, particularly with regard to CD8 T cells [53, 54]. On the other hand, highly abundant late proteins that are located in membrane structures of the poxvirus appear to be the main focus of the antibody and CD4 T-cell response [42, 43]. In the table *proteins*, we also provide annotations on whether the proteins have transmembrane region or leader signal sequence, as proteins with these features often interact with host cells and are important targets for subunit vaccine design [46, 47].

The EPIPOX web interface (Figure 2) allows querying of the database combining any annotation field in the database,

Table 4: Experimentally identified T-cell epitopes within the shared T-cell epitome predicted from pathogenic orthopoxvirus proteins.

(a)

CD8 T-cell epitopes	VARV GI	VARV ORF	Experimental HLA I restriction	Predicted HLA I restriction					
ALMRRIAVV	439013	F5R	HLA-A2	HLA-A0201	HLA-A0202	HLA-A0203	HLA-A0205	HLA-A0206	HLA-A6802
YLLSLFSTL	439056	A35L	HLA-A2	HLA-A0201	HLA-A0202	HLA-A0203	HLA-A0205	HLA-A0206	HLA-A6802
YLAKLTALV	438985	H5R	HLA-A2	HLA-A0201	HLA-A0202	HLA-A0203	HLA-A0205	HLA-A0206	HLA-A6802
NLLCHIYSL	438979	K7L	HLA-A2	HLA-A0201	HLA-A0202	HLA-A0203	HLA-A0205	HLA-A0206	HLA-Cw0702
IVIEAIHTV	439072	J2R	HLA-A0201	HLA-A0201	HLA-A0202	HLA-A0203	HLA-A0205	HLA-A0206	HLA-Cw0304
SLSAYIIRV	439004	I3L	HLA-A0201	HLA-A0201	HLA-A0202	HLA-A0203	HLA-A0205	HLA-A0206	HLA-A0207
YLDGQLARL	438965	E6R	HLA-A0201	HLA-A0201	HLA-A0202	HLA-A0203	HLA-A0205	HLA-A0206	HLA-A0207
YLPEVISTI	438988	H7L	HLA-A0201	HLA-A0201	HLA-A0202	HLA-A0203	HLA-A0205	HLA-A0206	HLA-Cw0102
TYNDHIVNL	439072	J2R	HLA-A2301	HLA-A2301	HLA-A2402	HLA-A2403	HLA-A2405	HLA-A2407	HLA-Cw0702
RPPSFYKPL	439046	A25R	HLA-B7	HLA-B0702	HLA-B3501	HLA-B5101	HLA-B5301	HLA-B5401	HLA-Cw0102
ALDEKLFLI	439045	A24R	HLA-A0201	HLA-A0201	HLA-A0202	HLA-A0203	HLA-A0205	HLA-A0206	HLA-A0207
FPYEGGKVF	438968	E9L	HLA-B0702	HLA-B0702	HLA-B1502	HLA-B3501	HLA-B5101	HLA-B5301	HLA-B5401
RLYDYFTRV	438973	K1L	HLA-A0201, HLA-A2	HLA-A0201	HLA-A0202	HLA-A0203	HLA-A0205	HLA-A0206	
ILDDNLYKV	438985	H5R	HLA-A0201, HLA-A2	HLA-A0201	HLA-A0202	HLA-A0205	HLA-A0207	HLA-Cw0702	
LLSYYVVYV	439009	F1R	HLA-A2	HLA-A0201	HLA-A0202	HLA-A0203	HLA-A0205	HLA-A0206	
FLIDLAFLI	438960	E1L	HLA-A2	HLA-A0202	HLA-A0203	HLA-A0205	HLA-A0206	HLA-Cw0304	
FPRSMLSIF	438994	M4R	HLA-B07:02	HLA-B0702	HLA-B3501	HLA-B4402	HLA-B5301	HLA-B5401	
YLFDFVISL	438996	L1R	HLA-A2	HLA-A0201	HLA-A0202	HLA-A0203	HLA-A0205	HLA-A0206	
YLIKLIEPV	439009	F1R	HLA-A0201, HLA-A2	HLA-A0201	HLA-A0202	HLA-A0203	HLA-A0205	HLA-A0206	
SPSNHHILL	439025	A4L	HLA-B07:02	HLA-B0702	HLA-B3501	HLA-B5101	HLA-B5301	HLA-B5401	
YPSNKNYEI	439033	A12R	HLA-B07:02	HLA-B0702	HLA-B3501	HLA-B5101	HLA-B5301	HLA-B5401	
MLMETMFFI	439007	I6R	HLA-A2	HLA-A0201	HLA-A0202	HLA-A0203	HLA-A0205	HLA-A0206	
ILNPVASSL	438998	L3R	HLA-A2	HLA-A0201	HLA-A0202	HLA-A0205	HLA-A0206	HLA-B1501	
FPSVFINPI	438968	E9L	HLA-B0702	HLA-B0702	HLA-B3501	HLA-B5101	HLA-B5301	HLA-B5401	
KYQSPVNIF	439043	A21R	HLA-A24, HLA-class I	HLA-A2301	HLA-A2402	HLA-A2403	HLA-A2405	HLA-A2407	
YLFGGFSTL	438980	K8R	HLA-A2	HLA-A0201	HLA-A0202	HLA-A0203	HLA-A0205	HLA-A0206	
YLYETYHLI	438981	H1L	HLA-A2	HLA-A0201	HLA-A0202	HLA-A0205	HLA-A0206		
VLYNGVNYL	439009	F1R	HLA-A2	HLA-A0201	HLA-A0202	HLA-A0205	HLA-A0206		
LIQEIVHEV	439029	A8L	HLA-A0201	HLA-A0201	HLA-A0202	HLA-A0205	HLA-A0206		
VELGSGNSF	439043	A21R	HLA-B3701	HLA-B1501	HLA-B1502	HLA-B4402	HLA-Cw0304		
RMIAISAKV	438934	P1L	HLA-A2	HLA-A0201	HLA-A0202	HLA-A0203	HLA-A0206		
FILGIIITV	439036	A15L	HLA-A0201	HLA-A0202	HLA-A0203	HLA-A0205	HLA-A0206		
LLSKNTFYL	438981	H1L	HLA-A2	HLA-A0201	HLA-A0202	HLA-A0205	HLA-A0207		
RPRDAIRFL	438961	E2L	HLA-B0702	HLA-B0702	HLA-B3501	HLA-B5301	HLA-B5401		
KLFNKVPIV	438996	L1R	HLA-A2	HLA-A0201	HLA-A0202	HLA-A0206	HLA-A6802		
SLFMILCTR	438979	K7L	HLA-A0301, HLA-A1101	HLA-A1101	HLA-A3101	HLA-A3301	HLA-A6801		
ILNDEQLNL	439029	A8L	HLA-A0201	HLA-A0201	HLA-A0205	HLA-A0207			
YLLGDSDSV	439038	A17L	HLA-A2	HLA-A0201	HLA-A0205	HLA-A0206			
QLMYALEPR	438985	H5R	HLA-A0301, HLA-A1101	HLA-A3101	HLA-A3301	HLA-A6801			
LMDENTYAM	439066	A45R	HLA-A2	HLA-A0205	HLA-A0207	HLA-Cw0702			
GLLLGCFWV	438955	C17L	HLA-A2	HLA-A0202	HLA-A0203	HLA-A0206			
LLSHFYPAV	438952	C14L	HLA-A2	HLA-A0201	HLA-A0205	HLA-A6802			

(a) Continued.

CD8 T-cell epitopes	VARV GI	VARV ORF	Experimental HLA I restriction	Predicted HLA I restriction		
NLFTFLHEI	439045	A24R	HLA-class I	HLA-A0201	HLA-A0203	HLA-A0206
GLFDFVNFV	439070	A49R	HLA-A2, HLA-A0201	HLA-A0202	HLA-A0203	HLA-A0206
YLGPRVCWL	439038	A17L	HLA-A2	HLA-A0202	HLA-A0205	HLA-A0206
ILKSLGFKV	438980	K8R	HLA-A2	HLA-A0202	HLA-A0203	HLA-A0205
DEVASTHDW	439025	A4L	HLA-B4403	HLA-B4402	HLA-B5801	
FLVIAINAM	439029	A8L	HLA-A2, HLA-A0201	HLA-A0206	HLA-Cw0304	
LSDLKKTIY	439040	A19R	HLA-A1, HLA-class I	HLA-A0101	HLA-B1501	
LLYFKVFGI	439019	N1L	HLA-A2	HLA-A0202	HLA-A0205	
SSNIMSESY	439014	F6R	HLA-A0101, HLA-A3002	HLA-A0101	HLA-B1501	
DTRGIFSAY	439032	A11L	HLA-A26, HLA-class I	HLA-A0101	HLA-B5801	
QIDVEKKIV	439029	A8L	HLA-A0201	HLA-A0207	HLA-A6802	
YLFRCVDAV	439030	A9R	HLA-A2	HLA-A0205	HLA-A0206	
KIEDLINQL	438973	K1L	HLA-A0201	HLA-A0203	HLA-A0207	
FTIDFKLKY	439009	F1R	HLA-A1, HLA-A2601, HLA-A2902	HLA-A0101	HLA-Cw0702	
WLKIKRDYL	439074	J4R	HLA-B0801	HLA-B0801		
AINVEKIEL	473688	L6R	HLA-A0201	HLA-A0207		
RIFVRVYNV	439007	I6R	HLA-A2	HLA-A0202		
SIIDLIDEY	438942	C4R	HLA-B1501	HLA-A0203		
EERHIFLDY	439009	F1R	HLA-B4403	HLA-B4402		
ILSDENYLL	439028	A7L	HLA-A2, HLA-A0201	HLA-A0205		
HISALKRRY	439027	A6R	HLA-A0101, HLA-A2902	HLA-A0101		
FLNISWFYI	438968	E9L	HLA-A2, HLA-A02:01	HLA-A0205		
SEVKFKYVL	439002	I1L	HLA-B44	HLA-B4402		
KLLLWFNYL	438980	K8R	HLA-A2	HLA-A0203		
YIDISDVKV	438973	K1L	HLA-A0201	HLA-A0207		
VWINNSWKF	439013	F5R	HLA-A24, HLA-A2301, HLA-A2402	HLA-Cw0702		
VLPFDIKKL	439014	F6R	HLA-A0201	HLA-Cw0102		
VETSISDYY	439043	A21R	HLA-B3701	HLA-B1501		
SQIIDISLR	439022	A1L	HLA-A0301, HLA-A1101	HLA-B2705		
HDVYGVSNF	439045	A24R	HLA-B4403	HLA-B4402		

(b)

CD4 T-cell epitope	VARV GI	VARV ORF	Experimental HLA II restriction	Predicted HLA II restriction									
FLIDLAFLI	438960	E1L	HLA-class II	DRB1∗0101	DRB1∗0102	DRB1∗0301	DRB1∗0311	DRB1∗0401	DRB1∗1201	DRB1∗1302	DRB1∗1502	DRB3∗0101	DRB5∗0101
IHWQIISSE	439072	J2R	DRB1∗04:05	DRB1∗0405	DRB1∗0406	DRB1∗0410	DRB1∗1304	DRB3∗0101					
YIDAYVSRL	439021	N3L	DRB1∗15:01	DRB1∗0901	DRB1∗1103	DRB3∗0202							
LMDENTYAM	439066	A45R	HLA-class II	DRB1∗1103									
IDAYVSRLL	439021	N3L	DRB1∗15:01	DRB1∗1201									
RMIAISAKV	438934	P1L	HLA-class II	DRB1∗0407									

T-cell epitopes in this table are a subset of those provided in Additional File S1.

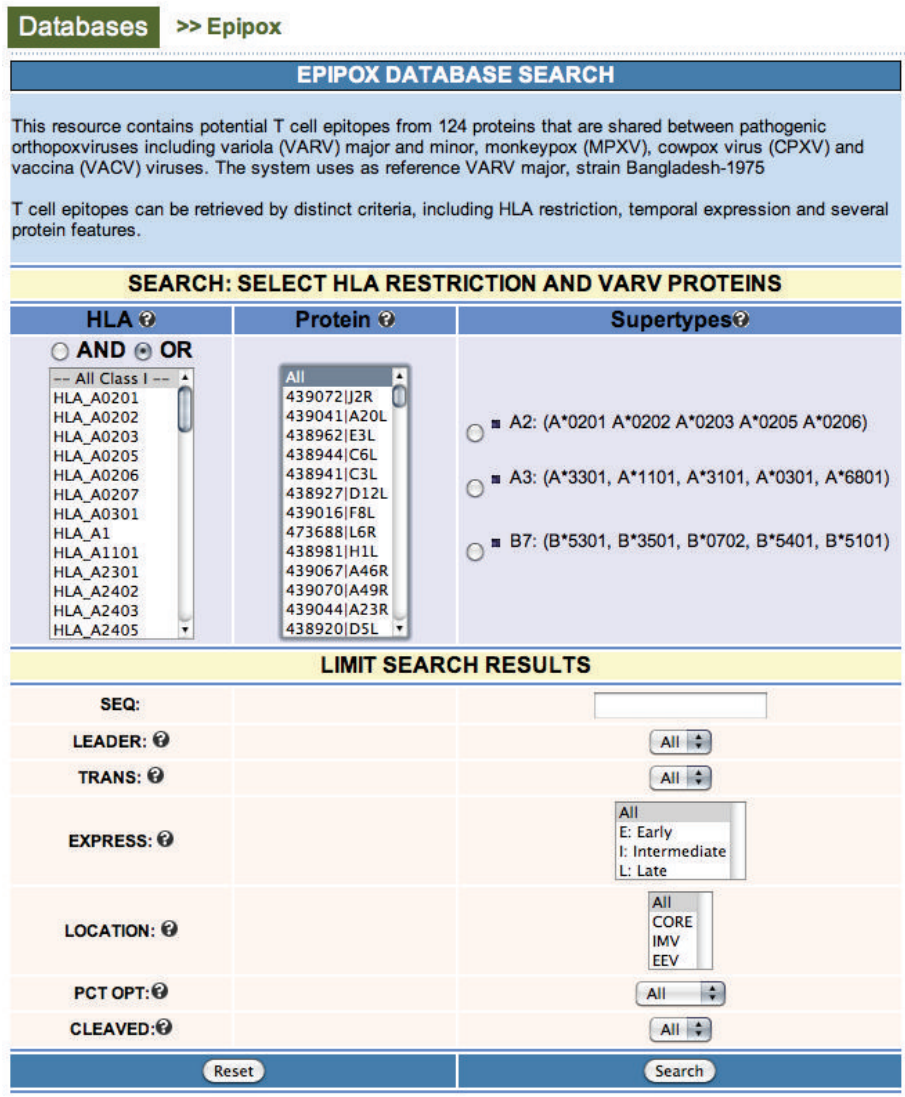

Figure 2: EPIPOX input page. The input page of EPIPOX is divided in two main sections for intuitive use. In the first part (SEARCH), users select HLA molecules and proteins to retrieve T-cell epitopes (multiple selection is allowed) while in the second part the user can limit the search output according to various criteria. These criteria include temporal expression of gene products (E: early; I: intermediate; L: late), location of proteins in relevant structures of the virus (CORE, IMV, and EEV), and the presence of leader and transmembrane regions. In addition, users can select only those peptides with a relative score above some selectable value. HLA-specific profiles used to score T-cell epitopes can reach a maximum score, which is used to set the relative score in percentage of each peptide. For HLA I-restricted epitopes, users can also restrict the search to those epitopes potentially generated by the proteasome.

as described above. For intuitive use, the interface is divided in two main sections. In the first section (SEARCH), users select proteins and restriction elements for epitope retrieval. In this section, EPIPOX also provides the option to query the database for promiscuous T-cell epitopes binding to three HLA I supertypes (A2, A3, and B7). The alleles belonging to these supertypes are present in 88% of the population regardless of their ethnic groups. Selecting promiscuous peptides restricted by these 3 supertypes facilitates maximizing the population coverage of vaccines with minimum numbers of peptides [49, 50, 55]. In the second section (LIMIT), users can select annotation criteria to restrict the results. As an example, in Figure 3, we show the page resulting from a sample query consisting of promiscuous peptides from CORE binding to the A2 supertype. From the EPIPOX output, users can also access additional information available from the Virus Pathogen Resource database (Figure 3) [56].

EPIPOX is related somewhat to certain existing databases. On the one hand, it shares features with generic epitope databases such as EPIMHC [25], AntiJen [40], and IEDB [24] and on the other hand it shares features with poxvirus genome annotation-orientated databases such as the *Poxviridae* database [28] (no longer operating) and the Virus Pathogen Resource (http://www.viprbrc.org/) [56].

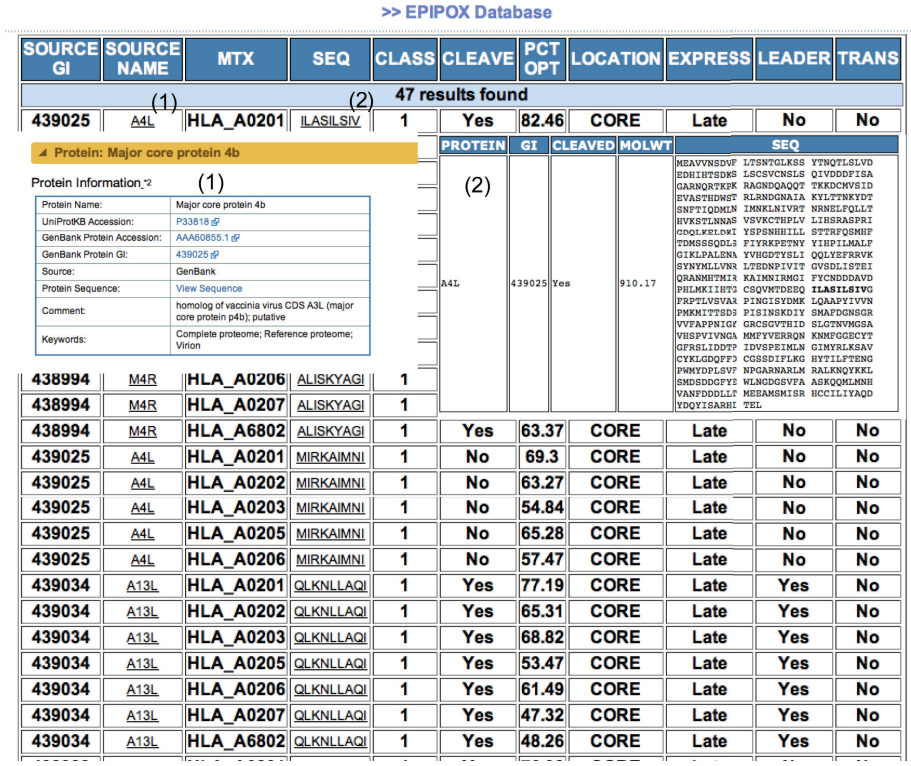

Figure 3: EPIPOX result page. The figure shows a slice of the output resulting from promiscuous CORE protein peptides binding to the A2 supertype. The output consists of a tabulated list, with information on each of the fields of the search query (columns). From field *SOURCE NAME* (1), users can access proteins from the Virus Pathogen Database (http://www.viprbrc.org/) (1) and by clicking on the epitope sequence, field *SEQ* (2), users will get the amino acid sequence of the protein showing the peptide in bold (2).

This later resource contains information on virus sequences, functional annotations and epitopes derived from IEDB [24]. However, the Virus Pathogen Resource does not allow selection of epitopes or antigens by criteria that are relevant to epitope vaccine design. In fact, EPIPOX is the only dedicated immunologic resource that has been designed to facilitate the rational selection of epitopes and antigens for subunit vaccine design.

4. Conclusions and Future Development

The availability of the VARV genomes enables the use of predictive tools that reveal entire T-cell epitomes and facilitate the development of epitope-based vaccines. However, in large and complex viruses, such as VARV, the potential T-cell epitome can be so sizeable that it will challenge experimental validation. Therefore, in this work we applied a rational strategy to limit the list of potential T-cell epitopes. First, we reduced the number of antigens by half by simply selecting those that are conserved among pathogenic orthopoxviruses related to VARV. Second, we enriched the antigens with annotations such as temporal expression and location. Lastly, we created a resource and *de facto* analysis pipeline (EPIPOX) with which to interrogate the resulting T-cell epitome and enable users to select immunologically relevant subsets of T-cell epitopes suitable for experimental validation.

We expect that this work and EPIPOX will be instrumental in developing safer smallpox vaccines and thereby in preventing zoonosis caused by other orthopoxviruses, including MPXV, which is also a potential terrorist bioweapon. In the future, we plan to enhance EPIPOX with validated and/or experimentally determined epitopes, upgrade protein annotations with functional information, and include additional features such as TAP transport [57], ERAAP cleavage [58], and T-cell epitope immunodominance. In sum, we would expect EPIPOX to establish itself as a facilitating resource of true utility in *inter alia* immunoinformatic characterization of viral genomics and computational reverse vaccinology.

Conflict of Interests

The authors declare that they have no conflict of interests.

Acknowledgments

The authors want to specially thank Dr. Ellis L Reinherz for his continuous support, inspiration, and future collaborative work. The authors also wish to thank *Immunotek, SL*, for financial support of MMA, and the Spanish Department of Science at MINECO for supporting the group's research through Grants SAF2006:07879, SAF2009:08301, and BIO2014:54164-R to Pedro A. Reche. Finally, The authors

wish to acknowledge Hong Zhang for programming assistance.

References

[1] D. R. Hopkins, *The Greatest Killer: Smallpox in History, with a New Introduction*, University of Chicago Press, Chicago, Ill, USA, 2002.

[2] F. Fenner, R. Wittek, and K. Dumbell, *The Orthopoxviruses*, Academic Press, San Diego, Calif, USA, 1998.

[3] R. M. L. Buller and G. J. Palumbo, "Poxvirus pathogenesis," *Microbiological Reviews*, vol. 55, no. 1, pp. 80–122, 1991.

[4] D. Baxby, "Poxvirus hosts and reservoirs. Brief review," *Archives of Virology*, vol. 55, no. 3, pp. 169–179, 1977.

[5] B. Moss, "Poxviridae. The virus and their replication," in *Fields Virology*, B. N. Fields, D. M. Knipe, and P. M. Howley, Eds., pp. 2849–2883, Lippincott-Raven Publishers, Hagerstown, Md, USA, 2001.

[6] K. L. Roberts and G. L. Smith, "Vaccinia virus morphogenesis and dissemination," *Trends in Microbiology*, vol. 16, no. 10, pp. 472–479, 2008.

[7] I. V. Babkin and I. N. Babkina, "The origin of the variola virus," *Viruses*, vol. 7, no. 3, pp. 1100–1112, 2015.

[8] S. N. Shchelkunov, S. S. Marennikova, and R. W. Moyer, *Orthopoxviruses Pathogenic for Humans*, Springer, Berlin, Germany, 2005.

[9] S. Parker, A. Nuara, R. M. L. Buller, and D. A. Schultz, "Human monkeypox: an emerging zoonotic disease," *Future Microbiology*, vol. 2, no. 1, pp. 17–34, 2007.

[10] G. McFadden, "Poxvirus tropism," *Nature Reviews Microbiology*, vol. 3, no. 3, pp. 201–213, 2005.

[11] D. A. Henderson and B. Moss, "Smallpox and vaccinia," in *Vaccines*, S. A. Plotkin and W. A. Orenstein, Eds., W.B. Saunders Company, Philadelphia, Pa, USA, 1999.

[12] L. Sánchez-Sampedro, B. Perdiguero, E. Mejías-Pérez, J. García-Arriaza, M. Di Pilato, and M. Esteban, "The evolution of poxvirus vaccines," *Viruses*, vol. 7, no. 4, pp. 1726–1803, 2015.

[13] E. R. Tulman, G. Delhon, C. L. Afonso et al., "Genome of horsepox virus," *Journal of Virology*, vol. 80, no. 18, pp. 9244–9258, 2006.

[14] B. L. Jacobs, J. O. Langland, K. V. Kibler et al., "Vaccinia virus vaccines: past, present and future," *Antiviral Research*, vol. 84, no. 1, pp. 1–13, 2009.

[15] E. Jenner, *An Inquiry into the Causes and Effects of the Variolae Vaccinae: A Disease Discovered in Some of the Western Counties of England, Particularly Gloucestershire, and Known by the Name of the Cow Pox*, Sampson Low, London, UK, 1798.

[16] H. Nishiura and M. Eichner, "Estimation of the duration of vaccine-induced residual protection against severe and fatal smallpox based on secondary vaccination failure," *Infection*, vol. 34, no. 5, pp. 241–246, 2006.

[17] D. A. Henderson, T. V. Inglesby, J. G. Bartlett et al., "Smallpox as a biological weapon: medical and public health management. Working Group on Civilian Biodefense," *The Journal of the American Medical Association*, vol. 281, no. 22, pp. 2127–2137, 1999.

[18] E. A. Fenn, "Biological warfare in eighteenth-century North America: beyond Jeffery Amherst," *Journal of American History*, vol. 86, no. 4, pp. 1552–1580, 2000.

[19] D. M. Maurer, B. Harrington, and J. M. Lane, "Smallpox vaccine: contraindications, administration, and adverse reactions," *American Family Physician*, vol. 68, no. 5, pp. 889–896, 2003.

[20] R. B. Kennedy, I. G. Ovsyannikova, R. M. Jacobson, and G. A. Poland, "The immunology of smallpox vaccines," *Current Opinion in Immunology*, vol. 21, no. 3, pp. 314–320, 2009.

[21] G. Chaudhri, V. Tahiliani, P. Eldi, and G. Karupiah, "Vaccine-induced protection against orthopoxvirus infection is mediated through the combined functions of CD4 T cell-dependent antibody and CD8 T cell responses," *Journal of Virology*, vol. 89, no. 3, pp. 1889–1899, 2015.

[22] M. Bray and M. E. Wright, "Progressive vaccinia," *Clinical Infectious Diseases*, vol. 36, no. 6, pp. 766–774, 2003.

[23] J. E. Stajich, D. Block, K. Boulez et al., "The Bioperl toolkit: perl modules for the life sciences," *Genome Research*, vol. 12, no. 10, pp. 1611–1618, 2002.

[24] R. Vita, J. A. Overton, J. A. Greenbaum et al., "The immune epitope database (IEDB) 3.0," *Nucleic Acids Research*, vol. 43, no. 1, pp. D405–D412, 2015.

[25] P. A. Reche, H. Zhang, J.-P. Glutting, and E. L. Reinherz, "EPIMHC: a curated database of MHC-binding peptides for customized computational vaccinology," *Bioinformatics*, vol. 21, no. 9, pp. 2140–2141, 2005.

[26] J. D. Bendtsen, H. Nielsen, G. von Heijne, and S. Brunak, "Improved prediction of signal peptides: SignalP 3.0," *Journal of Molecular Biology*, vol. 340, no. 4, pp. 783–795, 2004.

[27] E. L. Sonnhammer, G. von Heijne, and A. Krogh, "A hidden Markov model for predicting transmembrane helices in protein sequences," in *Proceedings of the International Conference on Intelligent Systems for Molecular Biology (ISMB '98)*, vol. 6, pp. 175–182, Montreal, Canada, June-July 1998.

[28] E. J. Lefkowitz, C. Upton, S. S. Changayil, C. Buck, P. Traktman, and R. M. L. Buller, "Poxvirus Bioinformatics Resource Center: a comprehensive Poxviridae informational and analytical resource," *Nucleic Acids Research*, vol. 33, pp. D311–D316, 2005.

[29] P. A. Reche, J.-P. Glutting, and E. L. Reinherz, "Prediction of MHC class I binding peptides using profile motifs," *Human Immunology*, vol. 63, no. 9, pp. 701–709, 2002.

[30] P. A. Reche, J.-P. Glutting, H. Zhang, and E. L. Reinherz, "Enhancement to the RANKPEP resource for the prediction of peptide binding to MHC molecules using profiles," *Immunogenetics*, vol. 56, no. 6, pp. 405–419, 2004.

[31] P. A. Reche and E. L. Reinherz, "Prediction of peptide-MHC binding using profiles," *Methods in Molecular Biology*, vol. 409, pp. 185–200, 2007.

[32] P. A. Reche and E. L. Reinherz, "Sequence variability analysis of human class I and class II MHC molecules: functional and structural correlates of amino acid polymorphisms," *Journal of Molecular Biology*, vol. 331, no. 3, pp. 623–641, 2003.

[33] C. M. Diez-Rivero, E. M. Lafuente, and P. A. Reche, "Computational analysis and modeling of cleavage by the immunoproteasome and the constitutive proteasome," *BMC Bioinformatics*, vol. 11, article 479, 2010.

[34] J. S. Blum, P. A. Wearsch, and P. Cresswell, "Pathways of antigen processing," *Annual Review of Immunology*, vol. 31, no. 1, pp. 443–473, 2013.

[35] W. E. Demkowicz Jr., R. A. Littaua, J. Wang, and F. A. Ennis, "Human cytotoxic T-cell memory: long-lived responses to vaccinia virus," *Journal of Virology*, vol. 70, no. 4, pp. 2627–2631, 1996.

[36] B. Moss, "Smallpox vaccines: targets of protective immunity," *Immunological Reviews*, vol. 239, no. 1, pp. 8–26, 2011.

[37] M. Moutaftsi, S. Salek-Ardakani, M. Croft et al., "Correlates of protection efficacy induced by vaccinia virus-specific $CD8^+$ T-cell epitopes in the murine intranasal challenge model," *European Journal of Immunology*, vol. 39, no. 3, pp. 717–722, 2009.

[38] W. Kastenmuller, I. Drexler, H. Ludwig et al., "Infection of human dendritic cells with recombinant vaccinia virus MVA reveals general persistence of viral early transcription but distinct maturation-dependent cytopathogenicity," *Virology*, vol. 350, no. 2, pp. 276–288, 2006.

[39] C. M. Diez-Rivero, M. Garcia-Boronat, and P. A. Reche, "Integrating T-cell epitope annotations with sequence and structural information using DAS," *Bioinformation*, vol. 3, no. 4, pp. 156–158, 2008.

[40] C. P. Toseland, D. J. Clayton, H. McSparron et al., "AntiJen: a quantitative immunology database integrating functional, thermodynamic, kinetic, biophysical, and cellular data," *Immunome Research*, vol. 1, no. 1, article 4, 2005.

[41] C. Oseroff, F. Kos, H.-H. Bui et al., "HLA class I-restricted responses to vaccinia recognize a broad array of proteins mainly involved in virulence and viral gene regulation," *Proceedings of the National Academy of Sciences of the United States of America*, vol. 102, no. 39, pp. 13980–13985, 2005.

[42] C. L. Smith, F. Mirza, V. Pasquetto et al., "Immunodominance of poxviral-specific CTL in a human trial of recombinant-modified vaccinia Ankara," *The Journal of Immunology*, vol. 175, no. 12, pp. 8431–8437, 2005.

[43] L. Jing, D. H. Davies, T. M. Chong et al., "An extremely diverse CD4 response to vaccinia virus in humans is revealed by proteome-wide T-cell profiling," *Journal of Virology*, vol. 82, no. 14, pp. 7120–7134, 2008.

[44] H. Meyer, G. Sutter, and A. Mayr, "Mapping of deletions in the genome of the highly attenuated vaccinia virus MVA and their influence on virulence," *Journal of General Virology*, vol. 72, no. 5, pp. 1031–1038, 1991.

[45] J. W. Golden and J. W. Hooper, "The strategic use of novel smallpox vaccines in the post-eradication world," *Expert Review of Vaccines*, vol. 10, no. 7, pp. 1021–1035, 2011.

[46] M. Kim, H. Yang, S.-K. Kim et al., "Biochemical and functional analysis of smallpox growth factor (SPGF) and anti-SPGF monoclonal antibodies," *The Journal of Biological Chemistry*, vol. 279, no. 24, pp. 25838–25848, 2004.

[47] H. Yang, S.-K. Kim, M. Kim et al., "Antiviral chemotherapy facilitates control of poxvirus infections through inhibition of cellular signal transduction," *Journal of Clinical Investigation*, vol. 115, no. 2, pp. 379–387, 2005.

[48] E. M. Lafuente and P. A. Reche, "Prediction of MHC-peptide binding: a systematic and comprehensive overview," *Current Pharmaceutical Design*, vol. 15, no. 28, pp. 3209–3220, 2009.

[49] P. A. Reche and E. L. Reinherz, "PEPVAC: a web server for multi-epitope vaccine development based on the prediction of supertypic MHC ligands," *Nucleic Acids Research*, vol. 33, no. 2, pp. W138–W142, 2005.

[50] A. Sette and J. Sidney, "HLA supertypes and supermotifs: a functional perspective on HLA polymorphism," *Current Opinion in Immunology*, vol. 10, no. 4, pp. 478–482, 1998.

[51] M. Molero-Abraham, E. M. Lafuente, D. R. Flower, and P. A. Reche, "Selection of conserved epitopes from hepatitis c virus for pan-populational stimulation of T-cell responses," *Clinical and Developmental Immunology*, vol. 2013, Article ID 601943, 10 pages, 2013.

[52] W. Zhong, P. A. Reche, C.-C. Lai, B. Reinhold, and E. L. Reinherz, "Genome-wide characterization of a viral cytotoxic T lymphocyte epitope repertoire," *Journal of Biological Chemistry*, vol. 278, no. 46, pp. 45135–45144, 2003.

[53] W. Kastenmuller, G. Gasteiger, J. H. Gronau et al., "Cross-competition of $CD8^+$ T cells shapes the immunodominance hierarchy during boost vaccination," *Journal of Experimental Medicine*, vol. 204, no. 9, pp. 2187–2198, 2007.

[54] C. M. Diez-Rivero and P. A. Reche, "CD8 T cell epitope distribution in viruses reveals patterns of protein biosynthesis," *PLoS ONE*, vol. 7, no. 8, Article ID e43674, 2012.

[55] P. A. Reche and E. L. Reinherz, "Definition of MHC supertypes through clustering of MHC peptide-binding repertoires," *Methods in Molecular Biology*, vol. 409, pp. 163–173, 2007.

[56] B. E. Pickett, E. L. Sadat, Y. Zhang et al., "ViPR: an open bioinformatics database and analysis resource for virology research," *Nucleic Acids Research*, vol. 40, no. 1, pp. D593–D598, 2012.

[57] C. M. Diez-Rivero, B. Chenlo, P. Zuluaga, and P. A. Reche, "Quantitative modeling of peptide binding to TAP using support vector machine," *Proteins: Structure, Function, and Bioinformatics*, vol. 78, no. 1, pp. 63–72, 2010.

[58] L. Saveanu, O. Carroll, V. Lindo et al., "Concerted peptide trimming by human ERAP1 and ERAP2 aminopeptidase complexes in the endoplasmic reticulum," *Nature Immunology*, vol. 6, no. 7, pp. 689–697, 2005.

Hindawi Publishing Corporation
Journal of Immunology Research
Volume 2015, Article ID 541282, 8 pages
http://dx.doi.org/10.1155/2015/541282

Research Article

Applying the Concept of Peptide Uniqueness to Anti-Polio Vaccination

Darja Kanduc,[1] Candida Fasano,[1] Giovanni Capone,[1] Antonella Pesce Delfino,[2] Michele Calabrò,[2] and Lorenzo Polimeno[2]

[1]*Department of Biosciences, Biotechnologies, and Biopharmaceutics, University of Bari, 70126 Bari, Italy*
[2]*Department of Emergency and Organ Transplantation (DETO), University of Bari, 70124 Bari, Italy*

Correspondence should be addressed to Darja Kanduc; d.kanduc@biologia.uniba.it

Received 5 February 2015; Accepted 28 April 2015

Academic Editor: Yoshihiko Hoshino

Background. Although rare, adverse events may associate with anti-poliovirus vaccination thus possibly hampering global polio eradication worldwide. *Objective*. To design peptide-based anti-polio vaccines exempt from potential cross-reactivity risks and possibly able to reduce rare potential adverse events such as the postvaccine paralytic poliomyelitis due to the tendency of the poliovirus genome to mutate. *Methods*. Proteins from poliovirus type 1, strain Mahoney, were analyzed for amino acid sequence identity to the human proteome at the pentapeptide level, searching for sequences that (1) have zero percent of identity to human proteins, (2) are potentially endowed with an immunologic potential, and (3) are highly conserved among poliovirus strains. *Results*. Sequence analyses produced a set of consensus epitopic peptides potentially able to generate specific anti-polio immune responses exempt from cross-reactivity with the human host. *Conclusion*. Peptide sequences unique to poliovirus proteins and conserved among polio strains might help formulate a specific and universal anti-polio vaccine able to react with multiple viral strains and exempt from the burden of possible cross-reactions with human proteins. As an additional advantage, using a peptide-based vaccine instead of current anti-polio DNA vaccines would eliminate the rare post-polio poliomyelitis cases and other disabling symptoms that may appear following vaccination.

1. Introduction

Vaccine-associated paralytic poliomyelitis (VAPP) [1] is the consequence of the replication of vaccine-derived polioviruses (VDPVs) that originate by genetic mutations from the strain contained in the oral polio vaccine (OPV). In fact, the poliovirus (PV) genetic mutability [2] appears to be the molecular basis of VAPP, which throws a shadow over the great success represented by vaccination in fighting PV infection [3, 4].

Currently, two new monovalent OPVs [5] and the change of the schedule from OPV to the exclusive use of inactivated polio vaccine (IPV) [6] represent options to interrupt PV transmission. However, it has been observed that reduction of exposure to a live attenuated virus such as that contained in OPV will inevitably lead to a decrease in herd immunity to a live microorganism and to natural boosters [7]. Such considerations, along with recent PV infection outbreaks, further complicate the issue of polio eradication [8].

In this scenario, new vaccine formulations and renewed research efforts might help to specifically fight PV infection. Recently, we analyzed the peptide overlap between PV1, strain Mahoney, and the human proteome and described a high extent of peptide sharing involving human proteins linked to fundamental cellular functions [9]. These data appeared to be of interest also because PV has been studied mainly at the nucleotide level [10], and, in general, there is a lack of knowledge of the interaction(s) between PV and the human host at the peptide/protein level. Actually, phenetic analyses of PV might help define peptide-based therapeutic approaches against PV infection, given that, for example,

(i) one single amino acid (aa) change, that is, His to Tyr at aa position 142 of virion protein 2 (VP2) or Val to

Ile at aa position 160 of virion protein 1 (VP1), on the capsid surface of PV1 Sabin allows the establishment of persistent infections in HEp-2c cell cultures [11];

(ii) replacement of the Ala residue with Asp at aa position 3 is linked to 50% loss of virion protein 4 (VP4) precursor myristoylation and severe reduction in specific infectivity [12];

(iii) the 25th aa, Ile, of PV 2C protein interacts with human reticulon 3, a protein involved in viral replication and/or pathogenesis [13].

Moreover, since the 1980s we have known that small aa groupings can play a critical role in neutralizing PV. For example, the discontinuous E^4T^7T/S^8R^9 tetrapeptide, which is present in PV VP1, is crucial for neutralizing PV3 by anti-PV3 25-1-14 monoclonal antibody (mAb) [14]. Additional examples of short immune determinants in the immune response against PV are the following ones:

(i) A linear heptapeptide (DNNQTSP) is an Ab-binding site mapped to aa residues 164–170 of VP2 [15].

(ii) Short synthetic peptides (e.g., DNTVRET, RSRSES, RSRSESSIESF, and STTNKDK) from PV VP1 prime the immune system of rabbits for a long-lasting, virus-neutralizing IgG Ab response following a single inoculation of intact virus [16].

(iii) The Immune Epitope Database (IEDB; http://www.immuneepitope.org) [17] includes the continuous linear pentapeptide STTNK (IEDB ID: 61944) [18, 19] and the discontinuous pentapeptide $T^{141}E^{143}S^{312}E^{315}P^{417}$ (IEDB ID: 91064) [20] as PV-derived epitopes.

Following the mathematical quantification of pentapeptide sharing between PV1 and human proteins, we reported that 2,040 out of the 2,204 pentamers composing the PV1 proteome are shared with the human proteome for a total of 18,223 matches, including multiple occurrences [9]. In general, a vast peptide sharing with human proteins is a characteristic of viral proteomes [21]. This peptide commonality suggests the existence of common evolutionary links between entities widely different as viruses and *Homo sapiens* and, in addition, indicates that potential cross-reactivity may affect antivirus vaccine formulations [22] and serological analyses [23]. Hence, it is reasonable to postulate that vaccines based on peptides unique to a virus and absent in the host proteome would guarantee high specificity and, at the same time, eliminate potential cross-reactivity.

Pursuing the objectives of overcoming the difficulties posed by the PV tendency to mutate and eliminating the viral reactivation-related VAPP in order to contribute to the global eradication of poliomyelitis, here we examine PV1 Mahoney polyprotein primary sequence and describe a set of pentapeptides uniquely owned by PV1, endowed with immunologic potential, and conserved among 43 PV strains. We propose that this set of pentapeptides might be used in preclinical and *in vivo* protocols with the ultimate aim of formulating effective, safe, and universal anti-PV vaccines.

2. Methods

The primary aa sequence of human PV1 polyproteins, strain Mahoney (NCBI taxonomic identifier: 12081; Swiss-Prot/UniProtKB entry: P03300), consisting of 11 viral proteins, 2,209 aa long [25] (further details at http://www.uniprot.org/uniprot/P03300), was analyzed for aa sequence similarity to the human proteome at the pentapeptide level. In brief, the viral polyprotein was dissected into 5-mers sequentially overlapped by four residues: MGAQV, GAQVS, AQVSS, QVSSQ, VSSQK, and so forth; then, each viral pentapeptide was used as a probe to scan the human proteome for instances of the same pentapeptide, as already described [9]. The similarity analysis used the Protein Information Resource (PIR) peptide match program (http://pir.georgetown.edu/) [26].

PV-derived epitopes were retrieved from the Immune Epitope Database (IEDB; http://www.immuneepitope.org) [17]. Only PV epitopes that had been experimentally validated in the human host were considered in this study.

Consensus peptide sequences were defined by ClustalW multialignment analysis (http://www.uniprot.org/program/?query=clustalw&sort=score) [24] of sequences from 43 PV strains retrieved from UniProt database (http://www.uniprot.org/) on the basis of the following characteristics: (1) described in scientific literature; (2) corresponding to the entire PV polyprotein; (3) derived from PV1 and PV3; (4) derived from PV variants isolated from VAPP or acute flaccid paralysis (AFP) patients or from immunocompromised patients with residual paralysis. Description and references of the 43 PV sequences used for multialignment analysis are reported in detail at http://www.uniprot.org/; the relative Swiss-Prot/UniProtKB entries are P03300, P03301, P03302, P06209, Q9Q281, Q9Q280, Q71AZ9, Q5TLH5, D1YSI9, D1YSJ1, D1YSJ2, D1YSJ3, D1YSJ4, D1YSJ5, D1YSJ6, D1YSJ7, D1YSJ9, D1YSK1, D1YSK2, D1YSK3, D1YSK4, D1YSK5, D1YSK6, D1YSK7, D1YSK8, D1YSK9, D1YSL0, D1YSL1, D1YSL2, D1YSL3, D1YSL4, D1YSL5, D2X673, D8L541, B4YUL3, B4YUL4, Q84792, C5HJY2, C5HJY3, D1GE40, D2E679, D1GE41, and D2XUS9.

3. Results and Discussion

3.1. Identification of Pentapeptides Unique to PV Type 1, Strain Mahoney. Using the procedure described under Section 2, we searched the human PV1, strain Mahoney, primary sequence for pentapeptides not shared with human proteins. We used pentapeptides as probes since a pentapeptide is a minimal functional unit in immunology [27], thus representing an appropriate length unit in measuring the qualitative/quantitative parameters of immunological phenomena [28].

Table 1 reports the pentapeptide platform that characterizes PV1 Mahoney polyprotein when compared to the *Homo sapiens* proteome. We find that 164 pentapeptides are unique to the viral polyprotein and absent in human proteins. In a few instances, viral 5-mers consecutively overlap (Table 1, pentapeptides in bold), thus forming 6-, 7-, and 8-mer stretches (e.g., $PV_{163–169}$QNMYYHY, $PV_{446–453}$NYYTHWAG,

Table 1: Pentapeptides unique to PV type 1, strain Mahoney, and absent in the human proteome.

Pos[a]	Sequence[b,c]	Pos[a]	Sequence[b,c]	Pos[a]	Sequence[b,c]	Pos[a]	Sequence[b,c]	Pos[a]	Sequence[b,c]	Pos[a]	Sequence[b,c]
11	GAHEN	393	MIPLN	746	PAKWD	969	YYPAR	1399	CHQPA	1750	**EIQWM**
29	TINYY	403	KNTMD	748	KWDDY	974	YQSHI	1403	ANFKR	1751	**IQWMR**
72	NIEAC	404	NTMDM	749	WDDYT	996	CHHGV	1413	CGKAI	1752	**QWMRP**
73	IEACG	408	MYRVQ	752	YTWQT	1014	FADIR	1418	QLMDK	1762	YPIIN
104	YGRWP	414	NDNPH	763	FYTYG	1021	YAYEE	1437	IVNER	1810	YVGNK
106	RWPEY	436	LSHTM	783	**AYSHF**	1084	ITRNY	1458	PIQYK	1840	TEQMC
107	WPEYL	446	**NYYTH**	784	**YSHFY**	1105	VSPWQ	1475	ECIND	1849	MYGTD
130	CRFYT	447	**YYTHW**	785	**SHFYD**	1136	TEACN	1489	VRNYC	1933	VAMRM
145	RGWWW	448	**YTHWA**	835	KIRVY	1139	CNAAK	1490	RNYCE	1935	MRMAF
146	GWWWK	449	**THWAG**	841	KPKHI	1188	STIHQ	1496	**KGWIV**	1946	FHKNP
148	WWKLP	464	SMMAT	847	VWCPR	1190	IHQSC	1497	**GWIVN**	1947	HKNPG
149	WKLPD	465	MMATG	857	AYYGP	1204	FNNVR	1498	**WIVNI**	1966	WSKIP
163	**QNMYY**	494	HVIWD	863	VDYKD	1205	NNVRW	1513	NRAMT	1979	AFDYT
164	**NMYYH**	495	VIWDI	880	TYGFG	1209	WLSIQ	1532	VYVMY	1983	TGYDA
165	**MYYHY**	497	WDIGL	881	YGFGH	1231	LEHTI	1534	VMYKL	1993	WFEAL
179	VQCNA	507	MVVPW	883	FGHQN	1291	FDGYK	1536	YKLFA	2028	YCVKG
199	MCLAG	510	PWISN	884	GHQNK	1311	GADMK	1588	GEFTM	2070	KMIAY
242	RFCPV	518	RQTTN	894	GYKIC	1314	MKLFC	1592	MLGIH	2073	AYGDD
244	CPVDY	534	FYQTR	895	YKICN	1326	FIPPM	1594	**GIHDN**	2115	TWENV
271	TNNCA	556	SACND	897	ICNYH	1340	FTSNY	1595	**IHDNV**	2131	KYPFL
292	KHNNW	557	ACNDF	912	VSTMW	1341	TSNYV	1596	**HDNVA**	2148	SIRWT
293	HNNWG	558	CNDFS	914	TMWDR	1368	RFAFD	1660	TETND	2158	TQDHV
295	NWGIA	568	DTTHI	934	ARCNC	1369	FAFDM	1677	MFVPV	2168	LAWHN
323	PMCC	569	TTHIG	942	VYYCE	1371	FDMDI	1699	**RTLMY**	2201	LYRRW
324	PMCCE	588	MIDNT	948	RRKYY	1388	DMTMA	1700	**TLMYN**		
326	CCEFN	665	CVSII	959	PTFQY	1389	MTMAT	1701	**LMYNF**		
327	CEFNG	708	RFDME	961	FQYME	1394	EMCKN	1702	**MYNFP**		
391	DTMIP	735	QIMYV	962	QYMEA	1398	NCHQP	1742	SYFTQ		

[a]aa position along the human PV type 1, strain Mahoney, primary sequence.
[b]aa sequences given in one-letter code.
[c]Consecutively overlapping pentapeptides forming 7- and 8-mer stretches unique to PV are given in bold.

$PV_{783–789}$AYSHFYD, $PV_{1496–1498}$KGWIVNI, $PV_{1594–1600}$GIHDNVA, $PV_{1699–1706}$RTLMYNFP, and $PV_{1750–1756}$EIQWMRP).

3.2. Analysis of the Immunologic Potential of Peptides Unique to PV. Next, the pentapeptides described in Table 1 were analyzed for their immunologic potential as follows. PV-derived epitopes were retrieved from IEDB, and the epitopes that had been experimentally validated in the human host were analyzed for the presence of pentapeptides unique to PV1 (see Table 1).

As reported in Table 2, the search through IEDB produced a final list of 78 viral epitopes derived from PV1 Mahoney, PV3 Sabin, and PV3 (P3/LEON/37 and P3/LEON 12A (1)B). Epitopes derived from PV2 strains were not considered since only data from immunoassays in mice, rats, and/or rabbits were available in IEDB for PV2 strains at the time of this study. Following sequence analysis, it was found that 20 of the 78 epitopes (i.e., IEDB IDs: 31814, 48785, 58511, 59797, 71769, 79272, 79480, 99910, 100138, 100244, 100349, 100382, 100536, 100576, 100631, 100667, 100672, 146181, 146248, and 146390; see IEDB IDs in bold in Table 2) have a total of 12 viral pentapeptides that are absent in the human proteome (pentapeptides in capital letters in Table 2). That is, a first conclusion from Table 2 is that 12 out of the 164 pentapeptides unique to PV1, strain Mahoney, are part of 20 PV epitopic sequences endowed with an immunologic potential in the human host.

Moreover, it can be seen that the 12 unique PV1 pentapeptides are not distributed at random among the PV-derived epitopes. For example, three unique pentapeptides (KWDDY, WDDYT, and YTWQT) overlap each other in the epitope IEDB ID 48785, sequence ppgapvpeKWDDYTWQTssnp (with unique overlapping pentapeptides in capital); the heptapeptide AYSHFYD, formed by three overlapping unique

Table 2: Twelve pentapeptides unique to PV1, Mahoney strain, and absent in the human proteome are distributed among twenty PV-derived epitopes recognized by human sera and/or T cells.

IEDB ID[a]	Epitope sequence[b,c]	PV antigen	PV strain	Immune context
30661	kevpaltavetgat	VP1	PV3 Sabin	B
31814	**klefftysRFDMEltfvvtan**	VP1	PV1 Mahoney	T
46859	paltavetgatnpl	VP1	PV1 Mahoney	B-T
48785	**ppgapvpeKWDDYTWQTssnp**	VP1	PV1 Mahoney	T
55952	rsrsessiesf	VP1	PV1 Mahoney	B
58511	**siFYTYGtaparisvpyvgi**	VP1	PV1 Mahoney	T
59797	**snAYSHFYDgfskvplkdqs**	VP1	PV1 Mahoney	T
66978	tvdnsasttnkdklfavwk	Polyprotein	PV1 Mahoney	T
71769	**vvndhnptkvtsKIRVYlkp**	Polyprotein	PV1 Mahoney	T
79155	altlslpkqqdslpdtka	Polyprotein	PV3 (P3/LEON/37 and P3/LEON 12A (1)B)	T
79160	atnplapsdtvqtrhvvq	Polyprotein	PV3 (P3/LEON/37 and P3/LEON 12A (1)B)	T
79186	dneqpttraqklfam	Polyprotein	PV3 (P3/LEON/37 and P3/LEON 12A (1)B)	T
79269	kevpaltavetgatnpla	Polyprotein	PV3 (P3/LEON/37 and P3/LEON 12A (1)B)	T
79272	**khvrVWCPRppravpyyg**	Polyprotein	PV3 (P3/LEON/37 and P3/LEON 12A (1)B)	T
79318	nghalnqvyqimyippga	Polyprotein	PV3 (P3/LEON/37 and P3/LEON 12A (1)B)	T
79350	qklfamwritykdtv	Polyprotein	PV3 (P3/LEON/37 and P3/LEON 12A (1)B)	T
79354	qpttraqklfamwri	Polyprotein	PV3 (P3/LEON/37 and P3/LEON 12A (1)B)	T
79433	traqklfamwrityk	Polyprotein	PV3 (P3/LEON/37 and P3/LEON 12A (1)B)	T
79434	traqklfamwritykdtv	Polyprotein	PV3 (P3/LEON/37 and P3/LEON 12A (1)B)	T
79435	trhvvqrrsrsestiesf	Polyprotein	PV3 (P3/LEON/37 and P3/LEON 12A (1)B)	T
79436	tskvriymkpkhvrvw	Polyprotein	PV3 (P3/LEON/37 and P3/LEON 12A (1)B)	T
79443	vaiievdneqpttraqkl	Polyprotein	PV3 (P3/LEON/37 and P3/LEON 12A (1)B)	T
79461	vrvvndhnptkvtskvri	Polyprotein	PV3 (P3/LEON/37 and P3/LEON 12A (1)B)	T
79480	**yippgaptpksWDDYTwq**	Polyprotein	PV3 (P3/LEON/37 and P3/LEON 12A (1)B)	T
80446	argacvtimtvdnpa	VP1	PV1 Mahoney	B
81394	easgpthskeipalt	VP1	PV1 Mahoney	B
82831	gpthskeipaltave	VP1	PV1 Mahoney	B
83234	hskeipaltavetga	VP1	PV1 Mahoney	B
88446	sdtvqtrhvvqhrsr	VP1	PV1 Mahoney	B
88495	sessiesffargacv	VP1	PV1 Mahoney	B
99863	aaparisvpyvgla	Polyprotein	PV3 Sabin	B
99886	ahskevpaltavet	Polyprotein	PV3 Sabin	B
99901	arisvpyvglanay	Polyprotein	PV3 Sabin	B
99910	**AYSHFYDgfakvpl**	Polyprotein	PV3 Sabin	B
99933	dfgvlavrvvndhn	Polyprotein	PV3 Sabin	B
99963	dtvqlrrkleffty	Polyprotein	PV3 Sabin	B
100029	famwritykdtvql	Polyprotein	PV3 Sabin	B
100101	hfydgfakvplktd	Polyprotein	PV3 Sabin	B
100117	hnptkvtskvriym	Polyprotein	PV3 Sabin	B
100138	**iFYTYGaaparisv**	Polyprotein	PV3 Sabin	B
100244	**lanAYSHFYDgfak**	Polyprotein	PV3 Sabin	B
100349	**npsiFYTYGaapar**	Polyprotein	PV3 Sabin	B
100382	**pkhvrVWCPRppra**	Polyprotein	PV3 Sabin	B
100391	psdtvqtrhvvqrr	Polyprotein	PV3 Sabin	B
100425	qklfamwritykdt	Polyprotein	PV3 Sabin	B
100430	qlrrklefftysrf	Polyprotein	PV3 Sabin	B
100439	qpttraqklfamwr	Polyprotein	PV3 Sabin	B
100482	rppravpyygpgvd	Polyprotein	PV3 Sabin	B
100492	samtvddfgvlavr	Polyprotein	PV3 Sabin	B

Table 2: Continued.

IEDB ID[a]	Epitope sequence[b,c]	PV antigen	PV strain	Immune context
100504	sevaqgaltlslpk	Polyprotein	PV3 Sabin	B
100536	**svpyvglanAYSHF**	Polyprotein	PV3 Sabin	B
100559	tkvtskvriymkpk	Polyprotein	PV3 Sabin	B
100573	traqklfamwrity	Polyprotein	PV3 Sabin	B
100575	tskvriymkpkhvr	Polyprotein	PV3 Sabin	B
100576	**tssnpsiFYTYGaa**	Polyprotein	PV3 Sabin	B
100580	tvddfgvlavrvvn	Polyprotein	PV3 Sabin	B
100583	tvqtrhvvqrrsrs	Polyprotein	PV3 Sabin	B
100585	twqtssnpsifyty	Polyprotein	PV3 Sabin	B
100586	tygaaparisvpyv	Polyprotein	PV3 Sabin	B
100587	tykdtvqlrrklef	Polyprotein	PV3 Sabin	B
100613	vlavrvvndhnptk	Polyprotein	PV3 Sabin	B
100619	vndhnptkvtskvr	Polyprotein	PV3 Sabin	B
100628	vriymkpkhvrvwc	Polyprotein	PV3 Sabin	B
100630	vrvvndhnptkvts	Polyprotein	PV3 Sabin	B
100631	**vrVWCPRppravpy**	Polyprotein	PV3 Sabin	B
100638	wcprppravpyygp	Polyprotein	PV3 Sabin	B
100644	writykdtvqlrrk	Polyprotein	PV3 Sabin	B
100667	**ymkpkhvrVWCPRp**	Polyprotein	PV3 Sabin	B
100672	**yvglanAYSHFYDg**	Polyprotein	PV3 Sabin	B
146178	ayappgaqpptsrk	Polyprotein	PV3 Sabin	B
146181	**cgSMMATGkilvay**	Polyprotein	PV3 Sabin	B
146248	**flfcgSMMATGkil**	Polyprotein	PV3 Sabin	B
146311	hqgalgvfaipeyc	Polyprotein	PV3 Sabin	B
146333	ilvayappgaqppt	Polyprotein	PV3 Sabin	B
146390	**kftflfcgSMMATG**	Polyprotein	PV3 Sabin	B
146494	phqiinlrtnnsat	Polyprotein	PV3 Sabin	B
146496	ppgaqpptsrkeam	Polyprotein	PV3 Sabin	B
146516	ravpyygpgvdyrn	Polyprotein	PV3 Sabin	B

[a]PV-derived epitopes are listed according to increasing IEDB ID number. Further details and reference(s) on each IEDB ID are reported at http://www.immuneepitope.org [17].

[b]Only PV-derived epitopes that had been experimentally validated in the human host are reported.

[c]The twenty PV-derived epitopes (and related IDs) containing PV-pentapeptide(s) absent in the human proteome are in bold, with the pentapeptide(s) absent in the human proteome given in capital.

pentapeptides shifted by one residue, characterizes four PV-derived epitopes (IEDB IDs: 59797, 99910, 100244, and 100672); the hexapeptide SMMATG formed by two overlapped 5-mers is present in three epitopes (IEDB IDs: 146181, 146248, and 146390).

Theoretically, vaccines based on such PV epitopic peptides (i.e., KWDDYTWQT, AYSHFYD, and SMMATG) might evoke highly specific anti-PV immune responses exempt of possible collateral cross-reactions in the human host.

3.3. Identification of Consensus Pentapeptides Unique to PVs and Endowed with Immunologic Potential. We reasoned that using epitopic peptides unique to the virus and conserved among PV strains might help develop a global anti-PV peptide-based vaccination protocol. Such an approach would be of special importance in providing an effective and wide coverage to the human population worldwide, thus allowing reaching the goal of PV eradication [29, 30]. To this aim, we searched for unique conserved sequences by analysing a set of 43 PV polyproteins selected as described under Section 2 and comprehending also PV variants isolated from faeces of VAPP or AFP or from immunocompromised patient(s) with residual paralysis. The 43 PV polyprotein sequences were aligned using multialignment ClustalW program [24] and the peptide sequences present in PV-derived epitopes (see Table 2) and absent in the human proteome were localized.

Table 3 shows that seven potentially immunogenic peptides (in the order $PV_{465–469}$MMATG, $PV_{708–712}$RFDME, $PV_{752–756}$DYTWQT, $PV_{763–767}$FYTYG, $PV_{783–789}$AYSHFYD, $PV_{835–839}$KIRVY, and $PV_{847–851}$VWCPR), derived from epitopes corresponding to (or formed of) pentapeptides unique

Table 3: Conservativeness of epitopic PV peptide regions among 43 PV strains and variants.

PV strain	UniProt/Swiss-Prot entry	aa Pos 464	aa Pos 708	aa Pos 748	aa Pos 763	aa Pos 783	aa Pos 835	aa Pos 847
PV1 Mahoney	P03300	FMMATG	RFDME	KWDDYTWQT	FYTYG	AYSHFYD	KIRVY	VWCPR
PV1 Sabin	P03301	SMMATG	RFDME	KWDDYTWQT	FYTYG	AYSHFYD	KIRVY	VWCPR
PV3 P3/Leon/37	P03302	SMMATG	RFDME	sWDDYTWQT	FYTYG	AYSHFYD	KvRiY	VWCPR
PV3 23127	P06209	SMMATG	RFDME	sWDDYTWQT	FYTYG	AYSHFYD	KvRvY	VWCPR
PV1 isolated	Q9Q281	SMMATG	RFDME	KWDDYTWQT	FYTYG	AYSHFYD	KvRVY	VWCPR
PV1 isolated	Q9Q280	SMMATG	RFDME	KWDDYTWQT	FYTYG	AYSHFYD	KIRVY	VWCPR
PV1 isolated	Q71AZ9	SMMATG	RFDME	KWDDYTWQT	FYTYG	AYSHFYD	KIRVY	VWCPR
PV1 isolated	Q5TLH5	SMMATG	RFDME	KWDDYTWQT	FYTYG	AYSHFYD	KIRVY	VWCPR
PV1-HAI01008C2	D1YSI9	SMMATG	RFDME	KWDDYTWQT	FYTYG	AYSHFYD	KIRVY	VWCPR
PV1-HAI01009	D1YSJ1	SMMATG	RFDME	KWDDYTWQT	FYTYG	AYSHFYD	KIRVY	VWCPR
PV1-HAI01008	D1YSJ2	SMMATG	RFDME	KWDDYTWQT	FYTYG	AYSHFYD	KIRVY	VWCPR
PV1-HAI01002	D1YSJ3	SMMATG	RFDME	KWDDYTWQT	FYTYG	AYSHFYD	KIRVY	VWCPR
PV1-HAI01001	D1YSJ4	SMMATG	RFDME	KWDDYTWQT	FYTYG	AYSHFYD	KIRVY	VWCPR
PV1-DOR01012	D1YSJ5	SMMATG	RFDME	KWDDYTWQT	FYTYG	AYSHFYD	KIRVY	VWCPR
PV1-DOR01002C	D1YSJ6	SMMATG	RFDME	KWDDYTWQT	FYTYG	AYSHFYD	KIRVY	VWCPR
PV1-DOR01002	D1YSJ7	SMMATG	RFDME	KWDDYTWQT	FYTYG	AYSHFYD	KIRVY	VWCPR
PV1-DOR01001C1	D1YSJ9	SMMATG	RFDME	KWDDYTWQT	FYTYG	AYSHFYD	KIRVY	VWCPR
PV1-DOR00042C2	D1YSK1	SMMATG	RFDME	KWDDYTWQT	FYTYG	AYSHFYD	KIRVY	VWCPR
PV1-DOR00042C1	D1YSK2	SMMATG	RFDME	KWDDYTWQT	FYTYG	AYSHFYD	KIRVY	VWCPR
PV1-DOR00042	D1YSK3	SMMATG	RFDME	KWDDYTWQT	FYTYG	AYSHFYD	KIRVY	VWCPR
PV1-DOR00041C3	D1YSK4	SMMATG	RFDME	KWDDYTWQT	FYTYG	AYSHFYD	KIRVY	VWCPR
PV1-DOR00041C2	D1YSK5	SMMATG	RFDME	KWDDYTWQT	FYTYG	AYSHFYD	KIRVY	VWCPR
PV1-DOR00044	D1YSK6	SMMATG	RFDME	KWDDYTWQT	FYTYG	AYSHFYD	KIRVY	VWCPR
PV1-DOR00028C	D1YSK7	SMMATG	RFDME	KWDDYTWQT	FYTYG	AYSHFYD	KIRVY	VWCPR
PV1-DOR00028	D1YSK8	SMMATG	RFDME	KWDDYTWQT	FYTYG	AYSHFYD	KIRVY	VWCPR
PV1-DOR00023C	D1YSK9	SMMATG	RFDME	KWDDYTWQT	FYTYG	AYSHFYD	KIRVY	VWCPR
PV1-DOR00025	D1YSL0	SMMATG	RFDME	KWDDYTWQT	FYTYG	AYSHFYD	KIRVY	VWCPR
PV1-DOOR24	D1YSL1	SMMATG	RFDME	KWDDYTWQT	FYTYG	AYSHFYD	KIRVY	VWCPR
PV1-DOR00015	D1YSL2	SMMATG	RFDME	KWDDYTWQT	FYTYG	AYSHFYD	KIRVY	VWCPR
PV1-DOR00016	D1YSL3	SMMATG	RFDME	KWDDYTWQT	FYTYG	AYSHFYD	KIRVY	VWCPR
PV1-HAI01013all	D1YSL4	SMMATG	RFDME	KWDDYTWQT	FYTYG	AYSHFYD	KIRVY	VWCPR
PV1-HAI01015	D1YSL5	SMMATG	RFDME	KWDDYTWQT	FYTYG	AYSHFYD	KIRVY	VWCPR
PV1-S302	D2X673	SMMATG	RFDME	KWDDYTWQT	FYTYG	AYSHFYD	KIRVY	VWCPR
CHN8184/GZ/CHN/2004	D8L541	SMMATG	RFDME	KWDDYTWQT	FYTYG	AYSHFYD	KIRVY	VWCPR
PV3 isolated	B4YUL3	SMMATG	RFDME	sWDDYTWQT	FYTYG	AYSHFYD	KvRVY	VWCPR
PV3 isolated	B4YUL4	SMMATG	RFDME	sWDDYTWQT	FYTYG	AYSHFYD	KvRVY	VWCPR
PV3 (vacc.StrainSabin3 (Leon 12a1b))	Q84792	SMMATG	RFDME	sWDDYTWQT	FYTYG	AYSHFYD	KvRiY	VWCPR
PV3-33239	C5HJY2	SMMATG	RFDME	sWDDYTWQT	FYTYG	AYSHFYD	KvRiY	VWCPR
PV3-31974	C5HJY3	SMMATG	RFDME	sWDDYTWQT	FYTYG	AYSHFYD	KvRiY	VWCPR
PV3-FIN84-60212	D1GE40	SMMATG	RFDME	sWDDYTWQT	FYTYG	AYSHFYD	KvRiY	VWCPR
PV3-SWI10947	D2E679	SMMATG	RFDME	sWDDYTWQT	FYTYG	AYSHFYD	KvRiY	VWCPR
PV3-FIN84-2493	D1GE41	SMMATG	RFDME	sWDDYTWQT	FYTYG	AYSHFYD	KvRiY	VWCPR
PV3-P3/Jinan/1/09	D2XUS9	SMMATG	RFDME	sWDDYTWQT	FYTYG	AYSHFYD	KvRiY	VWCPR

The 43 PV sequences were aligned using ClustalW multialignment program (http://www.uniprot.org/align/) [24]. The analyzed PV sequences and related references are described at http://www.uniprot.org/ and reported by Swiss-Prot/UniProtKB accession number. Peptide sequences present in PV-derived epitopes (see Table 2) and absent in the human proteome were localized along the 43 aligned PV sequences and analyzed for conservativeness. Peptide sequences are indicated by their position along the PV polyprotein. Mutated aa residues are in lower case.

to PV1 (see Tables 1 and 2), have 100% conservation among the 43 PV strains/variants under analysis. The seven potentially immunogenic unique peptide sequences had the same level of conservativeness in PV2 derived strains (data not shown).

4. Conclusion

Anti-PV immunization has been one of the major public health measures of the last century. International campaigns to eliminate polio reduced the incidence of this disease in the world. However, problematic issues remain, such as the tendency of the PV genome to mutate, the potential risk to develop postvaccine paralytic poliomyelitis, and the difficulty to completely eradicate PV infection in the world. In fact, according to the World Health Organization, in 2012, still three countries in the world remain polio-endemic: Nigeria, Pakistan, and Afghanistan [31].

The present data propose the concept of sequence uniqueness as a tool to define specific immunotherapies exempt of collateral effects [22] and describe a methodology to identify PV peptides that have zero percent identity to human proteins, are endowed with an immunologic potential, and are highly conserved among PV strains (e.g., $PV_{465–469}$MMATG, $PV_{708–712}$RFDME, $PV_{752–756}$DYTWQT, $PV_{763–767}$FYTYG, $PV_{783–789}$AYSHFYD, $PV_{835–839}$KIRVY, and $PV_{847–851}$VWCPR; see Table 3). Importantly, polio peptide sequences alternate through the human proteome with a frequency versus rarity pattern that characterizes other pathogens too [32–35].

Theoretically, such viral consensus epitopic peptides appear to be ideal tools to generate anti-PV immune responses promising of high specificity, thus avoiding serological cross-reactivity between human polyomaviruses [23], as well as possible cross-reactions with the human host [22]. As an example, a construct composed of the coding frames corresponding to the immunogenic consensus sequences described above (Table 2) might determine a specific anti-PV immune response and, at the same time, by being based on peptides, might eliminate the issues inherent to the tendency of the PV genome to mutate (i.e., VAPP). Such viral peptide sequences might also be used in passive anti-PV immunotherapies, that is, to produce specific antibodies capable of reacting with intact viral protein antigens.

Actually, the present report is intended to represent a first approach to preclinical and animal studies. As a matter of fact, the solidity of a large body of theoretical and *in silico* data is the mandatory basis to design *in vivo* experimentation and validation protocols especially when considering that (i) although monkeys can be experimentally infected, humans are the only known natural hosts of poliovirus; (ii) small animal models for testing polio pathogenesis mainly relate to transgenic mice to express a human receptor to poliovirus [36]; and, moreover, (iii) current laws on *in vivo* experimentation are increasingly restrictive.

Conflict of Interests

The authors declare that this paper is based on research that was not funded entirely or partially by an outside source.

Authors' Contribution

Darja Kanduc proposed the original idea, supervised the work, interpreted the data, and wrote the paper. All authors contributed to the computational analyses; Giovanni Capone also contributed to the project definition. All authors discussed and approved the paper.

References

[1] T. J. John, "A developing country perspective on vaccine-associated paralytic poliomyelitis," *Bulletin of the World Health Organization*, vol. 82, no. 1, pp. 53–57, 2004.

[2] C. Runckel, O. Westesson, R. Andino, and J. L. DeRisi, "Identification and manipulation of the molecular determinants influencing poliovirus recombination," *PLoS Pathogens*, vol. 9, no. 2, Article ID e1003164, 2013.

[3] R. J. D. Tebbens, M. A. Pallansch, J.-H. Kim et al., "Oral poliovirus vaccine evolution and insights relevant to modeling the risks of circulating vaccine-derived polioviruses (cVDPVs)," *Risk Analysis*, vol. 33, no. 4, pp. 680–702, 2013.

[4] W. R. Dowdle, E. De Gourville, O. M. Kew, M. A. Pallansch, and D. J. Wood, "Polio eradication: the OPV paradox," *Reviews in Medical Virology*, vol. 13, no. 5, pp. 277–291, 2003.

[5] R. B. Aylward and C. Maher, "Interrupting poliovirus transmission—new solutions to an old problem," *Biologicals*, vol. 34, no. 2, pp. 133–139, 2006.

[6] S. C. Arya and N. Agarwal, "Re: world wide experience with inactivated poliovirus vaccine," *Vaccine*, vol. 27, no. 1, p. 1, 2009.

[7] M.-C. Bonnet and A. Dutta, "World wide experience with inactivated poliovirus vaccine," *Vaccine*, vol. 26, no. 39, pp. 4978–4983, 2008.

[8] B. T. Mayer, J. N. S. Eisenberg, C. J. Henry, M. G. M. Gomes, E. L. Ionides, and J. S. Koopman, "Successes and shortcomings of polio eradication: a transmission modeling analysis," *American Journal of Epidemiology*, vol. 177, no. 11, pp. 1236–1245, 2013.

[9] G. Novello, G. Capone, C. Fasano, S. L. Bavaro, A. N. Polito, and D. Kanduc, "A quantitative description of the peptide sharing between poliovirus and *Homo* sapiens," *Immunopharmacology and Immunotoxicology*, vol. 34, no. 3, pp. 373–378, 2012.

[10] E. Cherkasova, M. Laassri, V. Chizhikov et al., "Microarray analysis of evolution of RNA viruses: evidence of circulation of virulent highly divergent vaccine-derived polioviruses," *Proceedings of the National Academy of Sciences of the United States of America*, vol. 100, no. 16, pp. 9398–9403, 2003.

[11] I. Pelletier, G. Duncan, and F. Colbère-Garapin, "One amino acid change on the capsid surface of poliovirus sabin 1 allows the establishment of persistent infections in HEp-2c cell cultures," *Virology*, vol. 241, no. 1, pp. 1–13, 1998.

[12] N. Moscufo, J. Simons, and M. Chow, "Myristoylation is important at multiple stages in poliovirus assembly," *Journal of Virology*, vol. 65, no. 5, pp. 2372–2380, 1991.

[13] W.-F. Tang, S.-Y. Yang, B.-W. Wu et al., "Reticulon 3 binds the 2C protein of enterovirus 71 and is required for viral replication," *The Journal of Biological Chemistry*, vol. 282, no. 8, pp. 5888–5898, 2007.

[14] D. M. A. Evans, P. D. Minor, G. S. Schild, and J. W. Almond, "Critical role of an eight-amino acid sequence of VP1 in neutralization of poliovirus type 3," *Nature*, vol. 304, no. 5925, pp. 459–462, 1983.

[15] K. J. Wiegers, K. Wetz, and R. Dernick, "Molecular basis for linkage of a continuous and discontinuous neutralization epitope on the structural polypeptide VP2 of poliovirus type 1," *Journal of Virology*, vol. 64, no. 3, pp. 1283–1289, 1990.

[16] E. A. Emini, B. A. Jameson, and E. Wimmer, "Priming for and induction of anti-poliovirus neutralizing antibodies by synthetic peptides," *Nature*, vol. 304, no. 5928, pp. 699–703, 1983.

[17] R. Vita, L. Zarebski, J. A. Greenbaum et al., "The immune epitope database 2.0," *Nucleic Acids Research*, vol. 38, supplement 1, pp. D854–D862, 2010.

[18] K. Wiegers, H. Uhlig, and R. Dernick, "N-AgIB of poliovirus type 1: a discontinuous epitope formed by two loops of VP1 comprising residues 96-104 and 141-152," *Virology*, vol. 170, no. 2, pp. 583–586, 1989.

[19] R. Ketterlinus and K. Wiegers, "Mapping of antigenic domains in poliovirus VP1 involved in structural rearrangements during virus morphogenesis and antigenic alterations of the virion," *Virology*, vol. 204, no. 1, pp. 27–37, 1994.

[20] C. Reynolds, G. Page, H. Zhou, and M. Chow, "Identification of residues in VP2 that contribute to poliovirus neutralization antigenic site 3B," *Virology*, vol. 184, no. 1, pp. 391–396, 1991.

[21] D. Kanduc, A. Stufano, G. Lucchese, and A. Kusalik, "Massive peptide sharing between viral and human proteomes," *Peptides*, vol. 29, no. 10, pp. 1755–1766, 2008.

[22] D. Kanduc, "Peptide cross-reactivity: the original sin of vaccines," *Frontiers in Bioscience*, vol. 4, no. 4, pp. 1393–1401, 2012.

[23] U. Moens, M. van Ghelue, X. Song, and B. Ehlers, "Serological cross-reactivity between human polyomaviruses," *Reviews in Medical Virology*, vol. 23, no. 4, pp. 250–264, 2013.

[24] J. D. Thompson, D. G. Higgins, and T. J. Gibson, "CLUSTAL W: improving the sensitivity of progressive multiple sequence alignment through sequence weighting, position-specific gap penalties and weight matrix choice," *Nucleic Acids Research*, vol. 22, no. 22, pp. 4673–4680, 1994.

[25] V. R. Racaniello and D. Baltimore, "Molecular cloning of poliovirus cDNA and determination of the complete nucleotide sequence of the viral genome," *Proceedings of the National Academy of Sciences of the United States of America*, vol. 78, no. 8, pp. 4887–4891, 1981.

[26] C. H. Wu, L.-S. Yeh, H. Huang et al., "The protein information resource," *Nucleic Acids Research*, vol. 31, no. 1, pp. 345–347, 2003.

[27] D. Kanduc, "Homology, similarity, and identity in peptide epitope immunodefinition," *Journal of Peptide Science*, vol. 18, no. 8, pp. 487–494, 2012.

[28] D. Kanduc, "Pentapeptides as minimal functional units in cell biology and immunology," *Current Protein & Peptide Science*, vol. 14, no. 2, pp. 111–120, 2013.

[29] N. C. Grassly, "The final stages of the global eradication of poliomyelitis," *Philosophical Transactions of the Royal Society of London, Series B: Biological Sciences*, vol. 368, no. 1623, Article ID 20120140, 2013.

[30] P. Minor, "The polio endgame," *Human Vaccines & Immunotherapeutics*, vol. 10, no. 7, pp. 2106–2108, 2014.

[31] Z. A. Bhutta, "Conflict and polio: winning the polio wars," *Journal of the American Medical Association*, vol. 310, no. 9, pp. 905–906, 2013.

[32] D. Kanduc, L. Tessitore, G. Lucchese, A. Kusalik, E. Farber, and F. M. Marincola, "Sequence uniqueness and sequence variability as modulating factors of human anti-HCV humoral immune response," *Cancer Immunology, Immunotherapy*, vol. 57, no. 8, pp. 1215–1223, 2008.

[33] G. Lucchese, A. Stufano, and D. Kanduc, "Proposing low-similarity peptide vaccines against *Mycobacterium tuberculosis*," *Journal of Biomedicine and Biotechnology*, vol. 2010, Article ID 832341, 8 pages, 2010.

[34] G. Capone, G. Lucchese, M. Calabrò, and D. Kanduc, "West Nile virus diagnosis and vaccination: using unique viral peptide sequences to evoke specific immune responses," *Immunopharmacology and Immunotoxicology*, vol. 35, no. 1, pp. 64–70, 2013.

[35] A. Lucchese, A. Guida, G. Capone, M. Petruzzi, D. Lauritano, and R. Serpico, "Designing a peptide-based vaccine against *Porphyromonas gingivalis*," *Frontiers in Bioscience*, vol. 5, no. 2, pp. 631–637, 2013.

[36] S. Khan, H. Toyoda, M. Linehan et al., "Poliomyelitis in transgenic mice expressing CD155 under the control of the Tage4 promoter after oral and parenteral poliovirus inoculation," *Journal of General Virology*, vol. 95, part 8, pp. 1668–1676, 2014.

Hindawi Publishing Corporation
Journal of Immunology Research
Volume 2015, Article ID 527395, 13 pages
http://dx.doi.org/10.1155/2015/527395

Research Article

Evaluation of Humoral Immunity to *Mycobacterium tuberculosis*-Specific Antigens for Correlation with Clinical Status and Effective Vaccine Development

Mamiko Niki,[1] Maho Suzukawa,[2] Shunsuke Akashi,[2] Hideaki Nagai,[2] Ken Ohta,[2] Manabu Inoue,[1] Makoto Niki,[1] Yukihiro Kaneko,[1] Kozo Morimoto,[3] Atsuyuki Kurashima,[3] Seigo Kitada,[4] Sohkichi Matsumoto,[1,5] Koichi Suzuki,[6] and Yoshihiko Hoshino[6]

[1]*Department of Bacteriology, Osaka City University Graduate School of Medicine, Abeno, Osaka 545-8585, Japan*
[2]*National Hospital Organization, National Tokyo Hospital, Takeoka, Kiyose, Tokyo 204-8585, Japan*
[3]*Division of Respiratory Medicine, Fukujuji Hospital, Japan Anti-Tuberculosis Association, Matsuyama, Kiyose, Tokyo 204-8522, Japan*
[4]*National Hospital Organization, National Toneyama Hospital, Toneyama, Toyonaka, Osaka 560-8552, Japan*
[5]*Department of Infectious Disease Control and International Medicine, Niigata University Graduate School of Medical and Dental Sciences, Niigata 951-8510, Japan*
[6]*Department of Mycobacteriology, Leprosy Research Center, National Institute of Infectious Diseases, Aoba, Higashimurayama, Tokyo 189-0002, Japan*

Correspondence should be addressed to Yoshihiko Hoshino; yhoshino@nih.go.jp

Received 30 December 2014; Revised 27 February 2015; Accepted 2 March 2015

Academic Editor: Pedro A. Reche

Although tuberculosis remains a major global health problem, Bacille Calmette-Guérin (BCG) is the only available vaccine. However, BCG has limited applications, and a more effective vaccine is needed. Cellular mediated immunity (CMI) is thought to be the most important immune response for protection against *Mycobacterium tuberculosis* (Mtb). However, the recent failure of a clinical trial for a booster BCG vaccine and increasing evidence of antibody-mediated immunity prompted us to evaluate humoral immunity to Mtb-specific antigens. Using Enzyme-Linked ImmunoSpot and Enzyme-Linked ImmunoSorbent Assays, we observed less correlation of both CMI and IgG titers with patient clinical status, including serum concentration of C reactive protein. However, IgA titers against Mtb were significantly correlated with clinical status, suggesting that specific IgA antibodies protect against Mtb proliferation. In addition, in some cases, IgA antibody titers were significantly associated with the serum concentration of total albumin, which supports the idea that humoral immunity can be influenced by the nutritional status. Based on these observations, we propose that the induction of humoral immunity should be included as an option in TB vaccine development strategies.

1. Introduction

Tuberculosis (TB) remains a leading cause of death in many regions of the world and one-third of the world's population is thought to be asymptomatic carriers of the causative agent, *Mycobacterium tuberculosis* (Mtb). The World Health Organization estimates that approximately 8.6 million people contracted the disease and 1.3 million died in 2012 [1]. Bacillus Calmete-Guerin (BCG), the only approved and available TB vaccine, is made using an attenuated strain of *Mycobacterium bovis*, a relative of Mtb [2]. The primary use of the BCG vaccine is the immunization of children in areas with a high prevalence of TB. However, BCG is considered an inadequate vaccine because it offers no protection for adults [3]. A novel approach is needed to create a more effective vaccine.

Several novel approaches to vaccine production are in development. Recent progress in methods of vaccine development has been covered in several excellent reviews and will not be addressed here [4, 5]. The majority of these candidate vaccines focus on improving cell-mediated immunity (CMI) to Mtb by modifying the current BCG platform or boosting BCG with a different format, and some candidate vaccines

Table 1: Characteristics of patients in this study.

	Active disease	Past disease	LTBI	Control
n	88	84	18	77
Age (mean ± SD)	59.9 ± 20.2	60.5 ± 19.6	58.8 ± 17.7	63.9 ± 10.7
Age range	21–97	19–92	21–87	35–87
Sex (male/female)	65/23	59/25	11/6	55/19
Positivity of QFT-IT	69.3%	59.5%	64.7% (100%[a])	ND

[a]Patients were all positive for any IRGA (QFT-GIT and/or ELISPOT IFN-γ).
ND: not done.

have shown promise in mice and/or nonhuman primates [6, 7]. Modified Vaccinia Ankara (MVA) 85A is one of the more advanced vaccine candidates that use BCG with a booster of Mtb major secreted antigen complex 85A (Ag85A) [8], which boosts BCG-primed Th1 immune responses. It was expected that MVA85A would reduce the incidence of TB cases in an endemic area (i.e., South Africa) by 60%. However, the phase 2b clinical trial found that MVA85A conferred no detectable improvement against Mtb infection [9].

Although CMI has been established as a major component in the control of mycobacterial infections, serology analyses indicate that Mtb infection also induces humoral immune responses against various mycobacterial antigens [10]. In addition, BCG vaccination can induce antibody responses to several mycobacterial antigens [11–13], which elicits both innate and cell-mediated immunity against mycobacteria [13]. Humoral immunity could modify the fate of intracellular bacteria through mechanisms ranging from simple opsonization to complicated FcR activation [14].

The consensus for many years was that the control of vigorous granuloma formation following infection by pathogenic fungi (i.e., intracellular pathogens) was achieved by activating CMI, while humoral immunity was believed to have no role in protection. However, recent studies using hybridoma technology found protective monoclonal antibodies against numerous pathological fungi [15]. Two ongoing vaccine trials for the fungus *Candida albicans*, a major human pathogen, are expected to transduce protection by inducing antibody-mediated immunity [16].

These studies suggest that humoral immunity might also play an important role in protection against Mtb infection, a function which could be used to develop a new technology for more effective vaccine development. To evaluate the feasibility of using humoral immunity against mycobacterial antigens for effective vaccine development, we compared IgG and IgA antibody titers using a variety of clinical and immunological parameters. The results suggest that IgA antibodies against Mtb components would make suitable Mtb vaccine candidates.

2. Subjects and Methods

2.1. Participants. Patients of National Tokyo Hospital, Tokyo, Japan, were consecutively enrolled in the study, after giving informed consent, from May 2010 through May 2011. A total of 190 Japanese patients (age: 60.1 ± 19.6 yr, male: 71.1%) were recruited. The following information was obtained from all patients at the time of enrollment: history of prior TB disease, work history in any healthcare setting or recent exposure to a patient with active TB, and other TB risk factors such as having immunodeficiency disorders or taking immunosuppressive drugs [17]. We used the same inclusion/exclusion criteria as in a previous study [18]. Information on previous medical history, clinical signs and symptoms, and radiological and microbiological data including the values of serum C reactive protein (CRP) and the concentration of total albumin were also collected. The patients were then divided into three categories: (1) Active disease: patients having positive TB symptom(s) and positive smear results and/or positive demonstration of Mtb in culture; (2) Past disease: previously diagnosed with TB, treated and currently free from symptom(s); and (3) Latent TB infection (LTBI): no symptoms with normal chest X-ray, but having positive results from an interferon gamma release assay (IGRA). Among the 190 patients recruited, 88 (46%) were classified as "Active disease," 84 (45%) as "Past disease," and 18 (9%) as LTBI. We enrolled age- and gender-matched patients with respiratory disease who were confirmed not to have any mycobacterial diseases as negative controls. All medical, radiological, and microbiological information was collected to confirm their eligibility. A total of 77 Japanese adults (age: 63.9 ± 10.7 yr, male: 71.4%) were recruited as a control group (Table 1). In Japan, more than 90% of the population has been vaccinated with BCG since 1929, suggesting that most of the control group have received the BCG vaccine. The research protocol was approved by the Institutional Review Boards of Osaka City University Graduate School of Medicine, Osaka, Japan, National Tokyo Hospital, Tokyo, Japan, Fukujuji Hospital, Tokyo, Japan, and National Toneyama Hospital, Osaka, Japan, and by the Research Ethics Committee of the National Institute of Infectious Disease, Tokyo, Japan.

2.2. Evaluation of Clinical Status. The clinical status of patients with active disease was evaluated as previously described with modification [19] (see Supplemental Table 1 in Supplementary Material available online at http://dx.doi.org/10.1155/2015/527395). (1) "Smear at entry" (entry = point of diagnosis before treatment): sputum smear taken at entry was stained and inspected by microscopy. The severity was subdivided as 0 (no acid fast bacilli (AFB) on smear), ± (1-2 AFB per 300 field), 1+ (1–9 AFB per 100 field), 2+ (more than 10 AFB per 100 field), and 3+ (more than 10 AFB per field). (2) "Positive conversion time": duration (weeks) between entry and positive MGIT results. (3) Duration of culture negative:

time (days) from initiation of treatment to negative smear results (= 0 AFB per field) by sputum microscopy. (4) Several routine laboratory tests including serum concentration of "C reactive protein (CRP) at entry," (total) "Albumin at entry," and "CRP after 60 days of treatment" were simultaneously performed. (5) Severity of chest radiography at entry: "The Japanese Society for Tuberculosis Classification" (1959) was applied [20]. Briefly, tuberculosis lesions are classified by chest X-ray findings as type (cavity) and extent. "X-ray type (cavity)" was subdivided from III to I (III: no cavity, II: morbid foci other than I, and I: widespread cavities) and "X-ray extent" from 1 to 3 (1: minimal, 2: moderate, and 3: severe). These markers and classifications were chosen because serum albumin levels reaction to the tuberculin skin test, the Gaffky scale, and negative conversion time are significantly correlated with both type and extent [20]. If patients contracted hilar glandular tuberculosis and/or tuberculosis lymphadenopathy, the evaluation of (1), (2), and (3) was excluded and that of (4) and (5) was included for the analysis because bacterial presentation in the sputum is rare.

2.3. QuantiFERON-TB Gold In-Tube (QFT-GIT) Assay. The QFT-GIT assay was performed using fresh whole blood in accordance with the manufacturer's instructions (Cellestis, Chadstone, Australia). The results were interpreted with software provided by Cellestis. The antigen used in this assay is the 6 kDa early secreted antigenic target from *M. tuberculosis* (ESAT-6), the 10 kDa culture filtrate protein (CFP-10), and TB7.7. However, there was no response to TB7.7 in Japanese patients [17]. Results were scored as "positive" when the IFN-γ concentration in the tube with TB-specific antigen was >0.35 IU/mL, after subtracting the value of the nil control, and at least >25% of the negative control value. When the net IFN-γ response was <0.35 IU/mL for the antigens and the response to the mitogen-positive control was >0.5 IU/mL, the response was considered "negative" [17, 19]. Stimulation with mitogen induced more than 0.5 IU/mL in all subjects, supporting the contention that immunosuppressed participants were not included in the study (data not shown).

2.4. ELISPOT Assay. The IFN-γ ELISPOT assay was performed as previously described [17]. Briefly, peripheral blood mononuclear cells (PBMCs) were seeded in precoated IFN-γ ELISPOT plates (Becton, Dickinson and Company, Franklin Lakes, NJ, USA) with 2.5×10^5 cells per well in AIM-V medium (GIBCO) and incubated with a protein (10 μM) of each antigen at 37°C in 5% CO_2 for 16 hr. A negative control (no mitogen or antigen) and a positive control (phytohemagglutinin, PHA, 5 μg/mL) were also included. After incubation, the wells were washed and developed with a conjugate against the antibody used and an enzyme substrate. Spot-forming units were counted using a KS ELISPOT imaging system (Carl Zeiss, Hallbergmoos, Germany) and labeled spot-forming cells (SFC). ELISPOT results were interpreted according to the following criteria: the test result was positive when (1) the negative control had 0–5 spots and (2) the spot count (negative control spot count) was greater than six. The test result was negative when the above criteria were not met and the positive control was valid (≥20) [17, 21]. Data were plotted as the numbers of SFC/1×10^6 cells.

2.5. ELISA Assay. Concentrations of IgG and IgA antibodies against Mtb were determined by ELISA using recombinant proteins as previously described, with modification [22]. Ninety-six well microplates (Sumilon Type H, LMS, Tokyo, Japan) were coated with each recombinant antigen in bicarbonate buffer, pH 9.6 overnight at 4°C (Supplemental Table 2). The plates were blocked with phosphate buffered saline (PBS) containing 0.05% Tween 20 and 5% skim milk for 12 hr at 4°C and washed four times with PBS containing 0.05% Tween 20. Human serum samples diluted 1 : 200 (for IgG) or 1 : 100 (for IgA) in PBS containing 0.05% Tween 20 and 0.5% skim milk were then added in duplicate (IgG) or triplicate (IgA) to the antigen-coated wells and incubated for 12 hr at 4°C. After washing the wells, HRP-conjugated antihuman IgG or IgA antibodies were added at a 1 : 2000 or 1 : 1000 dilution, respectively. Following a one hr incubation at 37°C, the plates were washed four times before 100 μL of SureBlue reserve-TMB was added to each well. The reactions were stopped after 10 min by adding 50 μL of 0.1 M HCl, and absorbance was measured at 450 nm using a Multiskan Spectrophotometer (Thermo Fisher Scientific, Yokohama, Japan). The results of the IgG-ELISA were expressed as absorbance at 450 nm, whereas results of the IgA-ELISA were expressed as ELISA-Index, $S/(B + 3SD)$ [23, 24], where S is the average OD value of the duplicate test samples and $B + 3SD$ corresponds to the average OD value of the duplicate negative controls (B) plus three times the standard deviation (SD).

2.6. Reagents and Recombinant Protein Preparation. pET-21b, pET-22b, and Bugbuster HT were obtained from Novagen (Darmstadt, Germany); *Escherichia coli* BL21 (DE3) cells were from Toyobo (Osaka, Japan); Lowenstein-Jensen Luria-Bertani medium and carbenicillin were from Sigma (St. Louis, MO, USA); isopropyl-1-thio-beta-d-galactopyranoside and Ni-NTA agarose were from Qiagen (Gaithersburg, MD, USA); skim milk was from Morinaga (Tokyo, Japan); horseradish peroxidase-conjugated antihuman IgG or IgA antibodies and Envision kits were from Dako (Carpinteria, CA, USA); SureBlue reserve TMB microwell peroxidase substrate was from KPL (Gaithersburg, MD, USA); and monoclonal Acr antibody was from HyTest (Turku, Finland).

A pET-21b or pET-22b-based vector expressing 16 kDa α-crystallin homolog (Acr, 16 kDa protein, hspX or TB16.3: Rv2031c), Ag85A (Rv3804c), CFP-10 (Rv3874), ESAT-6 (Rv3875), heparin-binding haemagglutinin adhesin (HBHA: Rv0475), heat-stress-induced ribosome binding protein A (HrpA, 20 kDa protein, Acr2 or hsp20: Rv0251c), and mycobacterial DNA-binding protein 1 (MDP1: Rv2986c) were produced by a PCR-based approach using a bacterial chromosome. Each PCR product containing coding regions was designed to allow expression of C-terminal, 6 histidine-tagged variants of the recombinant proteins following ligation into pET-21b. After construction, expression vectors were confirmed by DNA sequencing. Recombinant Mtb proteins were purified using Ni-NTA columns (1 mL bed

volume, GE Healthcare, Piscataway, NJ, USA) according to the manufacturer's instructions. Purified proteins were used as mycobacterial antigens for ELISAs and ELISPOT assays.

2.7. Statistical Analysis. The Mann-Whitney U test was used to compare IgG and IgA levels between two independent groups, whereas one-way ANOVA was used for the comparison of three or more unmatched groups. Spearman's rank correlation coefficient was used to determine the correlation between ELISA values and the severity of clinical status values. Pairwise comparisons were made between areas under the receiver operating characteristic curve (AUROC) for the categorized groups. Optimal cut-off values were chosen when Youden's index (sensitivity and specificity − 1) was maximal. All analyses were performed using online statistics calculators (http://www.socscistatistics.com/tests/Default.aspx, http://vassarstats.net/index.html, http://molpath.charite.de/cutoff/index.jsp). The threshold of significance was set at $P < 0.05$.

3. Results

3.1. Antibody Titers in Active Disease, Past Disease, LTBI Cases, and Controls. Titers of IgG and IgA antibodies against recombinant mycobacterial antigens were measured separately in the sera of "Active disease" ($n = 88$), "Past disease" ($n = 84$), LTBI ($n = 18$) cases, and control ($n = 77$). We chose mycobacteria-specific antigens based on (1) proteome analysis of antibody responses to Mtb from active TB patients (included Acr, Ag85, CFP-10, and HrpA) [25, 26]; (2) *in silico* studies performed to identify TB vaccine candidates (included Acr, Ag85, and ESAT-6) [27]; and (3) publications identifying HBHA and MDP1 as mycobacteria-specific antigens [22, 28, 29]. Active disease patients had higher levels of IgG antibodies against all antigens tested compared to controls. In particular, significant increases in serum IgG levels were observed against ESAT-6, CFP-10, Acr, HBHA, and HrpA (Figure 1). Titers of past disease were lower than those of active disease except for MDP1, Ag85A, and HrpA (Figure 1). In contrast, IgA antibody titers for MDP1 and HrpA were higher in the control group than in the active disease group (Figure 2). The individual values of antibodies against the seven antigens were used to generate receiver operating characteristic curves (ROC). The Area under the ROC curves (AUROC) was calculated in both Tables 2 and 3.

3.2. ELISPOT and QFT Titers in Active Disease, Past Disease, and LTBI and Comparison between CMI Assays and Humoral ELISA Assays. CMI against various recombinant antigens was measured by ELISPOT assay for the active disease, past disease, and LTBI groups. Ninety-six participants (age: 58.6 ± 18.9 yr, male: 68.8%) were randomly chosen for the analysis of IFN-γ ELISPOT assay for ESAT-6 and CFP-10 antigens. A portion of the participants were also randomly recruited for the ELISPOT assay (MDP1: $n = 37$ (age: 55.9 ± 18.2 yr, male: 67.6%); Acr: $n = 36$ (age: 55.7 ± 18.4 yr, male: 66.7%); HBHA: $n = 20$ (age: 56.2 ± 17.7 yr, male: 100%); and HrpA: $n = 29$ (age: 56.7 ± 16.8 yr, male: 100%)).

No significant difference was observed in CMI, except for MDP1, in which past disease and LTBI patients had significantly more SFCs than active disease patients (Figure 3). Stimulation with PHA induced more than 80 SFC per 1×10^6 cells in all subjects (data not shown), indicating the lack of immunosuppressed participants in the study. When the results from CMI (ELISPOT) and humoral immunity (ELISA to IgG and IgA) were compared, there was no association between ELISPOT positivity and the values of IgG or IgA (Supplemental Figure 1). Also, there were no significant differences in the values of QFT-GIT assay among the active disease, past disease, and LTBI groups (Supplemental Figure 2).

3.3. "CRP at Entry" as a Surrogate Marker of Other Clinical Markers. We divided serum CRP values at entry into two categories: CRP < 2 mg/mL (negative or minimal inflammation) and CRP ≥ 2 mg/mL (intermediate or severe inflammation) because CRP is a more sensitive inflammation marker than erythrocyte sedimentation rate, another systemic inflammation marker. Other clinical markers were also divided into several categories (from negative to severe, Supplemental Table 1). All other clinical markers, such as "Smear at entry," "Positive conversion time," "Duration of culture negative," "Albumin at entry," "CRP at the time after 60 days," "X-ray type (cavity)," and "X-ray extent" were evaluated with the scores of "CRP at entry" (Figure 4). The "Smear at entry" ($r = 0.296$, $P < 0.05$), "Duration of culture negative" ($r = 0.391$, $P < 0.01$), "Albumin at entry" ($r = 0.687$, $P < 0.01$), "CRP after 60 days" ($r = 0.528$, $P < 0.01$), "X-ray type (cavity)" ($r = 0.271$, $P < 0.05$), and "X-ray extent" ($r = 0.445$, $P < 0.01$) scores were significantly associated with those of "CRP at entry," suggesting that "CRP at entry" could serve as a surrogate for other clinical markers. Only "Positive conversion time" was not associated with "CRP at entry" ($r = 0.09$, $P = 0.45$, data not shown).

3.4. Reverse Association between IgA Titers against HrpA and "CRP at Entry". Finally, we compared the results of immunological scores and clinical scores, such as "Smear at entry," "Positive conversion time," "Duration of culture negative," "CRP at entry," "Albumin at entry," "CRP at the time after 60 days," "X-ray type (cavity)," and "X-ray extent." There was no association among IgG antibodies. Among IgA antibodies, "CRP at entry" was significantly associated with HrpA IgA levels ($r = -0.2505$, $P < 0.05$); ESAT-6 IgA was significantly associated with "Albumin at entry" ($r = 0.3304$, $P < 0.01$); and Acr IgA was also associated with "Albumin at entry" ($r = 0.3334$, $P < 0.01$) (Figure 5). No association was found between immunological markers and clinical markers for other measured parameters (Supplemental Figures 3–10 and data not shown).

4. Discussion

We compared serum antibody titers and IGRA against components of Mtb to evaluate humoral and cell-mediated immunity for improvements in vaccine development. We also

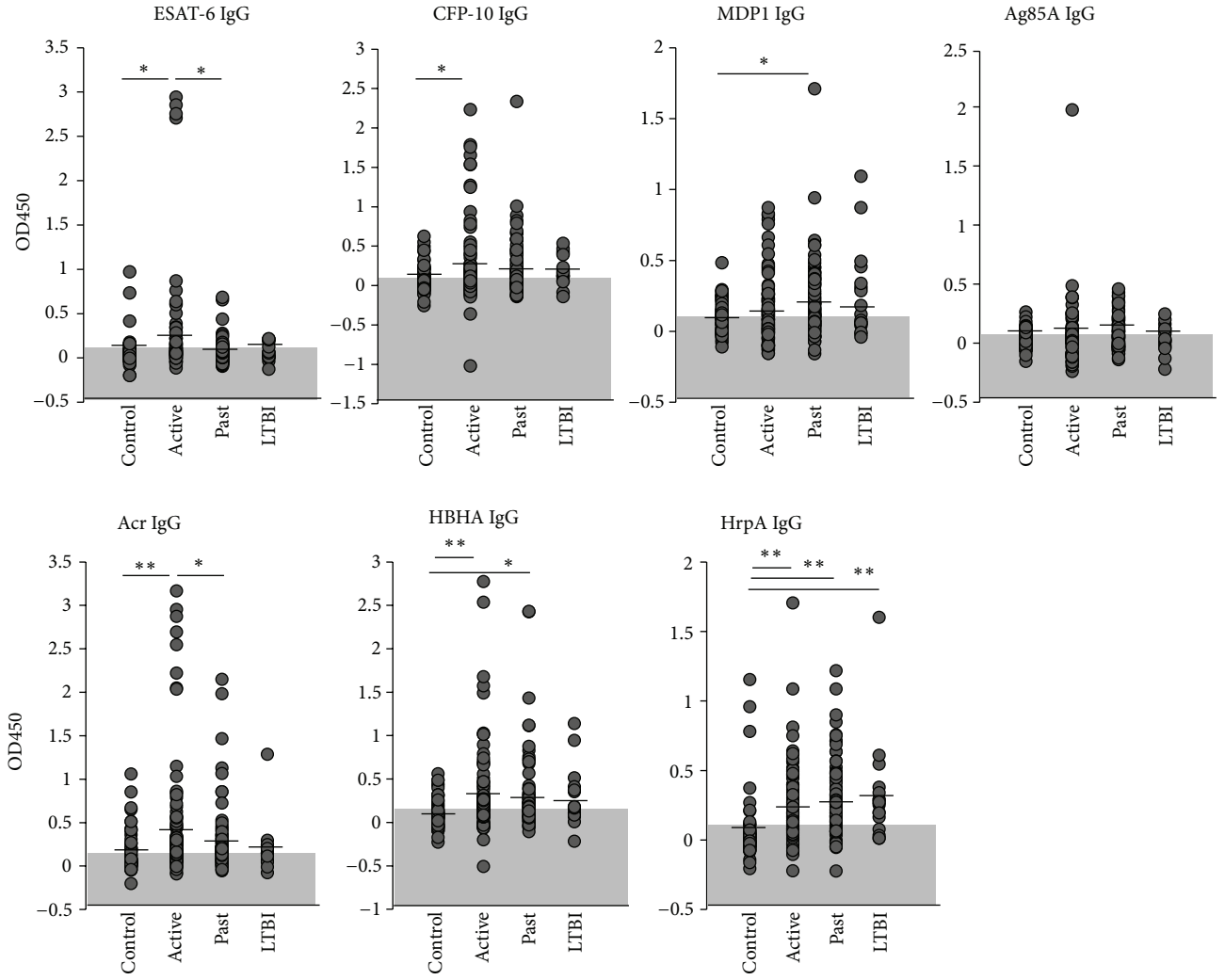

Figure 1: IgG responses to Mtb antigens. The levels of serum IgG against 7 antigens (ESAT-6, CFP-10, MDP1, Ag85A, Acr, HBHA, and HrpA) in active disease (labeled as "Active"), past disease ("Past"), latent TB infection ("LTBI"), and controls ("Control") were analyzed by ELISA. Data shown are the average of triplicate experiments. Shaded areas: areas under cut-off values, vertical lines: mean values, $^{*}P < 0.05$, $^{**}P < 0.01$.

compared these data with several clinical indices to evaluate a possible link for disease progression. Some IgA titers were elevated in the controls and lower in the active disease group. "CRP at entry" was significantly associated with several other clinical parameters. IgA antibody levels against HrpA in active disease patient were significantly associated with the clinical inflammation status measured by "CRP at entry." In addition, IgA antibodies against ESAT-6 and Acr were significantly associated with clinical nutrition status as measured by "Albumin at entry." Notably, an inverse correlation was found between "CRP at entry" and the IgA titer for HrpA, and a positive correlation was revealed between "Albumin at entry" and IgA titers for ESAT-6 and Acr. These findings suggest that some IgA antibodies targeting mycobacterial antigens can protect against the bacterial expansion or replication and corresponding lung inflammation previously reported in murinestudies *in vivo* [23, 30–32] and that antibody production could be influenced by the nutritional status of the patients, as has been reported in many studies [33–36].

CMI induction of the Th1 response should be the center of the principal immunity to Mtb infection. However, a recent study revealed this is not always the case. Strong immunological pressure on microbes usually drives an antigen shift, whereas a whole genome analysis of human T cell epitopes of Mtb showed they are evolutionarily hyperconserved [37]. If humans eliminate Mtb primarily through CMI, bacterial antigens might be exposed by the high level of immunological pressure; therefore, the epitopes should be hypermutated as they are in other pathogens such as hepatitis B virus, hepatitis C virus, HIV, or influenza virus [38–41]. We also found that most CMI measured by IFN-γ ELISPOT showed no difference among active, past, and LTBI patients. In addition, the frequency of IL-17+ CD4 cells (Th17 cells) was increased in HBHA or MDP1 responded populations in active or

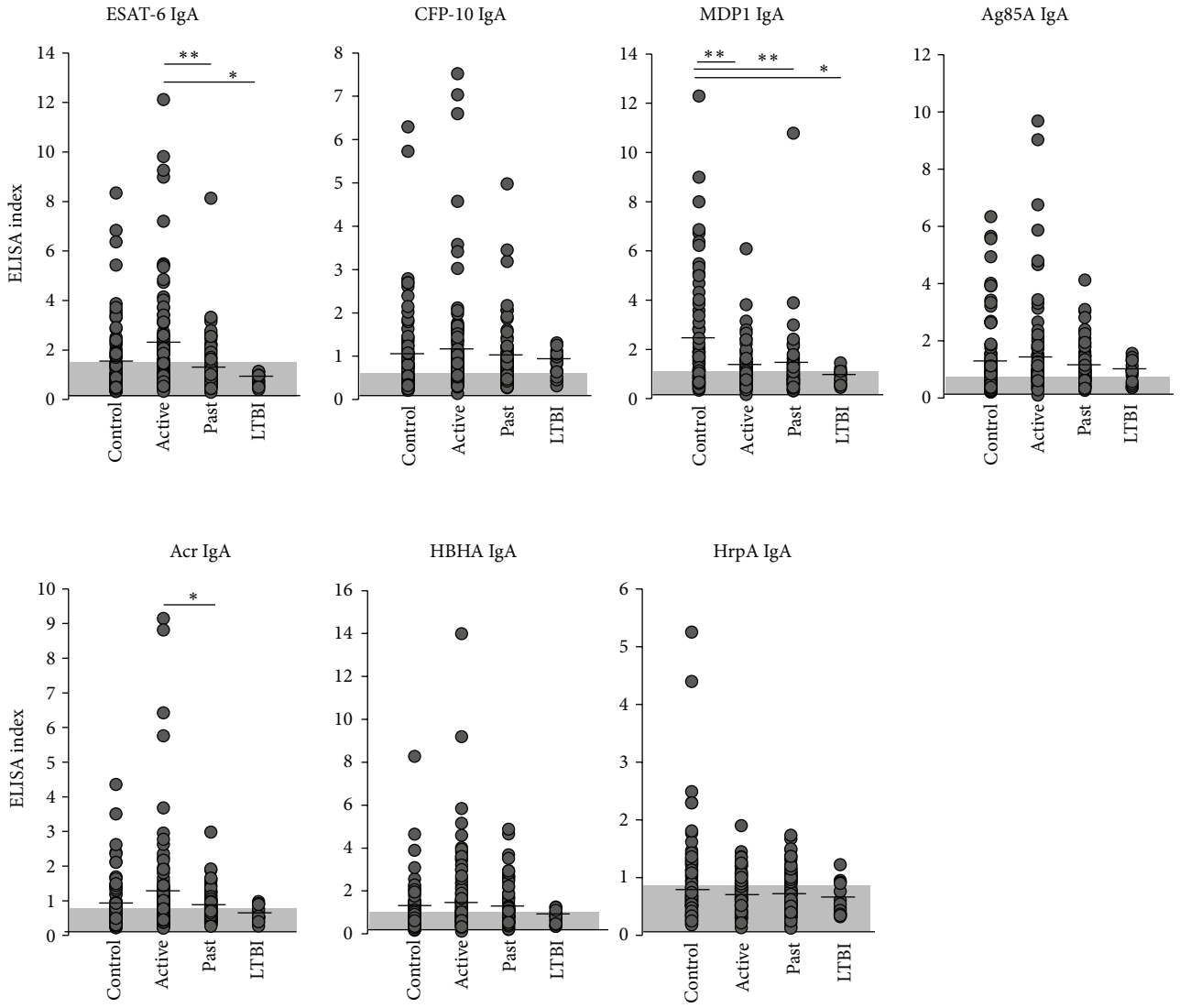

Figure 2: IgA responses to Mtb antigens. The levels of serum IgA against 7 antigens (ESAT-6, CFP-10, MDP1, Ag85A, Acr, HBHA, and HrpA) in active disease (labeled as "Active"), past disease ("Past"), latent TB infection ("LTBI"), and controls ("Control") were analyzed by ELISA. Data shown are the average of triplicate experiments. Shaded areas: areas under cut-off values, vertical lines: mean values, $^{*}P < 0.05$, $^{**}P < 0.01$.

past TB patients [28]. These observations led us to initiate the present study in order to examine the possibility of an additional immune response to mycobacterial infection.

Our study of cellular gene expression, derived by bronchoalveolar lavage (BAL) in active TB patients as well as normal volunteers using DNA microarray analysis, indicated a shift from a Th2 to Th1 phenotype in lung immune cells during the course of tuberculosis [42]. Most of the BAL cells from active patients showed a Th1 phenotype whereas all normal volunteers and some TB patients were Th2. Notably, the phenotype shifted from Th2 to Th1 in a patient during the course of the disease, supporting the premise that humoral immunity is predominant in the early stage of infection [16]. This observation suggests that humoral immunity might be an effective target for adjuvant enhancement in a new TB vaccine.

Recent studies have revealed that approximately 10% of bacterial proteomes could generate a human antibody response and a much smaller fraction of antigens (estimated as less than 1%) could be preferentially recognized by serum antibodies in active TB patients [25, 26]. We noted that the titers of some IgA antibodies were lower in active TB patients than in the controls, suggesting that BCG-induced humoral immunity to Mtb is maintained even after adolescence, but active disease can occur when the immunity diminishes. Several studies have also confirmed that vaccination with specific Mtb antigens such as Acr, Ag85, CFP-10, ESAT-6, or HBHA efficiently induces IgA and/or IgG antibodies as well as IFN-γ and other cytokines [35–40]. It is possible that DNA vaccination can induce humoral immunity in addition to CMI, which is important in protecting against the growth of Mtb. [30–32, 43–49].

Table 2: Serum IgG responses to seven mycobacterial antigens.

Group	Optical density at 450 nm (mean ± SD) and positive rate (%)						
	ESAT-6	CFP-10	MDP1	Ag85A	Acr	HBHA	HrpA
Cut-off values	0.067	0.077	0.118	0.037	0.129	0.140	0.072
Negative control	0.068 ± 0.155 36.4%	0.084 ± 0.160 41.9%	0.103 ± 0.108 36.5%	0.037 ± 0.074 44.6%	0.143 ± 0.213 32.4%	0.091 ± 0.157 23.0%	0.050 ± 0.210 16.2%
Active disease	0.248 ± 0.590[a] 55.7%	0.252 ± 0.508[a] 58.0%	0.157 ± 0.240 48.9%	0.068 ± 0.246 51.1%	0.487 ± 0.714[b] 76.1%	0.351 ± 0.502[b] 59.3%	0.256 ± 0.276[b] 77.3%
Past disease	0.068 ± 0.129[c] 39.3%	0.230 ± 0.345 64.3%	0.207 ± 0.259[d] 54.8%	0.080 ± 0.136 56.0%	0.277 ± 0.381[c] 66.7%	0.300 ± 0.436[d] 58.3%	0.290 ± 0.264[e] 79.8%
Latent TB infection	0.079 ± 0.100 41.2%	0.195 ± 0.190 76.5%	0.257 ± 0.320 52.9%	0.040 ± 0.115 41.2%	0.210 ± 0.292 64.7%	0.277 ± 0.334 64.7%	0.325 ± 0.368[f] 82.4%
AUROC	0.63	0.59	0.52	0.51	0.74	0.74	0.82

[a] $P < 0.05$ (active versus control), [b] $P < 0.01$ (active versus control), [c] $P < 0.05$ (active versus past), [d] $P < 0.05$ (past versus control), [e] $P < 0.01$ (past versus control), [f] $P < 0.01$ (latent versus control).
Optimal cut-off values were chosen when the Youden's index (sensitivity and specificity − 1) was maximal.
AUROC: areas under the receiver operating characteristic curve.

Table 3: Serum IgA responses to seven mycobacterial antigens.

Group	ELISA index at 450 nm (mean ± SD) and positive rate (%)						
	ESAT-6	CFP-10	MDP1	Ag85A	Acr	HBHA	HrpA
Cut-off values	1.496	0.567	1.115	0.577	0.738	1.015	0.901
Negative control	1.564 ± 1.533 32.4%	1.007 ± 1.041 58.1%	2.290 ± 2.277 63.5%	1.354 ± 1.382 64.9%	0.881 ± 0.739 41.9%	1.132 ± 1.140 35.1%	0.932 ± 0.813 39.2%
Active disease	2.189 ± 2.192 59.5%	1.246 ± 1.312 78.4%	1.137 ± 0.828[a] 30.7%	1.470 ± 1.664 85.2%	1.252 ± 1.549[b] 58.0%	1.713 ± 1.955 55.7%	0.751 ± 0.333 29.5%
Past disease	1.336 ± 1.128[c] 23.8%	0.976 ± 0.715 72.6%	1.166 ± 1.232[d] 34.5%	1.037 ± 0.686 79.8%	0.831 ± 0.495 50.0%	1.283 ± 0.954 50.0%	0.771 ± 0.356 35.7%
Latent TB infection	0.783 ± 0.246[e] 0.0%	0.793 ± 0.307 64.7%	0.879 ± 0.297[f] 11.8%	0.898 ± 0.395 58.8%	0.606 ± 0.221 23.5%	0.772 ± 0.299 17.6%	0.595 ± 0.285 17.6%
AUROC	0.63	0.53	0.66	0.57	0.59	0.62	0.53

[a] $P < 0.01$ (active versus control), [b] $P < 0.05$ (active versus past), [c] $P < 0.01$ (active versus past), [d] $P < 0.01$ (past versus control), [e] $P < 0.05$ (active versus latent), [f] $P < 0.05$ (latent versus control).
Optimal cut-off values were chosen when the Youden's index (sensitivity and specificity − 1) was maximal.
AUROC: areas under the receiver operating characteristic curve.

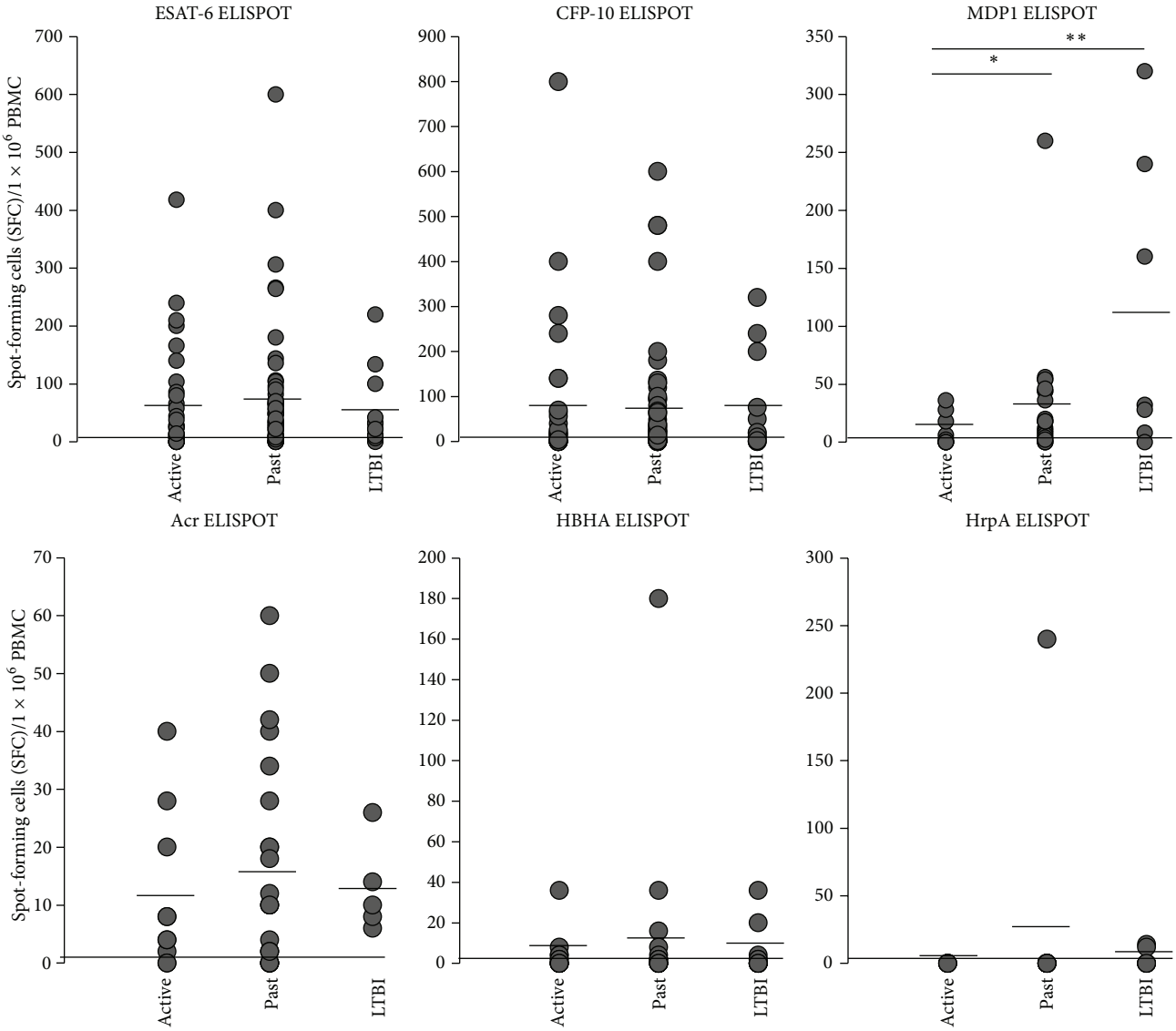

Figure 3: ELISPOT responses to Mtb antigens. ELISPOT SFCs against 6 antigens (ESAT-6, CFP-10, MDP1, Acr, HBHA, and HrpA) in active disease (labeled as "Active"), past disease ("Past") and latent TB infection ("LTBI"). Data shown are the average of triplicate experiments. Vertical lines: mean values, $^{*}P < 0.05$, $^{**}P < 0.01$.

There are many reports analyzing the level of IgG antibody titers in different clinical stages of TB [22, 50–52]. The major conclusion of these studies is that most IgG antibodies increase in the active phase and decline following treatment or during a LTBI, suggesting that the bacterial load is associated with the production of IgG and that the clinical cure lowers immunoglobulin levels. In this study, we confirmed that Mtb-specific IgG antibody levels are associated with bacterial load, because most IgG values were higher in active patients than past patients. However, we noted that IgA antibody titers of HrpA and MDP1 were quite different from those of IgG antibodies as they were higher in controls than in active patients. These results suggest that IgA levels toward some Mtb antigens are modified after infection, even if the patients had previously received a BCG vaccination as most Japanese should. Based on these findings, it can be hypothesized that a decline in IgA levels for these antigens, which is initially induced by BCG vaccination, might be related to bacterial growth. Although the DNA sequence of these antigens is almost homologous between BCG and Mtb (Supplemental Table 3), there may be a difference in protein structure and/or an amino acid sequence that is essential for the induction of humoral immune responses.

Both Acr and HrpA are mycobacterial heat shock proteins or chaperones that were revealed by a whole genome analysis of H37Rv [53]. Acr is a well characterized mycobacterial protein that possesses immune-dominancy [31, 32, 48, 54, 55]. Acr plays important roles during log phase growth and transition to the stationary phase of Mtb proliferation [56, 57]. Moreover, there are some studies concluding that monoclonal IgA antibody against Acr protects mycobacterial proliferation *in vivo*. Williams et al. compared the effect of

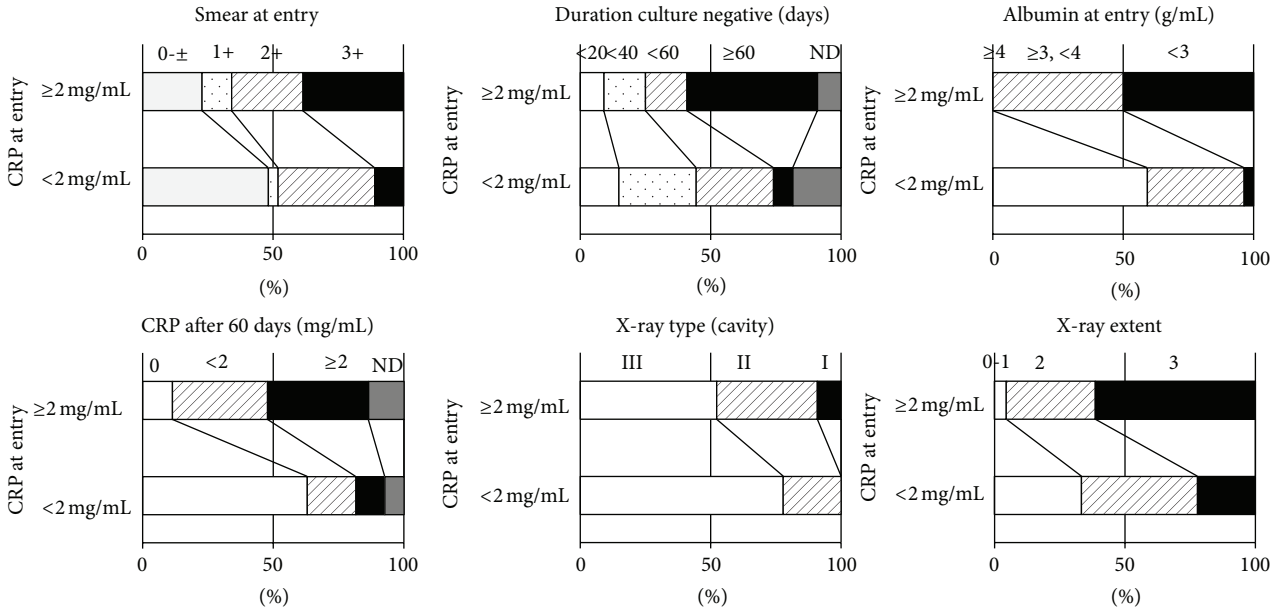

Figure 4: Clinical markers evaluated with "CRP at entry." All markers were significantly associated with "CRP at entry." "CRP at entry" was significantly associated with "Smear at entry" ($r = 0.296$, $P < 0.05$), "Duration of culture negative" ($r = 0.391$, $P < 0.01$), "Albumin at entry" ($r = 0.687$, $P < 0.01$), "CRP at 60 days" after treatment ($r = 0.528$, $P < 0.01$), X-ray type (cavity) ($r = 0.271$, $P < 0.05$), and X-ray extent ($r = 0.445$, $P < 0.01$).

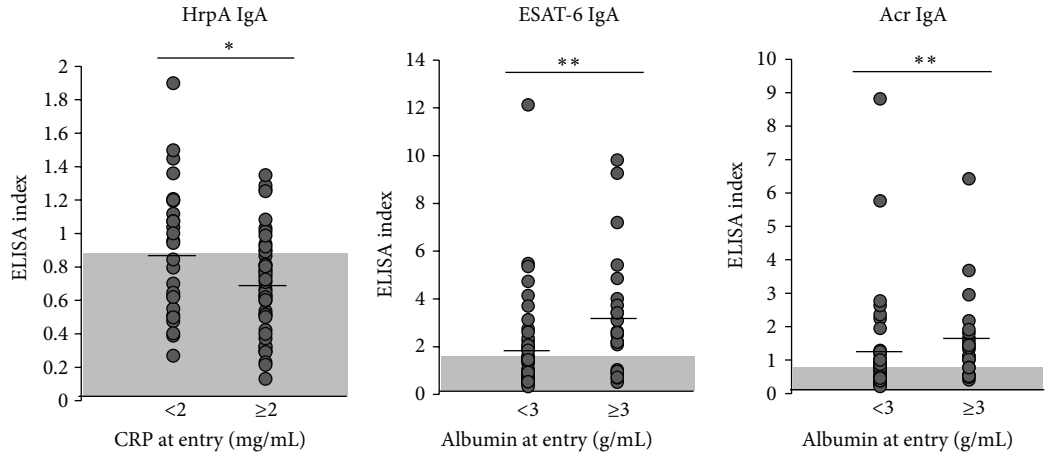

Figure 5: Association between immunological scores and clinical scores. HrpA IgA was negatively associated with "CRP at entry." ESAT-6 IgA and Acr IgA were positively associated with "Albumin at entry." Shaded areas: areas under cut-off values, vertical lines: mean values. $^{*}P < 0.05$, $^{**}P < 0.01$.

TBA61 (anti-Acr monoclonal IgA) and TBA68 (IgG of the same epitope as TBA61) on Mtb growth and observed that IgA antibody contributed more to a reduction in the number of bacteria in mouse lung space [31]. López et al. reported a greater reduction of bacteria and pathological severity of the disease when using TBA 61 compared with TBA84 (IgA to PstS-1, 38 kDa secreted glycoprotein [58, 59]) [32]. Although these experiments were performed using mouse models, they suggested that humoral immunity could at least modify or reduce the growth of Mtb [31, 32]. HrpA was identified by Ohara et al. in 1997 [60] with a 30% homology to Acr, which increases to 40% when comparing Acr core residues [61]. It was later demonstrated that the expression of HrpA is upregulated by heat-shock, nitrate, or macrophage engulfment, suggesting that HrpA is one of the early immune targets of Mtb antigens [62]. We found that the IgA to Acr or HrpA was associated with some of the parameters used to measure the clinical status of active patients and that it could support inhibition of the mycobacterial burden.

We also revealed that "CRP at entry" is a good surrogate marker for other clinical markers, a finding which is consistent with reports of previous studies [63]. Hypoalbuminemia has emerged as an independent factor of poor prognosis in several studies [33–36]. In this study, IgA antibody titers

generated by certain Mtb-specific antigens were significantly correlated with the scores of clinical markers such as CRP or albumin levels at first admission, which appears to be one of the host immune responses against Mtb. There was a significant association between IgA antibody titer and albumin. The importance of nutritional status for the clinical manifestation of TB has been evidenced by the fact that the incidence of TB is much higher in developing countries. This position is also supported by the correlations of serum IgA titers and higher albumin levels in the present study. The fact that humoral immunity had no association with CMI suggests that mycobacterial antigens influence humoral and cellular mediated immunity by different mechanisms. These findings suggest that induction of the IgA response could be a good strategy for Mtb vaccine design.

5. Conclusion

IgA antibody titers against several Mtb antigens, but not IgG antibodies nor CMI, significantly correlate with the clinical status of TB patients, raising the possibility that specific IgA antibodies protect against promotion of Mtb. These observations also suggest that induction of humoral immunity, especially for the IgA response, should be included as an option for TB vaccine strategies.

Conflict of Interests

The authors declare that they have no conflict of interests.

Authors' Contribution

Mamiko Niki, Manabu Inoue, Makoto Niki, and Yoshihiko Hoshino performed the laboratory experiments. Maho Suzukawa, Shunsuke Akashi, Hideaki Nagai, Kozo Morimoto, Atsuyuki Kurashima, Seigo Kitada, and Sohkichi Matsumoto contributed to the experimental system and statistical analysis. Mamiko Niki, Sohkichi Matsumoto, and Yoshihiko Hoshino contributed to the planning and proposal of the work. Yukihiro Kaneko, Ken Ohta, Koichi Suzuki, and Yoshihiko Hoshino coordinated the work.

Acknowledgments

The authors are thankful to all healthcare workers and tuberculosis patients who participated in this study. Sincere appreciation goes to Ms. Ayako Watanabe and Ms. Yasuko Inoue for their assistance with the laboratory assays. This work was supported in part by a Grant-in-Aid for Research on Emerging and Reemerging Infectious Diseases from the Ministry of Health, Labour and Welfare of Japan for H. Nagai, S. Matsumoto, and Y. Hoshino, by a Grant-in- Aid for Scientific Research (B) and (C) from the Japan Society for the Promotion of Science for S. Matsumoto and Y. Hoshino, and by a Grant-in-Aid for Adaptive and Seamless Technology transfer Program from Japan Science and Technology Agency for S. Matsumoto.

References

[1] WHO, *Global Tuberculosis Report 2013*, 2013, http://www.who.int/tb/publications/global_report/en/.

[2] P. E. M. Fine, "Variation in protection by BCG: implications of and for heterologous immunity," *The Lancet*, vol. 346, no. 8986, pp. 1339–1345, 1995.

[3] B. B. Trunz, P. Fine, and C. Dye, "Effect of BCG vaccination on childhood tuberculous meningitis and miliary tuberculosis worldwide: a meta-analysis and assessment of cost-effectiveness," *The Lancet*, vol. 367, no. 9517, pp. 1173–1180, 2006.

[4] T. H. M. Ottenhoff and S. H. E. Kaufmann, "Vaccines against tuberculosis: where are we and where do we need to go?" *PLoS Pathogens*, vol. 8, no. 5, Article ID e1002607, 2012.

[5] P. Andersen and S. H. E. Kaufmann, "Novel vaccination strategies against tuberculosis," *Cold Spring Harbor Perspectives in Medicine*, vol. 4, no. 6, 2014.

[6] C. Aagaard, T. Hoang, J. Dietrich et al., "A multistage tuberculosis vaccine that confers efficient protection before and after exposure," *Nature Medicine*, vol. 17, no. 2, pp. 189–195, 2011.

[7] P. L. Lin, J. Dietrich, E. Tan et al., "The multistage vaccine H56 boosts the effects of BCG to protect cynomolgus macaques against active tuberculosis and reactivation of latent *Mycobacterium tuberculosis* infection," *The Journal of Clinical Investigation*, vol. 122, no. 1, pp. 303–314, 2012.

[8] H. McShane, A. A. Pathan, C. R. Sander et al., "Recombinant modified vaccinia virus Ankara expressing antigen 85A boosts BCG-primed and naturally acquired antimycobacterial immunity in humans," *Nature Medicine*, vol. 10, no. 11, pp. 1240–1244, 2004.

[9] M. D. Tameris, M. Hatherill, B. S. Landry et al., "Safety and efficacy of MVA85A, a new tuberculosis vaccine, in infants previously vaccinated with BCG: a randomised, placebo-controlled phase 2b trial," *The Lancet*, vol. 381, no. 9871, pp. 1021–1028, 2013.

[10] K. R. Steingart, N. Dendukuri, M. Henry et al., "Performance of purified antigens for serodiagnosis of pulmonary tuberculosis: a meta-analysis," *Clinical and Vaccine Immunology*, vol. 16, no. 2, pp. 260–276, 2009.

[11] U. Beyazova, S. Rota, C. Cevheroglu, and T. Karsligil, "Humoral immune response in infants after BCG vaccination," *Tubercle and Lung Disease*, vol. 76, no. 3, pp. 248–253, 1995.

[12] R. M. Brown, O. Cruz, M. Brennan et al., "Lipoarabinomannan-reactive human secretory immunoglobulin A responses induced by mucosal bacille Calmette-Guérin vaccination," *The Journal of Infectious Diseases*, vol. 187, no. 3, pp. 513–517, 2003.

[13] S. De Vallière, G. Abate, A. Blazevic, R. M. Heuertz, and D. F. Hoft, "Enhancement of innate and cell-mediated immunity by antimycobacterial antibodies," *Infection and Immunity*, vol. 73, no. 10, pp. 6711–6720, 2005.

[14] A. Casadevall, "Antibody-mediated immunity against intracellular pathogens: two-dimensional thinking comes full circle," *Infection and Immunity*, vol. 71, no. 8, pp. 4225–4228, 2003.

[15] A. Casadevall, "Antibody immunity and invasive fungal infections," *Infection and Immunity*, vol. 63, no. 11, pp. 4211–4218, 1995.

[16] A. Casadevall and L.-A. Pirofski, "Immunoglobulins in defense, pathogenesis, and therapy of fungal diseases," *Cell Host & Microbe*, vol. 11, no. 5, pp. 447–456, 2012.

[17] H. Nagai, M. Suzukawa, Y. Sakakibara et al., "Immunological responses and epitope mapping by tuberculosis-associated antigens within the RD1 region in Japanese patients," *Journal of*

Immunology Research, vol. 2014, Article ID 764028, 8 pages, 2014.

[18] K. Komiya, H. Ariga, H. Nagai et al., "Reversion rates of QuantiFERON-TB gold are related to pre-treatment IFN-gamma levels," *Journal of Infection*, vol. 63, no. 1, pp. 48–53, 2011.

[19] H. Ariga, H. Nagai, A. Kurashima, Y. Hoshino, S. Shoji, and Y. Nakajima, "Stratified threshold values of QuantiFERON assay for diagnosing tuberculosis infection in immunocompromised populations," *Tuberculosis Research and Treatment*, vol. 2011, Article ID 940642, 9 pages, 2011.

[20] T. Murate, K. Shimokata, A. Watanabe et al., "Chest roentgenogram classification and clinical parameters in patients with active pulmonary tuberculosis," *Internal Medicine*, vol. 31, no. 2, pp. 185–188, 1992.

[21] K. Komiya, H. Ariga, H. Nagai et al., "Impact of peripheral lymphocyte count on the sensitivity of 2 IFN-γ release assays, QFT-G and ELISPOT, in patients with pulmonary tuberculosis," *Internal Medicine*, vol. 49, no. 17, pp. 1849–1855, 2010.

[22] M. Osada-Oka, Y. Tateishi, Y. Hirayama et al., "Antigen 85A and mycobacterial DNA-binding protein 1 are targets of immunoglobulin G in individuals with past tuberculosis," *Microbiology and Immunology*, vol. 57, no. 1, pp. 30–37, 2013.

[23] M. Legesse, G. Ameni, G. Medhin et al., "IgA response to ESAT-6/CFP-10 and Rv2031 antigens varies in patients with culture-confirmed pulmonary tuberculosis, healthy *Mycobacterium tuberculosis*-infected and non-infected individuals in a tuberculosis endemic setting, Ethiopia," *Scandinavian Journal of Immunology*, vol. 78, no. 3, pp. 266–274, 2013.

[24] A. M. M. Mattos, C. S. de Almeida, K. L. M. C. Franken et al., "Increased IgG1, IFN-γ, TNF-α and IL-6 responses to *Mycobacterium tuberculosis* antigens in patients with tuberculosis are lower after chemotherapy," *International Immunology*, vol. 22, no. 9, pp. 775–782, 2010.

[25] S. Kunnath-Velayudhan, A. L. Davidow, H.-Y. Wang et al., "Proteome-scale antibody responses and outcome of *Mycobacterium tuberculosis* infection in nonhuman primates and in tuberculosis patients," *The Journal of Infectious Diseases*, vol. 206, no. 5, pp. 697–705, 2012.

[26] S. Kunnath-Velayudhan, H. Salamon, H.-Y. Wang et al., "Dynamic antibody responses to the Mycobacterium tuberculosis proteome," *Proceedings of the National Academy of Sciences of the United States of America*, vol. 107, no. 33, pp. 14703–14708, 2010.

[27] A. Zvi, N. Ariel, J. Fulkerson, J. C. Sadoff, and A. Shafferman, "Whole genome identification of *Mycobacterium tuberculosis* vaccine candidates by comprehensive data mining and bioinformatic analyses," *BMC Medical Genomics*, vol. 1, no. 1, article 18, 2008.

[28] Y. Yamashita, Y. Hoshino, M. Oka et al., "Multicolor flow cytometric analyses of $CD4^+$ T cell responses to *Mycobacterium tuberculosis*-related latent antigens," *Japanese Journal of Infectious Diseases*, vol. 66, no. 3, pp. 207–215, 2013.

[29] H. R. Ramage, L. E. Connolly, and J. S. Cox, "Comprehensive functional analysis of *Mycobacterium tuberculosis* toxin-antitoxin systems: Implications for pathogenesis, stress responses, and evolution," *PLoS Genetics*, vol. 5, no. 12, Article ID e1000767, 2009.

[30] S. Balu, R. Reljic, M. J. Lewis et al., "A novel human IgA monoclonal antibody protects against tuberculosis," *Journal of Immunology*, vol. 186, no. 5, pp. 3113–3119, 2011.

[31] A. Williams, R. Reljic, I. Naylor et al., "Passive protection with immunoglobulin A antibodies against tuberculous early infection of the lungs," *Immunology*, vol. 111, no. 3, pp. 328–333, 2004.

[32] Y. López, D. Yero, G. Falero-Diaz et al., "Induction of a protective response with an IgA monoclonal antibody against *Mycobacterium tuberculosis* 16 kDa protein in a model of progressive pulmonary infection," *International Journal of Medical Microbiology*, vol. 299, no. 6, pp. 447–452, 2009.

[33] H.-R. Kim, S. S. Hwang, H. J. Kim et al., "Impact of extensive drug resistance on treatment outcomes in non-HIV-infected patients with multidrug-resistant tuberculosis," *Clinical Infectious Diseases*, vol. 45, no. 10, pp. 1290–1295, 2007.

[34] E. D. Matos and A. C. M. Lemos, "Association between serum albumin levels and in-hospital deaths due to tuberculosis," *International Journal of Tuberculosis and Lung Disease*, vol. 10, no. 12, pp. 1360–1366, 2006.

[35] K. Okamura, N. Nagata, K. Wakamatsu et al., "Hypoalbuminemia and lymphocytopenia are predictive risk factors for in-hospital mortality in patients with tuberculosis," *Internal Medicine*, vol. 52, no. 4, pp. 439–444, 2013.

[36] J.-Y. Wang, L.-N. Lee, and P.-R. Hsueh, "Factors changing the manifestation of pulmonary tuberculosis," *The International Journal of Tuberculosis and Lung Disease*, vol. 9, no. 7, pp. 777–783, 2005.

[37] Ĩ. Comas, J. Chakravartti, P. M. Small et al., "Human T cell epitopes of *Mycobacterium tuberculosis* are evolutionarily hyperconserved," *Nature Genetics*, vol. 42, no. 6, pp. 498–503, 2010.

[38] J. Bailey, J. N. Blankson, M. Wind-Rotolo, and R. F. Siliciano, "Mechanisms of HIV-1 escape from immune responses and antiretroviral drugs," *Current Opinion in Immunology*, vol. 16, no. 4, pp. 470–476, 2004.

[39] D. G. Bowen and C. M. Walker, "Mutational escape from $CD8^+$ T cell immunity: HCV evolution, from chimpanzees to man," *Journal of Experimental Medicine*, vol. 201, no. 11, pp. 1709–1714, 2005.

[40] M. P. Cooreman, G. Leroux-Roels, and W. P. Paulij, "Vaccine- and hepatitis B immune globulin-induced escape mutations of hepatitis B virus surface antigen," *Journal of Biomedical Science*, vol. 8, no. 3, pp. 237–247, 2001.

[41] C. Scholtissek, "Source for influenza pandemics," *European Journal of Epidemiology*, vol. 10, no. 4, pp. 455–458, 1994.

[42] B. Raju, Y. Hoshino, I. Belitskaya-Lévy et al., "Gene expression profiles of bronchoalveolar cells in pulmonary TB," *Tuberculosis*, vol. 88, no. 1, pp. 39–51, 2008.

[43] S. Buccheri, R. Reljic, N. Caccamo et al., "Prevention of the post-chemotherapy relapse of tuberculous infection by combined immunotherapy," *Tuberculosis*, vol. 89, no. 1, pp. 91–94, 2009.

[44] S. Chang-Hong, W. Xiao-Wu, Z. Hai, Z. Ting-Fen, W. Li-Mei, and X. Zhi-Kai, "Immune responses and protective efficacy of the gene vaccine expressing Ag85B and ESAT6 fusion protein from *Mycobacterium tuberculosis*," *DNA and Cell Biology*, vol. 27, no. 4, pp. 199–207, 2008.

[45] P. K. Giri, I. Verma, and G. K. Khuller, "Enhanced immunoprotective potential of *Mycobacterium tuberculosis* Ag85 complex protein based vaccine against airway *Mycobacterium tuberculosis* challenge following intranasal administration," *FEMS Immunology and Medical Microbiology*, vol. 47, no. 2, pp. 233–241, 2006.

[46] A. Grover, M. F. Ahmed, B. Singh, I. Verma, P. Sharma, and G. K. Khuller, "A multivalent combination of experimental antituberculosis DNA vaccines based on Ag85B and regions of difference antigens," *Microbes and Infection*, vol. 8, no. 9-10, pp. 2390–2399, 2006.

[47] K. Huygen, J. Content, O. Denis et al., "Immunogenicity and protective efficacy of a tuberculosis DNA vaccine," *Nature Medicine*, vol. 2, no. 8, pp. 893–898, 1996.

[48] H. Niu, L. Hu, Q. Li et al., "Construction and evaluation of a multistage *Mycobacterium tuberculosis* subunit vaccine candidate Mtb10.4-HspX," *Vaccine*, vol. 29, no. 51, pp. 9451–9458, 2011.

[49] C. Palma, E. Iona, F. Giannoni et al., "The LTK63 adjuvant improves protection conferred by Ag85B DNA-protein prime-boosting vaccination against *Mycobacterium tuberculosis* infection by dampening IFN-γ response," *Vaccine*, vol. 26, no. 33, pp. 4237–4243, 2008.

[50] C. Sánchez-Rodríquez, C. Estrada-Chávez, J. García-Vigil et al., "An IgG antibody response to the antigen 85 complex is associated with good outcome in Mexican Totonaca Indians with pulmonary tuberculosis," *International Journal of Tuberculosis and Lung Disease*, vol. 6, no. 8, pp. 706–712, 2002.

[51] X. Wu, Y. Yang, J. Zhang et al., "Comparison of antibody responses to seventeen antigens from *Mycobacterium tuberculosis*," *Clinica Chimica Acta*, vol. 411, no. 19-20, pp. 1520–1528, 2010.

[52] R. Baumann, S. Kaempfer, N. N. Chegou et al., "Serologic diagnosis of tuberculosis by combining Ig classes against selected mycobacterial targets," *The Journal of Infection*, vol. 69, no. 6, pp. 581–589, 2014.

[53] S. T. Cole, R. Brosch, J. Parkhill et al., "Deciphering the biology of *Mycobacterium tuberculosis* from the complete genome sequence," *Nature*, vol. 393, no. 6685, pp. 537–544, 1998.

[54] A. Geluk, M. Y. Lin, K. E. van Meijgaarden et al., "T-cell recognition of the HspX protein of *Mycobacterium tuberculosis* correlates with latent *M. tuberculosis* infection but not with *M. bovis* BCG vaccination," *Infection and Immunity*, vol. 75, no. 6, pp. 2914–2921, 2007.

[55] A. Purkayastha, L. A. McCue, and K. A. McDonough, "Identification of a *Mycobacterium tuberculosis* putative classical nitroreductase gene whose expression is coregulated with that of the acr gene within macrophages, in standing versus shaking cultures, and under low oxygen conditions," *Infection and Immunity*, vol. 70, no. 3, pp. 1518–1529, 2002.

[56] Y. Yuan, D. D. Crane, and C. E. Barry III, "Stationary phase-associated protein expression in *Mycobacterium tuberculosis*: function of the mycobacterial α-crystallin homolog," *Journal of Bacteriology*, vol. 178, no. 15, pp. 4484–4492, 1996.

[57] Y. Yuan, D. D. Crane, R. M. Simpson et al., "The 16-kDa α-crystallin (Acr) protein of *Mycobacterium tuberculosis* is required for growth in macrophages," *Proceedings of the National Academy of Sciences of the United States of America*, vol. 95, no. 16, pp. 9578–9583, 1998.

[58] G. Falero-Diaz, S. Challacombe, D. Rahman et al., "Transmission of IgA and IgG monoclonal antibodies to mucosal fluids following intranasal or parenteral delivery," *International Archives of Allergy and Immunology*, vol. 122, no. 2, pp. 143–150, 2000.

[59] J. Ivanyi, J. A. Morris, and M. Keen, "Studies with monoclonal antibodies to mycobacteria," in *Monoclonal Antibodies Against Bacteria*, A. J. L. Macario and E. C. Macario, Eds., pp. 59–90, Academic Press, New York, NY, USA, 1985.

[60] N. Ohara, M. Naito, C. Miyazaki, S. Matsumoto, Y. Tabira, and T. Yamada, "HrpA, a new ribosome-associated protein which appears in heat-stressed *Mycobacterium bovis* bacillus Calmette-Guerin," *Journal of Bacteriology*, vol. 179, no. 20, pp. 6495–6498, 1997.

[61] G. R. Stewart, L. Wernisch, R. Stabler et al., "Dissection of the heat-shock response in *Mycobacterium tuberculosis* using mutants and microarrays," *Microbiology*, vol. 148, part 10, pp. 3129–3138, 2002.

[62] K. A. Wilkinson, G. R. Stewart, S. M. Newton et al., "Infection biology of a novel α-crystallin of *Mycobacterium tuberculosis*: Acr2," *Journal of Immunology*, vol. 174, no. 7, pp. 4237–4243, 2005.

[63] J. F. Djoba Siawaya, N. B. Bapela, K. Ronacher et al., "Immune parameters as markers of tuberculosis extent of disease and early prediction of anti-tuberculosis chemotherapy response," *The Journal of Infection*, vol. 56, no. 5, pp. 340–347, 2008.

Hindawi Publishing Corporation
Journal of Immunology Research
Volume 2015, Article ID 763461, 11 pages
http://dx.doi.org/10.1155/2015/763461

Research Article

Automatic Generation of Validated Specific Epitope Sets

Sebastian Carrasco Pro,[1,2] John Sidney,[2] Sinu Paul,[2] Cecilia Lindestam Arlehamn,[2] Daniela Weiskopf,[2] Bjoern Peters,[2] and Alessandro Sette[2]

[1]*Laboratorio de Bioinformática y Biología Molecular, Laboratorios de Investigación y Desarrollo, Universidad Peruana Cayetano Heredia, Lima, Peru*
[2]*Division of Vaccine Discovery, La Jolla Institute for Allergy and Immunology, La Jolla, CA 92037, USA*

Correspondence should be addressed to Alessandro Sette; alex@liai.org

Received 24 December 2014; Accepted 2 March 2015

Academic Editor: Pedro A. Reche

Accurate measurement of B and T cell responses is a valuable tool to study autoimmunity, allergies, immunity to pathogens, and host-pathogen interactions and assist in the design and evaluation of T cell vaccines and immunotherapies. In this context, it is desirable to elucidate a method to select validated reference sets of epitopes to allow detection of T and B cells. However, the ever-growing information contained in the Immune Epitope Database (IEDB) and the differences in quality and subjects studied between epitope assays make this task complicated. In this study, we develop a novel method to automatically select reference epitope sets according to a categorization system employed by the IEDB. From the sets generated, three epitope sets (EBV, mycobacteria and dengue) were experimentally validated by detection of T cell reactivity *ex vivo* from human donors. Furthermore, a web application that will potentially be implemented in the IEDB was created to allow users the capacity to generate customized epitope sets.

1. Introduction

Adaptive immunity is based on the recognition of specific molecular structures, named epitopes, by either antibodies/B cell receptors or T cell receptors. Antibodies and B cell receptors bind a wide variety of structures, including proteins and carbohydrates. In the case of protein ligands, antibodies can recognize either a series of contiguous residues (linear epitopes) or a set of residues encoded in disparate regions of the protein sequence and brought together in the three dimensional structure of the protein ligand (discontinuous epitopes).

T cells recognize a complex between MHC molecules (named HLA in humans and H-2 in mouse) and, in most cases, a peptidic epitope of 8–16 residues in length [1, 2]. T cell responses are a key component of adaptive immunity. In concert with antibody responses, CD8 T cells, recognizing class I binding epitopes, and CD4 T cells, recognizing their class II counterparts, are key players in immunity to viruses and bacteria [3]. In the case of allergic reactions, CD4 T cell responses play a key role in pathogenesis both directly and indirectly through the regulation of antibody responses of the Ig E class [4].

Accurate measurement of B and T cell responses is a valuable tool to study autoimmunity, allergies, immunity to pathogens, and host-pathogen interactions and assist in the design and evaluation of T cell-based vaccines and immunotherapies [5–8]. Accordingly, a large number of studies have been devoted to defining B and T cell epitopes, a process that has been facilitated by an ever-increasing expansion and refinement of experimental methods.

As immune investigations proceed over time, many different epitopes from various organisms have been identified. Alternatively, large-scale epitope identification can reveal hundreds of potential epitopes [9–12]. The Immune Epitope Database (IEDB) [13, 14] is a freely available resource that serves as a repository of experimentally derived immune epitope information available in the peer-reviewed published literature, as well as from direct submission from NIH-NIAID funded large-scale epitope identification studies. The IEDB content covers a broad range of indications, to include infectious diseases (excluding HIV), allergies, transplantation, and

autoimmune disease and a similarly broad range of hosts, including humans, nonhuman primates, mice, and livestock, amongst others. The database, as of October 2014, hosts experimental data related to 121,812 different peptidic epitope structures.

This large amount of information might, in some cases, pose a challenge for the identification and selection of appropriate sets of epitopes for use in specific contexts. Thus, it is clearly desirable, given the ever-growing body of information contained in the IEDB, to develop tools to enable the efficient generation of sets of validated reference epitopes for any antigenic source of interest.

While an epitope, according to classic definitions, is any structure capable of interacting with T and B cell receptors, in practice the consensus in the scientific community is that certain types of assays identify the most relevant and validated epitopes. In the context of antibody reactivity, by way of example, epitopes identified on the basis of X-ray structures of Ag/antibody complexes, biological activity, and *in vivo* assays or recognized by IgE in the case of allergens are considered more biologically relevant than linear epitopes recognized in ELISA assays and elicited by peptide immunization. In the case of T cell reactivity, again by way of example, multimer/tetramer staining assays or readouts based on ICS or ELISPOT assays, are preferred over older assay platforms such as Thymidine incorporation following multiple *in vitro* restimulations with peptides. These high quality assays have been selected based on our experience and judgment; however, in the web tool developed, the user will be capable of customizing it by his/her needs, that is, select only epitopes derived from neutralization or ELISA assays or any other desired selection.

Indeed, for many applications, it is desirable to study T cells *ex vivo*, without manipulation. This is because manipulations, such as *in vitro* expansion, are known to profoundly change the phenotype and characteristic of the T cells [15–17], thus questioning the physiological relevance of some of the experimental observations. However, direct *ex vivo* detection of human T cell responses is often difficult, largely because the immune response in any individual may target many different epitopes, and different individuals typically recognize unique epitope repertoires. Simultaneous use of many different epitopes as a pool might represent a powerful approach to detecting T cell responses, because even if the frequency of T cells recognizing each individual epitope may be below the limit of detection, a pool of a large number of epitopes (i.e., responses) might pass the limit of detection.

An important consideration in the definition of reference sets of epitopes is how to factor the number of individual donors or experiments in which a given structure is reported to elicit a positive response, and particularly if this validation is provided in multiple independent studies. For example, different studies often report on essentially the same epitope but utilize different nested, truncated, or frame-shifted version of the same sequence, leaving uncertainty on how to combine the data or which particular version of the epitope to select for testing. Clarification of a general approach for combining data from such disparate studies would greatly facilitate the generation of nonredundant sets of epitopes.

In the present study, we have attempted the definition of an automated process to generate reference sets of high quality epitopes for various disease indications. The resulting tool, made available to the scientific community, provides a standardized and reproducible platform to automatically extract and process relevant data from the IEDB without the need of complex analysis and judgment calls from the user. At the same time, the tool also offers flexibility to enable the end user to design sets meeting specific user-defined criteria. We have also analyzed the data currently available in the IEDB, to determine how many sets of pathogen or autoantigen specific epitopes could be identified on the basis of the data available to date.

2. Materials and Methods

2.1. Database, Processing, and Implementation. Epitope data was derived from the IEDB database as of October 2014. MySQL was used to run queries and directly work with the database itself. The web page application is written in PHP/HTML code with a MySQL connection that allows communication between the database and the user interface.

2.2. Ranking Scores on the Basis of Response Frequency and Assay Type. Two independent scoring systems were developed to allow ranking and sorting of the epitopes. The first was based on the type of assays used to characterize the epitopes and the second on the frequency by which each epitope was recognized.

Regarding the assay type scoring system for MHC class I or class II epitopes, in our selection we included epitopes defined by multimer/tetramer staining, ELISPOT, and ICS assays. We arbitrarily associate a numerical parameter value of 3, 2, and 1 to these assay types, respectively. Each of these assay types can be used in either an *ex vivo* or *in vitro* configuration. To provide that *ex vivo* assays are always ranked higher, we assigned an *ex vivo* configuration a value of 4, and an *in vitro* configuration a value of 1, and calculated a final assay score by multiplying the assay type and configuration values. In the case of B cell epitopes, X-ray structure, biological activity, and *in vivo* assays were assigned a score of 1, as well as epitopes that present IgE; for these epitopes, the effector origin was not taken in consideration. Since each epitope can be associated with multiple records, each describing different assays and thus with different assay scores, the highest assay score, reflecting the highest level of validation reached for that epitope, was selected and carried forward.

In terms of scoring each epitope on the basis of the frequency by which it was recognized, we utilized a previously described Response Frequency (RF) score [18]. The RF score is calculated as

$$\frac{R - \sqrt{R}}{N}, \tag{1}$$

where N is the total of subjects tested and R is the number of positive responses. The square root is a correction factor, approximating one standard deviation for the number of

responding donors. This gives a higher score to epitopes studied with larger sample sizes. In case there is no information of subjects tested, the epitope will be assigned $R = 1, N = 1$ if the assay outcome is positive and $R = 0, N = 1$ if it was negative. The RF score (RFS) also takes into account all data for a given epitope across all publications. We decided to use an older and simpler RF definition, as compared to the one used in [19], as it is more suitable to filter epitopes based on their RFS. As an example, consider an epitope 1 with positive responses (P) = 1 and total subjects (T) = 1; the new definition gives a RFS = 1 (0.04–1.00) whereas the older version gives an RFS = 0. In contrast with epitope 2 with $P = 8$ and $T = 11$, the new version gives RFS = 0.73 (0.43 : 0.92) and the older RFS = 0.47. In order for the RFS to reflect the difference between epitopes 1 and 2 in terms of the total number of subjects, the latter should be assigned a higher score to be used for ranking and filtering the data, which at the end benefits the user giving simpler and useful results.

Both the assay score and RF score are calculated for each epitope and provided in the results. This allows further ranking or selecting epitopes based on different thresholds for these criteria.

2.3. Generation of Consensus Sequences for Overlapping and Nested MHC Class I and Class II Epitopes. For MHC class I epitopes, it is generally observed that a length of about 8–11 residues is optimal for T cell recognition and use in assays. Because of the structure of the class I binding groove, distinct class I sequences typically represent unique epitopes, even if they are nested within a longer sequence that is also recognized by T cells. Accordingly, for the present study, we have not subjected class I epitopes of nested or overlapping character to further processing.

For MHC class II epitopes, however, optimal epitopes are usually longer than the minimal T cell recognized 9-mer core. In general, class II epitopes are optimally of 13–20 residues in length [1]. Peptides of varying length but that carry the same core may all be similarly active and/or recognized by the same T cell specificity. Thus, many of the epitope structures contained in the IEDB for class II epitopes are redundant, nested or largely overlapping. For this reason, it is desirable to devise strategies to reduce the complexity of class II epitope sets. Here, we developed a clustering algorithm to generate consensus sequences or cluster of epitopes, an illustration of such a process can be found in Table 1. In order to solve this problem, our approach first sorts the peptides based on their RF scores. Then, taking the highest ranked peptide as starting sequence, we move down the ranked list aligning the sequences to find nested or overlapping epitopes by at least 9 residues. For this approach, we only consider identical matches over the region of overlap and identical nested peptides; given this definition, mismatches will be treated as separate epitopes. When a nested peptide is found, we will keep only the larger peptide and calculate a new RF score using the sum of all responded and tested subjects per epitope in the cluster. For overlapping epitopes, a consensus epitope or cluster will be generated combining the sequences, if the cluster length is up to 20 residues. In these cases, the RF score will be calculated as a new RF score as in the nested case. For the assay type scoring system, the highest ranked assay and application of all the assays associated with the set of nested epitopes will be considered.

Table 1: Example of a dataset reduction of MHC class II epitopes.

(a) Epitopes before being processed by the clustering tool; epitopes forming a potential consensus sequence or cluster are in bold

Epitope/cluster	RF score	Assay score
MLVLLVAVLVTAVYAFVHA	0.67	8
IQGNVTIHSLLDEGK	**0.66**	**8**
VPSPSMGRDIKVQFQSGGAN	0.65	12
NVTSIHSLLDEGKPT	0.63	12
QGNVTIHSLLDEGKPT	**0.59**	**12**
AQAAVVRFQEAANKQKQELD	0.47	12
GNVTSIHSLLDEG	**0.46**	**4**
FAGIEAAASAIQGNV	0.42	12

(b) The cluster generated by combining the sequences and associated information is in bold

Epitope/cluster	RF score	Assay score
MLVLLVAVLVTAVYAFVHA	0.67	8
VPSPSMGRDIKVQFQSGGAN	0.65	12
IQGNVTIHSLLDEGKPT	**0.57**	**12**
AQAAVVRFQEAANKQKQELD	0.47	12
FAGIEAAASAIQGNV	0.42	12

2.4. Human Study Subjects. In the case of donors with latent tuberculosis infection (LTBI), leukapheresis or whole unit blood samples from 10 adults were obtained from the University of California, San Diego, Antiviral Research Center (AVRC) clinic. Donors were classified as LTBI based on positive QuantiFERON-TB Gold In-Tube (Cellestis), as well as a physical exam and/or chest X-ray that was not consistent with active tuberculosis. Because Dengue virus (DENV) prevalence is low in the San Diego area, most LTBIs are DENV naïve.

To obtain DENV seropositive samples, anonymous blood donations from healthy adults were obtained by the National Blood Center, Ministry of Health, in the area of Colombo, Sri Lanka. Plasma of the associated donation was tested for serology using the flow-based U937+DC-SIGN neutralization assay (conducted at the University of North Carolina, Chapel Hill) as previously described [11, 20]. Because TB prevalence is low in the Colombo area, most DENV seropositive donors can be assumed to be TB negative.

All Samples were collected and used following guidelines from the Institutional Review Boards (IRB) of LJI and the Medical Faculty, University of Colombo (serving as National Institutes of Health-approved IRB for Genetech Research Institute).

2.5. Peptides and PBMC Isolation. 15-mer peptides were synthesized as crude material on a small (1 mg) scale by Mimotopes (Victoria, Australia) and/or A and A (San Diego).

PBMCs were purified by density gradient centrifugation (Ficoll-Hypaque, Amersham Biosciences) from 100 mL of leukapheresis sample or 450 mL of whole blood, according to manufacturer's instructions. Cells were cryopreserved in liquid nitrogen suspended in fetal bovine serum (Gemini Bio-products) containing 10% dimethyl sulfoxide.

2.6. Intracellular Cytokine Staining (ICS). PBMCs (2×10^6 cells/well) were incubated with peptide pools (1 μg/mL) for 2 hrs. Brefeldin A (1 μg/mL) (BD Bioscience) was added to the mixture and incubated for another 4 hours (i.e., a total of 6 hrs with peptide). Cells were then washed and stained for cell surface markers using anti-CD3-Alexa Fluor 700 (UCHT1), anti-CD8-V500 (RPA-T8) (both from BD Biosciences), anti-CD4-APC EFluor780 (RPA-T4), anti-CD45RA-EFluor450 (HI100), and anti-CCR7(CD197)-PerCPCy5.5 (G043H7) (all three from Affymetrix eBioscience) for 30 mins on ice. Cells were then washed, fixed with 4% paraformaldehyde, blocked with human sera, and stained for intracellular IFNγ using anti-IFNγ-FITC (4S.B3, Affymetrix eBiosciences). Samples were acquired on a BD LSR II flow cytometer. The frequency of cells responding to the TB/DENV-specific peptides was quantified by determining the total number of gated subset+ and cytokine+ cells and background values subtracted (as determined from the medium alone control) using FlowJo software (Tree Star).

3. Results and Discussion

3.1. Filtering Datasets to Select Human Peptidic Epitopes of Appropriate Size, Defined Restriction, and Assay Type. As a preliminary step towards deriving sets of reference epitopes associated with preferred validated assays, we processed the data contained in the IEDB relating to T cell epitopes. As of October 2014, a total of 28370 epitopes are associated with positive results in at least one T cell assay.

As an example of filtering strategies, we first considered only peptidic epitopes associated with infectious agents and allergies (Figure 1) and initially focused on bacteria, viruses, and nonhuman eukaryotes as epitope sources. Next, we only considered data in which humans were the host of the immune response and for which data was available to allow specifically characterizing responses as either class I or class II restricted. In the case of class I, we further considered only epitopes of 8–11 residues, and in the case of class II, only peptides of 13–20 residues were considered.

The next step in our process was to filter the results further by selecting epitopes that have been tested in "high quality" assays. This is possible because the IEDB curates the specific assays that are used to define and characterize the specific epitopes reported in the literature or provided to the database by direct submission. While obviously any desired assay set could be used, here we selected for inclusion the multimer/tetramer staining, ELISPOT and ICS assays. This assay-based filtering resulted in a final total of 6345 epitopes, 2512 and 3833 for class I and class II epitopes, respectively (Figure 1), representing about 20% of the initial 28370 epitopes.

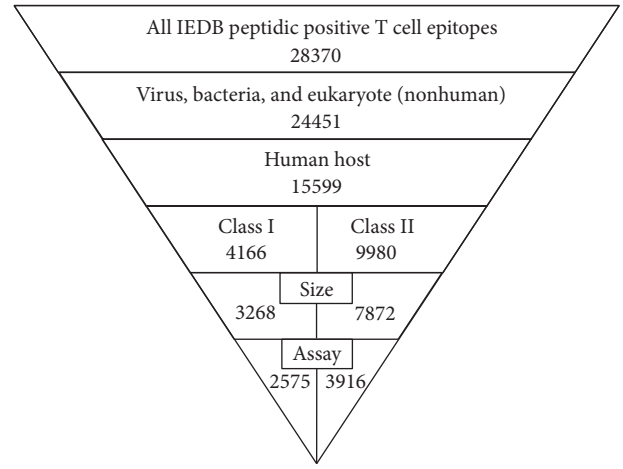

Figure 1: Diagram of the filtering steps towards the generation of the validated sets of epitopes, including the number of epitopes found in each step.

3.2. Identification of Epitope Categories Supported by Current IEDB Data. We surveyed the epitope data in the IEDB in terms of the species and antigens of provenance (epitope sources). For this purpose we adapted the categorization adopted by Seymour et al. [21]. The relative population of these categories in the IEDB as of the 2009 date was discussed by Davies et al. [22].

In Table 2, we list 43 categories for which at least ten class I or class II epitopes were identified for viruses/bacteria (Table 2(a)), nonhuman eukaryotes (Table 2(b)), and autoantigens (Table 2(c)). The data were further classified according to the source organism of the epitope. The number of epitopes contained in each category is also listed in Table 2. The table also lists B cell epitopes as identified and discussed further below.

3.3. Definition of Epitope Tables. As a result of the processes described above, we generated sets of epitopes for the various categories. As an example, Table 3 details the 21 epitopes defined for the Parvoviridae human class I category. In addition to the epitope sequence, source organism and protein, and MHC restriction, the IEDB Epitope ID is provided to facilitate retrieval of additional information from the IEDB pertaining to the epitope. Finally, the Response Frequency, Assay Score, the types of assay, and effector origin (*ex vivo* or *in vitro*), utilized to derive the Assay Score, are also given. All epitope tables from the categories shown in Table 2 can be found in the supplemental file "Epitope Tables.zip" in the Supplementary Material available online at http://dx.doi.org/10.1155/2015/763461.

3.4. Expanding the Tool to Address Autoimmune Epitopes, B Cell Epitopes, and Murine Epitopes. Having established the conceptual framework for selection of epitope sets, we next expanded our applicability. Autoimmune epitopes are identified by the fact that both source antigen and host organism are the same (e.g., both the T cells and the epitope

Table 2: (a) Number of epitopes per category for viruses and bacteria. (b) Number of epitopes per category for eukaryotes (nonhuman). (c) Number of epitopes per category for autoimmune epitopes (human and mouse).

(a)

	Class I		Class II		B cell			
					Linear		Discontinuous	
	HLA	H-2	HLA	H-2	Human	Mouse	Human	Mouse
Virus								
ssRNA (−) strand virus								
H1N1 subtype influenza A	41	77	207	206		15	11	27
H3N2 subtype influenza A	18	18	92	17		11	22	81
Other influenza A subtypes (not H3N2 or H1N1)	116	43	179	25		43	16	81
Influenza B/C			13					36
Paramyxoviridae (respiratory syncytial virus, measles, mumps)	47	80	28	27		33		71
Hantavirus	14							
ssRNA (+) strand virus								
Dengue virus	432	116	58	139		24	29	97
Hepatitis C virus	405	65	241	20	53	32	27	12
West Nile virus	33		99	103				24
Yellow fever	18	34	94	118				
Japanese encephalitis virus			33					
Picornaviridae (coxsackie, hepatitis A)	14	12		52		77		94
Coronaviruses	22	38	38	25	23	28		27
Retrotranscribing virus								
Hepatitis B virus	59	72	38	18		13		
Deltaretrovirus (HTLV)	25							
dsDNA virus								
Adenoviruses	13		45			10		
Alphaherpesvirinae (human herpesvirus 1/2, Varicellovirus)	91	52	35	13		32		32
Betaherpesvirinae (CMV, human herpesvirus 5, roseolovirus, murid herpesvirus)	204	48	141	20				
Gammaherpesvirinae (Epstein-Barr virus, *Rhadinovirus*, human herpesvirus 4)	237	63	59					
Papillomaviridae (human papillomavirus)	80	44	72			30		
Poxviridae (vaccinia, pox)	228	343	76	30				
Polyomavirus (Simian vacuolating virus)	31	14						
Parvoviridae	21		24		10			
Bacteria								
Actinobacteria/proteobacteria								
Alphaproteobacteria (Rhizobiales, *Rickettsia*, and *Anaplasmas*)			31					
Betaproteobacteria (*Neisseria*, *Bordetella*, and *Burkholderia*)			324	158		33		
Mycobacterium	129	33	478	33				11

(a) Continued.

	Class I		Class II		B cell			
					Linear		Discontinuous	
	HLA	H-2	HLA	H-2	Human	Mouse	Human	Mouse
Firmicutes/other bacteria								
Chlamydiales (chlamydia)	15	38				37		
Clostridiales			70					
Other Bacilli (anthracis, cereus, *Geobacillus*, and *Enterococcus*)			106			19		

(b)

	Class I		Class II		B cell			
					Linear		Discontinuous	
	HLA	H-2	HLA	H-2	Human	Mouse	Human	Mouse
Alveolata								
Plasmodium (*P. falciparum*, *P. vinckeia*, and *P. yoelli*)	64	29	186	33	16	49		
Euglenozoa								
Trypanosomatidae (*Trypanosoma*, *Leishmania*)	91	30		14				
Fungi								
Aspergillus			50	50	73			
Other fungi			77		54	11		
Plants								
Fabaceae (peas, soybean, peanut family)			17		419			
Betulaceae (birch family)			30		24			
Cupressaceae (cypress, cedar family)			21		22			
Gluten, coeliac Disease[1]			23		245	36		
Timothy-grass			474		19			
Other grass			98		124			
Amaranthaceae			20					
Animals								
Insects			67		23			
Arachnid			97		33	13	14	
Mammals		119	41	69	707	80		15

[1]Only epitopes derived from gliadin protein and high molecular weight glutenin [23] were included.

(c)

	Class I		Class II		B cell			
					Linear		Discontinuous	
	HLA	H-2	HLA	H-2	Human	Mouse	Human	Mouse
Rheumatoid arthritis	27		11					
Diabetes	73	76	46	17				
Multiple sclerosis			11		13			

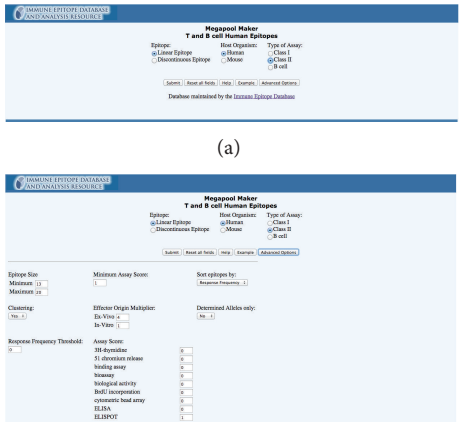

Figure 2: (a) Web application main page interface. (b) Web application "advanced options" page interface.

are originated from a human source). As listed in Table 2(c), all autoimmunity epitope categories relevant to a given disease are condensed into a single category. A protein tree functionality available on the IEDB [14] and a list of the most common antigens associated with each disease were used to extract autoimmune epitopes. The identified categories for which at least ten class I or class II epitopes were available are listed in Table 2(c), along with the number of epitopes contained in each category.

We considered expanding the scope of the study to also select epitopes recognized by species other than humans. In this case, the second most frequently represented host species is mouse. Accordingly, an option was created in the web application (next section) to allow selection of murine epitopes. The number of murine epitopes identified is listed as a separate column in Table 2.

Finally, we also expanded our analysis to allow selection of B cell/antibody epitopes. In this case, we set a 5 to 20 residue size window and initially selected X-ray structure, biological activity, and *in vivo* assays as most biologically relevant. In addition, we included induction of IgE subclass responses, as this type is most relevant in the context of allergic diseases. The number of B cell epitopes identified accordingly is also listed as a separate column in Table 2.

3.5. Implementation of a Web Application to Automatically Generate Epitope Sets. Finally, we developed a tool, which will be hosted by the IEDB as an additional link in the search results page and will be part of the next IEDB update release in fall 2015. This tool allows generation of specific epitope sets following the default criteria described above but also allows users to customize the generation of novel sets.

A sample screen shot of the main interface is shown in Figure 2(a). The main interface automatically obtains query results from IEDB searches and adds them to the query parameters of the tool. There, the user may choose to generate sets of class I, class II, antibody linear, or antibody discontinuous epitopes, relating to either human or mouse as the host organism from which the epitopes are derived. Because of the flexibility of the design, additional host organisms may be included, provided sufficient data becomes available in the literature. The user is offered results obtained with the default settings.

An "advanced options" webpage can be accessed from the main page, and a sample screen shot of this option is shown in Figure 2(b). In the advanced options, the user can set their custom RF score threshold and Assay score threshold, rank the results using the RF score or Assay Score, include the clustering tool, filtering by determined alleles (known MHC allele), and set the minimum and maximum size if the epitopes. Also, a number of additional assays, generally considered as being less rigorous, are provided, allowing the user to set custom parameters. Every field in the advance options dynamically changes to fit the default values for a given query. For example, if the user selects MHC class II epitopes, the web tool will set the clustering field to "yes" and the epitope size to 13–20.

3.6. Selection and Synthesis of Peptide Sets for Experimental Validation. To experimentally validate the usefulness of the tool we decided to synthesize some of the actual peptide sets identified by the tool and experimentally test them for recognition by human T cell responses. One of the main challenges for testing large pools for T cell recognition is that *ex vivo* T cells assays require relatively substantial amounts of each epitope (in the 1–0.1 microgram/mL range), compounded by the fact that peptide solubility in solvents most widely applicable to preparing peptide stock solutions, such as DMSO, is usually limited to about 20–40 mg/mL. Since solvents like DMSO are toxic in cellular assays at concentrations above 0.5%, this would seem to effectively limit the number of peptides that can be safely included in a pool to about 20.

However, in many cases the solubility of one peptide is not drastically influenced by the presence of other peptides (especially if the sequences, isolectric point, and general solubility are different). For this reason, we predicted that it might be possible to make pools of peptides already dissolved in a solvent like DMSO, mix the solutions, and relyophilize the pool of pools. Indeed, we routinely find these "sequentially lyophilized" pools, once resuspended, to be much more soluble than the individual components.

Accordingly, we synthetized a set of 207 EBV human CD8/class I epitopes, identified by the default setting described above (Supplemental Table 1A). In addition, we also synthetized a set of 92 CD8/class I epitopes derived from DENV virus, obtained by selecting only peptides with RF >= 0.01 (Supplemental Table 1B), and a set of 86 epitopes CD4/class II epitopes derived from *Mycobacterium tuberculosis*, based on an RF score >= 0.1 and being recognized *ex vivo* (Supplemental Table 1C).

3.7. Experimental Validation of the Use of Reference Epitope Sets to Detect T Cell Reactivity Ex Vivo. Peptides corresponding to these three sets of epitopes were pooled and tested with human PBMC as a source of T cells. For these experiments

Table 3: Parvoviridae virus validated epitope set downloaded from the web tool.

Epitope/cluster	Epitope ID	Source organism	Source protein	MHC restriction	RF score	Assay score	Assay type	Effector origin
FYTPLADQF	18474	Human parvovirus B19	Noncapsid protein NS-1	HLA-A*24:02	0.51	12	Multimer/tetramer, 51 chromium, ELISPOT	Direct *ex vivo*, cell line/clone
GLCPHCINV	20786	Human parvovirus B19	Noncapsid protein NS-1	HLA-A*02:01, HLA-A2	0.46	4	ELISPOT, 51 chromium	Direct *ex vivo*
QPTRVDQKM	51981	Human parvovirus B19	Noncapsid protein NS-1	HLA-B35	0.29	3	ELISPOT, 51 chromium, multimer/tetramer	Cell line/clone
LLHTDFEQV	37397	Human parvovirus B19	Noncapsid protein NS-1	HLA-A*02:01, HLA-A2	0.21	4	ELISPOT, 51 chromium	Direct *ex vivo*
TAKSRVHPL	62900	Human parvovirus B19	Viral protein 2	HLA-B8	0.12	4	ELISPOT, 51 chromium	Direct *ex vivo*
TEADVQQWL	63285	Human parvovirus B19	Noncapsid protein NS-1	HLA-B40	0.1	4	ELISPOT, 51 chromium	Direct *ex vivo*
SSHSGSFQI	61077	Human parvovirus B19	Noncapsid protein NS-1	HLA-Class I	0	4	ELISPOT, 51 chromium	Direct *ex vivo*
SESSFFNLI	57628	Human parvovirus B19	Noncapsid protein NS-1	HLA-B40	0	4	ELISPOT	Direct *ex vivo*
VQQWLTWCN	70634	Human parvovirus B19	Noncapsid protein NS-1	HLA-Class I	0	4	51 chromium, ELISPOT	Direct *ex vivo*
VPQYGYLTL	70458	Adeno-associated virus - 2	Major coat protein VP1	HLA-B*07:02	0	2	ICS, biological activity, ELISA	Short term restimulated
SALKLAIYKA	56861	Human parvovirus B19	Noncapsid protein NS-1	HLA-Class I	0	8	RNA/DNA detection, ICS	Direct *ex vivo*
TEADVQQWLTW	63286	Human parvovirus B19	Non-capsid protein NS-1	HLA-B44	0	4	ELISPOT	Direct *ex vivo*
QSALKLAIYK	52287	Human parvovirus B19	Noncapsid protein NS-1	HLA-Class I	0	8	ICS	Direct *ex vivo*
IDTCISATFR	25677	Human parvovirus B19	Noncapsid protein NS-1	HLA-Class I	0	4	ELISPOT	Direct *ex vivo*
HAKALKERMV	23542	Human parvovirus B19	Noncapsid protein NS-1	HLA-Class I	0	4	ELISPOT	Direct *ex vivo*
GLFNNVLYH	20861	Human parvovirus B19	Noncapsid protein NS-1	HLA-Class I	0	4	51 chromium, ELISPOT	Direct *ex vivo*
LHTDFEQVM	36432	Human parvovirus B19	Noncapsid protein NS-1	HLA-Class I	0	4	ELISPOT, 51 chromium	Direct *ex vivo*
LLHTDFEQVM	37398	Human parvovirus B19	Noncapsid protein NS-1	HLA-A*02:01	0	8	ICS	Direct *ex vivo*

Table 3: Continued.

Epitope/cluster	Epitope ID	Source organism	Source protein	MHC restriction	RF score	Assay score	Assay type	Effector origin
GLCPHCINVG	20787	Human parvovirus B19	Noncapsid protein NS-1	HLA-Class I	0	8	ICS, RNA/DNA detection	Direct *ex vivo*
EADVQQWLT	11014	Human parvovirus B19	Noncapsid protein NS-1	HLA-Class I	0	4	ELISPOT, 51 chromium	Direct *ex vivo*
RMTENIVEV	145986	Human parvovirus 4	ORF1	HLA-A*02:01	0	12	Multimer/tetramer, ICS	Short term restimulated, direct *ex vivo*

we selected PBMC from 5 individuals infected with DENV virus and likely uninfected with TB (see methods for details) and PBMC from 5 LTBI individuals and likely uninfected with DENV. Because of the high incidence of EBV infection worldwide [24], we assumed that most if not all individuals tested would be latently infected with EBV.

PBMC were stimulated with the DENV CD8 pool, MTB CD4 pool, and EBV CD8 pool. After *ex vivo* stimulation, the IFNγ response was measured by ICS (Figures 3(a)–3(d)). The gating strategy for these experiments is presented in Figure 3(a). Representative plots of the responses for both $CD4^+$ and $CD8^+$ T cells are shown for a LTBI donor (Figure 3(b)) and a DENV donor (Figure 3(c)). The IFNγ responses induced by each epitope pool in the relevant CD4/CD8 compartments for all donors tested are summarized in Figure 3(d). In the case of the MTB CD4 pool, *ex vivo* CD4 but not CD8 T cell responses were seen in the LTBI ($P = 0.004$) and DENV donors. The reactivity was lower in the DENV donors than in the LTBI donors ($P = 0.03$). This lower, but detectable, reactivity is explained by the fact that the DENV seropositive individuals are vaccinated against MTB with *M. bovis* BCG and are likely exposed to nontuberculous mycobacteria [25]. In the case of the DENV CD8 pool, CD8 T cell responses, but not CD4, were detected in 3 out of 5 DENV donors. This *ex vivo* reactivity in 3 out of 5 donors is in line with what was detected in previous studies [11]. As expected, no CD4 responses were seen to the CD8 DENV pool, as also low CD8 and CD4 T cell reactivity was noted in the MTB donors with the DENV CD8 pool. Finally, as also expected, in both cohorts reactivity was detected against the EBV CD8 pool in CD8 but not in CD4 T cells ($P = 0.004$ for LTBI and $P = 0.05$ for DENV).

4. Conclusions

We devised a strategy that allows automatically filtering datasets to select epitopes of appropriate size, defined restriction, and assay type for use in characterizing responses to specific indications. While querying the IEDB database can also generate these sets, a certain degree of complexity in the queries and the setting of multiple parameters would be necessary. In our application, the epitope sets are automatically generated, while the user is still enabled to change the default settings to generate validated epitope sets matching specific criteria.

We further identified which epitope categories are supported by current IEDB data, and found that reference epitope sets could be produced for 43 categories with data currently available in the IEDB. The number of such categories, broadly based on previous epitope classification work [21], is undoubtedly destined to grow, allowing an ever more comprehensive study of immune responses in a broad variety of experimental systems. To further illustrate the broad applicability of the approach, we also extended our work to address autoimmune epitopes, B cell epitopes, and murine epitopes.

While these actual epitope sets are provided as tables within the paper, we implemented a web application to automatically generate epitope sets, based on the fact that the IEDB content is rapidly growing and new epitopes are added to the IEDB in each of its biweekly updates. We plan to continuously gather feedback on this web application from the scientific community, and to implement changes and modifications through the main IEDB website [14].

Finally, to illustrate applicability in an actual experimental setting, we selected and synthesized peptide sets corresponding to EBV, DENV, and MTB epitopes. These epitope sets were used to measure immune reactivity in human cells. The experimental testing of these epitope sets demonstrated the applicability of these sets as a valuable resource to allow detection of T cell responses *ex vivo*. As such, these sets of epitopes represent potentially valuable resources for diagnostic purposes, as well as for further detailed characterization of the immune response to specific targets of immunological interest.

Conflict of Interests

The authors declare that they have no conflict of interests in the research.

Acknowledgment

This project has been funded with federal funds from the National Institute of Allergy and Infectious Diseases,

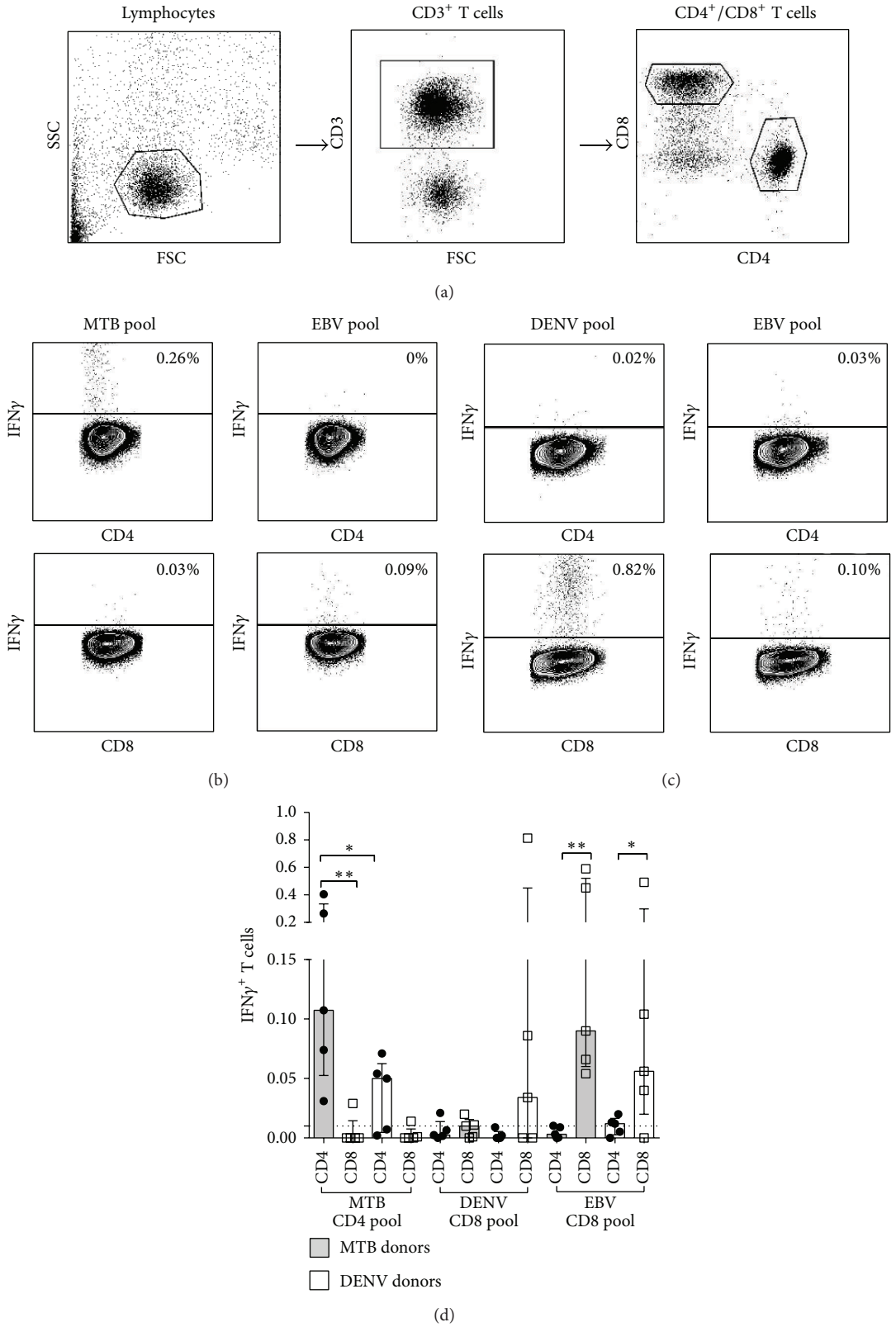

Figure 3: Predicted epitope pools induce a detectable *ex vivo* cytokine response. PBMC from donors with LTBI (MTB donor) or previously exposed to DENV were stimulated with their respective epitope pools and an EBV epitope pool. After *ex vivo* stimulation, the IFNγ response was measured by ICS using flow cytometry. Gating strategy (a) and representative plots of the responses for both $CD4^+$ and $CD8^+$ T cells are shown for a MTB donor (b) and DENV donor (c). (d) The ICS IFNγ responses induced by each epitope pool for all donors tested are summarized ($n = 10$). Statistical difference was determined using a one-tailed Mann-Whitney test. ($^*P \leq 0.05$; $^{**}P \leq 0.01$).

National Institutes of Health, and Department of Health and Human Services under Contract nos. HHSN272201200010C, HHSN272200900044C, and HHSN27220140045C and Grant no. U19 AI100275.

References

[1] D. R. Madden, "The three-dimensional structure of peptide-MHC complexes," *Annual Review of Immunology*, vol. 13, pp. 587–622, 1995.

[2] J. Neefjes, M. L. M. Jongsma, P. Paul, and O. Bakke, "Towards a systems understanding of MHC class i and MHC class II antigen presentation," *Nature Reviews Immunology*, vol. 11, no. 12, pp. 823–836, 2011.

[3] C. Kurts, B. W. Robinson, and P. A. Knolle, "Cross-priming in health and disease," *Nature Reviews Immunology*, vol. 10, no. 6, pp. 403–414, 2010.

[4] L. Borish, "Genetics of allergy and asthma," *Annals of Allergy, Asthma & Immunology*, vol. 82, no. 5, pp. 413–426, 1999.

[5] J.-M. Andrieu, S. Chen, C. Lai, W. Guo, and W. Lu, "Mucosal SIV vaccines comprising inactivated virus particles and bacterial adjuvants induce $CD8^+$ T-regulatory cells that suppress SIV-positive $CD4^+$ T-cell activation and prevent SIV infection in the macaque model," *Frontiers in Immunology*, vol. 5, article 297, 2014.

[6] J. Patterson-Bartlett, M. J. Levin, N. Lang, F. P. Schödel, R. Vessey, and A. Weinberg, "Phenotypic and functional characterization of ex vivo T cell responses to the live attenuated herpes zoster vaccine," *Vaccine*, vol. 25, no. 41, pp. 7087–7093, 2007.

[7] T. Prezzemolo, G. Guggino, M. P. la Manna, D. D. di Liberto, F. Dieli, and N. Caccamo, "Functional signatures of human CD4 and CD8 T cell responses to Mycobacterium tuberculosis," *Frontiers in Immunology*, vol. 5, article 180, 2014.

[8] A. Sette and R. Rappuoli, "Reverse vaccinology: developing vaccines in the era of genomics," *Immunity*, vol. 33, no. 4, pp. 530–541, 2010.

[9] C. Leisner, N. Loeth, K. Lamberth et al., "One-pot, mix-and-read peptide-MHC tetramers," *PLoS ONE*, vol. 3, no. 2, Article ID e1678, 2008.

[10] P. Braendstrup, B. K. Mortensen, S. Justesen et al., "Identification and HLA-tetramer-validation of human $CD4^+$ and $CD8^+$ T cell responses against HCMV proteins IE1 and IE2," *PLoS ONE*, vol. 9, no. 4, Article ID e94892, 2014.

[11] D. Weiskopf, M. A. Angelo, E. L. De Azeredo et al., "Comprehensive analysis of dengue virus-specific responses supports an HLA-linked protective role for $CD8^+$ T cells," *Proceedings of the National Academy of Sciences of the United States of America*, vol. 110, no. 22, pp. E2046–E2053, 2013.

[12] C. Oseroff, J. Sidney, M. F. Kotturi et al., "Molecular determinants of T cell epitope recognition to the common Timothy grass allergen," *Journal of Immunology*, vol. 185, no. 2, pp. 943–955, 2010.

[13] R. Vita, L. Zarebski, J. A. Greenbaum et al., "The immune epitope database 2.0," *Nucleic Acids Research*, vol. 38, no. 1, Article ID gkp1004, pp. D854–D862, 2009.

[14] R. Vita, J. A. Overton, J. A. Greenbaum et al., "The immune epitope database (IEDB) 3.0," *Nucleic Acids Research*, vol. 43, pp. D405–D412, 2015.

[15] E. J. Novak, A. W. Liu, J. A. Gebe et al., "Tetramer-guided epitope mapping: rapid identification and characterization of immunodominant CD4+ T cell epitopes from complex antigens," *Journal of Immunology*, vol. 166, no. 11, pp. 6665–6670, 2001.

[16] C. L. Day, N. P. Seth, M. Lucas et al., "Ex vivo analysis of human memory CD4 T cells specific for hepatitis C virus using MHC class II tetramers," *The Journal of Clinical Investigation*, vol. 112, no. 6, pp. 831–842, 2003.

[17] W. W. Kwok, M. Roti, J. H. DeLong et al., "Direct ex vivo analysis of allergen-specific $CD4^+$ T cells," *Journal of Allergy and Clinical Immunology*, vol. 125, no. 6, pp. 1407.e1–1409.e1, 2010.

[18] Y. Kim, K. Vaughan, J. Greenbaum, B. Peters, M. Law, and A. Sette, "A meta-analysis of the existing knowledge of immunoreactivity against hepatitis C virus (HCV)," *PLoS ONE*, vol. 7, no. 5, Article ID e38028, 2012.

[19] A. Bresciani, J. Greenbaum, C. S. L. Arlehamn, A. Sette, M. Nielsen, and B. Peters, "The interplay of sequence conservation and T cell immune recognition," in *Proceedings of the 5th ACM Conference on Bioinformatics, Computational Biology, and Health Informatics (BCB '14)*, pp. 739–743, Newport Beach, Calif, USA, September 2014.

[20] R. de Alwis and A. M. de Silva, "Measuring antibody neutralization of dengue virus (DENV) using a flow cytometry-based technique," *Methods in Molecular Biology*, vol. 1138, pp. 27–39, 2014.

[21] E. Seymour, R. Damle, A. Sette, and B. Peters, "Cost sensitive hierarchical document classification to triage PubMed abstracts for manual curation," *BMC Bioinformatics*, vol. 12, no. 1, article 482, 2011.

[22] V. Davies, K. Vaughan, R. Damle, B. Peters, and A. Sette, "Classification of the universe of immune epitope literature: representation and knowledge gaps," *PLoS ONE*, vol. 4, no. 9, Article ID e6948, 2009.

[23] M. F. Kagnoff, "Celiac disease: pathogenesis of a model immunogenetic disease," *The Journal of Clinical Investigation*, vol. 117, no. 1, pp. 41–49, 2007.

[24] H. Hjalgrim, J. Friborg, and M. Melbye, "The epidemiology of EBV and its association with malignant disease," in *Human Herpesviruses: Biology, Therapy, and Immunoprophylaxis*, A. Arvin, G. Campadelli-Fiume, E. Mocarski, P. S. Moore, B. Roizman, and R. Whitley, Eds., Cambridge University Press, Cambridge, UK, 2007.

[25] C. S. Lindestam Arlehamn, S. Paul, F. Mele et al., "Immunological consequences of intragenus conservation of *Mycobacterium tuberculosis* T-cell epitopes," *Proceedings of the National Academy of Sciences of the United States of America*, vol. 112, no. 2, pp. E147–E155, 2015.

Hindawi Publishing Corporation
Journal of Immunology Research
Volume 2015, Article ID 761820, 13 pages
http://dx.doi.org/10.1155/2015/761820

Review Article

Peptide-Based Treatment: A Promising Cancer Therapy

Yu-Feng Xiao, Meng-Meng Jie, Bo-Sheng Li, Chang-Jiang Hu, Rui Xie, Bo Tang, and Shi-Ming Yang

Department of Gastroenterology, Xinqiao Hospital, Third Military Medical University, Chongqing 400037, China

Correspondence should be addressed to Shi-Ming Yang; shimingyang@yahoo.com

Received 26 September 2014; Accepted 14 December 2014

Academic Editor: Masha Fridkis-Hareli

Many new therapies are currently being used to treat cancer. Among these new methods, chemotherapy based on peptides has been of great interest due to the unique advantages of peptides, such as a low molecular weight, the ability to specifically target tumor cells, and low toxicity in normal tissues. In treating cancer, peptide-based chemotherapy can be mainly divided into three types, peptide-alone therapy, peptide vaccines, and peptide-conjugated nanomaterials. Peptide-alone therapy may specifically enhance the immune system's response to kill tumor cells. Peptide-based vaccines have been used in advanced cancers to improve patients' overall survival. Additionally, the combination of peptides with nanomaterials expands the therapeutic ability of peptides to treat cancer by enhancing drug delivery and sensitivity. In this review, we mainly focus on the new advances in the application of peptides in treating cancer in recent years, including diagnosis, treatment, and prognosis.

1. Introduction

Peptides are molecules formed by combinations of amino acids linked by peptide bonds through the dehydration-condensation reaction. Peptides can be obtained conveniently from the products of proteolysis, direct synthesis by the body, or artificial synthesis [1]. Peptides play a large role in the treatment of diseases. Peptide-based therapy has been applied in various diseases, such as allergic diseases, infectious diseases, autoimmune diseases, fibrosis, and asthma. There are several advantages of peptides, such as easy availability and convenient purification and storage [2–4]. Peptide-based therapies have been tested in both in vitro and in vivo experimental models, and some may present promising outcomes. Larché demonstrated the basic mechanisms and feasibility of peptide therapy for allergic diseases [2]. Additionally, Iikuni et al. demonstrated encouraging efficacy using anti-DNA immunoglobulin peptide therapy against systemic lupus erythematosus (an autoimmune disease) in murine models [1]. Moreover, Oh and Lee reported the combined use of HMGB-1 box A peptide and S1PLyase siRNA in the treatment of acute lung injury [5]. Similarly, Nojiri et al. also certified that atrial natriuretic peptide (ANP) was significantly useful in inhibiting lipopolysaccharide-induced acute lung injury [6].

In addition, peptides also play an important role in cancer, including early diagnosis, prognostic predictors, and the treatment of cancer patients. Unlike other therapies, peptides show superiority due to their specificity. Recently, peptide-based therapy against cancer, such as peptide vaccines, has attracted increased attention [7]. Since sipuleucel-T was accepted by the US Food and Drug Administration (FDA) as the first standard peptide vaccine for prostate tumors, an increasing number of clinical trials have been conducted in many other cancer types, such as melanoma, glioblastoma, breast cancer, and gastric cancer [8]. However, the clinical response is considered limited and most of the current clinical trials showed limited efficacy [9]. Therefore, many novel methods, such as the combination with nanomaterials and chemotherapy, personalized peptide vaccination, and improved delivery systems, have been attempted in clinical trials and some may prolong the survival of cancer patients or result in tumor regression and show enhanced clinical efficacy.

In this view, we summarize the new progress of peptides in the application of cancer diagnosis (Table 1), prognostic

Table 1: Peptides applied in cancer diagnosis.

Cancer	Peptide	Year	Author	Reference
Pancreatic cancer	uMMP-2 and uTIMP-1	2014	Roy et al.	[10]
	MIC-1/GDF15	2014	Wang et al.	[11]
	RGS6	2014	Jiang et al.	[12]
Gastric cancer	LGR5	2013	Zheng et al.	[13]
	PGI/II, CA242	2014	Lu et al.	[14]
Prostate cancer	EN2	2013	McGrath et al.	[15]
	UCP2	2013	Li et al.	[16]
Breast cancer	HER-2	2014	Boku	[17]
	MUC1	2011	Zanetti et al.	[18]
Colorectal cancer	HNP1-3	2006	Albrethsen et al.	[19]
	CPAA-783-EPPT1	2012	Bloch et al.	[20]
	Serum C-peptide	2014	Comstock et al.	[21]
Lung cancer	Linear peptide antigen derived from ANXA1	2014	Wang et al.	[22]
	C-peptide in serum	2014	Zhang et al.	[23]
	11 novel peptides	2014	McGuire et al.	[24]
	Peptides from variable parts of antibodies	2014	de Costa et al.	[25]
	HCBP-1	2014	Wang et al.	[26]

predictors, and novel peptide therapies for cancer patients. We also discuss the prognosis and adverse effects of peptide vaccines in clinical trials.

2. Peptides and Colorectal Cancer

Colorectal cancer (CRC) is one of the most common cancers in the world, and it causes approximately 500,000 deaths worldwide per year, according to a recent report. Patients with metastatic CRC have a low 5-year survival rate, and early diagnosis of CRC leads to a better prognosis [19, 56]. At present, peptides also play an important role in CRC diagnosis. FITC-labeled peptide EPPT1 was linked to cationic polyacrylamide (CPAA) to form CPAA-783-EPPT1, which can target the cell transmembrane underglycosylated MUC-1 protein in the colorectal cell lines HT-29 and LS-174T [20]. In addition, in a recent clinical study, human neutrophil peptides 1–3 (HNP1–3) were reported to be present at high concentrations in CRC tissue, especially in Dukes' stages C and D [19]. Additionally, Comstock et al. also reported that a high concentration of serum C-peptide indicates a high risk of an adenoma in males [21]. These data suggested that peptides could be used as biomarkers for detecting CRC.

In addition to their function in the detection of CRC, peptides have also demonstrated their ability to treat CRC. Atrial natriuretic peptide (ANP), one of the cardiac and vascular derived peptide hormones, was reported to be a potential drug for CRC because it has antiproliferative effects in CRC cells [37]. Neovascularization is essential for tumor growth, and the neovasculature has been an attractive target for anticancer therapy. Li et al. reported that a peptide called TCP-1 could specifically target the blood vessels in tumor tissues [38]. Interestingly, they also found that TCP-1 could also deliver fluorescein and drugs for imaging detection and apoptosis in CRC, respectively [38]. Their findings suggested that TCP-1 could be a promising peptide for CRC therapy because it could carry anticancer drugs specifically to CRC tissue, without binding to normal tissue. In addition, Wang et al. also reported that F56 peptide conjugated nanoparticles loading vincristine (F56-VCR-NP) could target both primary lesions and the neovasculature of lung metastases, causing apoptosis of the neovasculature and necrosis of the CRC tissue [39].

Interestingly, peptides present in nondigestible fractions (NDF) of the common bean were reported to have an antiproliferative effect via increased p53 expression in a human CRC cell line [50]. In addition, researchers from the same team also found that the peptides in NDF from common beans could cause different gene expression in a human CRC cell line, which was related to cell death and survival, the cell cycle, cell proliferation, and so forth, leading to the induction of apoptosis and cell death. Their reports indicated that the role of peptides from the common bean could be used for anticancer treatment in CRC.

Additionally, the vaccine made by combined peptides has been well studied in treating CRC. Inoda et al. reported that the combined use of three peptides (Cep55/c10orf3_193(10), Cep55/c10orf3_402(11), and Cep55/c10orf3_283(12)) was effective in HLA-A24-positive CRC [51]. Recently, Hazama et al. reported a "peptide cocktail" treatment in CRC patients. In this study, researchers showed an improved median overall survival time in patients who received an injection of the "peptide cocktail" compared with the control group [57]. Then, in the following research, Hazama and colleagues found that the interleukin-6 level was increased due to the peptide vaccine, and it could also predict good prognosis in patients who accepted the peptide vaccine [52]. Similarly, Okuno et al. also reported that a 7-peptide cocktail vaccine with oral chemotherapy demonstrated an improved outcome in patients with metastatic CRC, as these subjects had a longer survival time compared with the control group [53].

From these data, we conclude that peptides could be used in detecting and treating CRC, and the combined use of peptides was most effective, including both peptides bound with a drug and the use of a "peptide cocktail" vaccine.

3. Peptides and Lung Cancer

Lung cancer is the leading cause of cancer-related mortality, and the 5-year survival remains low despite new therapies [58, 59]. The detection of lung cancer in early stages has attracted much attention in recent years. It has been many years since a peptide was first used as a predictor of lung cancer [60]. In recent years, new peptides have also demonstrated their ability in detecting lung cancer. Wang et al. reported that the linear peptide antigen derived from annexin A1 was higher in patients with non-small-cell lung cancer (NSCLC), compared with control subjects [22]. Zhang and colleagues also found that C-peptide in the serum was higher in patients with lung cancer, especially in the small cell lung cancer group, the stage III-IV group, and patients with lung cancer and diabetes [23]. Additionally, McGuire et al. found 11 novel peptides that specifically bind to a series of human NSCLC cell lines and are involved in a number of pathways, indicating that these peptides could be used as predictors for NSCLC [24]. Interestingly, peptides could also be used as carriers, because they have specific binding sites. Gniazdowska et al. reported that the vasopressin peptide conjugated with 99mTc (99mTc(NS3)(CN-AVP(an))) could be used as an ideal compound for imaging small cell lung cancer (SCLC) cells with its high stability and novel binding to the SCLC cell line H69 [61]. In addition, Hong et al. also found that 131I-anti-ProGRP(31–98)scFv, which can bind to progastrin-releasing peptide(31–98) (ProGRP(31–98)), had a high level of selective uptake by tumor tissues, but a low level in normal tissues, indicating that it could be used for SCLC radioimmunoimaging [62]. Impressively, de Costa et al. first found that peptides generated from variable antibodies were shared among lung cancer patients but not a control group [25], suggesting that these peptides could be novel biomarkers for screening lung cancer. Evidence also showed that the peptide HCBP-1 has exhibited specific binding to lung cancer stem cells, suggesting that this peptide may be used to identify lung cancer stem cells and as a drug carrier to lung cancer stem cells [26].

Peptides can also be used to treat lung cancer. Takahashi et al. reported that the dendritic cell vaccines pulsed with Wilms' tumor-1 peptide significantly improved the survival period of patients with advanced NSCLC [40]. Additionally, Kotsakis et al. also reported that the hTERT-targeting Vx-001 vaccine, which is a vaccine consisting of a TERT572Y optimized cryptic peptide that restricts target HLA-A*0201, could induce strong immune responses and improve the clinical outcome of the majority of NSCLC HLA-A2 (+) patients [41]. Recently, Ahsa et al. also reported that the synthesized peptide Disruptin decreased the clonogenicity of EGFR-dependent cancer cells [42]. They also found that Disruptin could inhibit the microvessel density in lung cancer cell line H1975 xenografts [42], indicating that Disruptin could be a potential drug for EGFR positive cancer. Similarly, Sigalov also designed a ligand-independent peptide-based TREM-1 (triggering receptor expressed on myeloid cells-1) inhibitor to specifically silence TREM-1, and this peptide delayed tumor growth in xenograft models of human NSCLC [43].

Interestingly, peptides from natural sources were also able to treat lung cancer. The peptide fractions from high oleic acid soybean showed an inhibitory effect in cancer cells (including colon cancer, liver cancer, and lung cancer), and this effect was dose dependent [54]. Additionally, peptides from the venom of the Eastern green mamba have toxic effects against the human NSCLC cell line A549 [55].

With the development of nanotechnology, peptides that are conjugated with nanomaterials have exhibited a great potential in treating diseases, especially cancer. Chittasupho et al. reported that a synthetic compound (LFC131-DOX NPs), which contained a peptide (LFC131, an inhibitor of CXCR4), PLGA nanoparticles, and doxorubicin, could specifically bind to the human lung cancer cell line A549, indicating that LFC131-DOX NPs could be used as a drug delivery system in treating lung cancer [44]. In addition, Guan and colleagues also reported that TH10 peptide conjugated nanoparticles loading docetaxel (TH10-DTX-NP) showed therapeutic efficacy in inhibiting vascular pericytes in a mouse lung metastasis model, indicating that TH10-DTX-NP could be a potential drug for treating cancer [46]. Similarly, Wang et al. also reported that bradykinin-potentiating peptide (BPP) decorated chitosan nanoparticles could enhance vascular permeability in tumors, resulting in drug accumulation in tumors and prolonging survival [45].

4. Peptides and Pancreatic Cancer

Pancreatic cancer (PC) remains a deadly malignant disease, with a 6% five-year survival rate, and increased incidence and mortality in recent years [63]. It has an extremely poor prognosis due to many factors, including low diagnosis rate, a high rate of metastasis, and the poor efficacy of conventional treatments [64].

Evidence showed that urinary matrix metalloproteases (uMMP-2) and urinary tissue inhibitor of metalloproteases (uTIMP-1) can be used to detect PC, and uTIMP-1 may be used to distinguish between pancreatic ductal adenocarcinoma (PDAC) and pancreatic neuroendocrine tumors [10]. Wang et al. reported that macrophage inhibitory cytokine 1 (MIC-1/GDF15) was overexpressed in PDAC tissues and may be a novel biomarker to screen for PDAC [11]. Moreover, Jiang et al. demonstrated that the expression of RGS6 was low in PC patients [12]. In general, the peptides mentioned above may serve as novel diagnostic biomarkers in PC.

Rothenberg et al. have identified that gemcitabine, as a first-line treatment, can improve the survival rate and quality of life in cases of advanced pancreatic cancer. However, the median survival and one-year survival rate were approximately 6 months and 18%, respectively [65]. In recent years, peptide-based vaccines, which elicit a specific anticancer response, have been considered to be a promising treatment option. Tumor-associated antigens (TAAs) can be recognized by the immune system and thus result in the disturbance

of cancer cells or even tumor regression [66]. However, peptide vaccines showed limited clinical efficacy, influenced by the ability of tumor cells to escape recognition by the immune system [66]. Multiple mechanisms might contribute to immune escape such as a loss or downregulation of molecules, including tumor antigens and human leukocyte antigen (HLA) [67]. To date, some novel potential solutions or modulations have been proposed, such as the modification of TAA peptides, vaccines against multiple TAA epitopes, and the combination of chemotherapy [66].

Recently, the Wilms tumor gene (WT1) peptide-based vaccine in combination with gemcitabine was found to be more effective than gemcitabine alone. The median survival and one-year survival rate of the combination therapy were 8.1 months and 29%, respectively [27]. WT1 is overexpressed in PC cells, and the WT1 protein acts similarly to TAA and is targeted by specific effector T cells in immunotherapies. WT1-specific cytotoxic T lymphocytes (CTLs) against PC cells and delayed type hypersensitivity (DTH) were induced in response to the WT1 peptide-based vaccine. Through the release of perforins and granzymes as well as FasL/Fas interactions, the target tumor cells were eliminated and regressed. Moreover, CTLs specific for WT1 only act on cells with elevated expression of WT1 but do not damage normal cells, such as hematopoietic cells [68]. Therefore, the WT1 vaccine has no significantly adverse effects on hematopoiesis [68].

Gemcitabine induces cell apoptosis through inhibiting DNA synthesis [69]. The drug has many immune-modulating functions, such as the selective depletion of B lymphocytes, the reinforcement of T-cell recall responses, the reduction of regulatory T-cells, and an increase in the cross-presentation and cross-priming of tumor antigens [70–72]. Furthermore, gemcitabine upregulates the expression of WT1 and enhances the sensitivity of pancreatic cancer cells to CTL-mediated killing [64, 73].

WT1 peptide-based vaccines upregulate WT1-specific CTLs, and gemcitabine contributes to the amplification of CTL proliferation and the antitumor response. Thus, the combination of the WT1 vaccine with gemcitabine was synergistic [73]. Nishida et al. proved that longer survival was significantly interrelated with a positive DTH to WT1 peptides, and a high frequency of memory-phenotype WT1-specific CTLs was observed among DTH-positive patients [27]. Positive DTH to WT1 and a higher frequency of memory-phenotype WT1-CTLs could serve as two useful prognostic markers of effective clinical results [27]. In addition, the WT1 vaccine led to pain relief and alleviated distressing symptoms. The side effects of combination therapy resemble those of gemcitabine alone except for topical skin reactions [27]. The combination of chemotherapy with immunotherapy against cancer proved to be effective and synergistic.

In addition, Suzuki et al. reported that a KIF20A-derived peptide combined with gemcitabine increased the number of peptide-specific IFN-γ producing cells and indicated promising clinical outcomes in advanced PC patients [28]. Moreover, a mixture of a telomerase (GV1001) vaccine and gemcitabine was found to be safe, however, with a weak and transient immune response [29].

5. Peptides and Gastric Cancer

In spite of decreased incidence and death rates of gastric cancer worldwide in recent years, gastric cancer still has high incidence rates, especially in Eastern Asia, Eastern Europe, and South America [63]. The incidence of gastric carcinoma has notably decreased due to improved hygiene leading to lower rates of *H. pylori* infection, the popularization of refrigeration, and reduced smoking rates [74]. Chemotherapy, such as docetaxel, cisplatin, 5-fluorouracil, and S-1, is the conventional treatment for advanced, recurrent, or unresectable gastric carcinoma and shows poor clinical prognosis [75]. Since the acceptance of Provenge (sipuleucel-T) as the first cancer vaccine in prostate cancer by the FDA, peptide vaccine therapy was widely attempted in other cancers, such as colorectal, pancreatic, and gastric cancer [8].

Peptides are capable of detecting and diagnosing cancer. Zheng and his colleagues reported that leucine-rich repeat-containing G protein-coupled receptor 5 (LGR5) levels were significantly elevated in gastric cancer tissues, thus serving as an early diagnostic biomarker [13]. In addition, the detection of serum pepsinogen I (PGI), pepsinogen II (PGII), and carbohydrate antigen 242 (CA242) may be useful in diagnosing gastric cancer [14].

Recently, clinical trials in patients with gastric cancer (GC) have been conducted using peptide-based vaccines, including vascular endothelial growth factor receptor 2-(VEGFR2-) 169, VEGFR1-1084, and lymphocyte antigen 6 complex locus K (LY6K-177) epitope peptides [30, 31].

VEGF is highly expressed in endothelial cells of newly formed tumor vessels and is considered to be a tumor angiogenic and vasculogenic factor [76]. VEGFR2 is responsible for mitogenesis, angiogenesis, and permeability-enhancing activity by binding with VEGF, while VEGFR1 plays a negative role in VEGF-induced responses by inhibiting the binding of VEGFR2 with VEGF [77]. A peptide vaccine targeting VEGFR1 and an anti-VEGFR2 antibody are effective in inhibiting tumor angiogenesis [77, 78]. Therefore, VEGFR1 and VEGFR2 are promising antiangiogenic targets [79]. A combination of a VEGFR1 and VEGFR2 peptide-based vaccine with S-1 plus cisplatin showed improved clinical efficacy, and no severe adverse events were observed in patients with advanced GC. The median overall survival and progression-free survival time were 14.2 months and 9.6 months, respectively, with the combined therapy, compared to 13 months and 6 months with the S-1 plus cisplatin treatment [30].

LY6K-177 is overexpressed in the majority of lung and esophageal cancer tissues [80]. Ishikawa et al. have demonstrated that the peptide vaccine derived from the HLA-A*2402-restricted LY6K-177 epitope was able to induce a specific CD8+ CTL response [81]. The suppression of LY6K expression with siRNA effectively inhibited the growth of LY6K-expressing lung and esophageal cancer cells [81]. Therefore, LY6K might be suitable to repress tumor growth as a targeting peptide in vaccine therapy. Clinical trials of vaccine therapy containing peptide LY6K-177 have verified that the LY6K-177 vaccine stimulated an antigen-specific CD8+ CTL response and significantly prolonged the survival of patients with esophageal squamous cell carcinoma [82].

An estimated 85% of GC patients have LY6K expression. A phase I clinical trial of an LY6K-177 peptide vaccine emulsified with Montanide ISA 51 was conducted in advanced gastric cancer patients [31]. The clinical response was effective, with nearly no side effects except for redness and induration at the injection sites [58].

To a great extent, the development of immunotherapy with peptide vaccines depends on the identification of novel vaccine targets, such as tumor-associated antigens [65]. However, few gastric cancer-targeting TAAs have been identified, and TAAs that can induce anticancer responses need to be further investigated.

6. Peptides and Prostate Cancer

Prostate cancer is the first leading cancer type of all newly diagnosed cancers and the second leading cause of cancer deaths among men in 2014 [63]. The incidence rate has declined but has fluctuated greatly since 2000 due to differences in prostate-specific antigen (PSA) testing prevalence and ethnicity [83]. A variety of chemotherapies have been employed to clinically treat prostate cancer, such as docetaxel and abiraterone [84]. Immunotherapy has been shown to be feasible to cope with chemotherapy-resistant cancer. Sipuleucel-T is the first FDA-approved cancer vaccine for the treatment of castration-resistant prostate cancer patients [85].

Mcgrath and his colleagues validated that EN2, a homeobox-containing transcription factor, was present in human fetuses but absent in healthy adults. However, the overexpression of EN2 in patients with prostate cancer can lead to the diagnosis of prostate tumors [15]. Similarly, mitochondrial uncoupling protein 2 is overexpressed in prostate cancer and may serve as a biomarker for diagnosis [16].

Faced with limited therapeutic efficacy, the identification of novel tumor antigens and the elevation of immunogenicity using vaccines are advisable approaches to improve clinical responses [66]. Noguchi et al. reported that personalized peptide vaccination (PPV) was well tolerated in the treatment of patients with castration-resistant prostate cancer (CRPC) in 2013 [47]. As we mentioned previously, although a large number of clinical trials have been conducted, outcomes showed limited responses and were less than satisfactory [86]. The limited clinical efficacy might be caused by not knowing the immunological status of patients, which contributed to mismatches between vaccine peptides and the heterogeneous immune cell repertoires [87].

Unlike other therapies, PPV is a novel immunotherapy tailored for individual patients. Many suitable candidate antigens are selected based on HLA type and the preexisting host immunity [88]. Conventional vaccines containing simply one peptide might not initiate a specific antitumor response against tumor cell variants because of the loss or reduction of TAA [88]. Therefore, a maximum of four peptides might increase the possibility of inducing immune responses and thus decrease the chance of tumor escape from immunosurveillance [89]. Two to four selected peptides were employed in patients during this trial along with incomplete Freund's adjuvant. The estimated median survival time was 18.8 months [47]. The result demonstrated that PPV was feasible for patients with CRPC and also recommended a surrogate marker for the evaluation of the clinical efficacy of cancer vaccine prostate-specific antigen doubling time (PSADT) [47].

In 2014, Saif reported that the PAP-114-128 epitope-based vaccine stimulated antigen-specific T-cell responses and reduced the growth of prostate cancer cells in C57BL/6 mice [32]. Prostatic acid phosphatase (PAP) is overexpressed in prostate cancer and may be an ideal vaccine target in the immunotherapy of prostate tumor patients [8]. Because long peptide vaccines are more efficient than ones that use whole proteins [90], the PAP-114-128 epitope peptide, which can induce CD4+ and CD8+ T cell responses, was screened from the PAP protein. The trial also validated that the PAP-114-128 peptide delivered through the ImmunoBody vector (IB-PAP-114-128) exhibited stronger CD4+ and CD8+ T cell specific responses and IFN-γ response than the PAP-114-128 peptide [32]. Furthermore, the IB-PAP-114-128 vaccine stimulated T cells that had higher avidity than PAP-114-128 emulsified with incomplete Freund's adjuvant [32]. ImmunoBody uses monoclonal IgG1 antibodies that were reconstructed to express specific antigenic epitopes to induce cellular immunity [91]. The Fc region of IgG1 can elicit high-affinity responses when targeting FcγR (CD64) expressed on DCs [92]. Thus, the fusion of the PAP-114-128 epitope peptide and ImmunoBody vector demonstrated effective antitumor benefits [32]. Further studies of this combined therapy are needed to assess its clinical efficacy.

Additionally, Fenoglio et al. confirmed the safety and immunological response against prostate tumors by using of a multipeptide, dual-adjuvant telomerase vaccine called GX301, which is composed of four telomerase peptides (peptide540–548, peptide611–626, peptide672–686, and peptide766–780) and two adjuvants, MontanideISA-51 and Imiquimod [48].

7. Peptides and Breast Cancer

Breast cancer is the second most common cause of cancer deaths among women in the United States in 2014 [63]. The increased incidence rates but decreased death rates of breast cancer might be attributed to the prevalence of screening examinations, early diagnosis that prevents tumors from developing into advanced stages and improvement in treatment [93, 94].

At present, treatments for breast cancer patients consist of chemotherapy, endocrine therapy, immunotherapy, and combination therapies [95]. Immunotherapies, including antibodies and peptide vaccines, are effective in the treatment of chemotherapy-resistant cancer [96]. Trastuzumab is a monoclonal antibody against human epidermal growth factor receptor 2 (HER-2) [97], which is overexpressed in almost 30% of breast cancer patients and is closely related to poor prognosis [17]. Ado-trastuzumab emtansine has been approved by the FDA as standard regimen for patients with HER-2 positive breast cancer [98].

The earlier the diagnosis occurs, the better the prognosis will be. Peptides play important roles in the early diagnosis of breast cancer, which results in decreased mortality. A list of antigens expressed in breast cancer cells including HER-2, carcinoembryonic antigen (CEA) mucin1 [18], p53, and telomerase reverse transcriptase has been investigated in humans [96, 99]. These peptides may be used to detect breast cancer.

In recent years, many strategies to improve immune efficacy have been proposed, such as the modification of peptide sequences at amino acid residues [66], using different vaccine delivery systems [95], PPV therapy as mentioned previously [87], and various combination therapies.

Takahashi et al. reported that personalized peptide vaccination applied clinically to metastatic recurrent triple-negative breast cancer (TNBC) patients has demonstrated feasible results [9]. The advantages of PPV over conventional immunotherapy methods have been reported previously. TNBCs, lacking the immunohistochemical expression of HER-2, the estrogen receptor, and the progesterone receptor, occur more frequently in younger women [100]. TNBC patients often have a poor prognosis and present with an aggressive grade and lymph node metastases at the time of diagnosis [101]. In this trial, most patients displayed augmented PPV-induced immune responses, showing considerable efficacy [9]. Moreover, no patient had severe therapy-related adverse events throughout the treatment [9].

According to previous studies, different vaccine delivery systems also greatly affect the clinical immune efficacy and demonstrated augmented immune responses [33]. Cationic liposome enhanced the amplitude of the antitumor effect and resulted in tumor regression when used as an adjuvant treatment [102]. There are many advantages that contribute to the adjuvant performance, such as versatility in lipid composition and size, the high efficiency of antigen loading, increased presentation of antigens, and the high ability of biodegradability and biocompatibility [103]. Mansourian et al. reported on a p5 peptide (HER-2 derived peptide) encapsulated in a delivery system that is composed of fusogenic dioleoyl phosphatidylethanolamine (DOPE) incorporated into 1,2-dioleoyl-3-trimethylammonium-propane (DOTAP) cationic liposome-cholesterol, and when the peptide was coadministered with CpG-ODN, the system increased the delivery of p5 and showed an elevated specific CTL response in mice inoculated with TUBO tumor cells [33]. TUBO is a cloned cell line that overexpresses the rat HER-2 protein [33]. The study demonstrated that further studies on its clinical effects in HER-2 positive breast cancer patients would be warranted. In addition, Shariat et al. investigated optimal methods of encapsulating the p5 peptide into liposomes to improve the peptide encapsulation efficiency [49]. Moreover, Karkada and colleagues designed a liposome-in-oil vaccine platform called DepoVax that can enhance immunogenicity of the vaccine [104]. Effective vaccine delivery systems play important roles in vaccine therapeutic efficacy.

Additionally, Ohtake and his colleagues validated that an artificial long peptide consisting of survivin-18 (SU18) and SU22 connected by a glycine linker was able to induce IFN-γ producing Th1 and Tc1 cells better than mixed short peptides [34]. In addition, Mittendorf et al. reported that the combination of E75 and granulocyte-macrophage colony-stimulating factor (GM-CSF) is safe and inhibits tumor recurrence [35]. Moreover, evidence has suggested that a multiepitope derived from an ErbB-2 vaccine suppressed the growth of breast cancer stem cells and consequently prevented tumorigenesis [36].

8. Discussion

Cancer is a threat to human health [105] due to its metastatic characteristic and high recurrence and mortality rates. Tumor cells can survive by escaping the host's immune system, synthesizing proteins to resist external treatment, and so forth [106, 107]. Traditional cancer treatments include chemotherapy, radiotherapy, and surgical resection. Among these treatments, chemotherapy remains a helpful and frequently used method to treat cancer. Commonly, traditional chemotherapeutical drugs target tumor cells by disrupting necessary cell products, such as DNA, RNA, or proteins [108]. However, chemotherapy is also insufficient. Because chemotherapy does not specifically target tumor cells, it causes many side effects in patients [109]. Additionally, multidrug resistance (MDR) is the main reason that chemotherapy fails to cure patients [108]. Under these limitations, chemotherapy based on peptides has received increased attention.

Peptides, which are short chains of amino acid monomers linked by peptide bonds, can specifically bind to tumor cells with low toxicity to normal tissues [110], indicating that they are a promising anticancer agent. This tumor-targeting ability of peptides is based on molecular structure [110]. Tumor cells have different membrane proteins on the cell membrane, such as endothelial cell growth factor receptors (EGFR) and cell surface proteoglycans [111, 112], making it possible for molecules to specifically bind to these proteins [113]. Peptides, derived from natural or synthetic sources, can selectively bind to these proteins [110] because they may share similar structures by containing arginine and lysine [114]. These amino acids can form hydrogen bonds with the negatively charged components on the cell membrane [114, 115], indicating that amino acids are the main reason why peptides may bind to tumor cell membranes. However, these properties are not sufficient for peptides to specifically target tumor cells. The specific selective ability of peptides may depend on their spatial structure [116], such as cartilage matrix proteins, which have a three-stranded a-helical coiled-coil structure in the C-terminal domain that may serve as a trimerization site [117]. Peptides are not the only molecule that can bind to tumor cell membranes, but they are the most ideal molecules because they have low molecular weights and good cellular uptake [110].

As we have summarized previously, peptides can be used to treat different types of cancer (lung cancer, CRC, pancreatic cancer, gastric cancer, prostate cancer, and breast cancer), from early diagnosis, treatment to prognosis. In addition to these types of cancer, peptides can also be used in skin cancer, renal cancer, osteosarcoma, and so forth. Wu et al. reported that properdistatin, a novel peptide

Table 2: Peptides applied in treating cancer.

Cancer type	Peptide	Model	Year	Author	Reference
Pancreatic cancer	WT1	In vivo	2014	Nishida et al.	[27]
	KIF20A	In vivo	2014	Suzuki et al.	[28]
	GV1001	In vivo	2014	Staff et al.	[29]
Gastric cancer	VEGFR1, 2	In vivo	2012	Masuzawa et al.	[30]
	LY6K-177	In vivo	2014	Ishikawa et al.	[31]
Prostate cancer	PAP-114-128	TRAMP C1	2014	Saif et al.	[32]
Breast cancer	p5	TUBO	2014	Mansourian et al.	[33]
	SU18, SU22	In vivo	2014	Ohtake et al.	[34]
	E75	In vivo	2014	Mittendorf et al.	[35]
	ErbB-2	MMC	2014	Gil et al.	[36]
Colorectal cancer	ANP	DHD/K12/Trb, SW620	2012	Serafino et al.	[37]
	TCP-1	HCT116 and HT-29	2010	Li et al.	[38]
	F56	HUVEC	2014	Wang et al.	[39]
NSCLC	WT1	In vivo	2013	Takahashi et al.	[40]
	TERT572Y	In vivo	2014	Kotsakis et al.	[41]
	Disruptin	H1975	2014	Ahsa et al.	[42]
	TREM-1	J774A.1	2014	Sigalov	[43]
Lung cancer	LFC131	A549	2014	Chittasupho et al.	[44]
	BPP	In vivo	2014	Wang et al.	[45]
Melanoma	TH10	B16F10-luc-G5	2014	Guan et al.	[46]

derived from the plasma protein properdin, could inhibit angiogenesis in A-07 human melanoma xenografts [110]. Liu and Miao also showed that the CycMSH peptide conjugated with Tc-99m has exhibited an ability to target metastatic melanoma, indicating the potential of metastatic melanoma detection by CycMSH [118]. González et al. reported that the peptides derived from the melanocortin 1 receptor could elicit cytotoxic T-lymphocyte responses to kill melanoma cells [119]. Additionally, peptides for renal cancer treatment have also been of great interest. Vacas et al. reported that a vasoactive intestinal peptide inhibited invasion and metastasis of ccRCCs, by decreasing the nuclear level of β-catenin [120]. In addition, a peptide-based vaccine has also been used to treat metastatic renal cell carcinoma. Yoshimura et al. reported that vaccination with a vascular endothelial growth factor receptor 1 peptide showed anticancer effects in 18 patients with metastatic renal cancer [121]. Rausch and colleagues also found that a vaccine based on the IMA901 peptide could elicit a T-cell response and prolong overall survival in patients with metastatic renal cell carcinoma [122]. In addition to the novel applications of peptides in diagnosing and treating cancer, peptides can be used in other aspects of cancer therapy. Liu et al. found that the peptide Myr-NR2B9c could be used to reduce bone cancer pain, suggesting that this peptide could be used in patients with advanced bone cancer [123]. From these data, we conclude that peptides could be used in treating many types of cancer, and this treatment has shown promising clinical outcomes.

Peptide based chemotherapy is also a type of immunotherapy (Table 2). Though the immune system can target tumor cells, the tumor cells develop a number of immune escape mechanisms to avoid immune system surveillance [124]. The mechanism of peptides used in cancer therapy can be divided into two aspects: (1) peptides can bind to specific molecular targets on tumor cells, and these peptides can either regulate the biosynthesis of tumor cells or serve as a drug delivery system. (2) Peptides can induce specific T cell responses to tumor cells, as González et al. reported [119].

Interestingly, peptides could also target tumor vessel as well as targeting tumor cells. Li and Cho thought that tumor vascular was a better target for peptide treatment, when compared to tumor cells [125]. The endothelial cells of tumor have unique advantages in attracting peptide, such as low drug resistance, distinct microenvironment, and better blood perfusion [38, 126–128]. These advantages also give the unique application of peptide treatment, such as direct molecular imaging of targeted vascular peptides [125]. These peptides could provide potential target in diagnosing and treating tumor.

In using peptides to treat cancer, peptide-based vaccines have drawn increased attention (Table 3). Peptide-based vaccines have been widely applied in various diseases, such as allergies, infectious diseases, autoimmune diseases, and even cancer. Recently, peptide-based vaccines against cancer have been used to elicit tumor regression. Since the acceptance of sipuleucel-T by the FDA as the first peptide vaccine for prostate tumors, an increasing number of clinical trials have been conducted in many other cancer types, such as melanoma, glioblastoma, breast cancer, and gastric cancer [8]. A peptide-based vaccine has many advantages, including (1) the convenient and inexpensive acquisition of peptides; (2) easy administration; (3) the specificity of targeting to tumor tissues but not normal tissues; (4) fewer or even no severe side effects [66].

Table 3: Peptide-based vaccine in clinical application.

Cancer	Treatment	Sample	Study phase	Year	Author	Reference
Pancreatic cancer	WT1 peptide-based vaccine combined with gemcitabine	32	I	2014	Nishida et al.	[27]
	KIF20A-derived peptide in combination with gemcitabine	9	I	2014	Suzuki et al.	[28]
	Telomerase GV1001 vaccine together with gemcitabine	21	I	2014	Staff et al.	[29]
Gastric cancer	VEGFR1-1084 and VEGFR2-169 combined with S-1 and cisplatin	22	I/II	2012	Masuzawa et al.	[30]
	LY6K-177 peptide vaccine emulsified with Montanide ISA 51	6	I	2014	Ishikawa et al.	[31]
Prostate cancer	PPV (2-4 positive peptides selected from 31 candidate peptides)	100	II	2013	Noguchi et al.	[47]
	IB-PAP-114-128 vaccine therapy	—	—	2014	Saif et al.	[32]
	A multipeptide, dual-adjuvant telomerase vaccine (GX301)	11	I/II	2013	Fenoglio et al.	[48]
mrTNBC	PPV	18	II	2014	Takahashi et al.	[9]
Breast cancer	P5 encapsulated in DOTAP-cholesterol-DOPE liposomes coadministered with CpG-ODN	—	—	2014	Mansourian et al.	[33]
	Optimized encapsulation of p5 into liposomes	—	—	2014	Shariat et al.	[49]
	An artificial long peptide consisting of SU18 and SU22	—	—	2014	Ohtake et al.	[34]
	Combination therapy of E75 and GM-CSF	187	I/II	2014	Mittendorf et al.	[35]
	Multiepitope derived from ErbB-2 vaccine	—	—	2014	Gil et al.	[36]
Colorectal cancer	Atrial natriuretic peptide (ANP)	—	—	2012	Serafino et al.	[37]
	TCP-1 peptide	—	—	2010	Li et al.	[38]
	F56-VCR-NP	—	—	2014	Wang et al.	[39]
	Peptides from common bean NDF	—	—	2014	Luna Vital et al.	[50]
	Cep55/c10orf3 derived peptide vaccine	—	—	2011	Inoda et al.	[51]
	A cocktail vaccine of 5 peptides	18	I	2014	Hazama et al.	[52]
	A combination of 7-peptide cocktail vaccine and tegafur-uracil plus leucovorin	30	I	2014	Okuno et al.	[53]
Lung cancer	Dendritic cell vaccines pulsed with WT-1 peptide	62	—	2013	Takahashi et al.	[40]
	hTERT-targeting Vx-001 vaccine	46	II	2014	Kotsakis et al.	[41]
	A synthesized peptide Disruptin	—	—	2014	Ahsa et al.	[42]
	A ligand-independent peptide-based TREM1 inhibitor	—	—	2014	Sigalov	[43]
	Peptide fractions from high oleic acid soybean	—	—	2013	Rayaprolu et al.	[54]
	Peptides from venom of Eastern green mamba	—	—	2014	Conlon et al.	[55]
	LFC131-DOX NPs delivery system	—	—	2014	Chittasupho et al.	[44]
	TH10-DTX-NP	—	—	2014	Guan et al.	[46]
	BPP-decorated chitosan nanoparticles	—	—	2014	Wang et al.	[45]

Tumor-associated antigens (TAAs) are expressed in tumor cells and can be recognized by T lymphocytes, resulting in activation of the immune system [66]. A TAA peptide vaccine, when injected into cancer patients, binds with the restricted major histocompatibility complex (MHC) molecule expressed in antigen presenting cells (APCs) [129]. Then the peptide/MHC complex is transported to the cell surface after intracellular processing and recognized by T cell receptor (TCR) on the surface of T cells, leading to the activation of T lymphocytes [130]. Therefore, a peptide cancer vaccine may elicit a specific immune response against tumors. Nevertheless, the clinical response is limited and shows limited efficacy [131]. These failures may be due to many factors, including the poor immunogenicity of TAAs, immune escape of tumor cells, and tumor heterogeneity [67]. New strategies for improving the clinical outcome include the modification of TAA peptides [132], vaccines against multiple TAA epitopes, personalized peptide vaccination [87], a combination with chemotherapy, and different administration routes and delivery systems [95]. Some novel methods have been tried, and some may improve the clinical efficacy and prolong the survival of cancer patients.

9. Conclusion

In this review, we mainly summarized new advances in using peptides to treat different types of cancer, indicating that peptides could be used as an ideal immunotherapy method in treating cancer due to the novel advantages of peptides, such as specifically targeting tumor cells, decreased toxicity and efficient immunoreaction. The development of identifying and synthesizing novel peptides could provide a promising choice to patients with cancer.

Abbreviation

FDA: Food and Drug Administration
CRC: Colorectal cancer
CPAA: Cationic polyacrylamide
NDF: Nondigestible fractions
NSCLC: Non-small-cell lung cancer
PC: Pancreatic cancer
HER-2: Human epidermal growth factor receptor 2
CEA: Carcinoembryonic antigen
TAA: Tumor-associated antigens
GC: Gastric cancer
HLA: Human leukocyte antigen.

Conflict of Interests

The authors declare that there is no conflict of interests regarding the publication of this paper.

Authors' Contribution

Yu-Feng Xiao and Meng-Meng Jie contributed equally to this study.

References

[1] N. Iikuni, B. H. Hahn, and A. La Cava, "Potential for anti-DNA immunoglobulin peptide therapy in systemic lupus erythematosus," *Expert Opinion on Biological Therapy*, vol. 9, no. 2, pp. 201–206, 2009.

[2] M. Larché, "Peptide therapy for allergic diseases: basic mechanisms and new clinical approaches," *Pharmacology & Therapeutics*, vol. 108, no. 3, pp. 353–361, 2005.

[3] L.-P. Boulet, "Allergen-derived T cell peptides and late asthmatic responses," *American Journal of Respiratory and Critical Care Medicine*, vol. 169, no. 1, pp. 2–3, 2004.

[4] S. P. Atamas, "Relief from within: a peptide therapy for fibrosis," *Science Translational Medicine*, vol. 4, no. 136, Article ID 136fs16, 2012.

[5] B. Oh and M. Lee, "Combined delivery of HMGB-1 box A peptide and S1PLyase siRNA in animal models of acute lung injury," *Journal of Controlled Release*, vol. 175, no. 1, pp. 25–35, 2014.

[6] T. Nojiri, H. Hosoda, T. Tokudome et al., "Atrial natriuretic peptide inhibits lipopolysaccharide-induced acute lung injury," *Pulmonary Pharmacology & Therapeutics*, vol. 29, no. 1, pp. 24–30, 2014.

[7] J. N. Francis and M. Larché, "Peptide-based vaccination: where do we stand?" *Current Opinion in Allergy and Clinical Immunology*, vol. 5, no. 6, pp. 537–543, 2005.

[8] M. A. Cheever and C. S. Higano, "PROVENGE (sipuleucel-T) in prostate cancer: the first FDA-approved therapeutic cancer vaccine," *Clinical Cancer Research*, vol. 17, no. 11, pp. 3520–3526, 2011.

[9] R. Takahashi, U. Toh, N. Iwakuma et al., "Feasibility study of personalized peptide vaccination for metastatic recurrent triple-negative breast cancer patients," *Breast Cancer Research*, vol. 16, no. 4, article R70, 2014.

[10] R. Roy, D. Zurakowski, J. Wischhusen et al., "Urinary TIMP-1 and MMP-2 levels detect the presence of pancreatic malignancies," *British Journal of Cancer*, vol. 111, no. 9, pp. 1772–1779, 2014.

[11] X. B. Wang, Y. F. Li, H. M. Tian et al., "Macrophage inhibitory cytokine 1 (MIC-1/GDF15) as a novel diagnostic serum biomarker in pancreatic ductal adenocarcinoma," *BMC Cancer*, vol. 14, no. 1, article 578, 2014.

[12] N. Jiang, R. H. Xue, F. F. Bu, X. Tong, J. K. Qiang, and R. Liu, "Decreased RGS6 expression is associated with poor prognosis in pancreatic cancer patients," *International Journal of Clinical and Experimental Pathology*, vol. 7, no. 7, pp. 4120–4127, 2014.

[13] Z.-X. Zheng, Y. Sun, Z.-D. Bu et al., "Intestinal stem cell marker LGR5 expression during gastric carcinogenesis," *World Journal of Gastroenterology*, vol. 19, no. 46, pp. 8714–8721, 2013.

[14] Y. Lu, B. Zhou, G. Q. Gao, D. Li, X. D. Liu, and B. Huang, "Clinical significance in combined detection of serum pepsinogen I, pepsinogen II and carbohydrate antigen 242 in gastric cancer," *Hepatogastroenterology*, vol. 61, no. 129, pp. 255–258, 2014.

[15] S. E. Mcgrath, A. Michael, R. Morgan, and H. Pandha, "EN2: a novel prostate cancer biomarker," *Biomarkers in Medicine*, vol. 7, no. 6, pp. 893–901, 2013.

[16] W. Li, K. Nichols, C.-A. Nathan, and Y. Zhao, "Mitochondrial uncoupling protein 2 is up-regulated in human head and neck, skin, pancreatic, and prostate tumors," *Cancer Biomarkers*, vol. 13, no. 5, pp. 377–383, 2013.

[17] N. Boku, "HER2-positive gastric cancer," *Gastric Cancer*, vol. 17, no. 1, pp. 1–12, 2014.

[18] J. S. Zanetti, D. F. Soave, J. P. Oliveira-Costa et al., "The role of tumor hypoxia in MUC1-positive breast carcinomas," *Virchows Archiv*, vol. 459, no. 4, pp. 367–375, 2011.

[19] J. Albrethsen, C. H. Møller, J. Olsen, H. Raskov, and S. Gammeltoft, "Human neutrophil peptides 1, 2 and 3 are biochemical markers for metastatic colorectal cancer," *European Journal of Cancer*, vol. 42, no. 17, pp. 3057–3064, 2006.

[20] M. Bloch, Y. Kam, E. Yavin et al., "The relative roles of charge and a recognition peptide in luminal targeting of colorectal cancer by fluorescent polyacrylamide," *European Journal of Pharmaceutical Sciences*, vol. 47, no. 5, pp. 904–913, 2012.

[21] S. S. Comstock, D. Xu, K. Hortos et al., "Association of insulin-related serum factors with colorectal polyp number and type in adult males," *Cancer Epidemiology, Biomarkers & Prevention*, vol. 23, no. 9, pp. 1843–1851, 2014.

[22] W. Wang, S. Guan, S. Sun et al., "Detection of circulating antibodies to linear peptide antigens derived from ANXA1 and DDX53 in lung cancer," *Tumor Biology*, vol. 35, no. 5, pp. 4901–4905, 2014.

[23] M. Zhang, X. Li, X. Zhang, Y. Yang, Z. Feng, and X. Liu, "Association of serum hemoglobin A1c, C-peptide and insulin-like growth factor-1 levels with the occurrence and development of lung cancer," *Molecular Clinical Oncology*, vol. 2, no. 4, pp. 506–508, 2014.

[24] M. J. McGuire, B. P. Gray, S. Li et al., "Identification and characterization of a suite of tumor targeting peptides for non-small cell lung cancer," *Scientific Reports*, vol. 4, article 4480, 2014.

[25] D. de Costa, I. Broodman, W. Calame et al., "Peptides from the variable region of specific antibodies are shared among lung cancer patients," *PLoS ONE*, vol. 9, no. 5, Article ID e96029, 2014.

[26] A. Wang, L. Chen, K. Pu, and Y. Zhu, "Identification of stem-like cells in non-small cell lung cancer cells with specific peptides," *Cancer Letters*, vol. 351, no. 1, pp. 100–107, 2014.

[27] S. Nishida, S. Koido, Y. Takeda et al., "Wilms tumor gene (WT1) peptide-based cancer vaccine combined with gemcitabine for patients with advanced pancreatic cancer," *Journal of Immunotherapy*, vol. 37, no. 2, pp. 105–114, 2014.

[28] N. Suzuki, S. Hazama, T. Ueno et al., "A phase i clinical trial of vaccination with KIF20A-derived peptide in combination with gemcitabine for patients with advanced pancreatic cancer," *Journal of Immunotherapy*, vol. 37, no. 1, pp. 36–42, 2014.

[29] C. Staff, F. Mozaffari, J.-E. Frodin, H. Mellstedt, and M. Liljefors, "Telomerase (GV1001) vaccination together with gemcitabine in advanced pancreatic cancer patients," *International Journal of Oncology*, vol. 45, no. 3, pp. 1293–1303, 2014.

[30] T. Masuzawa, Y. Fujiwara, K. Okada et al., "Phase I/II study of S-1 plus cisplatin combined with peptide vaccines for human vascular endothelial growth factor receptor 1 and 2 in patients with advanced gastric cancer," *International Journal of Oncology*, vol. 41, no. 4, pp. 1297–1304, 2012.

[31] H. Ishikawa, M. Imano, O. Shiraishi et al., "Phase I clinical trial of vaccination with LY6K-derived peptide in patients with advanced gastric cancer," *Gastric Cancer*, vol. 17, no. 1, pp. 173–180, 2014.

[32] J. M. S. Saif, J. Vadakekolathu, S. S. Rane et al., "Novel prostate acid phosphatase-based peptide vaccination strategy induces antigen-specific T-cell responses and limits tumour growth in mice," *European Journal of Immunology*, vol. 44, no. 4, pp. 994–1004, 2014.

[33] M. Mansourian, A. Badiee, S. A. Jalali et al., "Effective induction of anti-tumor immunity using p5 HER-2/neu derived peptide encapsulated in fusogenic DOTAP cationic liposomes co-administrated with CpG-ODN," *Immunology Letters*, vol. 162, no. 1, part A, pp. 87–93, 2014.

[34] J. Ohtake, T. Ohkuri, Y. Togashi, H. Kitamura, K. Okuno, and T. Nishimura, "Identification of novel helper epitope peptides of Survivin cancer-associated antigen applicable to developing helper/killer-hybrid epitope long peptide cancer vaccine," *Immunology Letters*, vol. 161, no. 1, pp. 20–30, 2014.

[35] E. A. Mittendorf, G. T. Clifton, J. P. Holmes et al., "Final report of the phase I/II clinical trial of the E75 (nelipepimut-S) vaccine with booster inoculations to prevent disease recurrence in high-risk breast cancer patients," *Annals of Oncology*, vol. 25, no. 9, pp. 1735–1742, 2014.

[36] E. Y. Gil, U. H. Jo, H. J. Lee et al., "Vaccination with ErbB-2 peptides prevents cancer stem cell expansion and suppresses the development of spontaneous tumors in MMTV-PyMT transgenic mice," *Breast Cancer Research and Treatment*, vol. 147, no. 1, pp. 69–80, 2014.

[37] A. Serafino, N. Moroni, R. Psaila et al., "Anti-proliferative effect of atrial natriuretic peptide on colorectal cancer cells: evidence for an Akt-mediated cross-talk between NHE-1 activity and Wnt/β-catenin signaling," *Biochimica et Biophysica Acta—Molecular Basis of Disease*, vol. 1822, no. 6, pp. 1004–1018, 2012.

[38] Z. J. Li, W. K. K. Wu, S. S. M. Ng et al., "A novel peptide specifically targeting the vasculature of orthotopic colorectal cancer for imaging detection and drug delivery," *Journal of Controlled Release*, vol. 148, no. 3, pp. 292–302, 2010.

[39] C. Wang, M. Zhao, Y.-R. Liu et al., "Suppression of colorectal cancer subcutaneous xenograft and experimental lung metastasis using nanoparticle-mediated drug delivery to tumor neovasculature," *Biomaterials*, vol. 35, no. 4, pp. 1215–1226, 2014.

[40] H. Takahashi, M. Okamoto, S. Shimodaira et al., "Impact of dendritic cell vaccines pulsed with Wilms' tumour-1 peptide antigen on the survival of patients with advanced non-small cell lung cancers," *European Journal of Cancer*, vol. 49, no. 4, pp. 852–859, 2013.

[41] A. Kotsakis, E. Papadimitraki, E. K. Vetsika et al., "A phase II trial evaluating the clinical and immunologic response of HLA-A2$^+$ non-small cell lung cancer patients vaccinated with an hTERT cryptic peptide," *Lung Cancer*, vol. 86, no. 1, pp. 59–66, 2014.

[42] A. Ahsa, S. G. Ramanand, I. L. Bergin et al., "Efficacy of an EGFR-specific peptide against EGFR-dependent cancer cell lines and tumor xenografts," *Neoplasia*, vol. 16, no. 2, pp. 105–114, 2014.

[43] A. B. Sigalov, "A novel ligand-independent peptide inhibitor of TREM-1 suppresses tumor growth in human lung cancer xenografts and prolongs survival of mice with lipopolysaccharide-induced septic shock," *International Immunopharmacology*, vol. 21, no. 1, pp. 208–219, 2014.

[44] C. Chittasupho, K. Lirdprapamongkol, P. Kewsuwan, and N. Sarisuta, "Targeted delivery of doxorubicin to A549 lung cancer cells by CXCR4 antagonist conjugated PLGA nanoparticles," *European Journal of Pharmaceutics and Biopharmaceutics*, vol. 88, no. 2, pp. 529–538, 2014.

[45] X. Wang, C. Yang, Y. Zhang, X. Zhen, W. Wu, and X. Jiang, "Delivery of platinum(IV) drug to subcutaneous tumor and lung metastasis using bradykinin-potentiating peptide-decorated chitosan nanoparticles," *Biomaterials*, vol. 35, no. 24, pp. 6439–6453, 2014.

[46] Y. Y. Guan, X. Luan, J. R. Xu et al., "Selective eradication of tumor vascular pericytes by peptide-conjugated nanoparticles for antiangiogenic therapy of melanoma lung metastasis," *Biomaterials*, vol. 35, no. 9, pp. 3060–3070, 2014.

[47] M. Noguchi, F. Moriya, S. Suekane et al., "A phase II trial of personalized peptide vaccination in castration-resistant prostate cancer patients: prolongation of prostate-specific antigen doubling time," *BMC Cancer*, vol. 13, article 613, 2013.

[48] D. Fenoglio, P. Traverso, A. Parodi et al., "A multi-peptide, dual-adjuvant telomerase vaccine (GX301) is highly immunogenic in patients with prostate and renal cancer," *Cancer Immunology, Immunotherapy*, vol. 62, no. 6, pp. 1041–1052, 2013.

[49] S. Shariat, A. Badiee, M. R. Jaafari, and S. A. Mortazavi, "Optimization of a method to prepare liposomes containing HER2/Neu-derived peptide as a vaccine delivery system for breast cancer," *Iranian Journal of Pharmaceutical Research*, vol. 13, pp. 15–25, 2014.

[50] D. A. L. Vital, E. G. de Mejía, V. P. Dia, and G. Loarca-Piña, "Peptides in common bean fractions inhibit human colorectal cancer cells," *Food Chemistry*, vol. 157, pp. 347–355, 2014.

[51] S. Inoda, R. Morita, Y. Hirohashi et al., "The feasibility of Cep55/c10orf3 derived peptide vaccine therapy for colorectal carcinoma," *Experimental and Molecular Pathology*, vol. 90, no. 1, pp. 55–60, 2011.

[52] S. Hazama, H. Takenouchi, R. Tsunedomi et al., "Predictive biomarkers for the outcome of vaccination of five therapeutic epitope peptides for colorectal cancer," *Anticancer Research*, vol. 34, no. 8, pp. 4201–4205, 2014.

[53] K. Okuno, F. Sugiura, K. Inoue, and Y. Sukegawa, "Clinical trial of a 7-peptide cocktail vaccine with oral chemotherapy for patients with metastatic colorectal cancer," *Anticancer Research*, vol. 34, no. 6, pp. 3045–3052, 2014.

[54] S. J. Rayaprolu, N. S. Hettiarachchy, P. Chen, A. Kannan, and A. Mauromostakos, "Peptides derived from high oleic acid soybean meals inhibit colon, liver and lung cancer cell growth," *Food Research International*, vol. 50, no. 1, pp. 282–288, 2013.

[55] J. M. Conlon, M. Prajeep, M. Mechkarska et al., "Peptides with *in vitro* anti-tumor activity from the venom of the Eastern green mamba, *Dendroaspis angusticeps* (Elapidae)," *Journal of Venom Research*, vol. 5, pp. 16–21, 2014.

[56] R. E. Schoen, "The case for population-based screening for colorectal cancer," *Nature Reviews Cancer*, vol. 2, no. 1, pp. 65–70, 2002.

[57] S. Hazama, Y. Nakamura, H. Takenouchi et al., "A phase I study of combination vaccine treatment of five therapeutic epitope-peptides for metastatic colorectal cancer; safety, immunological response, and clinical outcome," *Journal of Translational Medicine*, vol. 12, no. 1, article 63, 2014.

[58] A. Jemal, F. Bray, M. M. Center, J. Ferlay, E. Ward, and D. Forman, "Global cancer statistics," *CA: A Cancer Journal for Clinicians*, vol. 61, no. 2, pp. 69–90, 2011.

[59] M. Früh, D. de Ruysscher, S. Popat, L. Crinò, S. Peters, and E. Felip, "Small-cell lung cancer (SCLC): ESMO clinical practice guidelines for diagnosis, treatment and follow-up," *Annals of Oncology*, vol. 24, supplement 6, pp. vi99–vi105, 2013.

[60] T. J. McDonald, M. A. Ghatei, S. R. Bloom et al., "A qualitative comparison of canine plasma gastroenteropancreatic hormone responses to bombesin and the porcine gastrin-releasing peptide (GRP)," *Regulatory Peptides*, vol. 2, no. 5, pp. 293–304, 1981.

[61] E. Gniazdowska, P. Koźmiński, K. Bańkowski, and P. Ochman, "^{99m}Tc-labeled vasopressin peptide as a radiopharmaceutical for small-cell lung cancer (SCLC) diagnosis," *Journal of Medicinal Chemistry*, vol. 57, no. 14, pp. 5986–5994, 2014.

[62] Z. H. Hong, Y. Z. Shi, Z. L. Liu, X. L. Zhou, Y. Yang, and J. Tang, "Preliminary radioimmunoimaging and biodistribution of ^{131}iodine-labeled single-chain antibody fragment against progastrin-releasing peptide (31–98) in small cell lung cancer xenografts," *Chinese Medical Journal*, vol. 127, no. 11, pp. 2007–2011, 2014.

[63] R. Siegel, J. Ma, Z. Zou, and A. Jemal, "Cancer statistics, 2014," *CA: A Cancer Journal for Clinicians*, vol. 64, no. 1, pp. 9–29, 2014.

[64] A. Takahara, S. Koido, M. Ito et al., "Gemcitabine enhances Wilms' tumor gene WT1 expression and sensitizes human pancreatic cancer cells with WT1-speciWc T-cell-mediated antitumor immune response," *Cancer Immunology, Immunotherapy*, vol. 60, no. 9, pp. 1289–1297, 2011.

[65] M. L. Rothenberg, M. J. Moore, M. C. Cripps et al., "A phase II trial of gemcitabine in patients with 5-FU-refractory pancreas cancer," *Annals of Oncology*, vol. 7, no. 4, pp. 347–353, 1996.

[66] G. Parmiani, C. Castelli, P. Dalerba et al., "Cancer immunotherapy with peptide-based vaccines: what have we achieved? Where are we going?" *Journal of the National Cancer Institute*, vol. 94, no. 11, pp. 805–818, 2002.

[67] F. M. Marincola, E. M. Jaffee, D. J. Hicklin, and S. Ferrone, "Escape of human solid tumors from T-cell recognition: molecular mechanisms and functional significance," *Advances in Immunology*, vol. 74, pp. 181–273, 2000.

[68] L. Gao, I. Bellantuono, A. Elsässer et al., "Selective elimination of leukemic CD34$^+$ progenitor cells by cytotoxic T lymphocytes specific for WT1," *Blood*, vol. 95, no. 7, pp. 2198–2203, 2000.

[69] A. M. Storniolo, S. R. Allerheiligen, and H. L. Pearce, "Preclinical, pharmacologic, and phase I studies of gemcitabine," *Seminars in Oncology*, vol. 24, no. 2, supplement 7, pp. S7-2–S7-7, 1997.

[70] A. K. Nowak, B. W. S. Robinson, and R. A. Lake, "Gemcitabine exerts a selective effect on the humoral immune response: implications for combination chemo-immunotherapy," *Cancer Research*, vol. 62, no. 8, pp. 2353–2358, 2002.

[71] L. Rettig, S. Seidenberg, I. Parvanova, P. Samaras, A. Knuth, and S. Pascolo, "Gemcitabine depletes regulatory T-cells in human and mice and enhances triggering of vaccine-specific cytotoxic T-cells," *International Journal of Cancer*, vol. 129, no. 4, pp. 832–838, 2011.

[72] A. K. Nowak, R. A. Lake, A. L. Marzo et al., "Induction of tumor cell apoptosis in vivo increases tumor antigen cross-presentation, cross-priming rather than cross-tolerizing host tumor-specific CD8 T cells," *The Journal of Immunology*, vol. 170, no. 10, pp. 4905–4913, 2003.

[73] R. Ramakrishnan, D. Assudani, S. Nagaraj et al., "Chemotherapy enhances tumor cell susceptibility to CTL-mediated killing during cancer immunotherapy in mice," *The Journal of Clinical Investigation*, vol. 120, no. 4, pp. 1111–1124, 2010.

[74] E. Kawakami, R. S. Machado, S. K. Ogata, and M. Langner, "Decrease in prevalence of *Helicobacter pylori* infection during a 10-year period in Brazilian children," *Arquivos de Gastroenterologia*, vol. 45, no. 2, pp. 147–151, 2008.

[75] A. Ohtsu, "Current status and future prospects of chemotherapy for metastatic gastric cancer: a review," *Gastric Cancer*, vol. 8, no. 2, pp. 95–102, 2005.

[76] M. Clauss, "Molecular biology of the VEGF and the VEGF receptor family," *Seminars in Thrombosis and Hemostasis*, vol. 26, no. 5, pp. 561–569, 2000.

[77] H. Ishizaki, T. Tsunoda, S. Wada, M. Yamauchi, M. Shibuya, and H. Tahara, "Inhibition of tumor growth with antiangiogenic cancer vaccine using epitope peptides derived from human vascular endothelial growth factor receptor 1," *Clinical Cancer Research*, vol. 12, no. 19, pp. 5841–5849, 2006.

[78] M. Prewett, J. Huber, Y. Li et al., "Antivascular endothelial growth factor receptor (fetal liver kinase 1) monoclonal antibody inhibits tumor angiogenesis and growth of several mouse and human tumors," *Cancer Research*, vol. 59, no. 20, pp. 5209–5218, 1999.

[79] N. Ferrara, H.-P. Gerber, and J. LeCouter, "The biology of VEGF and its receptors," *Nature Medicine*, vol. 9, no. 6, pp. 669–676, 2003.

[80] B. Zhang, Z. Zhang, X. Zhang, X. Gao, K. H. Kernstine, and L. Zhong, "Serological antibodies against LY6K as a diagnostic biomarker in esophageal squamous cell carcinoma," *Biomarkers*, vol. 17, no. 4, pp. 372–378, 2012.

[81] N. Ishikawa, A. Takano, W. Yasui et al., "Cancer-testis antigen lymphocyte antigen 6 complex locus K is a serologic biomarker and a therapeutic target for lung and esophageal carcinomas," *Cancer Research*, vol. 67, no. 24, pp. 11601–11611, 2007.

[82] M. Iwahashi, M. Katsuda, M. Nakamori et al., "Vaccination with peptides derived from cancer-testis antigens in combination with CpG-7909 elicits strong specific CD8+ T cell response in patients with metastatic esophageal squamous cell carcinoma," *Cancer Science*, vol. 101, no. 12, pp. 2510–2517, 2010.

[83] A. L. Potosky, B. A. Miller, P. C. Albertsen, and B. S. Kramer, "The role of increasing detection in the rising incidence of prostate cancer," *The Journal of the American Medical Association*, vol. 273, no. 7, pp. 548–552, 1995.

[84] E. S. Antonarakis and M. A. Eisenberger, "Expanding treatment options for metastatic prostate cancer," *The New England Journal of Medicine*, vol. 364, no. 21, pp. 2055–2058, 2011.

[85] P. W. Kantoff, C. S. Higano, N. D. Shore et al., "Sipuleucel-T immunotherapy for castration-resistant prostate cancer," *The New England Journal of Medicine*, vol. 363, no. 5, pp. 411–422, 2010.

[86] K. Itoh and A. Yamada, "Personalized peptide vaccines: a new therapeutic modality for cancer," *Cancer Science*, vol. 97, no. 10, pp. 970–976, 2006.

[87] T. Sasada, A. Yamada, M. Noguchi, and K. Itoh, "Personalized peptide vaccine for treatment of advanced cancer," *Current Medicinal Chemistry*, vol. 21, no. 21, pp. 2332–2345, 2014.

[88] T. Sasada, M. Noguchi, A. Yamada, and K. Itoh, "Personalized peptide vaccination: a novel immunotherapeutic approach for advanced cancer," *Human Vaccines & Immunotherapeutics*, vol. 8, no. 9, pp. 1309–1313, 2012.

[89] A. Yamada, T. Sasada, M. Noguchi, and K. Itoh, "Next-generation peptide vaccines for advanced cancer," *Cancer Science*, vol. 104, no. 1, pp. 15–21, 2013.

[90] F. M. Speetjens, P. J. K. Kuppen, M. J. P. Welters et al., "Induction of p53-specific immunity by a p53 synthetic long peptide vaccine in patients treated for metastatic colorectal cancer," *Clinical Cancer Research*, vol. 15, no. 3, pp. 1086–1095, 2009.

[91] R. L. Metheringham, V. A. Pudney, B. Gunn, M. Towey, I. Spendlove, and L. G. Durrant, "Antibodies designed as effective cancer vaccines," *mAbs*, vol. 1, no. 1, pp. 71–85, 2009.

[92] L. G. Durrant, V. A. Pudney, and I. Spendlove, "Using monoclonal antibodies to stimulate antitumor cellular immunity," *Expert Review of Vaccines*, vol. 10, no. 7, pp. 1093–1106, 2011.

[93] C. A. Parise and V. Caggiano, "Disparities in race/ethnicity and socioeconomic status: risk of mortality of breast cancer patients in the California Cancer Registry, 2000–2010," *BMC Cancer*, vol. 13, article 449, 2013.

[94] C. Desantis, J. Ma, L. Bryan, and A. Jemal, "Breast cancer statistics, 2013," *CA: A Cancer Journal for Clinicians*, vol. 64, no. 1, pp. 52–62, 2014.

[95] E. Mohit, A. Hashemi, and M. Allahyari, "Breast cancer immunotherapy: monoclonal antibodies and peptide-based vaccines," *Expert Review of Clinical Immunology*, vol. 10, no. 7, pp. 927–961, 2014.

[96] S. E. Wright, "Immunotherapy of breast cancer," *Expert Opinion on Biological Therapy*, vol. 12, no. 4, pp. 479–490, 2012.

[97] S. Dhillon, "Trastuzumab emtansine: a review of its use in patients with her2-positive advanced breast cancer previously treated with trastuzumab-based therapy," *Drugs*, vol. 74, no. 6, pp. 675–686, 2014.

[98] L. Amiri-Kordestani, G. M. Blumenthal, Q. C. Xu et al., "FDA approval: ado-trastuzumab emtansine for the treatment of patients with HER2-positive metastatic breast cancer," *Clinical Cancer Research*, vol. 20, no. 17, pp. 4436–4441, 2014.

[99] L. Novellino, C. Castelli, and G. Parmiani, "A listing of human tumor antigens recognized by T cells: March 2004 update," *Cancer Immunology, Immunotherapy*, vol. 54, no. 3, pp. 187–207, 2005.

[100] G. J. Morris, S. Naidu, A. K. Topham et al., "Differences in breast carcinoma characteristics in newly diagnosed African-American and Caucasian patients: a single-institution compilation compared with the national cancer institute's surveillance, epidemiology, and end results database," *Cancer*, vol. 110, no. 4, pp. 876–884, 2007.

[101] B. D. Lehmann, J. A. Bauer, X. Chen et al., "Identification of human triple-negative breast cancer subtypes and preclinical models for selection of targeted therapies," *The Journal of Clinical Investigation*, vol. 121, no. 7, pp. 2750–2767, 2011.

[102] C. Wang, Y. Zhuang, Y. Zhang et al., "Toll-like receptor 3 agonist complexed with cationic liposome augments vaccine-elicited antitumor immunity by enhancing TLR3-IRF3 signaling and type I interferons in dendritic cells," *Vaccine*, vol. 30, no. 32, pp. 4790–4799, 2012.

[103] W. Yan, W. Chen, and L. Huang, "Mechanism of adjuvant activity of cationic liposome: phosphorylation of a MAP kinase, ERK and induction of chemokines," *Molecular Immunology*, vol. 44, no. 15, pp. 3672–3681, 2007.

[104] M. Karkada, N. L. Berinstein, and M. Mansour, "Therapeutic vaccines and cancer: focus on DPX-0907," *Biologics: Targets and Therapy*, vol. 8, pp. 27–38, 2014.

[105] D. Hanahan and R. A. Weinberg, "The hallmarks of cancer," *Cell*, vol. 100, no. 1, pp. 57–70, 2000.

[106] S. K. Bhutia and T. K. Maiti, "Targeting tumors with peptides from natural sources," *Trends in Biotechnology*, vol. 26, no. 4, pp. 210–217, 2008.

[107] K. Fernald and M. Kurokawa, "Evading apoptosis in cancer," *Trends in Cell Biology*, vol. 23, no. 12, pp. 620–633, 2013.

[108] W. Huang, J. Seo, S. B. Willingham et al., "Learning from host-defense peptides: cationic, amphipathic peptoids with potent anticancer activity," *PLoS ONE*, vol. 9, no. 2, Article ID e90397, 2014.

[109] D. Amit and A. Hochberg, "Development of targeted therapy for bladder cancer mediated by a double promoter plasmid

expressing diphtheria toxin under the control of H19 and IGF2-P4 regulatory sequences," *Journal of Translational Medicine*, vol. 8, article 134, 2010.

[110] D. D. Wu, Y. F. Gao, Y. M. Qi, L. X. Chen, Y. F. Ma, and Y. Z. Li, "Peptide-based cancer therapy: opportunity and challenge," *Cancer Letters*, vol. 351, no. 1, pp. 13–22, 2014.

[111] M. Trepel, R. Pasqualini, and W. Arap, "Screening phage-display Peptide libraries for vascular targeted peptides," in *Methods in Enzymology*, vol. 445 of *Angiogenesis: In Vivo Systems, Part B*, chapter 4, pp. 83–106, Elsevier, 2008.

[112] N. D'Onofrio, M. Caraglia, A. Grimaldi et al., "Vascular-homing peptides for targeted drug delivery and molecular imaging: meeting the clinical challenges," *Biochimica et Biophysica Acta—Reviews on Cancer*, vol. 1846, no. 1, pp. 1–12, 2014.

[113] M. Shadidi and M. Sioud, "Selective targeting of cancer cells using synthetic peptides," *Drug Resistance Updates*, vol. 6, no. 6, pp. 363–371, 2003.

[114] S. M. Farkhani, A. Valizadeh, H. Karami, S. Mohammadi, N. Sohrabi, and F. Badrzadeh, "Cell penetrating peptides: efficient vectors for delivery of nanoparticles, nanocarriers, therapeutic and diagnostic molecules," *Peptides*, vol. 57, pp. 78–94, 2014.

[115] A. Bolhassani, "Potential efficacy of cell-penetrating peptides for nucleic acid and drug delivery in cancer," *Biochimica et Biophysica Acta—Reviews on Cancer*, vol. 1816, no. 2, pp. 232–246, 2011.

[116] F.-S. Kao, Y.-R. Pan, R.-Q. Hsu, and H.-M. Chen, "Efficacy verification and microscopic observations of an anticancer peptide, CB1a, on single lung cancer cell," *Biochimica et Biophysica Acta—Biomembranes*, vol. 1818, no. 12, pp. 2927–2935, 2012.

[117] K. Beck, J. E. Gambee, C. A. Bohan, and H. P. Bächinger, "The C-terminal domain of cartilage matrix protein assembles into a triple-stranded α-helical coiled-coil structure," *Journal of Molecular Biology*, vol. 256, no. 5, pp. 909–923, 1996.

[118] L. Q. Liu and Y. B. Miao, "Metastatic melanoma targeting property of a novel Tc-99m-labeled HYNIC-conjugated lactam bridge-cyclized alpha-MSH peptide," *Nuclear Medicine and Biology*, vol. 41, no. 7, p. 622, 2014.

[119] F. E. González, M. Ramírez, E. B. Allerbring et al., "Melanocortin 1 receptor-derived peptides are efficiently recognized by cytotoxic T lymphocytes from melanoma patients," *Immunobiology*, vol. 219, no. 3, pp. 189–197, 2014.

[120] E. Vacas, A. M. Bajo, A. V. Schally, M. Sánchez-Chapado, J. C. Prieto, and M. J. Carmena, "Vasoactive intestinal peptide induces oxidative stress and suppresses metastatic potential in human clear cell renal cell carcinoma," *Molecular and Cellular Endocrinology*, vol. 365, no. 2, pp. 212–222, 2013.

[121] K. Yoshimura, T. Minami, M. Nozawa, and H. Uemura, "Phase I clinical trial of human vascular endothelial growth factor receptor 1 peptide vaccines for patients with metastatic renal cell carcinoma," *British Journal of Cancer*, vol. 108, no. 6, pp. 1260–1266, 2013.

[122] S. Rausch, S. Kruck, A. Stenzl, and J. Bedke, "IMA901 for metastatic renal cell carcinoma in the context of new approaches to immunotherapy," *Future Oncology*, vol. 10, no. 6, pp. 937–948, 2014.

[123] Y. Liu, X. Cui, Y.-E. Sun et al., "Intrathecal injection of the peptide Myr-NR2B9c attenuates bone cancer pain via perturbing N-methyl-D-aspartate receptor-PSD-95 protein interactions in mice," *Anesthesia & Analgesia*, vol. 118, no. 6, pp. 1345–1354, 2014.

[124] Z. Xu, S. Ramishetti, Y.-C. Tseng, S. Guo, Y. Wang, and L. Huang, "Multifunctional nanoparticles co-delivering Trp2 peptide and CpG adjuvant induce potent cytotoxic T-lymphocyte response against melanoma and its lung metastasis," *Journal of Controlled Release*, vol. 172, no. 1, pp. 259–265, 2013.

[125] Z. J. Li and C. H. Cho, "Peptides as targeting probes against tumor vasculature for diagnosis and drug delivery," *Journal of Translational Medicine*, vol. 10, article S1, 2012.

[126] E. Ruoslahti, S. N. Bhatia, and M. J. Sailor, "Targeting of drugs and nanoparticles to tumors," *The Journal of Cell Biology*, vol. 188, no. 6, pp. 759–768, 2010.

[127] J. Enbäck and P. Laakkonen, "Tumour-homing peptides: tools for targeting, imaging and destruction," *Biochemical Society Transactions*, vol. 35, no. 4, pp. 780–783, 2007.

[128] A. J. T. George, L. Lee, and C. Pitzalis, "Isolating ligands specific for human vasculature using in vivo phage selection," *Trends in Biotechnology*, vol. 21, no. 5, pp. 199–203, 2003.

[129] F. Aranda, E. Vacchelli, A. Eggermont et al., "Trial watch: peptide vaccines in cancer therapy," *OncoImmunology*, vol. 2, no. 12, Article ID e26621, 2013.

[130] M. Mohme, M. C. Neidert, L. Regli, M. Weller, and R. Martin, "Immunological challenges for peptide-based immunotherapy in glioblastoma," *Cancer Treatment Reviews*, vol. 40, no. 2, pp. 248–258, 2014.

[131] R. Takahashi, U. Toh, N. Iwakuma et al., "Feasibility study of personalized peptide vaccination for metastatic recurrent triple-negative breast cancer patients," *Breast Cancer Research*, vol. 16, no. 4, article R70, 2014.

[132] D. Valmori, J.-F. Fonteneau, C. M. Lizana et al., "Enhanced generation of specific tumor-reactive CTL in vitro by selected Melan-A/MART-1 immunodominant peptide analogues," *The Journal of Immunology*, vol. 160, no. 4, pp. 1750–1758, 1998.

Hindawi Publishing Corporation
Journal of Immunology Research
Volume 2015, Article ID 473909, 8 pages
http://dx.doi.org/10.1155/2015/473909

Clinical Study

Phase II Study of Personalized Peptide Vaccination with Both a Hepatitis C Virus-Derived Peptide and Peptides from Tumor-Associated Antigens for the Treatment of HCV-Positive Advanced Hepatocellular Carcinoma Patients

Shigeru Yutani,[1] Kazuomi Ueshima,[2] Kazumichi Abe,[3] Atsushi Ishiguro,[4] Junichi Eguchi,[5] Satoko Matsueda,[1] Nobukazu Komatsu,[6] Shigeki Shichijo,[1] Akira Yamada,[7] Kyogo Itoh,[1] Tetsuro Sasada,[1,6] Masatoshi Kudo,[2] and Masanori Noguchi[7]

[1]*Cancer Vaccine Center, Kurume University, Kurume 839-0863, Japan*
[2]*Department of Gastroenterology and Hepatology, Kinki University Faculty of Medicine, Osaka 589-8511, Japan*
[3]*Department of Digestive, Rheumatism and Collagen Internal Medicine, Fukushima Prefectural Medical College, Fukushima 960-1295, Japan*
[4]*Department of Medical Oncology, Hirosaki University Graduate School of Medicine, Hirosaki 036-8562, Japan*
[5]*Department of Gastroenterology, Showa University School of Medicine, Tokyo 142-8555, Japan*
[6]*Department of Immunology, Kurume University School of Medicine, Kurume 830-0011, Japan*
[7]*Research Center for Innovative Cancer Therapy, Kurume University, Kurume 830-0011, Japan*

Correspondence should be addressed to Shigeru Yutani; yutani@med.kurume-u.ac.jp

Received 27 September 2014; Accepted 24 December 2014

Academic Editor: Masha Fridkis-Hareli

Objective. To evaluate safety and immune responses of personalized peptide vaccination (PPV) for hepatitis C virus- (HCV-) positive advanced hepatocellular carcinoma (HCC). *Patients and Methods*. Patients diagnosed with HCV-positive advanced HCC were eligible for this study. A maximum of four HLA-matched peptides were selected based on the preexisting IgG responses specific to 32 different peptides, which consisted of a single HCV-derived peptide at core protein positions 35–44 (C-35) and 31 peptides derived from 15 different tumor-associated antigens (TAAs), followed by subcutaneous administration once per week for 8 weeks. Peptide-specific cytotoxic T lymphocyte (CTL) and IgG responses were measured before and after vaccination. *Results*. Forty-two patients were enrolled. Grade 3 injection site skin reaction was observed in 2 patients, but no other PPV-related severe adverse events were noted. Peptide-specific CTL responses before vaccination were observed in only 3 of 42 patients, but they became detectable in 23 of 36 patients tested after vaccination. Peptide-specific IgG responses were also boosted in 19 of 36 patients. Peptide-specific IgG1 responses to both C-35 and TAA-derived peptides could be potentially prognostic for overall survival. *Conclusion*. Further clinical study of PPV would be warranted for HCV-positive advanced HCC, based on the safety and strong immune induction.

1. Introduction

Although sorafenib has been approved for advanced hepatocellular carcinoma (HCC), which is defined as metastatic or locally advanced disease not amenable to locoregional therapies, the efficacy of this agent was modest and the median survival time (MST) was around 10 months [1, 2]. In addition, no other systemic treatments have shown obvious efficacy in the past 5 years [3, 4]. Nevertheless, new approaches to immunotherapy, such as glypican-3 targeting peptide vaccine and anti-CTLA4 treatment, have shown promising results in the early phase of clinical studies [5–9].

We have developed a novel regimen of personalized peptide vaccination (PPV) that can be used to treat cancer patients with many different HLA-class I types. In this approach, the preexisting host immunity is analyzed to select

4 peptides from among 31 pooled peptides derived from 15 different TAAs, which are then administered as a vaccination [10–15]. PPV has the potential to prolong overall survival (OS) in advanced cancer patients who fail to respond to standard chemotherapy. We also reported a prophylactic effect of PPV with hepatitis C virus- (HCV-) derived peptides against the development of HCC associated with HCV [16–18]. The HCV-core peptide at positions 35–44 (C-35 peptide), which can induce cytotoxic T lymphocyte (CTL) activity in many different HLA-class I types, is a key peptide in the prophylactic effect [19]. In the current study, therefore, we conducted a phase II study of PPV, in which 4 peptides were selected from among 32 different peptides that consisted of a C-35 peptide and 31 peptides derived from 15 TAAs, for HCV-positive advanced HCC patients in order to evaluate the safety and immune responses.

2. Patients and Methods

2.1. Patients. Patients who were diagnosed with HCV-positive advanced HCC as defined by metastatic or locally advanced disease and were not candidates for locoregional therapies were eligible for this study. Staging was carried out according to the Japanese integrated staging system (Liver Cancer Study Group of Japan) [8, 20]. The patients had to show positive IgG responses to at least 2 of the 32 different vaccine candidate peptides, as reported previously [10–18]. Other inclusion criteria were as follows: age between 20 and 80 years; an Eastern Cooperative Oncology Group (ECOG) performance status of 0 or 1 at the time of first visit; positive status for the human leukocyte antigens (HLA) A2, A24, A3 supertype (A3, A11, A31, or A33), or A26; life expectancy of at least 12 weeks; and adequate hematologic, hepatic, and renal function. Exclusion criteria included pulmonary, cardiac, or other systemic diseases; an acute infection; a history of severe allergic reactions; pregnancy or nursing; and other inappropriate conditions for enrollment as judged by clinicians. The protocol was approved by the Ethical Committee of each university and registered in the UMIN Clinical Trials Registry (UMIN000003520, UMIN000005634). All patients were given a full explanation of the protocol and provided their informed consent before enrollment.

2.2. Clinical Protocol. This was a phase II study conducted by Kurume University, Kinki University, Hirosaki University, Fukushima Prefectural College, and Showa University Hospitals. Primary endpoint was to evaluate the safety and immunological responses. Secondary endpoint was to evaluate a clinical benefit from the viewpoint of OS. C-35 peptide (YLLPRRGPRL) derived from the HCV core protein, which was applicable for all the above-listed HLA types as reported previously [16–19], and 31 peptides, which were derived from 15 different TAAs [12 peptides for HLA-A2, 16 peptides for HLA-A24, 9 peptides for HLA-A3 supertypes (-A3, -A11, -A31, and -A33), and 4 peptides for HLA-A26] (Supplementary Table 1, Supplementary Material available online at http://dx.doi.org/10.1155/2015/473909), were employed for vaccination. These peptides were prepared under the conditions of Good Manufacturing Practice by the Polypeptide Laboratories (San Diego, CA) and American Peptide Company (Vista, CA).

Two to four peptides for vaccination to individual patients were selected in consideration of the HLA typing and preexisting host immunity, as assessed by the titers of IgG specific to each of the 32 different vaccine candidates before vaccination [10–18]. The selected peptides were subcutaneously administered with incomplete Freund's adjuvant (Montanide ISA-51; Seppic, Paris, France) once a week for 8 consecutive weeks. During the PPV, only best supportive care was allowed except for patients who were receiving chemotherapy or targeted therapy at the time of entry. Tumor markers (TM), α-fetoprotein (AFP), and des-γ-carboxy prothrombin (DCP) were measured before and after the 8th vaccination. Adverse events were monitored according to the National Cancer Institute Common Terminology Criteria for Adverse Events version 4.0 (NCI-CTC Ver. 4.0).

2.3. Measurement of IgG and CTL Responses. Humoral immune responses specific to each of the 32 peptide candidates were determined by measuring the levels of peptide-specific IgG and IgG subclasses (IgG1, IgG2, IgG3, and IgG4) using the Luminex system (Luminex, Austin, TX), as previously reported [10–15]. If the titers of peptide-specific IgG to at least one of the vaccinated peptides after the 8th vaccination were more than twofold higher than those before vaccination, the changes were considered to be significant, as previously reported [10–15]. CTL responses specific to the vaccinated peptides were evaluated by interferon- (IFN-) γ ELISPOT assay using peripheral blood mononuclear cells (PBMCs) before and after vaccination as previously reported [10–15]. As a control, CTL responses specific to CEF peptides (MABTECH, Cincinnati, OH), a mixture of virus-derived CTL epitopes, were also examined.

2.4. Statistical Analyses. OS was calculated from the first day of peptide vaccination until the date of death or the last date when the patient was known to be alive. The survival analysis was performed with the Kaplan-Meier method, and a comparison of the survival curves was performed with the log-rank test or Wilcoxon test. Spearman's correlation index was utilized to examine the association among the values of IgG and IgG subclasses. Values of $P < 0.05$ were considered to indicate statistical significance. All statistical analyses were conducted using the JMP software package, version 10 (SAS Institute Inc., Cary, NC).

3. Results

3.1. Patients' Characteristics. Between December 2000 and May 2013, 42 patients with HCV-positive advanced HCC (Stage IVa: 15 patients; Stage IVb: 27 patients) were enrolled in this study (Table 1). The Japanese integrated staging (JIS) scores [20, 21] of the 42 patients were 3 ($n = 21$), 4 ($n = 18$), and 5 ($n = 3$). Previously conducted regimens of locoregional therapies included hepatectomy ($n = 14$), surgery other than hepatectomy ($n = 2$), radiation ($n = 9$), transcatheter

Table 1: Patients' characteristics ($n = 42$).

Factor	Number
Age	
Median (range)	70 (48–80)
Gender	
Male	34
Female	8
ECOG performance status	
0	32
1	10
HLA type	
A24	24
A2	21
A3 supertype	14
A26	13
Clinical stage	
IVa	15
IVb	27
JIS score	
3	21
4	18
5	3
Previously conducted treatments	
Locoregional	
Hepatectomy	14
Surgery other than hepatectomy	2
Radiation	9
Transcatheter arterial embolization (TAE)	23
Transcatheter arterial chemoembolization (TACE)	16
Hepatic arterial infusion chemotherapy (HAIC)	16
Radiofrequency ablation (RFA)	15
Percutaneous ethanol injection therapy (PEIT)	6
Microwave coagulation therapy (MCT)	3
Systemic	
Sorafenib	21
5-FU based chemotherapies	6
Other clinical trials	9
AFP at first visit	
Median (range), ng/mL	376 (3.7–103000)
DCP at first visit	
Median (range), mAU/mL	2335 (11–778000)
Number of vaccinations	
Median (range)	8 (3–8)
Combination therapy	
None	30
Sorafenib	10
Chemotherapy	2

ECOG: Eastern Cooperative Oncology Group; JIS: Japanese integrated staging; AFP: α-fetoprotein; DCP: des-γ-carboxy prothrombin.

arterial embolization (TAE) ($n = 23$), transcatheter arterial chemoembolization (TACE) ($n = 16$), hepatic arterial infusion chemotherapy (HAIC) ($n = 16$), radiofrequency ablation (RFA) ($n = 15$), percutaneous ethanol injection therapy (PEIT) ($n = 6$), and microwave coagulation therapy (MCT) ($n = 3$). The median number of these treatment regimens was 2, with a range of 0 to 5. Previously conducted systemic therapies for advanced HCC were sorafenib ($n = 21$), 5-FU based drugs ($n = 6$), and new clinical trials ($n = 9$), with a median regimen number of 1 and a range of 0 to 4.

The median value of AFP at the time of the first visit, two weeks before the 1st vaccination, was 376 ng/mL (3.7 to 103,000 ng/mL), while the median value of DCP was 2,335 mAU/mL (11 to 778,000 mAU/mL). Thirty-six patients received 8 vaccinations and completed the protocol, whereas the remaining 6 patients dropped from the protocol before the 8th vaccination due to rapid disease progression ($n = 5$) or of their own will ($n = 1$). The median number of peptide vaccinations was 8, with a range of 3 to 8. Thirty patients received PPV alone, 10 patients received PPV with sorafenib, 1 patient received PPV with S-1, and 1 patient received PPV with HAIC.

3.2. Adverse Events. Skin reactions of grades 1, 2, and 3 at the injection sites were observed in 15, 4, and 2 patients, respectively, but no other PPV-related severe adverse events were observed (Table 2). Fourteen grade 3 adverse events were observed during vaccination, with 10 events occurring in patients treated with PPV alone and 4 events occurring in those with PPV and combined therapies. No grade 4 adverse events were observed, whereas a grade 5 adverse event was observed in 1 patient with PPV and sorafenib (pleural infection). All of them except for skin reaction at injection sites were considered to be due to disease progression or combined therapies judged by an independent ethical committee.

3.3. Immune Responses. Both peptide-specific CTL and IgG responses were analyzed in prevaccination blood samples from all 42 patients and in postvaccination samples from 36 patients who completed the 8th vaccination. CTL responses to the vaccinated peptides were detectable in only 3 of 42 patients before vaccination (2 patients for C-35 peptide and 1 patient for TAA peptide) (Supplementary Table 2). However, it became detectable after vaccination in 23 of 36 patients: CTL responses specific to the C-35 peptide were observed in 19 of 36 patients tested, and those specific to the TAA-derived peptides were observed in 15 of 36 patients. We also tested CTL responses to CEF peptides, a mixture of virus-derived CTL epitopes, as a control. They were present in 15 of 42 patients before vaccination and in 19 of 36 patients after the 8th vaccination (Supplementary Table 2). Increase or decrease of CTL responses to CEF peptides was observed in 15 or 5 of 36 patients, respectively.

Peptide-specific IgG responses before vaccination were observed in all patients, with very high levels of IgG titers to the C-35 peptide in most of them. Augmentation of the IgG responses to at least one of the vaccinated peptides after vaccination was observed in 19 of 36 patients tested, with an increase of IgG specific to the C-35 peptide in 5 of 36 patients and an increase of IgG specific to TAA-derived peptides in 19 of 36 patients (Supplementary Table 2). To

Table 2: Adverse events during the PPV ($n = 42$).

Event	Number					
	Grade 1	Grade 2	Grade 3	Grade 4	Grade 5	Total (%)
Injection site skin reaction	15	4	2	0	0	21 (50%)
Blood/bone marrow						
Anemia	7	4	0	0	0	11 (26%)
Lymphopenia	9	1	0	0	0	10 (24%)
Neutropenia	0	2	0	0	0	2 (5%)
Thrombocytopenia	7	0	0	0	0	7 (17%)
Leukopenia	3	1	0	0	0	4 (10%)
Laboratory						
AST increase	4	6	4	0	0	14 (33%)
ALT increase	10	1	2	0	0	13 (31%)
ALP increase	9	2	0	0	0	11 (26%)
GGT increase	7	3	2	0	0	12 (29%)
Bilirubin increase	2	2	0	0	0	4 (10%)
Creatinine increase	2	1	0	0	0	3 (7%)
Gastrointestinal disorders						
Anorexia	5	3	0	0	0	8 (19%)
Abdominal distension	2	0	0	0	0	2 (5%)
Ascites	2	1	1	0	0	4 (10%)
Constipation	0	2	0	0	0	2 (5%)
Edema limbs	2	0	0	0	0	2 (5%)
Fever	5	0	0	0	0	5 (12%)
Malaise	3	0	0	0	0	3 (7%)
Pain	1	3	2	0	0	6 (14%)
Pruritus	2	0	0	0	0	2 (5%)
Eruption	2	1	0	0	0	3 (7%)
Urinary incontinence	0	1	0	0	0	1 (2%)
Pleural infection	0	0	0	0	1	1 (2%)
Hypertension	0	0	1	0	0	1 (2%)
Insomnia	0	1	0	0	0	1 (2%)

better understand humoral immune responses, the levels of IgG subclasses (IgG1, IgG2, IgG3, and IgG4) specific to the vaccinated peptides before and after vaccination were also measured (Supplementary Table 3). There was a significant correlation between peptide-specific IgG and IgG1 (Spearman rank correlation coefficient = 0.865), but not between IgG and IgG2, IgG3, or IgG4 (Spearman rank correlation coefficient: IgG versus IgG2 = 0.376, IgG versus IgG3 = 0.371, and IgG versus IgG4 = 0.310). In contrast, there were substantial correlations among peptide-specific IgG2, IgG3, and IgG4 (Spearman rank correlation coefficient: IgG2 versus IgG3 = 0.554, IgG2 versus IgG4 = 0.491, and IgG3 versus IgG4 = 0.556).

3.4. Clinical Responses. AFP was decreased after vaccination in 9 of 33 patients, who showed abnormal elevation of serum AFP (>10 ng/mL) before vaccination (Supplementary Table 2). Decrease in another tumor marker, DCP, after vaccination was also observed in 9 of 33 patients, who showed abnormal elevation of serum DCP (>40 mAU/mL) before vaccination (Supplementary Table 2). The MST of the 42 patients was 184 days (Figure 1(a)). It is of note that the MST of patients with a JIS score of 3 (189 days) was not substantially different from that of patients with a JIS score of 4 or 5 (164 days) (Figure 1(b), $P = 0.73$ by log-rank test). In addition, combination therapy with sorafenib had no effect on the MST (Figure 1(c), $P = 0.82$ by log-rank test). As expected, however, patients showing decrease in AFP or DCP after the 8th vaccination ($n = 13$; MST, 286 days) showed longer survival than those without such decreases ($n = 23$; MST, 180 days) (Figure 1(d); $P = 0.01$ by log-rank test, $P = 0.046$ by Wilcoxon test).

Notably, all 6 patients showing increased IgG1 responses to both C-35 peptide and TAA-derived peptides survived more than 210 days, and their MST (286 days) tended to be longer than that of patients showing an increased IgG1 response to either peptide ($n = 18$, 162 days) or that of patients showing no increase to any peptide ($n = 12$, 223 days) (Figure 2(a); $P = 0.12$ by log-rank test, $P = 0.06$ by Wilcoxon test). However, peptide-specific IgG (Figure 2(b); $P = 0.56$ by

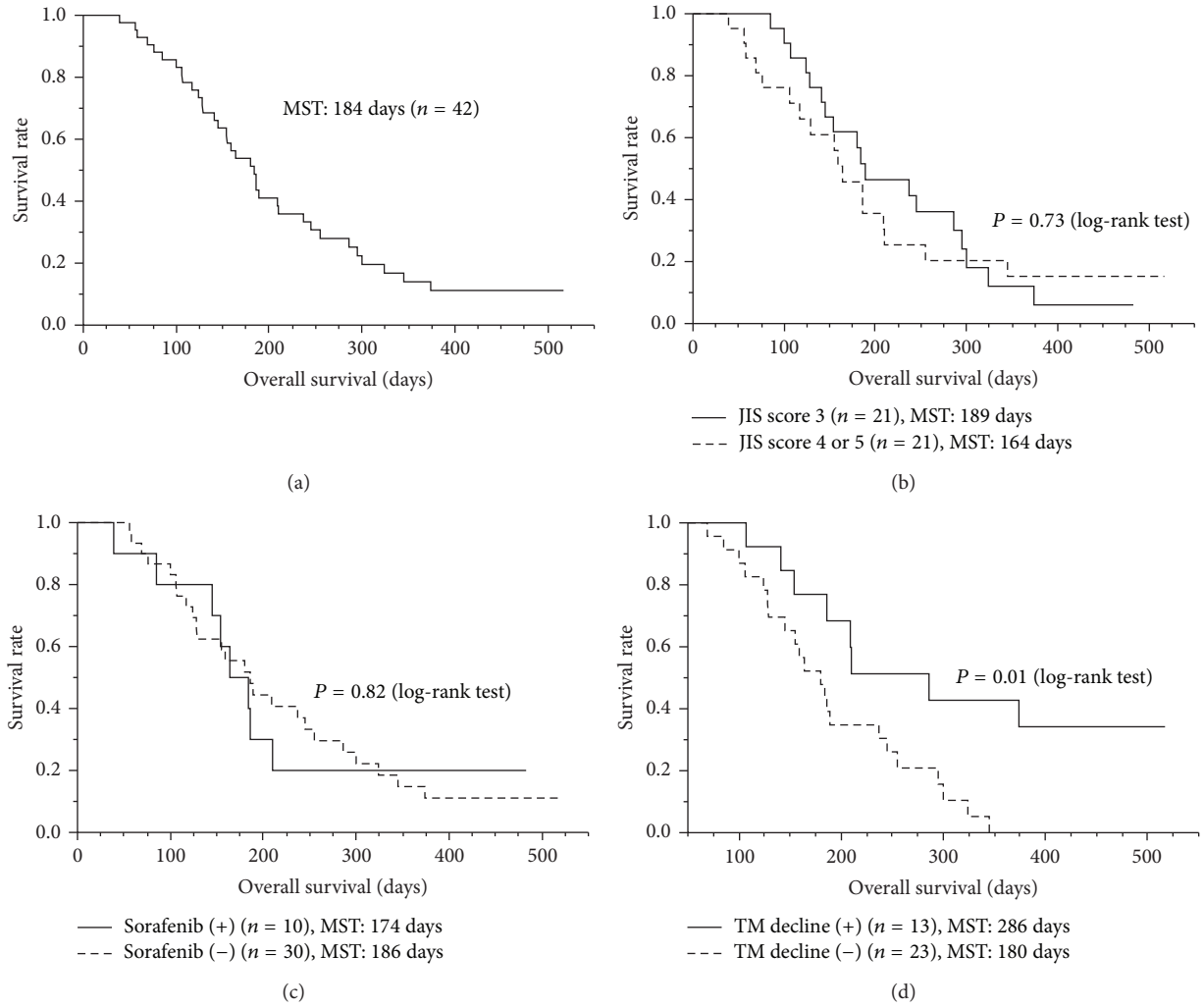

Figure 1: Survival analysis. The survival analysis was performed with the Kaplan-Meier method, and a comparison of the survival curves was performed with the log-rank test. (a) The median survival time (MST) from the first vaccination of PPV was 184 days in 42 patients. (b) The patients with a JIS score of 3 (MST, 189 days) did not show significantly different survival, compared to those with a JIS score of 4 or 5 (MST, 164 days) ($P = 0.73$). (c) Combination therapy with sorafenib did not affect OS ($P = 0.82$). (d) Patients with decreased TM (tumor markers), AFP, or DCP, after vaccination (MST, 286 days) showed longer survival than those without it (MST, 180 days) ($P = 0.01$).

log-rank test), IgG2 (Figure 2(c), $P = 0.64$ by log-rank test), IgG3, or IgG4 responses (data not shown) as well as peptide-specific CTL responses (Figure 2(d), $P = 0.69$ by log-rank test) did not show prognostic significance.

4. Discussion

The tumor immunity against HCV-positive advanced HCC was reported to be deeply suppressed [22]. For example, molecules involved in T cell check points have been suggested to inhibit CTL responses against tumor cells in advanced HCC [9]. As expected, the current study demonstrated that CTL responses to the vaccinated peptides, but not to virus-derived peptides, before vaccination were rarely observed, indicating that the antitumor immunity in the enrolled patients was severely depressed. However, CTL responses to the vaccinated peptides became detectable at the end of the 8th vaccination in 23 of 36 patients tested. In addition, PPV did not suppress but rather increased the CTL responses to virus-derived peptides. The peptide-specific IgG responses were also boosted in 19 of 36 patients tested. Severe PPV-related adverse events were rarely observed, in agreement with our previous reports [10–18]. In sum, these results indicate that PPV might be a useful approach for HCV-positive advanced HCC patients, who fail to respond to various locoregional and/or systemic treatment regimens, from the viewpoint of both safety and immunological responses.

The MST of the enrolled patients from the first vaccination of PPV was 184 days, with 189 days for the patients with JIS score of 3 and 164 days for those with JIS score of 4 or 5. The current data might be promising for the patients with the JIS score of 4 or 5, since the MST of these patients was reported to be around 3 to 4 months [20, 21]. The MSTs of patients treated with PPV alone or PPV in combination

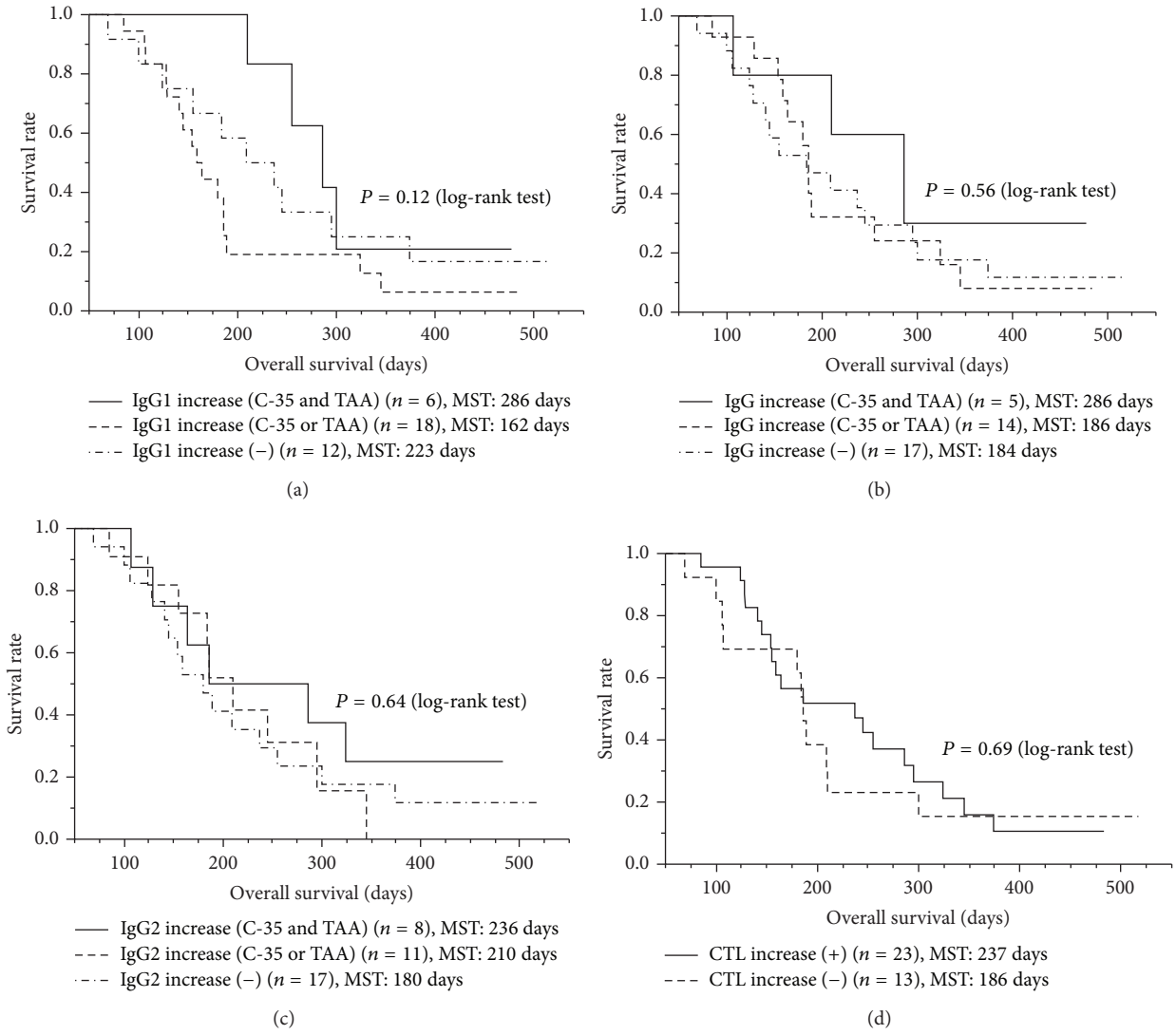

Figure 2: Immune response and overall survival. Association between immune responses and OS was examined with the Kaplan-Meier method, and a comparison of the survival curves was performed with the log-rank test. (a) The peptide-specific IgG1 response was potentially prognostic ($P = 0.12$ by log-rank test, $P = 0.06$ by Wilcoxon test); all 6 patients showing increased IgG1 responses to both the C-35 peptide and TAA-derived peptides survived more than 210 days, and their MST (286 days) tended to be longer than that of patients showing increased IgG1 responses to either peptide (162 days) or that of patients showing no increase to any peptide (223 days). (b) The peptide-specific IgG response was not prognostic ($P = 0.56$). (c) The peptide-specific IgG2 response was not prognostic ($P = 0.64$). (d) The peptide-specific CTL response was not prognostic ($P = 0.69$).

with sorafenib were 186 or 174 days, respectively. No grade 4 or 5 adverse events were observed in patients with PPV alone, whereas a grade 5 adverse event (pleural infection) was observed in a patient receiving PPV and sorafenib. These results suggested that the combination of sorafenib and PPV had no additive benefit, although the scale of the study was small.

From the viewpoint of biomarkers, the peptide-specific IgG1 response was suggested to be a potentially prognostic factor in this study, since all 6 patients showing boosted IgG1 responses to both C-35 peptide and TAA-derived peptides survived more than 210 days, and their MST (286 days) tended to be longer than that of patients showing boosted IgG1 responses to either peptide alone (162 days) or that of patients showing no increase in response to any peptide (223 days) ($P = 0.12$ by log-rank test, $P = 0.06$ by Wilcoxon test). In contrast, the peptide-specific IgG2 response did not show prognostic significance. Since IgG1, but not IgG2, is known to enhance antibody-mediated opsonization and phagocytosis of antigens, peptide-specific IgG1 may enhance antitumor immunity through phagocytosis and cross-presentation of antigen peptides [23]. Further studies will be needed to clarify the mechanisms.

In contrast to IgG1 responses as a potential prognostic biomarker, the peptide-specific CTL response was not well correlated with OS in these patients under PPV. This may

have been mainly due to the small size of patient numbers. Indeed, we suggested that the peptide-specific IgG response was more useful than the peptide-specific CTL response as a prognostic biomarker for patients under PPV, primarily because monitoring of IgG responses shows higher sensitivity than that of CTL responses [24].

5. Conclusion

The current study indicated that PPV with both a HCV-derived CTL epitope peptide and 31 peptides from TAAs could be recommended for the next step of a clinical trial in HCV-positive advanced HCC patients, because of safety and strong immune induction.

Conflict of Interests

One of the authors, Akira Yamada, is a board member of the Green Peptide Company, Ltd. Both Kyogo Itoh and Akira Yamada own stock in the Green Peptide Company, Ltd. Kyogo Itoh received research funds from Taiho Pharmaceutical Company, Ltd. The other authors declare that they have no competing interests.

Acknowledgments

This study was supported in part by grants from the Regional Innovation Cluster Program, by the Project for Development of Innovative Research on Cancer Therapeutics (P-Direct) of the Ministry of Education, Culture, Sports, Science and Technology of Japan, and by the Sendai Kousei Hospital.

References

[1] J. M. Llovet, S. Ricci, V. Mazzaferro et al., "Sorafenib in advanced hepatocellular carcinoma," *The New England Journal of Medicine*, vol. 359, no. 4, pp. 378–390, 2008.

[2] A.-L. Cheng, Y.-K. Kang, Z. Chen et al., "Efficacy and safety of sorafenib in patients in the Asia-Pacific region with advanced hepatocellular carcinoma: a phase III randomised, double-blind, placebo-controlled trial," *The Lancet Oncology*, vol. 10, no. 1, pp. 25–34, 2009.

[3] A.-L. Cheng, Y.-K. Kang, D.-Y. Lin et al., "Sunitinib versus sorafenib in advanced hepatocellular cancer: results of a randomized phase III trial," *Journal of Clinical Oncology*, vol. 31, no. 32, pp. 4067–4075, 2013.

[4] J. M. Llovet, T. Decaens, J.-L. Raoul et al., "Brivanib in patients with advanced hepatocellular carcinoma who were intolerant to sorafenib or for whom sorafenib failed: results from the randomized phase III BRISK-PS study," *Journal of Clinical Oncology*, vol. 31, no. 28, pp. 3509–3516, 2013.

[5] T. F. Greten, A. G. Duffy, and F. Korangy, "Hepatocellular carcinoma from an immunologic perspective," *Clinical Cancer Research*, vol. 19, no. 24, pp. 6678–6685, 2013.

[6] J. Heo, T. Reid, L. Ruo et al., "Randomized dose-finding clinical trial of oncolytic immunotherapeutic vaccinia JX-594 in liver cancer," *Nature Medicine*, vol. 19, no. 3, pp. 329–336, 2013.

[7] B.-H. Park, T. Hwang, T.-C. Liu et al., "Use of a targeted oncolytic poxvirus, JX-594, in patients with refractory primary or metastatic liver cancer: a phase I trial," *The Lancet Oncology*, vol. 9, no. 6, pp. 533–542, 2008.

[8] Y. Sawada, T. Yoshikawa, D. Nobuoka et al., "Phase I trial of a glypican-3-derived peptide vaccine for advanced hepatocellular carcinoma: immunologic evidence and potential for improving overall survival," *Clinical Cancer Research*, vol. 18, no. 13, pp. 3686–3696, 2012.

[9] B. Sangro, C. Gomez-Martin, M. de la Mata et al., "A clinical trial of CTLA-4 blockade with tremelimumab in patients with hepatocellular carcinoma and chronic hepatitis C," *Journal of Hepatology*, vol. 59, no. 1, pp. 81–88, 2013.

[10] M. Terasaki, S. Shibui, Y. Narita et al., "Phase I trial of a personalized peptide vaccine for patients positive for human leukocyte antigen-A24 with recurrent or progressive glioblastoma multiforme," *Journal of Clinical Oncology*, vol. 29, no. 3, pp. 337–344, 2011.

[11] R. Takahashi, Y. Ishibashi, K. Hiraoka et al., "Phase II study of personalized peptide vaccination for refractory bone and soft tissue sarcoma patients," *Cancer Science*, vol. 104, no. 10, pp. 1285–1294, 2013.

[12] M. Noguchi, T. Kakuma, H. Uemura et al., "A randomized phase II trial of personalized peptide vaccine plus low dose estramustine phosphate (EMP) versus standard dose EMP in patients with castration resistant prostate cancer," *Cancer Immunology, Immunotherapy*, vol. 59, no. 7, pp. 1001–1009, 2010.

[13] M. Noguchi, T. Sasada, and K. Itoh, "Personalized peptide vaccination: a new approach for advanced cancer as therapeutic cancer vaccine," *Cancer Immunology, Immunotherapy*, vol. 62, no. 5, pp. 919–929, 2013.

[14] K. Matsumoto, M. Noguchi, T. Satoh et al., "A phase I study of personalized peptide vaccination for advanced urothelial carcinoma patients who failed treatment with methotrexate, vinblastine, adriamycin and cisplatin," *BJU International*, vol. 108, no. 6, pp. 831–838, 2011.

[15] K. Yoshida, M. Noguchi, T. Mine et al., "Characteristics of severe adverse events after peptide vaccination for advanced cancer patients: analysis of 500 cases," *Oncology Reports*, vol. 25, no. 1, pp. 57–62, 2011.

[16] N. Komatsu, S. Yutani, A. Yamada et al., "Prophylactic effect of peptide vaccination against hepatocellular carcinoma associated with hepatitis C virus," *Experimental and Therapeutic Medicine*, vol. 1, no. 4, pp. 619–626, 2010.

[17] S. Yutani, A. Yamada, K. Yoshida et al., "Phase I clinical study of a personalized peptide vaccination for patients infected with hepatitis C virus (HCV) 1b who failed to respond to interferon-based therapy," *Vaccine*, vol. 25, no. 42, pp. 7429–7435, 2007.

[18] S. Yutani, N. Komatsu, S. Shichijo et al., "Phase I clinical study of a peptide vaccination for hepatitis C virus-infected patients with different human leukocyte antigen-class I-A alleles," *Cancer Science*, vol. 100, no. 10, pp. 1935–1942, 2009.

[19] Y. Niu, N. Komatsu, Y. Komohara et al., "A peptide derived from hepatitis C virus (HCV) core protein inducing cellularresponses in patients with HCV with various HLA class IA alleles," *Journal of Medical Virology*, vol. 81, no. 7, pp. 1232–1240, 2009.

[20] M. Kudo, H. Chung, S. Haji et al., "Validation of a new prognostic staging system for hepatocellular carcinoma: the JIS score compared with the CLIP score," *Hepatology*, vol. 40, no. 6, pp. 1396–1405, 2004.

[21] M. Winkel od, D. Nagel, J. Sappl et al., "Prognosis of patients with hepatocellular carcinoma. Validation and ranking of established staging-systems in a large western HCC-cohort," *PLoS ONE*, vol. 7, no. 10, Article ID e45066, 13 pages, 2012.

[22] S. M. Rushbrook, S. M. Ward, E. Unitt et al., "Regulatory T cells suppress in vitro proliferation of virus-specific $CD8^+$ T cells during persistent hepatitis C virus infection," *Journal of Virology*, vol. 79, no. 12, pp. 7852–7859, 2005.

[23] B. Platzer, M. Stout, and E. Fiebiger, "Antigen cross-presentation of immune complexes," *Frontiers in Immunology*, vol. 5, article 140, 2014.

[24] M. Noguchi, T. Mine, N. Komatsu et al., "Assessment of immunological biomarkers in patients with advanced cancer treated by personalized peptide vaccination," *Cancer Biology and Therapy*, vol. 10, no. 12, pp. 1266–1279, 2010.

Hindawi Publishing Corporation
Journal of Immunology Research
Volume 2015, Article ID 786501, 9 pages
http://dx.doi.org/10.1155/2015/786501

Research Article

The Peptide Vaccine Combined with Prior Immunization of a Conventional Diphtheria-Tetanus Toxoid Vaccine Induced Amyloid β Binding Antibodies on Cynomolgus Monkeys and Guinea Pigs

Akira Yano,[1] Kaori Ito,[2] Yoshikatsu Miwa,[3] Yoshito Kanazawa,[4] Akiko Chiba,[5] Yutaka Iigo,[6] Yoshinori Kashimoto,[6] Akira Kanda,[7] Shinji Murata,[7] and Mitsuhiro Makino[2]

[1] *Iwate Biotechnology Research Center, 22-174-4 Narita, Kitakami, Iwate 024-0003, Japan*
[2] *Venture Science Laboratories, R&D Division, Daiichi-Sankyo Co., Ltd., 1-2-58 Hiromachi, Shinagawa-ku, Tokyo 140-8710, Japan*
[3] *Quality Assurance Division, Hayashibara Co., Ltd., 675-1 Fujisaki, Naka-ku, Okayama 702-8006, Japan*
[4] *R&D Planning Department, R&D Division, Daiichi-Sankyo Co., Ltd., 1-2-58 Hiromachi, Shinagawa-ku, Tokyo 140-8710, Japan*
[5] *Development Oversight Function, R&D Division, Daiichi-Sankyo Co., Ltd., 1-2-58 Hiromachi, Shinagawa-ku, Tokyo 140-8710, Japan*
[6] *Biological Research Department, Drug Discovery and Biomedical Technology Unit, Daiichi-Sankyo R&D Novare Co., Ltd., 1-16-13 Kitakasai, Edogawa-ku, Tokyo 134-8630, Japan*
[7] *Biological Research Laboratories, R&D Division, Daiichi-Sankyo Co., Ltd., 1-2-58 Hiromachi, Shinagawa-ku, Tokyo 140-8710, Japan*

Correspondence should be addressed to Akira Yano; akiray@ibrc.or.jp

Received 2 May 2015; Accepted 21 July 2015

Academic Editor: Pedro A. Reche

The reduction of brain amyloid beta (Aβ) peptides by anti-Aβ antibodies is one of the possible therapies for Alzheimer's disease. We previously reported that the Aβ peptide vaccine including the T-cell epitope of diphtheria-tetanus combined toxoid (DT) induced anti-Aβ antibodies, and the prior immunization with conventional DT vaccine enhanced the immunogenicity of the peptide. Cynomolgus monkeys were given the peptide vaccine subcutaneously in combination with the prior DT vaccination. Vaccination with a similar regimen was also performed on guinea pigs. The peptide vaccine induced anti-Aβ antibodies in cynomolgus monkeys and guinea pigs without chemical adjuvants, and excessive immune responses were not observed. Those antibodies could preferentially recognize Aβ_{40}, and Aβ_{42} compared to Aβ fibrils. The levels of serum anti-Aβ antibodies and plasma Aβ peptides increased in both animals and decreased the brain Aβ_{40} level of guinea pigs. The peptide vaccine could induce a similar binding profile of anti-Aβ antibodies in cynomolgus monkeys and guinea pigs. The peptide vaccination could be expected to reduce the brain Aβ peptides and their toxic effects via clearance of Aβ peptides by generated antibodies.

1. Introduction

Alzheimer's disease (AD) is a neurodegenerative disease pathologically characterized by the deposition of the amyloid beta (Aβ) fragments derived from amyloid precursor protein (APP) in senile plaques and the accumulation of neurofibrillary tangles composed of tau protein [1, 2]. Increasing evidence suggests that accumulation of Aβ plays a central role in the onset and progression of AD, and therapeutic interventions have been directed toward the reduction of Aβ production using inhibitors of the β- and γ-secretase enzymes or enhancement of Aβ clearance by immunotherapy [3–5].

Regarding Aβ immunotherapy, both active immunization against Aβ and passive immunization with monoclonal Aβ antibodies were reported to attenuate amyloid plaque formation in the brains of APP transgenic mice [6–8]. These treatments also diminished the amyloid-associated pathology

[9–11] and improved learning deficits [12, 13]. In the clinical trials of the AN1792 vaccine, the aggregated $A\beta_{1-42}$ peptide with a QS-21 adjuvant, the long-term follow-up study analysis indicated that $A\beta_{1-42}$ immunization resulted in clearance of amyloid plaques in patients with AD; however, this clearance did not lead to the prevention of progressive neurodegeneration [14]. In recent clinical trials, passive immunization with the anti-Aβ antibody, bapineuzumab and solanezumab, and intravenous immunoglobulin treatment failed to show a significant clinical benefit in patients with mild to moderate AD [15]. Although the clinical results were disappointing, there is a consensus in the field that Aβ immunotherapy by earlier intervention, targeting patients with early AD or mild cognitive impairment or presymptomatic subjects, could be an effective therapeutic and prophylactic treatment. Anti-amyloid combination therapies were also expected as practical approach for AD by the results that inhibition of γ-secretase or β-secretase with anti-Aβ antibodies was more effective than either alone in animal models [16, 17].

Based on the clinical results of the study of AN1792, which was halted due to the development of meningoencephalitis potentially related to a proinflammatory T-cell-mediated immune response [18–20], next-generation vaccine strategies for AD treatment will remain promising if the vaccine induces autoantibodies (anti-Aβ antibodies) without excessive inflammatory responses.

We have previously reported an Aβ peptide vaccine constructed of two parts, a T-cell epitope peptide on the N-terminal side and a B-cell epitope peptide connected by a dilysine linker (KK) to the C-terminal side of the peptide [21]. In order to enhance the immunogenicity of the peptide, a cell-attachment motif (RGD) was added to the N-terminal side of the peptide [21], and a multiagretope-type T-cell epitope was used for induction of antibodies to a wide range of MHC-II type individuals [22]. Although the $A\beta_{1-42}$ peptide, the antigen of AN1792, is estimated to contain many T-cell epitopes including cytotoxic epitopes, the N-terminal region of Aβ was thought to be an effective and safer target [23–25]. Our vaccine contained only the $A\beta_{1-13}$ as a target B-cell epitope peptide, which is estimated to contain few cytotoxic T-cell epitopes by *in silico* analysis [22]. Because the $A\beta_{1-13}$ was as weak as the B-cell epitope, the utilization of the additional T-cell epitope peptide, recognizable by preexisting memory T-cells in the host, was necessary for induction of the antibody to $A\beta_{1-13}$ [26]. We used the multiagretope-type T-cell epitope peptide from diphtheria toxin ($DiTox_{382-401}$). The diphtheria toxin was used as a conventional vaccine antigen, such as diphtheria and tetanus (DT) vaccines designed to induce the toxin-neutralizing antibodies by Th2 type humoral immunities, and the major memory T-cells responding to DT epitopes were estimated to induce Th2 type immune responses. Our peptide vaccine, the RGD-$DiTox_{382-401}$-KK-$A\beta_{1-13}$ peptide, could induce the anti-Aβ antibodies to C57BL/6 by boosting the T-cell reaction preimmunized by DT vaccination without chemical adjuvants [26]. This result provided motivation to investigate whether our peptide vaccine will also be effective to other species.

In this study, we investigated the immunogenicity of the peptide with vaccination to cynomolgus monkeys and guinea pigs and studied the effects of antibodies by monitoring the Aβ peptides.

2. Methods

2.1. Peptides. A RGD-$DiTox_{382-401}$-KK-$A\beta_{1-13}$ peptide (RGD-AYNFVESIINLFQVVHNSYN-KK-DAEFRHDSGYEVH, the numbers following DiTox indicated the position of the amino acids on the precursor protein of diphtheria toxin including the 32-amino acids signal peptide), synthesized and verified by MALDI-TOF/MS as over the 95% purity, was obtained from Operon Biotechnologies K.K. (Tokyo, Japan). The single-letter universally accepted notation for amino acids is used throughout this text. Human Aβ peptide fragments used in this study were purchased from AnaSpec, Inc. (CA, USA).

2.2. Animals. The vaccination studies on male cynomolgus monkeys (3 to 4 years of age at the start of the study) were performed at Mitsubishi Chemical Medience Corporation (Shibaura, Tokyo, Japan). Male guinea pigs (Slc:Hartley) were purchased from Japan SLC, Inc. (Hamamatsu, Japan), and immunization began at 5 weeks of age. All experimental procedures were performed in accordance with the in-house guideline of the Institutional Animal Care and Use Committee of Daiichi Sankyo Co., Ltd.

2.3. Immunization. Cynomolgus monkeys were primed with 0.5 mL of absorbed diphtheria-tetanus combined toxoid (DT vaccine: The Kitasato Institute, Tokyo, Japan) three weeks before peptide immunization. The Aβ peptide vaccine was subcutaneously administrated with 0.5 or 2.5 mg/0.5 mL/head eight times every two weeks.

Guinea pigs were primed subcutaneously with 50 μL/head of DT vaccine before the peptide immunization. Three weeks after the DT vaccination, guinea pigs were immunized subcutaneously with 200 μg/200 μL/head of RGD-$DiTox_{382-401}$-KK-$A\beta_{1-13}$ peptide solution or 200 μL of vehicle (distilled water) for the control group. Four identical booster doses were given at 3-week intervals.

2.4. Sample Collection. Peripheral blood was collected every 2 weeks from the cynomolgus monkeys; then plasma and serum were prepared and stored at −20°C for the following experiments.

Approximately 100 μL of blood was collected from the guinea pigs by tail bleeding one week after each peptide administration. Plasma samples were prepared by centrifugation and stored individually with a complete protease inhibitor cocktail (Roche Diagnostics K.K., Tokyo, Japan). One week after the last booster dose, cerebrospinal fluid (CSF) was obtained; then the animals were bled and plasma samples were prepared. CSF and plasma samples were prepared by centrifugation and then stored at −20°C. The brains were removed, frozen on dry ice, and stored at −80°C for an ELISA assay.

2.5. ELISA for Anti-Aβ Antibodies. Plates were coated with $A\beta_{1-42}$ dissolved in distilled water and then washed with

wash buffer (0.05% Tween 20 in phosphate buffered saline; PBS). Next, the plates were blocked with 1% Block Ace (Bio-Rad Laboratories, Inc., Hercules, CA, USA) in PBS at room temperature and then washed with wash buffer. Plasma samples were diluted 100- to 1000-fold. The autologous 2H8 mouse monoclonal anti-Aβ antibody (Thermo Fisher Scientific K.K., Yokohama, Japan) was used to generate a calibration curve for antibody titers. Each sample was applied to a well and incubated at 4°C overnight. After washing the plate, the wells were incubated with horseradish peroxidase- (HRP-) conjugated anti-mouse IgG and anti-guinea pig antibody (Sigma-Aldrich Japan, Inc., Tokyo, Japan) at 4°C for 2 h. Next, they were incubated with 2,2′-azino-di-[3-ethylbenzothiazoline-6 sulfonic acid] diammonium salt (ABTS) substrate (Bio-Rad Laboratories, Inc.) at room temperature in the dark. After sufficient color development had occurred, 2 M phosphate buffer was added to stop the reaction. The absorbance of each well at 405 nm was measured with a spectrophotometer and antibody titers were then calculated.

ELISAs for antibody epitope-mapping were performed using the following Aβ peptides: RGD-DiTox$_{382-401}$-KK-Aβ_{1-13}, Aβ_{1-13}, Aβ_{1-40}, Aβ_{1-42}, and Aβ_{1-42} fibrils (fAβ_{1-42}) as an immobilized antigen, and ELISAs were performed in the same way as described above. The preparation of fAβ_{1-42} is described as follows: Lyophilized Aβ_{1-42} in PBS was incubated at 37°C for three days and then the resulting Aβ solution was centrifuged at 4°C for 10 min at 10,000 ×g; then the precipitated fraction was suspended in distilled water and used in this study.

2.6. ELISA for Brain and Plasma. The brains of guinea pigs were thawed on ice and then homogenized in 5 volumes (v/w) of 42% formic acid solution including protease inhibitors using a homogenizer and a sonicator and were incubated overnight at 37°C. The homogenates were centrifuged at 37,000 rpm for 60 min at 4°C (OptimaTM L-100XP, rotor 50.4Ti, Beckman Coulter, Inc., Tokyo, Japan) and the supernatants were neutralized with 11 volumes (v/v) of 1 M Tris solution and then centrifuged at 10000 rpm for 10 min at 4°C (himac CT13R, Hitachi Koki Co., Ltd., Tokyo, Japan). The supernatants were collected as a brain Aβ fraction.

Levels of Aβ_{40} and Aβ_{42} in brain and plasma samples were measured using a Human/Rat β Amyloid (40) ELISA Kit Wako II (Wako Pure Chemical Industries, Ltd., Tokyo, Japan), Human/Rat β Amyloid (42) ELISA Kit Wako, High-Sensitive (Wako Pure Chemical Industries, Ltd.), and Human Amyloid β Oligomers (82E1-specific) Assay Kit (IBL Co., Ltd., Gunma, Japan) and were used according to the manufacturer's instructions.

2.7. Detection of Cytokines from Peripheral Blood of Cynomolgus Monkeys. Plasma of cynomolgus monkeys at days 22 to 36, 64 to 78, and 106 to 120 was pooled and used for the ELISA. IL-2, IL-4, IL-10, and TNFα were measured by a Monkey ELISA Kit (Invitrogen) according to the manufacturer's instruction.

2.8. Aβ_{1-42} Toxicity Assay. The soluble Aβ_{1-42} peptide was added to the 7th day after passage of rat adrenal medulla derived pheochromocytoma, PC12 (Dainippon Sumitomo Pharma Co., Ltd., Tokyo, Japan), cell line at 0 to 2 μM, and the viability of the cells was evaluated by AlamarBlue (Pierce, Thermo Fisher Scientific, Inc., Waltham, MA, USA) according to the manufacturer's instructions. The anti-Aβ_{1-42} monoclonal antibody (0.33 μM of 6E10, abcam, Cambridge, USA) was used as a control for the protection of PC12 cells from cytotoxic Aβ_{1-42} peptide. The antibody (0.33 μM of mouse IgG, Sigma-Aldrich, St. Louis, MO, USA) was used as a negative control. The serum and antibodies were preincubated with Aβ_{1-42} peptides at 4°C for 2 h, then added to the cells, and cultured for 24 h.

2.9. Statistical Analysis. Data were expressed as mean ± standard error (SE). Data from the passive avoidance test and the brain, plasma, and CSF Aβ levels were analyzed by one-way analysis of variance (ANOVA). Data from the splenic T-cell proliferation assay were analyzed by the one-way layout and multiple comparison method of Dunnett. SAS System Release 8.2 (SAS Institute Inc.) was used to perform all analyses and P values of less than 0.05 were considered to be statistically significant.

3. Results

3.1. Immunization of Aβ Peptide in Cynomolgus Monkeys. The time courses of plasma antibody concentration against the Aβ peptides by subcutaneous administration of the RGD-DiTox$_{382-401}$-KK-Aβ_{1-13} peptide (0.5 and 2.5 mg/head) or vehicle (distilled water) in cynomolgus monkeys are shown in Figure 1(a). Compared to the vehicle group, the 2.5 mg peptide administrated group showed significantly higher antibody concentrations after the initial peptide administration (8 days after the first administration). To recognize the upper limit of the antibody concentration induced by the peptide, booster immunizations were continued over 100 days after the first immunization. The marked elevation following the third immunization was not observed and final serum antibody concentrations were reached about 8 times higher than that of the vehicle group. The plasma concentrations of Aβ_{40} were not significantly different between the groups, but the concentration of Aβ_{42} peptide in the 2.5 mg/head vaccination group was significantly higher than the vehicle group (Figure 1(b)). The result of epitope-mapping is indicated in Figure 1(c). The peptide induced antibodies recognized not only the Aβ vaccine peptide (KK-Aβ_{1-13}) but also the full-length Aβ_{1-40} and Aβ_{1-42} peptide. The antibodies were less reactive to Aβ fibrils (fAβ_{1-42}) than Aβ_{1-42} peptide. The antibody reactivities against the Aβ_{13-16} and Aβ_{1-10} peptide were relatively weaker than that against the Aβ_{1-13} peptide, suggesting that the C-terminal side of the Aβ_{1-13} peptide was the main epitope of the antibody generated by this peptide vaccination.

The cytokine responses to the peptide immunization were investigated by ELISA. Plasma of the cynomolgus monkeys at days 22 to 36, 64 to 78, and 106 to 120 was pooled and used for ELISA. IL-2, IL-4, IL-10, and TNFα were measured, but all cytokines remained under the detection limits (Table 1;

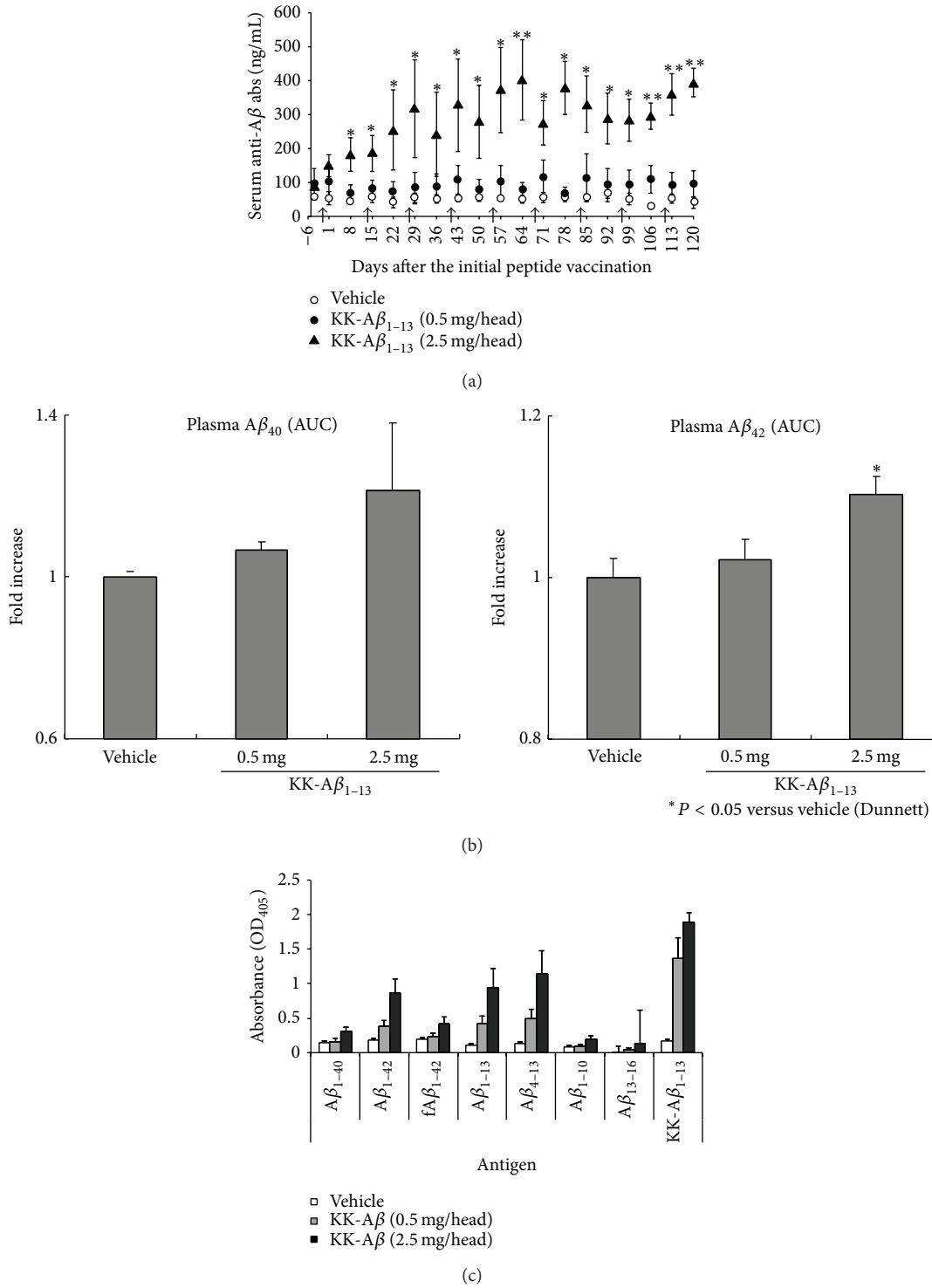

Figure 1: Induction of the anti-Aβ antibodies and Aβ peptides in the peripheral blood by immunization of the peptide vaccine to cynomolgus monkeys. The serum anti-Aβ antibody levels of the cynomolgus monkeys treated with vehicle or RGD-DiTox$_{20}$-KK-Aβ_{1-13} (a). The plasma Aβ_{40} and Aβ_{42} peptide (b) level (nM) of cynomolgus monkeys. Diphtheria and tetanus toxoids (DT, 0.5 mL/head, s.c.) were administered to cynomolgus monkeys. Three weeks after the DT treatment, vehicle or the peptide (0.5 or 2.5 mg/head, s.c.) was administered at intervals of 2 weeks (arrows; total 9 times). Blood sampling was performed every week after the initial treatment. Results are represented as mean ± SE ($n = 5$). $^{*}P < 0.05$ and $^{**}P < 0.01$ as compared with the vehicle control group (the Dunnett test). Epitope-mapping of plasma anti-Aβ antibodies immunized with vehicle or RGD-DiTox$_{382-401}$-KK-Aβ_{1-13} peptide (c). Epitope-mapping of antibodies was performed using each peptide-precoated ELISA with plasma collected at two weeks after the final treatment. Results are represented as mean ± SE ($n = 5$). KK-Aβ_{1-13}: RGD-DiTox$_{20}$-KK-Aβ_{1-13} peptide.

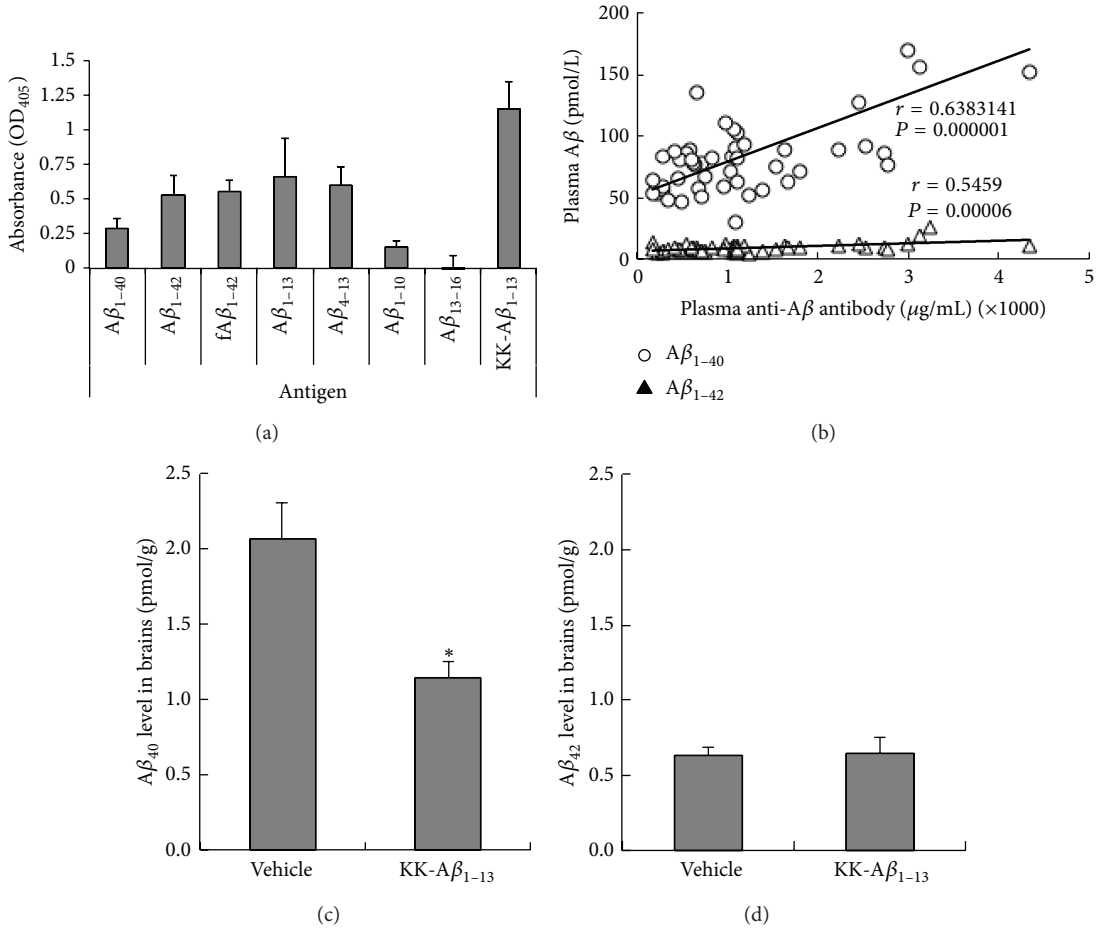

Figure 2: Induction of the anti-Aβ antibodies in the plasma and Aβ peptides in the brain by immunization of the peptide vaccine to guinea pigs. Epitope-mapping of plasma anti-Aβ antibodies immunized with RGD-DiTox$_{382–401}$-KK-A$\beta_{1–13}$ peptide (a). Epitope-mapping of antibodies was performed using each peptide-precoated ELISA with plasma collected at two weeks after the final treatment. Results are represented as mean ± SE. $n = 5$. The plasma anti-Aβ antibody levels of the guinea pigs treated with RGD-DiTox$_{20}$-KK-A$\beta_{1–13}$ peptides and the correlation of anti-Aβ antibody concentrations to Aβ_{40} and Aβ_{42} peptide doses in the plasma (b). The Aβ peptide levels in the brain of guinea pigs (c and d). Diphtheria and tetanus toxoids (DT, 200 μL/head, s.c.) were administered to guinea pigs. Three weeks after the DT treatment, vehicle or the peptide (200 μg/head) was administered at intervals of 3 weeks (arrows; total 6 times). Blood sampling was performed every week after the initial treatment. Results are represented as mean ± SE ($n = 5$). $^{*}P < 0.05$ and $^{**}P < 0.01$ as compared to the vehicle control group (the Dunnett test).

Table 1: Cytokines in the peripheral blood of cynomolgus monkeys.

	Th1 type		Th2 type	
	TNFα	IL-2	IL-4	IL-10
Control	n.d.	n.d.	n.d.	n.d.
0.5 mg/head-KK-Aβ peptide	n.d.	n.d.	n.d.	n.d.
2.5 mg/head-KK-Aβ peptide	n.d.	n.d.	n.d.	n.d.

Detection limits: TNF 2 pg/mL, Il-2 2 pg/mL, Il-4 3 pg/mL, and Il-10 10 pg/mL.

TNFα < 2 pg/mL, Il-2 < 2 pg/mL, Il-4 < 3 pg/mL, and Il-10 < 10 pg/mL).

3.2. Immunization of Aβ Peptide in Guinea Pigs. The Aβ peptide, RGD-DiTox$_{382–401}$-KK-A$\beta_{1–13}$ peptide (200 μg/head), or vehicle (distilled water) was subcutaneously administrated in guinea pigs. Compared to the vehicle group, the peptide administrated group showed 6 to 8 times higher antibody titers throughout the experiment (data not shown). The epitope-mapping performed with the serum from the final bleed indicated that the peptide vaccination induced antibodies in guinea pigs in the same patterns of epitopes as in cynomolgus monkeys except that the antibodies were reactive to fAβ as like as A$\beta_{1–42}$ peptide (Figure 2(a)).

The concentration of the plasma A$\beta_{1–40}$ peptide tended to increase due to the peptide immunization and showed a correlation with the level of anti-Aβ antibodies in the serum (Figure 2(b)). The concentration of the plasma Aβ_{42} peptide was ten times lower than Aβ_{40} peptide and their orders were unchanged by increasing anti-Aβ antibody concentration.

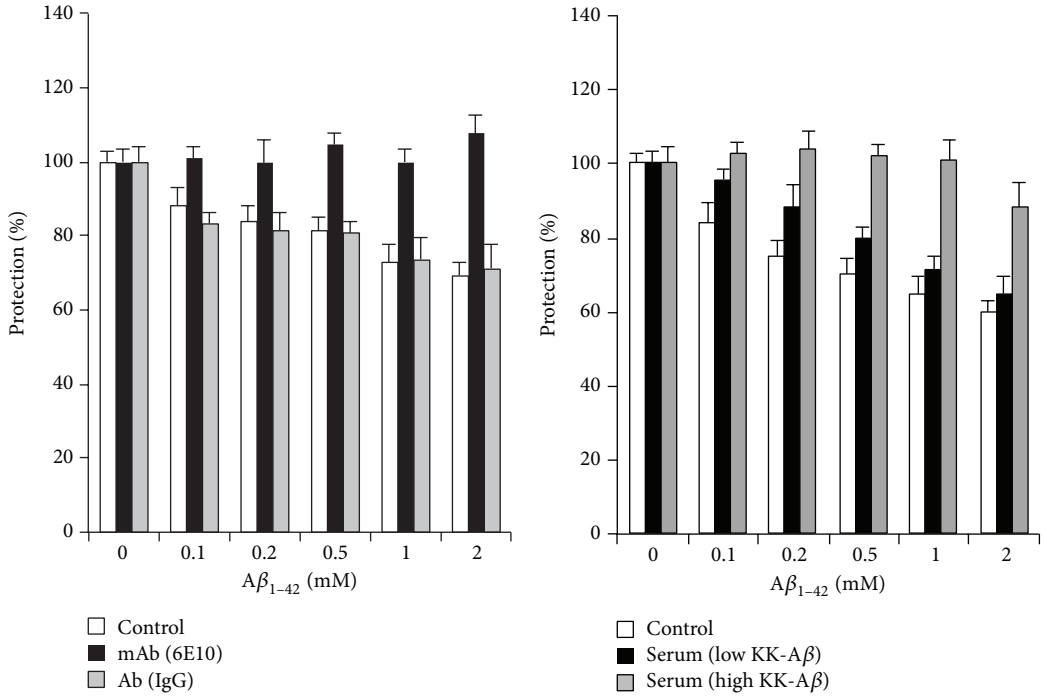

Figure 3: Effects of antiserum from cynomolgus monkeys vaccinated with RGD-DiTox$_{20}$-KK-Aβ_{1-13} peptides or vehicle on Aβ-induced cytotoxicity of PC12 cells. The effects of the anti-Aβ monoclonal antibodies (positive control: black bar) and nonspecific immunoglobulin (gray bar) on the cytotoxicity of Aβ peptides (base control of cytotoxicity: white bar) are indicated (a). The effects of the serum of Aβ_{1-42} peptide-immunized monkey (0.5 mg/head low dose: black bar, and 2.5 mg/head high dose: gray bar) on the cytotoxic Aβ_{42} peptides (buffer control: white bar) are indicated.

Aβ_{40} peptide levels in brains were significantly decreased by the peptide immunization group (Figure 2(c)), but the level of Aβ_{42} peptide did not change by immunization (Figure 2(d)).

3.3. Aβ_{1-42} Toxicity Assay with a Nerve Cell Culture. To evaluate the protective effect of the peptide induced anti-Aβ antibodies, Aβ_{1-42} toxicity assay with a PC12 cell culture was performed. The anti-Aβ serum (25% final concentration) in cynomolgus monkeys collected one week after the final peptide immunization was investigated. Only the anti-Aβ antibody could protect PC12 cells from the toxic Aβ peptide (Figure 3(a)). The anti-Aβ serum of high-dose peptide-immunized monkeys protected PC12 cells from the damage of Aβ_{1-42} peptide (Figure 3(b)).

4. Discussion

The RGD-DiTox$_{382-401}$-KK-Aβ_{1-13} peptide with preimmunized DT vaccine induced anti-Aβ antibodies in monkeys and guinea pigs without any chemical adjuvants. The vaccine peptide induced about 6 to 8 times higher anti-Aβ antibodies than vehicle-treated animals following third immunization. Those results clearly indicated the vaccine peptide was immunogenic to both kinds of animals. The multiagretope-type T-cell epitope peptide on the N-terminal side of our peptide worked as T-cell epitope of DT vaccine to the animals with many types of MHC [22], and the results of guinea pigs and cynomolgus monkeys showed the T-cell epitopes of each animal were included in the peptide.

The T-cell epitope sequence was derived from conventional DT vaccine for induction of antibodies to Aβ peptide. Davtyan et al. [27] reported the same concept of AD peptide vaccine, Lu AF20513, that used memory Th cells generated by tetanus toxoid vaccine for induction of Aβ antibodies. Lu AF20513 was immunized with strong adjuvants, CFA/IFA, Quil-A or Alhydrogel, and more than several hundred times higher titers of antibodies were induced. It supported the availability of our peptide vaccine, if the arrangement of the epitopes and the amino acid sequence of T-cell epitope were different from our peptide. Our peptide would also induce more strong immune responses immunized with strong chemical adjuvants (supplemental experiments; see Supplementary Material available online at http://dx.doi.org/10.1155/2015/786501). In this study, we tried to avoid the induction of the strong immune responses for reduction of the risk by unexpected immune responses, namely, cytotoxic responses reported in the clinical trial of AN1792 [14]. The excessive entry of antibodies in the brain also might be a risk of encephalitis. Following the 9 administrations of the peptide, significant levels of cytokines were not induced in cynomolgus monkeys (Table 1).

The result of the $A\beta_{1-42}$ toxicity assay using PC12 cells presented the effectiveness of the anti-Aβ serum induced by the weak immune responses by our peptide vaccination. In addition, our peptide vaccination induced antibodies working for clearance of Aβ peptides from the brain of the guinea pigs (Figure 2) [7]. The epitope-mapping of antibodies of both animals indicated the antibodies commonly recognize the C-terminal side of the $A\beta_{1-13}$, full-length $A\beta_{1-40}$, and $A\beta_{1-42}$ peptides (Figures 1(b) and 2(a)). $A\beta_{1-42}$ fibril was also recognized by antiserum of guinea pigs but less reactive to antiserum of cynomolgus monkeys (Figures 2(a) and 1(c)). The antisera of our peptide would be more suitable for nerve cell protection from $A\beta_{1-42}$ peptides than dissolution of the $A\beta_{1-42}$ fibrils. This might be a major difference between AN1792 and our peptide. Lu AF20513 also used the $A\beta_{1-12}$ peptide as B-cell epitope, and the epitope of the induced antibodies was thought to be common between Lu AF20513 and our peptide. The antibodies induced by our peptide significantly increased the plasma $A\beta_{1-40}$ peptides and reduced the $A\beta_{1-40}$ peptides in the brains (Figures 1 and 2). It would be considered that the anti-Aβ antibodies transport the Aβ peptides from the brain to the blood stream [28, 29]. In contrast, plasma and brain $A\beta_{1-42}$ peptide was always lower than $A\beta_{1-40}$ peptides and was not changed in the guinea pigs. It was expected that the basal level of $A\beta_{1-42}$ peptides in the wild type guinea pigs was three times lower than $A\beta_{1-40}$ peptide, and most of anti-Aβ antibodies would preferably react to $A\beta_{1-40}$ peptide compared to $A\beta_{1-42}$ peptide. Then it might be difficult to show the effects of the anti-$A\beta_{1-42}$ antibodies in Figure 2(d).

We also investigated the effect of the peptide vaccine by immunization of Tg2576 mice expressing the Swedish mutation of APP (APPK670N, M671L) (supplements). Unfortunately, the antibodies were not induced without chemical adjuvants and Freund's incomplete adjuvant (FIA) was used three weeks after the DT vaccination. Tg2576 mice expressed excessive APPs in all tissues and strong adjuvants were necessary for induction of antibodies to Aβ peptides (Figure S1). The peptide vaccine could induce anti-Aβ antibodies to APP-Tg mice. The binding patterns of antibodies showed the same epitopes to guinea pigs and cynomolgus monkeys (Figure S1A). The results of the Tg2576 indicated that the vaccine induced antibodies increased Aβ peptides in plasma, which is consistent with the results in monkeys and guinea pigs, and CSF (Figures S1B, C, D, and E). The brain Aβ deposition and Aβ oligomer of APP-Tg mice reduced compared to vehicle-treated animals (Figures S1F, G, H, and I). Those results suggested that antibodies transported the Aβ peptides from the brain to the blood stream through the cerebrospinal fluid.

We investigated memory changes in a passive avoidance test after the last booster vaccination. Compared to non-Tg mice, the learning impairment had already been initiated in Tg2576 mice at the initial immunization (data not shown). Six months after the initial immunization, the learning impairment in mice treated with Aβ peptide was significantly less than that in mice treated with vehicle, suggesting that Aβ peptide vaccination slowed the progression of learning impairment. Biochemical analysis indicated a significant reduction of the levels of insoluble $A\beta_{1-40}$, $A\beta_{1-42}$, and Aβ oligomers in the brain of KK-Aβ peptide vaccinated mice. A significant reduction of $A\beta_{1-42}$ immunostaining in the parietal cortex and hippocampus was also observed (data not shown) suggesting that the vaccination with the RGD-$DiTox_{382-401}$-KK-$A\beta_{1-13}$ peptide could have a potential to reduce and/or to inhibit the formation of senile plaques in the brains of Tg2576 mice. These results are similar to other findings of vaccinations [30, 31] and suggest that the vaccination with the RGD-$DiTox_{382-401}$-KK-$A\beta_{1-13}$ peptide might slow the progression of learning impairment mediated through the reduction of senile plaques, soluble Aβ oligomers, and/or inhibition of senile plaque formation in the brain. Those pharmaceutical effects, observed in Tg2576 mice, would be expected in wild type guinea pigs and cynomolgus monkeys.

5. Conclusions

RGD-$DiTox_{382-401}$-KK-$A\beta_{1-13}$ peptide vaccination in combination with a prior vaccination of the conventional diphtheria-tetanus combined toxoid vaccine induced anti-$A\beta_{40\text{ and }42}$ antibodies in cynomolgus monkeys and guinea pigs. It promoted Aβ clearance in the brains of guinea pigs. The peptide vaccination did not show any excessive immune responses in any tested animals. We propose that this peptide would be a possible therapeutic or prophylactic candidate for AD.

Abbreviations

Aβ: Amyloid beta
DT: Diphtheria-tetanus combined toxoid
APP: Amyloid precursor protein
AD: Alzheimer's disease
CSF: Cerebrospinal fluid
PBS: Phosphate buffered saline
HRP: Horseradish peroxidase
BBB: Blood-brain barrier.

Conflict of Interests

The authors declared that they have no competing interests.

Authors' Contribution

Akira Yano participated in the design of the study and in writing the paper. Kaori Ito, Yoshikatsu Miwa, Yoshito Kanazawa, and Mitsuhiro Makino participated in the design of the study and Kaori Ito, Mitsuhiro Makino, and Akiko Chiba performed the experiments. Yutaka Iigo and Yoshinori Kashimoto performed the data analysis. Akira Kanda and Shinji Murata supported the animal experiments. Akira Yano and Kaori Ito made equal contribution.

Acknowledgments

The authors would like to thank Chikako Nishimoto and Haruka Endo for their assistance in conducting the study. This work was supported by Daiichi-Sankyo Co., Ltd.

References

[1] J. Hardy and D. J. Selkoe, "The amyloid hypothesis of Alzheimer's disease: progress and problems on the road to therapeutics," *Science*, vol. 297, no. 5580, pp. 353–356, 2002.

[2] A. Nikolaev, T. McLaughlin, D. D. M. O'Leary, and M. Tessier-Lavigne, "APP binds DR6 to trigger axon pruning and neuron death via distinct caspases," *Nature*, vol. 457, no. 7232, pp. 981–989, 2009.

[3] M. S. Rafii and P. S. Aisen, "Recent developments in Alzheimer's disease therapeutics," *BMC Medicine*, vol. 7, article 7, 2009.

[4] D. M. Holtzman, J. C. Morris, and A. M. Goate, "Alzheimer's disease: the challenge of the second century," *Science Translational Medicine*, vol. 3, article 77sr1, 2011.

[5] M. Citron, "Alzheimer's disease: strategies for disease modification," *Nature Reviews Drug Discovery*, vol. 9, no. 5, pp. 387–398, 2010.

[6] D. Schenk, R. Barbour, W. Dunn et al., "Immunization with amyloid-β attenuates Alzheimer disease-like pathology in the PDAPP mouse," *Nature*, vol. 400, no. 6740, pp. 173–177, 1999.

[7] F. Bard, C. Cannon, R. Barbour et al., "Peripherally administered antibodies against amyloid β-peptide enter the central nervous system and reduce pathology in a mouse model of Alzheimer disease," *Nature Medicine*, vol. 6, no. 8, pp. 916–919, 2000.

[8] D. M. Wilcock, A. Rojiani, A. Rosenthal et al., "Passive immunotherapy against Aβ in aged APP-transgenic mice reverses cognitive deficits and depletes parenchymal amyloid deposits in spite of increased vascular amyloid and microhemorrhage," *Journal of Neuroinflammation*, vol. 1, article 24, 2004.

[9] J. A. Lombardo, E. A. Stern, M. E. McLellan et al., "Amyloid-β antibody treatment leads to rapid normalization of plaque-induced neuritic alterations," *The Journal of Neuroscience*, vol. 23, no. 34, pp. 10879–10883, 2003.

[10] S. Oddo, L. Billings, J. P. Kesslak, D. H. Cribbs, and F. M. LaFerla, "Aβ immunotherapy leads to clearance of early, but not late, hyperphosphorylated tau aggregates via the proteasome," *Neuron*, vol. 43, no. 3, pp. 321–332, 2004.

[11] R. P. Brendza, B. J. Bacskai, J. R. Cirrito et al., "Anti-Aβ antibody treatment promotes the rapid recovery of amyloid-associated neuritic dystrophy in *PDAPP* transgenic mice," *The Journal of Clinical Investigation*, vol. 115, no. 2, pp. 428–433, 2005.

[12] C. Janus, J. Pearson, J. McLaurin et al., "Aβ peptide immunization reduces behavioural impairment and plaques in a model of Alzheimer's disease," *Nature*, vol. 408, no. 6815, pp. 979–982, 2000.

[13] D. Morgan, D. M. Diamond, P. E. Gottschall et al., "A β peptide vaccination prevents memory loss in an animal model of Alzheimer's disease," *Nature*, vol. 408, no. 6815, pp. 982–985, 2000.

[14] C. Holmes, D. Boche, D. Wilkinson et al., "Long-term effects of Aβ42 immunisation in Alzheimer's disease: follow-up of a randomised, placebo-controlled phase I trial," *The Lancet*, vol. 372, no. 9634, pp. 216–223, 2008.

[15] M. Sarazin, G. Dorothée, L. C. de Souza, and P. Aucouturier, "Immunotherapy in Alzheimer's disease: do we have all the pieces of the puzzle?" *Biological Psychiatry*, vol. 74, no. 5, pp. 329–332, 2013.

[16] E. Giacobini and G. Gold, "Alzheimer disease therapy—moving from amyloid-β to tau," *Nature Reviews Neurology*, vol. 9, no. 12, pp. 677–686, 2013.

[17] H. Jacobsen, L. Ozmen, A. Caruso et al., "Combined treatment with a BACE inhibitor and anti-Aβ antibody gantenerumab enhances amyloid reduction in APPLondon mice," *The Journal of Neuroscience*, vol. 34, no. 35, pp. 11621–11630, 2014.

[18] J.-M. Orgogozo, S. Gilman, J.-F. Dartigues et al., "Subacute meningoencephalitis in a subset of patients with AD after Aβ42 immunization," *Neurology*, vol. 61, no. 1, pp. 46–54, 2003.

[19] J. A. R. Nicolll, D. Wilkinson, C. Holmes, P. Steart, H. Markham, and R. O. Weller, "Neuropathology of human Alzheimer disease after immunization with amyloid-β peptide: a case report," *Nature Medicine*, vol. 9, no. 4, pp. 448–452, 2003.

[20] I. Ferrer, M. Boada Rovira, M. L. Sánchez Guerra, M. J. Rey, and F. Costa-Jussá, "Neuropathology and pathogenesis of encephalitis following amyloid-β immunization in Alzheimer's disease," *Brain Pathology*, vol. 14, no. 1, pp. 11–20, 2004.

[21] A. Yano, A. Onozuka, K. Matin, S. Imai, N. Hanada, and T. Nisizawa, "RGD motif enhances immunogenicity and adjuvanicity of peptide antigens following intranasal immunization," *Vaccine*, vol. 22, no. 2, pp. 237–243, 2003.

[22] A. Yano, A. Onozuka, Y. Asahi-Ozaki et al., "An ingenious design for peptide vaccines," *Vaccine*, vol. 23, no. 17-18, pp. 2322–2326, 2005.

[23] D. S. Gelinas, K. DaSilva, D. Fenili, P. St. George-Hyslop, and J. McLaurin, "Immunotherapy for Alzheimer's disease," *Proceedings of the National Academy of Sciences of the United States of America*, vol. 101, no. 2, pp. 14657–14662, 2004.

[24] F. Bard, R. Barbour, C. Cannon et al., "Epitope and isotype specificities of antibodies to β-amyloid peptide for protection against Alzheimer's disease-like neuropathology," *Proceedings of the National Academy of Sciences of the United States of America*, vol. 100, no. 4, pp. 2023–2028, 2003.

[25] D. H. Cribbs, A. Ghochikyan, V. Vasilevko et al., "Adjuvant-dependent modulation of T_h1 and T_h2 responses to immunization with β-amyloid," *International Immunology*, vol. 15, no. 4, pp. 505–514, 2003.

[26] A. Yano, Y. Miwa, Y. Kanazawa et al., "A novel method for enhancement of peptide vaccination utilizing T-cell epitopes from conventional vaccines," *Vaccine*, vol. 31, no. 11, pp. 1510–1515, 2013.

[27] H. Davtyan, A. Ghochikyan, I. Petrushina et al., "Immunogenicity, efficacy, safety, and mechanism of action of epitope vaccine (Lu AF20513) for Alzheimer's disease: prelude to a clinical trial," *Journal of Neuroscience*, vol. 33, no. 11, pp. 4923–4934, 2013.

[28] R. B. DeMattos, K. R. Bales, D. J. Cummins, J.-C. Dodart, S. M. Paul, and D. M. Holtzman, "Peripheral anti-Aβ antibody alters CNS and plasma Aβ clearance and decreases brain Aβ burden in a mouse model of Alzheimer's disease," *Proceedings of the National Academy of Sciences of the United States of America*, vol. 98, no. 15, pp. 8850–8855, 2001.

[29] F. Lemiale, W.-P. Kong, L. M. Akyürek et al., "Enhanced mucosal immunoglobulin A response of intranasal adenoviral vector human immunodeficiency virus vaccine and localization in the central nervous system," *Journal of Virology*, vol. 77, no. 18, pp. 10078–10087, 2003.

[30] F. Goñi, F. Prelli, Y. Ji et al., "Immunomodulation targeting abnormal protein conformation reduces pathology in a mouse model of alzheimer's disease," *PLoS ONE*, vol. 5, no. 10, Article ID e13391, 2010.

[31] S. Rasool, R. Albay III, H. Martinez-Coria et al., "Vaccination with a non-human random sequence amyloid oligomer mimic results in improved cognitive function and reduced plaque deposition and micro hemorrhage in Tg2576 mice," *Molecular Neurodegeneration*, vol. 7, no. 1, article 37, 2012.

Hindawi Publishing Corporation
Journal of Immunology Research
Volume 2015, Article ID 723946, 11 pages
http://dx.doi.org/10.1155/2015/723946

Research Article

Experimental Immunization Based on *Plasmodium* Antigens Isolated by Antibody Affinity

Ali N. Kamali,[1,2] Patricia Marín-García,[1,3] Isabel G. Azcárate,[1,4] Antonio Puyet,[1,4] Amalia Diez,[1,4] and José M. Bautista[1,4]

[1]*Department of Biochemistry and Molecular Biology IV, Universidad Complutense de Madrid, Facultad de Veterinaria, Ciudad Universitaria, 28040 Madrid, Spain*
[2]*Department of Biology, Faculty of Basic Sciences, Islamic Azad University, Central Tehran Branch, Tehran 14676-86831, Iran*
[3]*Department of Medicine and Surgery, Psychology, Preventive Medicine and Public Health and Medical Immunology and Microbiology, Faculty of Health Sciences, Universidad Rey Juan Carlos, Alcorcón, 28922 Madrid, Spain*
[4]*Research Institute Hospital 12 de Octubre, Universidad Complutense de Madrid, 28040 Madrid, Spain*

Correspondence should be addressed to José M. Bautista; jmbau@ucm.es

Received 25 June 2015; Accepted 25 August 2015

Academic Editor: Yoshihiko Hoshino

Vaccines blocking malaria parasites in the blood-stage diminish mortality and morbidity caused by the disease. Here, we isolated antigens from total parasite proteins by antibody affinity chromatography to test an immunization against lethal malaria infection in a murine model. We used the sera of malaria self-resistant ICR mice to lethal *Plasmodium yoelii yoelii* 17XL for purification of their IgGs which were subsequently employed to isolate blood-stage parasite antigens that were inoculated to immunize BALB/c mice. The presence of specific antibodies in vaccinated mice serum was studied by immunoblot analysis at different days after vaccination and showed an intensive immune response to a wide range of antigens with molecular weight ranging between 22 and 250 kDa. The humoral response allowed delay of the infection after the inoculation to high lethal doses of *P. yoelii yoelii* 17XL resulting in a partial protection against malaria disease, although final survival was managed in a low proportion of challenged mice. This approach shows the potential to prevent malaria disease with a set of antigens isolated from blood-stage parasites.

This paper is dedicated to the memory of Professor Amando Garrido-Pertierra

1. Introduction

Human malaria infection can lead to a wide range of clinical symptoms that are influenced by epidemiological and immunological factors [1] along with the mechanisms of immune evasion of the parasite [2]. Protective humoral response against *Plasmodium falciparum* can be acquired after repeated infections of malaria; however, it does not persist over long periods of time and it is generally incomplete [1].

Despite concerted efforts worldwide, most advanced vaccines in development have shown moderate efficacy [3] maybe since they are based on parasite antigens, too polymorphic, and expressed only in brief periods of the parasite life cycle [4]. In addition, vaccine candidates represent less than 0.5% of the entire genome [5] and more than 50% of the vaccines currently designed are based independently on only three antigens: circumsporozoite protein (CSP), merozoite surface protein (MSP), and the apical membrane antigen 1 (AMA-1). Due to difficulties in identifying the widely dispersed immune responses to *Plasmodium*, only about 1% of the antigens encoded by the parasite have been studied so far [6]. Although the identification of immunological markers for protection has been intricate, several reports

suggest that humoral responses to a variety of antigens are involved in protection [5, 7].

Thus, a combination of antigen subunits of different parasite stages is the long-term objective of malaria vaccine [8]. Vaccines based on the inoculation of the whole organism enable a vast array of antigens to be delivered and therefore provide a multiepitope vaccine [9–11]. Nevertheless, the specific antigens mediating protective immunity induced by whole organism vaccination are still largely unknown [11]. The generation of protective responses in malaria induced by subunit vaccines is still under debate [11, 12]. In addition, there may be specific protective immune responses that do not arise during the normal course of infection but that can be primed by vaccination and boosted by infection [12] or by ultralow doses of drug-contained or killed parasites [13–15].

By using animal models, several laboratories have attempted to induce protective immune response by immunization with crude preparations of whole blood-stage antigens applying various adjuvants, and different degrees of protection have been reported [15–17]. Protective response in mice induced by undetermined whole blood-stage antigens has been shown to be dependent on $CD4^+$ T cells, interferon gamma, and nitric oxide [15]. Thus, with more than 5,000 proteins expressed during the life cycle of *Plasmodium* spp. [18] it remains to be known which combinations of them could be efficient antigens mediating protective immunity induced by whole organism vaccination. Moreover, a question arising from these studies is whether immune protection is elicited predominantly by a very limited or a large number of antigens [19].

Previous results from our laboratory show that a percentage of ICR mice naturally acquire a long-term protective humoral response against homologue reinfections of the lethal parasite *P. yoelii yoelii* 17XL (*PyL*) [20]. Moreover, sera of these mice are a suitable source of immunoglobulins for the isolation of antigenic plasmodial proteins by immunoaffinity [21]. Consequently, in the present study, we have investigated the use of the protective IgGs from pooled sera of malaria model in ICR mice [20] to isolate blood-stage parasite antigens by immunoaffinity as described earlier [21] to investigate their immunogenicity in BALB/c mice. The immunization elicited antigens and the level of protection achieved against a lethal malaria challenge is discussed.

2. Materials and Methods

2.1. Animals and Malaria Infection. The rodent malaria parasite *PyL* MRA-267 was obtained from Dr. Virgilio Do Rosario (Instituto de Higiene e Medicina Tropical, Universidade Nova de Lisboa) and stored in liquid nitrogen after serial blood passages in mice. Infected blood was kept in liquid nitrogen in a solution containing glycerol 28% (v/v), sorbitol 3% (w/v), and NaCl 0.65% (w/v). Inbred BALB/cAnNHsd and randombred ICR pathogen-free female mice (Hsd:ICR[CD-1]), aged 6–8 weeks, were purchased from Harlan Laboratories (Udine, Italy). The mice were housed under standard conditions of light (12 : 12 h light : dark cycles), temperature (22–24°C), and humidity (around 50%) in the Animal Housing Facility at Universidad Complutense de Madrid. All mice were fed a commercial diet (2018 Teklad Global 18% Protein Rodent Diet, Harlan Laboratories) *ad libitum*. All animal care and experimental procedures carried out at the Universidad Complutense de Madrid complied with Spanish (R.D. 32/2007) and European Union legislation (2010/63/CE) and were approved by the Animal Experimentation Committee of this institution. The experiments here described involving animals are reported following the ARRIVE guidelines [22].

For all challenges, parasite isolation, and immune sera sampling, mice were inoculated by intraperitoneal (i.p.) injection of 2×10^7 *PyL*-infected red blood cells (iRBCs) from infected mice. After infection, p-aminobenzoic acid at a final concentration of 0.05% (w/v) was included in the drinking water to enhance parasite growth [23, 24].

2.2. Total Parasite Protein Extraction. Protein lysates were extracted from the RBCs with a mixture of ring, trophozoite, and schizont-stage parasites of infected ICR mice showing >50% parasitaemia. Mice were anaesthetized with isoflurane, as recommended by the local Animal Experimentation Committee, and whole blood was collected from the aorta into tubes containing EDTA 0.1 M as anticoagulant and kept at −80°C until protein extraction. Protein isolation began with RBC lysis using 10 vol saponin 0.1% (w/v) in PBS. After centrifugation (320 ×g, 5 min, 4°C) and washing twice in cold PBS, the pellet was treated with extraction buffer (50 mM Tris-HCl, pH 8.0; 50 mM NaCl; 0.5% Mega 10) containing protease inhibitor cocktail (Roche, Indianapolis, IN, USA) and subjected to four freeze-thaw cycles. Finally, lysates were centrifuged (20,000 ×g, 15 min, 4°C) and total *PyL* protein samples stored at −80°C until use.

2.3. Purification of Mouse IgGs. Hsd:ICR (CD-1) malaria-resistant mice were generated as previously described by Azcárate et al. [20]. Briefly mice were infected intraperitoneally with 2×10^7 PyL-iRBCs obtained from donor *PyL*-infected mice. Mice that recovered from 1st infection were reinfected on days 60 and 420 after the first infection following the same infection protocol. IgGs from 150 μL of pooled serum samples obtained after three infections of malaria-resistant ICR mice were isolated using 0.2 mL NAb protein A/G column (Thermo Scientific, MA) according to the manufacturer's instructions. Briefly, serum was diluted in binding buffer (sodium phosphate 100 mM containing NaCl 150 mM, pH 7.2) and IgGs bound to the column were eluted in 400 μL fractions using the elution buffer provided (pH 2.8). Collecting tubes were previously preloaded with 40 μL of Tris-HCl 1 M, pH 8.5 for neutralization. After elution, purified IgGs were dialyzed in a Slid-A-Lyzer dialysis cassette (Thermo Scientific) against 500 mL of sodium phosphate 0.01 M containing NaCl 0.15 M, pH 7.2 during 2 h, with a total of 3 replacements. After the third replacement, equilibrium was continued overnight at 4°C and dialyzed IgGs were kept at −20°C until use. Purity and yield of IgGs were verified by sodium dodecyl sulfate-polyacrylamide gel electrophoresis and western blotting. Contaminating protein in the elution and loss of IgGs during purification, dialysis, and concentration were both negligible as previously reported [21].

2.4. Immobilization of Mice IgGs. Isolated mice IgGs were immobilized on agarose using the Pierce Direct IP kit (Thermo Scientific, MA), following the procedure previously reported [21]. Briefly, 100 μL of AminoLink Plus coupling resin was applied to each column and centrifuged at 1,000 ×g for 1 min. The columns were then washed twice with 200 μL of 1x coupling buffer (sodium phosphate 0.01 M containing NaCl 0.15 M, pH 7.2). Next, 50 μg of purified IgGs from malaria-resistant mice was loaded onto the column and the volume immediately adjusted to 200 μL using ultrapure water and coupling buffer. After addition of 3 μL of sodium cyanoborohydride 5 M to allow covalent binding, the column was incubated at room temperature with rotation for 2 h. Next, the column was washed twice with coupling buffer and prewashed with 200 μL of quenching buffer (Tris-HCl 1 M) to remove any uncoupled IgG. To block the remaining sites on the resin, 200 μL of quenching buffer and 3 μL of sodium cyanoborohydride were once again added, and the column was incubated for 15 min with gentle shaking. Finally, the column was washed twice with coupling buffer and 6 times with wash solution (NaCl 1 M) and subjected to a final wash with TBS (Tris-buffered saline, Tris 0.025 M, NaCl 0.15 M; pH 7.2).

2.5. Isolation of Parasite Antigens by Immunoaffinity. This procedure has been previously reported [21]. Briefly, total proteins extracted from *PyL* (500–1000 μg) diluted in a 600 μL volume of TBS were loaded onto each antibody-coupled spin column and incubated for 2 h with gentle shaking. To remove nonbound proteins, the complex was washed three times with TBS and once with conditioning buffer supplied with the kit. Sodium deoxycholate 1% (w/v) (Sigma-Aldrich, St. Louis, MO, USA) in PBS was used to dissociate the bound antigens from the immobilized antibody and the eluted antigens were recovered in PBS [25]. The eluted antigens were concentrated and buffer was exchanged with PBS using Pierce Concentrator 7 mL/9 K (Thermo Scientific, MA).

Protein concentration in all fractions, from parasite extracts to antigen isolation, was determined with the Bio-Rad DC Protein Assay (Bio-Rad, CA, USA).

2.6. Immunoblot Assays. Parasite total protein extracts, prepared as described above, were solubilized in SDS-polyacrylamide gel electrophoresis (SDS-PAGE) sample buffer containing SDS 2.5%, boiled for 5 minutes, and subsequently separated on 10% SDS-PAGE. After electrophoresis, proteins were transferred onto PVDF (Hybond-P, GE Healthcare) membranes following standard procedures. Blots were blocked for 1 h with PBS containing 5% nonfat dried milk. The blots were subsequently incubated overnight with individual mouse serum from any of the experimental groups of immunized mice, diluted in PBS containing 0.05% Tween-20 at concentration of 0.05%. Bound IgGs were detected using HRP-conjugated anti-mouse IgG (GE Healthcare) at 1/5000 dilution. Detection was performed using the SuperSignal chemiluminescence substrate (Thermo Scientific, MA) and exposure to X-ray film.

2.7. Adjuvants and Immunizations. To compare CPG ODN-1826 (InvivoGen) and Freund's adjuvants, 60 BALB/c mice were divided into 6 groups ($n = 10$ each) and inoculated with same volume (50 μL) containing 2 μg of the immunoaffinity-purified antigens in different preparations as follows. Group 1: intramuscular (i.m.) injection of one volume of antigens plus 50 μg CpG ODN_{1826} plus one volume of incomplete Freund's adjuvant (IFA). Group 2: i.p. injection of one volume of antigens plus one volume of Complete Freund's Adjuvant (CFA). Group 3: i.p. injection of antigens alone. Group 4: i.m. injection of one volume of 50 μg CpG ODN_{1826} plus one volume of IFA. Group 5: i.p. injection of CFA. Group 6: i.p. injection of PBS. Inoculations were performed twice on days 1 and 27. Four weeks later, at day 55, animals were i.p. infected with 2×10^7 *PyL* parasitized RBCs. Parasitemia was monitored by thin tail-blood smears, stained with Wright's eosin methylene blue. For boosting, CFA (1 : 1 emulsion) was replaced with the IFA (1 : 1 emulsion) in groups 2 and 5.

For the second vaccination trial, immunizations were performed only with the Freund's adjuvant system. At days 1, 25, 50 and 85, three groups of mice were immunized subcutaneously (s.c.) with 10 μg of the immunoaffinity-purified antigenic preparations plus adjuvant (group 1), with only adjuvant (group 2), and with PBS (group 3). CFA was used only in the primary immunization and was replaced with IFA for the following boosts. Two weeks after the last immunization, animals were infected intraperitoneally as indicated above.

2.8. Statistical Analysis. Differences between individual groups were analyzed using Student's t-test or the Mann-Whitney test in Prism 5 software (GraphPad Software Inc.). Significance was set at $P < 0.05$.

3. Results

3.1. Diversity of Blood-Stage Antigens Isolated by Immunoaffinity. As shown in Figure 1(a), a wide range of molecular weight proteins between 22 and 250 kDa were detected by the immune sera, demonstrating that the isolated immune affinity antigens have functional binding and recognition. Moreover, analysis of the antigens with only anti-mouse IgG/HRP linked F(ab) did not show any signal in the membranes (Figure 1(b)), establishing that either complete or fraction IgGs did not coelute in the flow-through during purification. This initial screening of the immunoaffinity isolated antigens that were subsequently used for immunization demonstrated their richness in multiple native IgGs recognition and consequently their potential use for vaccination purposes.

3.2. Blood-Stage Antigens Required Adjuvant to Elicit Immune Response. *PyL* antigens purified with IgGs antibodies from ICR resistant-mouse sera were used as a vaccine to determine their capacity to induce protection in a uniformly lethal model of malaria as BALB/c mice infected with *PyL*. Due to the difficulties in developing a vaccine formulation, in a first trial the antigens were explored with different adjuvants to test their stimulatory capacity. Mice were challenged with only 2 μg of purified antigens accompanied by CpG ODN_{1826},

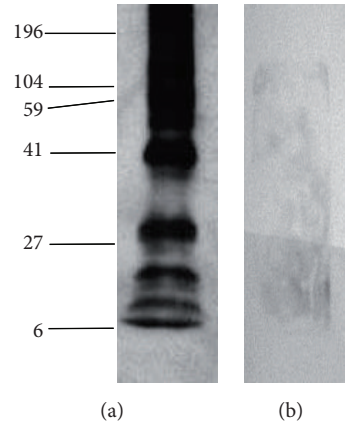

Figure 1: Immunoreactivity against isolated antigens. Representative western blot analysis of *PyL* antigens obtained through immunoaffinity chromatography with immobilized IgGs from malaria surviving ICR mice. (a) shows the specificity of immune sera from ICR mice against purified antigens followed by the incubation with the secondary antibody anti-mouse IgG/HRP linked Fab and (b) was incubated only with the secondary antibody. Lanes were loaded with 10 μg of protein.

IFA, or CFA on days 1 and 27 and infected on day 55 (Figure 2). The number of days of life of mice from groups immunized with 2 μg of purified antigens together with any of the tested adjuvant systems (groups 1 and 2) was significantly higher than their control groups 3, 4, and 6; and 3, 5, and 6, respectively ($P < 0.05$) (Figure 3(a)), suggesting that the presence of adjuvants is necessary for the acquisition of some degree of protection. Apart from increasing survival rates, significant lower parasitemia was also observed on day 4 post-infection (pi) between groups 1 and 2 and their own controls (Figure 3(b)).

Since adjuvant CpG is especially effective when small amounts of antigen are applied [26], it was considered potentially suitable for this type of vaccination, particularly due to the difficulty in obtaining large amounts of highly purified antigens. However, although a slight delay in mortality was observed, this adjuvant failed to increase protection against lethal challenging infection with *PyL* (mouse group 1) showing that the choice of an appropriate adjuvant system is critical in the immunization effectiveness with the purified antigens in our mouse model. The most effective adjuvant in our experiments was Freund's. Mice treated with antigens and CFA appeared to be partially protected, as death was delayed for about 2 days, and one mouse survived the challenge.

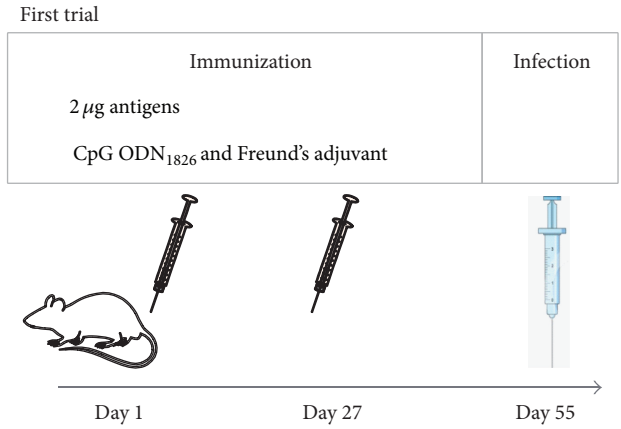

Figure 2: Experimental design of immunization with purified antigens and different adjuvants. IgGs, from naturally surviving ICR mice to *PyL* infection, were purified and used to isolate blood-stage parasite antigens. BALB/c mice divided into 6 groups were then inoculated with 2 μg of purified antigens using CpG ODN$_{1826}$ and/or Freund's adjuvant systems or with proper controls on days 1 and 27 and infected with 2×10^7 *PyL*-RBCs on day 55.

3.3. Immunization Elicits Progressive IgG Response to Multiple Blood-Stage Parasite Antigens. The results obtained using 2 μg of purified antigens for immunization (Figure 3) suggested that the vaccine dose used could be limiting to observe a consistent response. Hence, we increased the amount of immunoaffinity-purified antigens for vaccination to 10 μg, doubled to 4 inoculations along 12 weeks, and tested subcutaneous (s.c.) route of inoculation in order to improve immunogenicity [27]. Thus, BALB/c mice were inoculated with antigens using the Freund's adjuvant system on days 1, 25, 50, and 85 (Figure 4). Our objective was to induce B lymphocytes to synthesize antibodies as they are crucial components of the protective immune response against malaria in human and animal models [28, 29]. Consequently, to ascertain the possible humoral response developed by mice we conducted a time-course IgG immunoblot analysis prior to infection at days 40, 70, and 100 using total *PyL* protein extracts.

A progressive increase of the amount of IgGs and the range of parasite Ags recognized was observed along the vaccination period (Figure 5). At day 40, vaccinated mice sera showed a strong recognition of high molecular weight antigens ranging between 250 and 95 kDa (Figure 5(a)). Moreover, both repertoire and intensity recognition increased at day 70 and subsequently at day 100, when the maximum was observed (Figures 5(b) and 5(c)). From inspection of individual serum reactivity it became apparent that the later

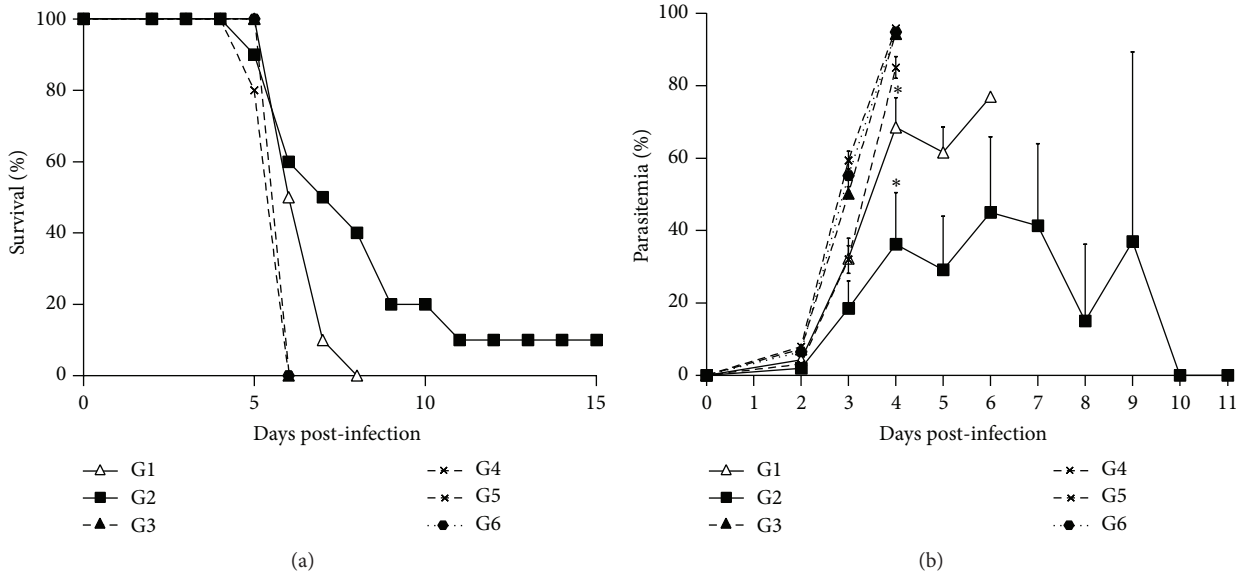

Figure 3: Course of infection after vaccination with different adjuvants in BALB/c mice. Mice were divided into 6 groups ($n = 10$ each) to be immunized on days 1 and 27. Group (G) 1 with 2 μg of purified antigens and CpG ODN_{1826} plus IFA, G2 with 2 μg antigens plus CFA, G3 with 2 μg of antigens, G4 with PBS and CpG ODN_{1826} plus IFA, G5 with PBS and CFA, and G6 with PBS. On day 27 CFA was replaced with IFA. At day 55, all mice were challenged with 2×10^7 *PyL*-RBCs. Percentages of (a) survival and (b) parasitemia are shown as mean (± SEM). $^*P < 0.05$ comparing to controls with antigens or same adjuvant alone or PBS (G2 versus G3, G5, and G6; G1 versus G3, G4, and G6).

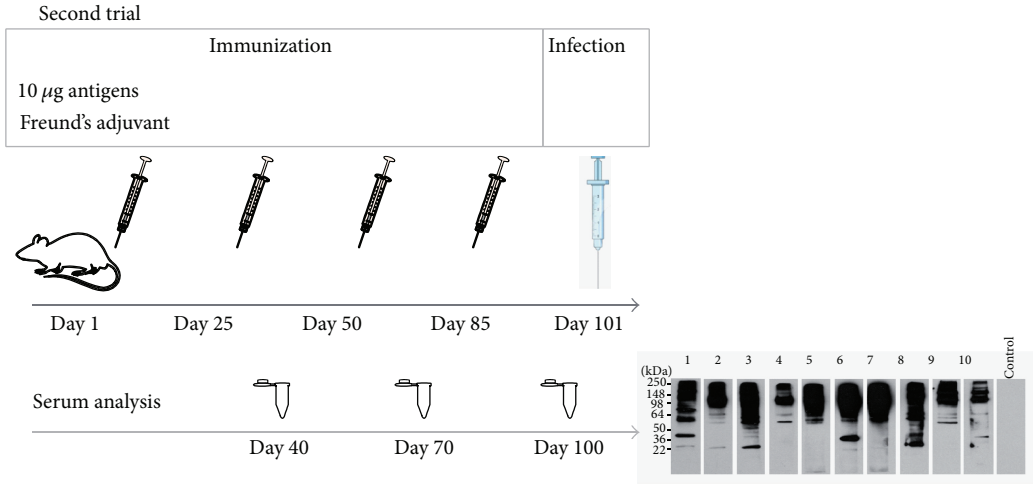

Figure 4: Experimental design of immunization with purified antigens and Freund's adjuvant. Blood-stage parasite antigens were isolated by using IgGs from surviving ICR mice to *PyL* infection and were inoculated together with Freund's adjuvant in BALB/c mice on days 1, 25, 50, and 85. Two weeks later mice were infected with 2×10^7 *PyL*-RBCs. Mouse sera obtained on days 40, 70, and 100 were subjected to immunoblot analysis.

IgGs to show up were those recognizing small molecular weight antigens, particularly in the range 64–36 kDa, in which certain degree of heterogeneity was observed between individual mice. Nevertheless, there was no evidence in the individual western blot patterns that could differentiate surviving from nonsurviving mice (Figure 5(c)).

3.4. Immunization Elicits Partial Protection against Lethal Blood-Stage Malaria Infection. After confirming the immune stimulatory capacity of our antigens with Freund's adjuvant, mice were challenged two weeks after the last immunization to determine their state of immunity to the live parasite. Vaccinated mice survived more days than untreated or adjuvant-treated mice (Figure 6(a)) ($P < 0.05$). In addition, one vaccinated mouse survived up to day 18 pi and another fully survived after clearing parasitemia (Figures 6(a) and 6(b)). Interestingly, parasitemia on these two mice reached a maximum of 30.5% on day 7 pi, much lower than the maximum of 92.4% by day 5 pi reached in control mice, and progressively declined during the following days (Figure 6(c)). At day 17 pi,

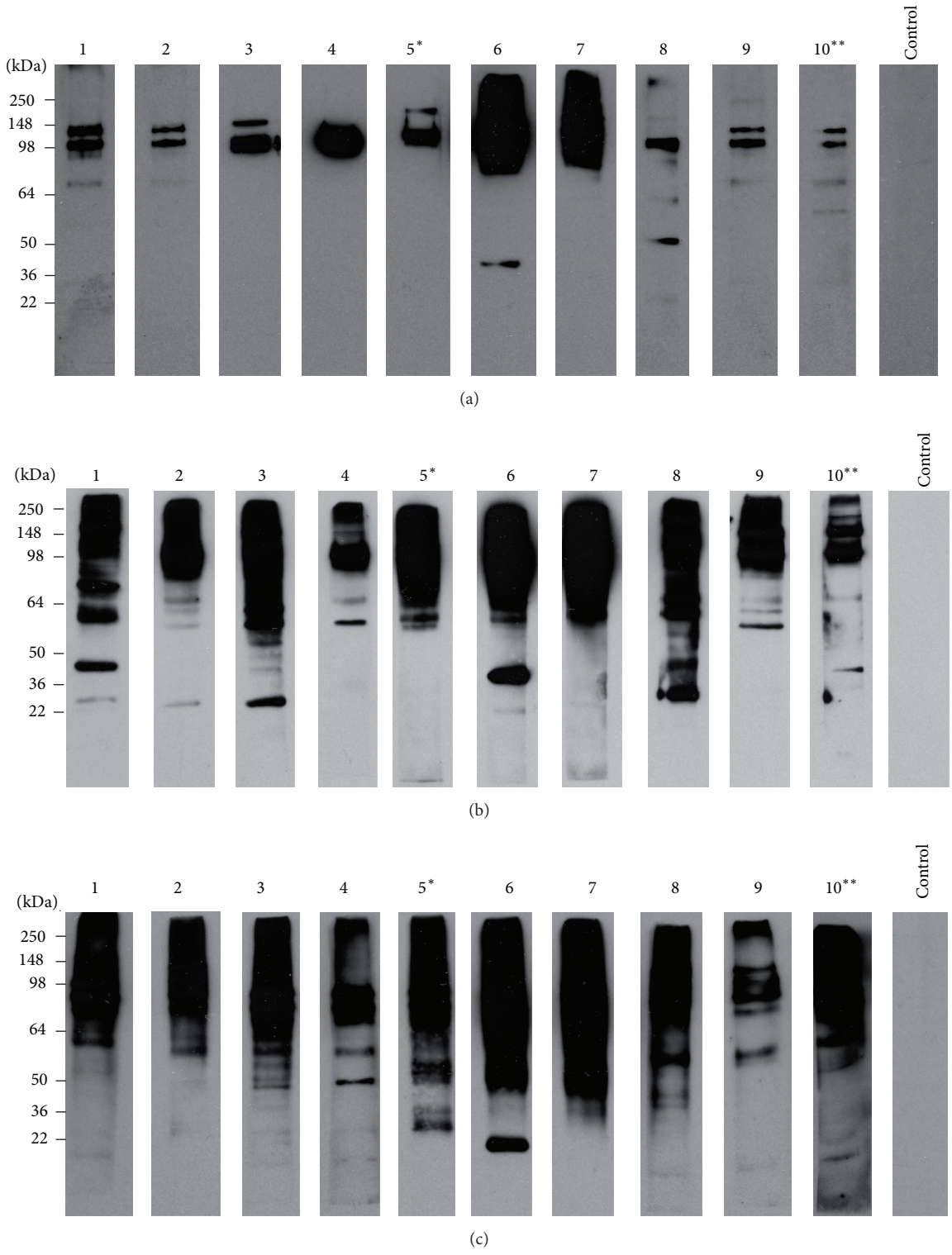

Figure 5: Humoral response of BALB/c mice after immunization with purified *PyL* antigens and Freund's adjuvant. The reactivity of sera obtained from mice previously immunized with highly affinity-purified antigens plus Freund's adjuvant ($n = 10$) was assayed on immunoblots of total *P. yoelii* blood-stage antigen (10 μg/lane) at days 40 (a), 70 (b) and 100 (c). A representative nonvaccinated mouse serum (Control) served as the negative control at corresponding day. Two weeks after last immunization mice were infected with *PyL* and mouse number 5* survived the infection and mouse number 10** lived until day 17 pi. Antigen-specific antibodies were detected with anti-mouse IgG/HRP linked F(ab).

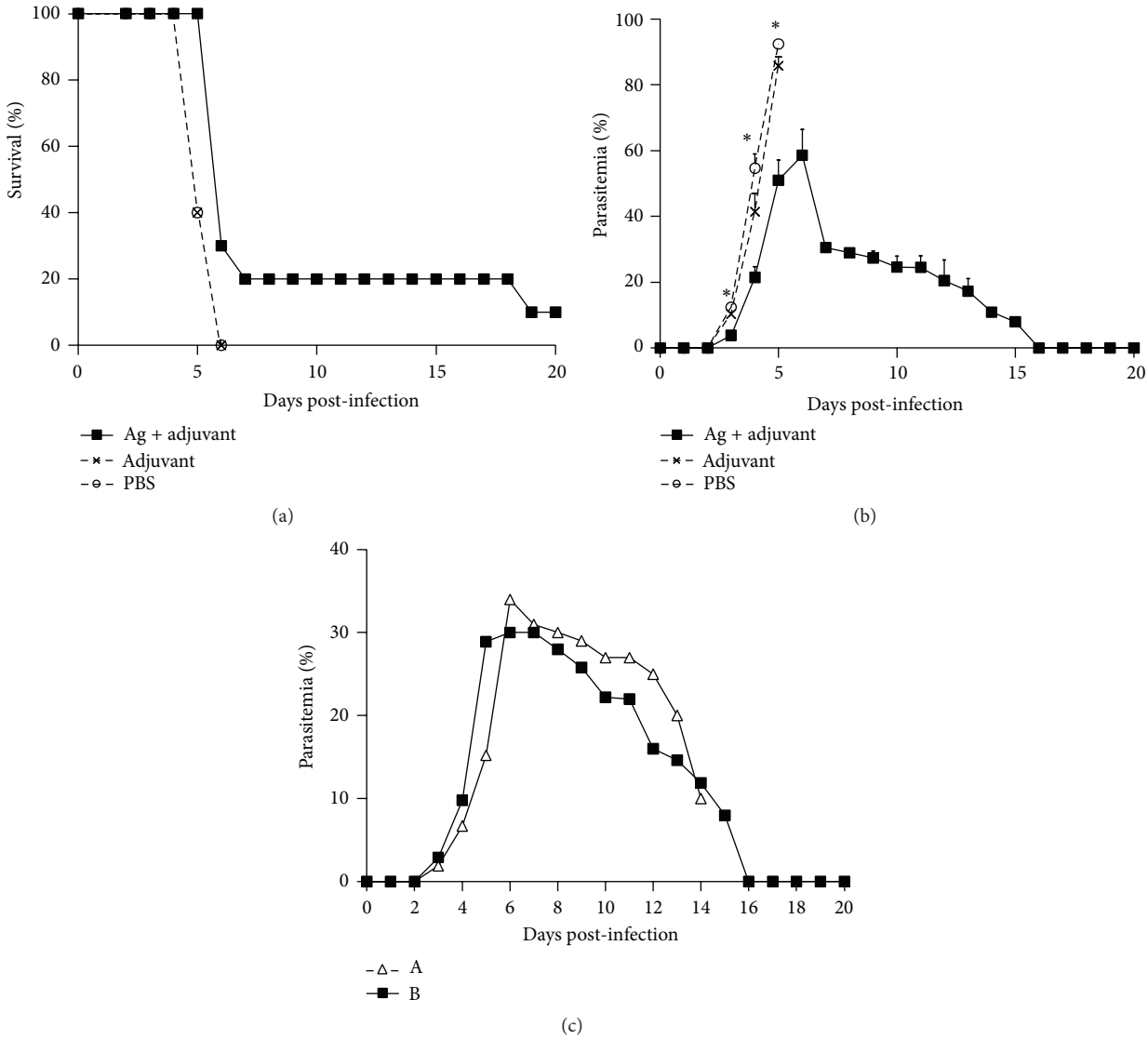

Figure 6: Course of infection in BALB/c mice after antigen and Freund's adjuvant vaccination. Groups of BALB/c mice were immunized with 10 μg of purified antigens formulated with Freund's adjuvant (Ag + adjuvant, $n = 10$), Freund's adjuvant plus PBS (Adjuvant, $n = 10$), or PBS alone (PBS, $n = 5$). Two weeks after the fourth immunization, mice were challenged with 2×10^7 *PyL*-RBCs. Percentages of (a) survival and (b) parasitemia from a total of 500 RBCs are shown as mean (± SEM). (c) Parasitemia course of mice with longer surviving rates after vaccination: mouse which survived around two weeks (Δ) or completely survived (■). Data is shown as mean (± SEM). $^*P < 0.05$ comparing group "Ag + adjuvant" to both controls.

one out of two vaccinated mice died with a status of severe anaemia, while the surviving mouse cleared all parasites in blood as observed by microscopy inspection.

4. Discussion

The incomplete immune response to malaria together with the lack of a licensed vaccine and the spread of drug resistant parasites hinder malaria control and turn malaria disease into a major public health problem [30]. Numerous vaccine strategies are being researched in the malaria field and are mainly based on three different antigens separately used: circumsporozoite protein (CSP), merozoite surface protein (MSP), and apical membrane antigen 1 (AMA-1). However, these strategies do not emulate the naturally acquired immunity against malaria which is based on years of repetitive infections allowing contact with a large range of different antigens [5, 7, 31]. Actually, immunizations with a broad spectrum of antigens from different parasite stages are considered to counteract the parasite's immune evasion improving protection [8]. According to this concept, experimental vaccination with whole parasites through irradiation [32] or genetically [33] attenuated *Plasmodium* sporozoites or with parasites in hepatic or blood-stages under treatment with different drugs [13, 14, 34] is providing excellent results of malaria protection as they can more easily fight against the antigenic

polymorphism of the parasite. Thus, in the present work, we aimed to produce an immunogenic combination based on *P. yoelii* blood-stage antigens isolated with immobilized affinity-purified antibodies from malaria-resistant mice. During blood-stage malaria infection, parasite-specific antibodies have been shown to play a key role in controlling parasitemia [28, 35]. However, malaria infection also gives rise to strongly elevated blood concentrations of non-malaria-specific immunoglobulin [36] and IgG responses specific for *P. falciparum* antigens are often unexpectedly short-lived and fail to consistently boost upon reinfection [37]. For that reason, the research of protective antigens is still difficult and here we proposed to use the total *Plasmodium*-specific IgGs produced in response to malaria reinfection in ICR immune mice to isolate total antigens in which protective antigens will also be present. Although resistance to malaria can be generated through antimalarial treatment in mice [38], drugs can alter the natural mechanisms of immune protection. Consequently, to test the protective capacity of *PyL* antigens we chose to use antibodies produced under a naturally developed immune response in the ICR malaria model in which a 20% of mice naturally develop immunity to the infection [20].

We have previously demonstrated the protective role of antibodies against the infection through the passive transfer of pooled sera from resistant ICR mice containing 150–200 μg of total IgG to naïve BALB/c mice, 2 hours after a challenge with 2×10^7 *PyL* iRBCs, being able to cure 40% of transferred mice [20]. BALB/c mice are uniformly susceptible to fatal malaria infection with *PyL* so their use for vaccine and drug preclinical trials is consolidated [24].

This procedure allows us to previously identify well-known and new malaria antigens including protein disulfide isomerase (PDI), the HSPA5 member of the heat shock protein-70 family (also called binding immunoglobulin protein BiP), the aspartic proteinase plasmepsin, and the eukaryotic translation initiation factor 3 (IF3) as antigenic proteins [21]. In addition to these proteins, other unidentified bands are also detected on 1D-electrophoresis within the immune-affinity purified proteins, suggesting that the partial protection of BALB/c mice against the lethal infection dose is not only due to the above indicated identified proteins. Nonetheless the potential role of those four highly prevalent antigens to immunize the surviving mice may contribute to the increase of the components of a more effective blood-stage malaria vaccine. Immune responses to malaria HSPs have been repeatedly demonstrated in patients with malaria [39]. Further, several reports characterizing malarial HSPs indicated that this protein class might play important roles in the life cycle of the parasites [40]. The ability of HSP 70 to regulate parasite actin polymerization during invasion of RBCs suggests that HSP 70 is correlated with infectivity of malaria parasites [40, 41]. The remaining three identified plasmodial immunogenic antigens, for which their functionality in blood-stage malaria has been well defined elsewhere [21], are similarly worth being explored as candidates to raise antibodies during *in vivo* vaccination screens with purified antigens.

Among the criteria for selecting a vaccine formulation, the antigenic components are crucial to later investigate adjuvants, route of delivery, potential adverse effects, and stability. Given the large variety of responses that the same antigens can generate with different adjuvants [42–44], we chose to compare the effect of two different adjuvants to test the *in vivo* protective immunity with our set of *P. yoelii* purified antigens. Results obtained using 2 μg of purified antigens as potential immunogenic mixture showed some degree of protective response, which was dependent on the adjuvants used.

It has been reported that CPG ODNs binding to TLR9 receptor results in the production of proinflammatory cytokines and chemokines stimulating the recruitment of additional inflammatory mediators. However, our isolated antigens plus CpG ODN adjuvant did not confer protection against the malaria infection in mice. Actually, immunization with CpG ODN has shown a wide variety of results in infectious disease trials [45]. Factors as conjugation rate of protein and ODN, infection dose, and administration route play a role in its effectiveness as adjuvant [46–48].

On the other hand, Freund's adjuvant decreased parasitemia and increased survival in the vaccinated mice. It has been reported that early immune response caused by IFA/CFA includes rapid uptake of adjuvant components by dendritic cells, enhanced phagocytosis, secretion of cytokines by mononuclear phagocytes as well as transient activation and proliferation of CD4+ lymphocytes [49] in addition to antibody production against denatured epitopes of proteins [50]. Given that Freund's adjuvant was more effective in our experiments we chose this adjuvant in the formulation of the following vaccine trial.

In the second trial, the humoral response developed by BALB/c mice after the four vaccination challenges was characterized by immunoblot which confirmed the immunogenicity of our isolated antigens. A large variety of *PyL* specific IgGs were developed against a wide range of parasite proteins, similar to the build-up of the humoral response observed in partially immunized humans [51]. The key role of B cells in controlling malaria infections has been clearly revealed in rodent models lacking these cells, which are not able to eliminate *P. yoelii* [35] and *P. chabaudi* infections [52]. Moreover, the protective role of Abs against malaria infection is supported by the transfer of immune serum into infected nonimmune humans as an efficient treatment strategy [28] that is also efficient in mouse models [29]. Specific anti-malarial Abs might protect by several attributes, including merozoite invasion blocking, cooperation with monocytes, NKs or DCs; or by inhibiting iRBCs cytoadherence [36].

Infection of our vaccinated mice showed that all individuals prolonged their survival rate but only a small fraction was really protected against the lethal infection. Further experiments with lower infective doses could permit a progressive encounter of immune system with the parasite and influence Th1/Th2 activity [53]. Besides, the inoculation of a higher quantity of antigen could probably improve the percentage of protection. Immune responses in endemic infections in humans can be partially protective, allowing the individual to tolerate significant parasite densities without

overt disease [54], but the mechanisms of immune protection are poorly understood [1, 55]. In fact, we were not able to identify differential antibody production between protected and unprotected individuals which could be the reason of the low duration of the protection, as it has also been described following the administration of the RTS, S/AS01, the most advanced vaccine candidate in humans [56–58].

5. Conclusions

In conclusion, immunoaffinity-purified antigens using IgGs from protected individuals deserve further research, either by fractionation of some of the isolated set or by complementation with additional components, to improve efficacy of a potential multiantigen blood-stage malaria vaccine.

Conflict of Interests

All authors reported no conflict of interests in the research presented in the paper.

Acknowledgments

The authors thank Susana Pérez-Benavente for excellent technical assistance. This work was supported by Spanish National Grants (MICINN BIO2010-17039 and MINECO BIO2013-44565-R) and by the Programme of Consolidate Research Teams from UCM-Comunidad de Madrid (Research Team 920267).

References

[1] D. L. Doolan, C. Dobano, and J. K. Baird, "Acquired immunity to malaria," *Clinical Microbiology Reviews*, vol. 22, no. 1, pp. 13–36, 2009.

[2] H. Hisaeda, K. Yasutomo, and K. Himeno, "Malaria: immune evasion by parasites," *International Journal of Biochemistry and Cell Biology*, vol. 37, no. 4, pp. 700–706, 2005.

[3] N. J. White, S. Pukrittayakamee, T. T. Hien, M. A. Faiz, O. A. Mokuolu, and A. M. Dondorp, "Malaria," *The Lancet*, vol. 383, no. 9918, pp. 723–735, 2014.

[4] T. L. Richie and A. Saul, "Progress and challenges for malaria vaccines," *Nature*, vol. 415, no. 6872, pp. 694–701, 2002.

[5] D. L. Doolan, Y. Mu, B. Unal et al., "Profiling humoral immune responses to *P. falciparum* infection with protein microarrays," *Proteomics*, vol. 8, no. 22, pp. 4680–4694, 2008.

[6] J. Langhorne, F. M. Ndungu, A.-M. Sponaas, and K. Marsh, "Immunity to malaria: more questions than answers," *Nature Immunology*, vol. 9, no. 7, pp. 725–732, 2008.

[7] J. C. Gray, P. H. Corran, E. Mangia et al., "Profiling the antibody immune response against blood stage malaria vaccine candidates," *Clinical Chemistry*, vol. 53, no. 7, pp. 1244–1253, 2007.

[8] E. M. Riley and V. A. Stewart, "Immune mechanisms in malaria: new insights in vaccine development," *Nature Medicine*, vol. 19, no. 2, pp. 168–178, 2013.

[9] M. F. Good, "A whole parasite vaccine to control the blood stages of *Plasmodium*—the case for lateral thinking," *Trends in Parasitology*, vol. 27, no. 8, pp. 335–340, 2011.

[10] L. Rénia, A. C. Grüner, M. Mauduit, and G. Snounou, "Vaccination against malaria with live parasites," *Expert Review of Vaccines*, vol. 5, no. 4, pp. 473–481, 2006.

[11] M. F. Good and D. L. Doolan, "Malaria vaccine design: immunological considerations," *Immunity*, vol. 33, no. 4, pp. 555–566, 2010.

[12] J. M. Burns Jr., P. D. Dunn, and D. M. Russo, "Protective immunity against *Plasmodium yoelii* malaria induced by immunization with particulate blood-stage antigens," *Infection and Immunity*, vol. 65, no. 8, pp. 3138–3145, 1997.

[13] D. J. Pombo, G. Lawrence, C. Hirunpetcharat et al., "Immunity to malaria after administration of ultra-low doses of red cells infected with *Plasmodium falciparum*," *The Lancet*, vol. 360, no. 9333, pp. 610–617, 2002.

[14] M. Roestenberg, A. C. Teirlinck, M. B. B. McCall et al., "Long-term protection against malaria after experimental sporozoite inoculation: an open-label follow-up study," *The Lancet*, vol. 377, no. 9779, pp. 1770–1776, 2011.

[15] A. Pinzon-Charry, V. McPhun, V. Kienzle et al., "Low doses of killed parasite in CpG elicit vigorous $CD4^+$ T cell responses against blood-stage malaria in mice," *The Journal of Clinical Investigation*, vol. 120, no. 8, pp. 2967–2978, 2010.

[16] T. L. M. ten Hagen, A. J. Sulzer, M. R. Kidd, A. A. Lal, and R. L. Hunter, "Role of adjuvants in the modulation of antibody isotype, specificity, and induction of protection by whole blood-stage *Plasmodium yoelii* vaccines," *Journal of Immunology*, vol. 151, no. 12, pp. 7077–7085, 1993.

[17] J. Yuan, B. Xu, and B.-F. Liu, "Protective immune mechanisms induced by cellular vaccine made of the erythrocytic *Plasmodium yoelii*," *Zhongguo Yi Xue Ke Xue Yuan Xue Bao*, vol. 26, no. 1, pp. 47–51, 2004.

[18] M. J. Gardner, N. Hall, E. Fung et al., "Genome sequence of the human malaria parasite *Plasmodium falciparum*," *Nature*, vol. 419, no. 6906, pp. 498–511, 2002.

[19] D. L. Doolan, "*Plasmodium* immunomics," *International Journal for Parasitology*, vol. 41, no. 1, pp. 3–20, 2011.

[20] I. G. Azcárate, P. Marín-García, A. N. Kamali et al., "Differential immune response associated to malaria outcome is detectable in peripheral blood following plasmodium yoelii infection in mice," *PLoS ONE*, vol. 9, no. 1, Article ID e85664, 2014.

[21] A. N. Kamali, P. Marín-García, I. G. Azcárate, A. Diez, A. Puyet, and J. M. Bautista, "*Plasmodium yoelii* blood-stage antigens newly identified by immunoaffinity using purified IgG antibodies from malaria-resistant mice," *Immunobiology*, vol. 217, no. 8, pp. 823–830, 2012.

[22] C. Kilkenny, W. Browne, I. C. Cuthill, M. Emerson, and D. G. Altman, "Animal research: reporting in vivo experiments: the ARRIVE guidelines," *British Journal of Pharmacology*, vol. 160, no. 7, pp. 1577–1579, 2010.

[23] G. A. Kicska, L.-M. Ting, V. L. Schramm, and K. Kim, "Effect of dietary p-aminobenzoic acid on murine Plasmodium yoelii infection," *Journal of Infectious Diseases*, vol. 188, no. 11, pp. 1776–1781, 2003.

[24] A. W. Taylor-Robinson, "Regulation of immunity to malaria: valuable lessons learned from murine models," *Parasitology Today*, vol. 11, no. 9, pp. 334–342, 1995.

[25] A. A. Holder and R. R. Freeman, "Immunization against blood-stage rodent malaria using purified parasite antigens," *Nature*, vol. 294, no. 5839, pp. 361–364, 1981.

[26] R. Weeratna, L. Comanita, and H. L. Davis, "CPG ODN allows lower dose of antigen against hepatitis B surface antigen in BALB/c mice," *Immunology and Cell Biology*, vol. 81, no. 1, pp. 59–62, 2003.

[27] R. E. Bégué and H. Sadowska-Krowicka, "Protective efficacy of recombinant urease B and aluminum hydroxide against Helicobacter pylori infection in a mouse model," *FEMS Immunology and Medical Microbiology*, vol. 60, no. 2, pp. 142–146, 2010.

[28] S. Cohen, I. A. McGregor, and S. Carrington, "Gamma-globulin and acquired immunity to human malaria," *Nature*, vol. 192, no. 4804, pp. 733–737, 1961.

[29] A. N. Jayawardena, G. A. T. Targett, E. Leuchars, and A. J. S. Davies, "The immunological response of CBA mice to *P. yoelii*. II. The passive transfer of immunity with serum and cells," *Immunology*, vol. 34, no. 1, pp. 157–165, 1978.

[30] WHO, *World Malaria Report*, World Health Organization, Geneva, Switzerland, 2012.

[31] A. Trieu, M. A. Kayala, C. Burk et al., "Sterile protective immunity to malaria is associated with a panel of novel *P. falciparum* antigens," *Molecular & Cellular Proteomics*, vol. 10, no. 9, Article ID M111.007948, 2011.

[32] S. L. Hoffman, L. M. L. Goh, T. C. Luke et al., "Protection of humans against malaria by immunization with radiation-attenuated *Plasmodium falciparum* sporozoites," *Journal of Infectious Diseases*, vol. 185, no. 8, pp. 1155–1164, 2002.

[33] A.-K. Mueller, M. Labaled, S. H. I. Kappe, and K. Matuschewski, "Genetically modified *Plasmodium* parasites as a protective experimental malaria vaccine," *Nature*, vol. 433, no. 7022, pp. 164–167, 2005.

[34] M. Roestenberg, M. McCall, J. Hopman et al., "Protection against a malaria challenge by sporozoite inoculation," *The New England Journal of Medicine*, vol. 361, no. 5, pp. 468–477, 2009.

[35] F. I. Weinbaum, C. B. Evans, and R. E. Tigelaar, "Immunity to *Plasmodium berghei* yoelii in mice. I. The course of infection in T cell and B cell deficient mice," *Journal of Immunology*, vol. 117, no. 5, part 2, pp. 1999–2005, 1976.

[36] P. Perlmann and M. Troye-Blomberg, "Malaria and the immune system in humans," *Chemical Immunology*, vol. 80, pp. 229–242, 2002.

[37] P. Bejon, J. Mwacharo, O. Kai et al., "A phase 2b randomised trial of the candidate malaria vaccines FP9 ME-TRAP and MVA ME-TRAP among children in Kenya," *PLoS Clinical Trials*, vol. 1, no. 6, article e29, 2006.

[38] E. Belnoue, T. Voza, F. T. M. Costa et al., "Vaccination with live *Plasmodium yoelii* blood stage parasites under chloroquine cover induces cross-stage immunity against malaria liver stage," *The Journal of Immunology*, vol. 181, no. 12, pp. 8552–8558, 2008.

[39] C. O. P. Alexandre, L. M. A. Camargo, D. Mattei et al., "Humoral immune response to the 72 kDa heat shock protein from *Plasmodium falciparum* in populations at hypoendemic areas of malaria in western Brazilian Amazon," *Acta Tropica*, vol. 64, no. 3-4, pp. 155–166, 1997.

[40] G. Banumathy, V. Singh, S. R. Pavithra, and U. Tatu, "Heat shock protein 90 function is essential for *Plasmodium falciparum* growth in human erythrocytes," *Journal of Biological Chemistry*, vol. 278, no. 20, pp. 18336–18345, 2003.

[41] I. Tardieux, I. Baines, M. Mossakowska, and G. E. Ward, "Actin-binding proteins of invasive malaria parasites and the regulation of actin polymerization by a complex of 32/34-kDa proteins associated with heat shock protein 70kDa," *Molecular and Biochemical Parasitology*, vol. 93, no. 2, pp. 295–308, 1998.

[42] E. Mata, M. Igartua, R. M. Hernández, J. E. Rosas, M. E. Patarroyo, and J. L. Pedraz, "Comparison of the adjuvanticity of two different delivery systems on the induction of humoral and cellular responses to synthetic peptides," *Drug Delivery*, vol. 17, no. 7, pp. 490–499, 2010.

[43] A. Rafi-Janajreh, J. E. Tongren, C. Kensil et al., "Influence of adjuvants in inducing immune responses to different epitopes included in a multiepitope, multivalent, multistage *Plasmodium falciparum* candidate vaccine (FALVAC-1) in outbred mice," *Experimental Parasitology*, vol. 101, no. 1, pp. 3–12, 2002.

[44] C. Yang, W. E. Collins, L. Xiao et al., "Influence of adjuvants on murine immune responses against the C-terminal 19 kDa fragment of *Plasmodium vivax* merozoite surface protein-1 (MSP-1)," *Parasite Immunology*, vol. 18, no. 11, pp. 547–558, 1996.

[45] J. Scheiermann and D. M. Klinman, "Clinical evaluation of CpG oligonucleotides as adjuvants for vaccines targeting infectious diseases and cancer," *Vaccine*, vol. 32, no. 48, pp. 6377–6389, 2014.

[46] H. Tighe, K. Takabayashi, D. Schwartz et al., "Conjugation of protein to immunostimulatory DNA results in a rapid, long-lasting and potent induction of cell-mediated and humoral immunity," *European Journal of Immunology*, vol. 30, no. 7, pp. 1939–1947, 2000.

[47] M. Roman, E. Martin-Orozco, J. S. Goodman et al., "Immunostimulatory DNA sequences function as T helper-1-promoting adjuvants," *Nature Medicine*, vol. 3, no. 8, pp. 849–854, 1997.

[48] H. Shirota, K. Sano, N. Hirasawa et al., "Novel roles of CpG oligodeoxynucleotides as a leader for the sampling and presentation of CpG-tagged antigen by dendritic cells," *The Journal of Immunology*, vol. 167, no. 1, pp. 66–74, 2001.

[49] A. Billiau and P. Matthys, "Modes of action of Freund's adjuvants in experimental models of autoimmune diseases," *Journal of Leukocyte Biology*, vol. 70, no. 6, pp. 849–860, 2001.

[50] G. Wolberg, C. T. Liu, and F. L. Adler, "Passive hemagglutination. II. Titration of antibody against determinants unique for aggregated denatured bovine serum albumin and further studies on gelatin," *Journal of Immunology*, vol. 105, no. 4, pp. 797–801, 1970.

[51] M. Linares, E. Albizua, D. Méndez et al., "Malaria hidden in a patient with diffuse large B-cell lymphoma and sickle cell trait," *Journal of Clinical Microbiology*, vol. 49, no. 12, pp. 4401–4404, 2011.

[52] T. von der Weid, N. Honarvar, and J. Langhorne, "Gene-targeted mice lacking B cells are unable to eliminate a blood stage malaria infection," *Journal of Immunology*, vol. 156, no. 7, pp. 2510–2516, 1996.

[53] J. Wipasa, S. Elliott, H. Xu, and M. F. Good, "Immunity to asexual blood stage malaria and vaccine approaches," *Immunology and Cell Biology*, vol. 80, no. 5, pp. 401–414, 2002.

[54] R. W. Sauerwein, E. M. Bijker, and T. L. Richie, "Empowering malaria vaccination by drug administration," *Current Opinion in Immunology*, vol. 22, no. 3, pp. 367–373, 2010.

[55] J. G. Beeson, F. H. A. Osier, and C. R. Engwerda, "Recent insights into humoral and cellular immune responses against

malaria," *Trends in Parasitology*, vol. 24, no. 12, pp. 578–584, 2008.

[56] K. E. Kester, J. F. Cummings, O. Ofori-Anyinam et al., "Randomized, double-blind, phase 2a trial of falciparum malaria vaccines RTS,S/AS01B and RTS,S/AS02A in malaria-naive adults: safety, efficacy, and immunologic associates of protection," *Journal of Infectious Diseases*, vol. 200, no. 3, pp. 337–346, 2009.

[57] D. Ansong, K. P. Asante, J. Vekemans et al., "T cell responses to the RTS,S/AS01$_E$ and RTS,S/AS02$_D$ malaria candidate vaccines administered according to different schedules to Ghanaian children," *PLoS ONE*, vol. 6, no. 4, Article ID e18891, 2011.

[58] J. M. Lumsden, R. J. Schwenk, L. E. Rein et al., "Protective immunity induced with the RTS,S/AS vaccine is associated with IL-2 and TNF-α producing effector and central memory CD4$^+$ T cells," *PLoS ONE*, vol. 6, no. 7, Article ID e20775, 2011.

Hindawi Publishing Corporation
Journal of Immunology Research
Volume 2015, Article ID 395371, 12 pages
http://dx.doi.org/10.1155/2015/395371

Research Article

Modulating p56Lck in T-Cells by a Chimeric Peptide Comprising Two Functionally Different Motifs of Tip from *Herpesvirus saimiri*

Jean-Paul Vernot,[1,2] Ana María Perdomo-Arciniegas,[1] Luis Alberto Pérez-Quintero,[1] and Diego Fernando Martínez[1]

[1] *Fisiología Celular y Molecular, Facultad de Medicina, Universidad Nacional de Colombia, Bogotá 11001, Colombia*
[2] *Instituto de Investigaciones Biomédicas, Facultad de Medicina, Universidad Nacional de Colombia, Bogotá 11001, Colombia*

Correspondence should be addressed to Jean-Paul Vernot; jpvernoth@unal.edu.co

Received 17 March 2015; Revised 28 April 2015; Accepted 27 May 2015

Academic Editor: Darren R. Flower

The Lck interacting protein Tip of *Herpesvirus saimiri* is responsible for T-cell transformation both *in vitro* and *in vivo*. Here we designed the chimeric peptide hTip-CSKH, comprising the Lck specific interacting motif CSKH of Tip and its hydrophobic transmembrane sequence (hTip), the latter as a vector targeting lipid rafts. We found that hTip-CSKH can induce a fivefold increase in proliferation of human and *Aotus* sp. T-cells. Costimulation with PMA did not enhance this proliferation rate, suggesting that hTip-CSKH is sufficient and independent of further PKC stimulation. We also found that human Lck phosphorylation was increased earlier after stimulation when T-cells were incubated previously with hTip-CSKH, supporting a strong signalling and proliferative effect of the chimeric peptide. Additionally, Lck downstream signalling was evident with hTip-CSKH but not with control peptides. Importantly, hTip-CSKH could be identified in heavy lipid rafts membrane fractions, a compartment where important T-cell signalling molecules (LAT, Ras, and Lck) are present during T-cell activation. Interestingly, hTip-CSKH was inhibitory to Jurkat cells, in total agreement with the different signalling pathways and activation requirements of this leukemic cell line. These results provide the basis for the development of new compounds capable of modulating therapeutic targets present in lipid rafts.

1. Introduction

Selective phosphorylation of tyrosine residues in the T-cell receptor- (TCR-) associated CD3 complex and ζ chains follows TCR engagement and activation by the MHC-peptide complex [1]. Tyrosine phosphorylation is mediated by protein members of the nonreceptor Src tyrosine kinase family, mainly p56Lck (Lck) and p59Fyn (Fyn) [2]. Lck is lymphoid-specific and essential for T-cell development and function [3, 4]; it associates with surface molecules such as CD2, CD4, CD8, CD45, and IL-2 receptor [4–6]. Lck can be either phosphorylated by serine-threonine or tyrosine kinases but it is well known that its activity is mainly positively and negatively regulated by tyrosine phosphorylation in positions 394 and 505, respectively [7, 8]. Stimulation of T-cell lines defective in Lck expression has shown an abnormal tyrosine phosphorylation pattern of downstream protein targets [9]. Lck has acquired importance as a therapeutic target for regulating T-cell response due to this central role in T-cell function [10–12].

Lck, as well as other Src family members, is also the target of viral proteins as a strategy for lymphotropic viruses [13], such as human immunodeficiency virus [14], Epstein-Barr virus [15], or *Herpesvirus saimiri* (HVS), to escape immune control and maintain latency [16]. In particular, HVS is a lymphotropic γ-herpesvirus, which is nonpathogenic in its natural host *Saimiri sciureus*, but in some New World primate species induces fulminant T-cell lymphomas [17]. HVS infection has been used *in vitro* in human and non-human primates (*Aotus* spp.) as a strategy for T-cell transformation

[18–20]. This would suggest that transformation mechanisms in human and *Aotus* T-cells could have the same molecular basis.

Two HVS gene products, Tip (tyrosine kinase interacting protein) and StpC (*Saimiri* transforming protein), seem to be essential for the observed oncogenic phenotype [21]. Tip was able to induce T-cell lymphoma in transgenic mice and is therefore very likely to be responsible for the oncogenicity in T-cells [22]. A mechanistic model in which Tip participates in TCR signalling and CD4 downregulation has been proposed to explain HVS-infected T-cell longevity with consequences on viral persistence and pathogenesis [23]. Some studies have shown that Tip specifically associates with Lck, increasing its phosphorylation and activity and thus T-cell proliferation [24–26]. Moreover, Tip has been extensively implicated in oncogenic transformation [13, 27].

Nevertheless, in Jurkat T-cell lines or primary T-cells immortalized by lentiviral transduction, other authors have shown that Tip induces downregulation of Lck and an overall decrease in cellular tyrosine phosphorylation of several proteins, including Lck and ZAP70 [16, 28]. Early work has shown differences in signalling molecule expression and altered requirements for Jurkat cells activation [29], explaining in part the opposite effect of Tip in primary T-cells versus Jurkat cells or immortalized T-cells.

The Lck-binding domains (LBD) of Tip have been mapped to the carboxyl terminal portion of the molecule involving two independent binding motifs, SH3B (SH3 binding) and CSKH (C-terminal Src kinase homology). They are included within a highly conserved region between amino acids 146 to 182 [30–33]. The SH3B motif (residues 172 to 182) binds to the SH3 domain on Lck, while the CSKH motif (residues 146 to 155) binds to the kinase catalytic domain [24]. Interestingly, mutants of Tip, containing either only SH3B or only CSKH domains, bind to Lck although to a reduced extent [32]. Also a truncated form of Tip lacking SH3B is still able to induce lymphomas *in vivo* [34] and coexpression of Lck with a Tip mutant lacking SH3B stimulated tyrosine phosphorylation of cellular proteins [32]. This suggests a suitable and sufficient role of the CSKH domain for Lck binding, T-cell signalling, proliferation, and eventually cell transformation.

As it would be expected for a protein regulating Lck, Tip has been shown to be constitutively present in lipid rafts [23, 35], a signalling platform for T-cell activation [36, 37], where early signals are induced allowing subsequently specific gene expression and proliferation [26, 38, 39]. The carboxyl terminal hydrophobic (hTip) sequence of Tip is responsible for its localization to lipid rafts [40]. In the present work, we have explored the intriguing possibility of inducing T-cell activation and proliferation by using a short Lck binding motif of Tip (CSKH) properly delivered to lipid rafts. In fact, the hTip-CSKH chimera was delivered to detergent resistant membranes allowing us to specifically target Lck, to induce intracellular signalling and T-cell proliferation. Of great relevance, this work suggests that using a lipid raft targeting sequence from the transforming Tip protein could be a novel strategy to activate or inhibit signal transduction pathways, in other cell types and conditions, in which lipid raft dynamic is involved.

2. Methods

2.1. Peptide Synthesis and Characterization. Peptides were synthesized by solid phase as previously described [41]. The hTip sequence corresponds to the carboxyl-terminal residues 232–250 (CLVVVILAVLLLVTVLSIL); the CSKH motif EDLQSFLEKY plus a 6-residue extension (PPDFRK) adjacent to the CSKH motif was used as the hTip cargo, forming the chimera (CLVVVILAVLLLVTVLSILEDLQSFLEKYPPDFRK), here called hTip-CSKH. hTip, CSKH, and a chimeric peptide with the CSKH sequence in a scrambled configuration (hTip-CSKHsc) were also used in some experiments as controls. Peptides were analyzed by RP-HPLC and mass spectrometry to ascertain molecular weight and purity.

2.2. Blood Samples, Cell Isolation, and Cell Line. Human blood samples were obtained from healthy donors after informed consent. *Aotus nancymaae* from the Colombian Amazon region were housed according to NIH guidelines for animal handling. Both human and *Aotus* peripheral blood mononuclear cells (PBMC) were isolated by Ficoll-Hypaque density gradient centrifugation (Sigma-Aldrich Co., St. Louis, MO, USA). The Jurkat T-cell leukemia cell line (ATCC) was cultured under standard conditions. Cell viability was routinely assessed by Trypan-blue dye exclusion and only samples having >90% viability were further used.

2.3. Aotus nancymaae Lck Sequence Determination. RNA from 1×10^7 lymph node cells was extracted by TRIZOL (Gibco, Invitrogen Corp., New York, NY, USA) as described elsewhere. Lck coding and proximal 5′ and 3′ UTR regions were amplified by RT/PCR using SuperScript III One Step RT/PCR with Platinum Taq (end point) (Invitrogen Life Technologies, Carlsbad, CA, USA) with sense primer LckRs17 (5′GCCTGGACCATGTGAAT3′) and antisense primer LckRa20 (5′TGACTATGGCACAAGAACTC3′). Three clones were obtained and sequenced using 6 different primers: LckRs17, LckRa20, M13 forward, M13 reverse primers, and two internal primers LckIntF (5′TGGACAGTTCGGGGAGG3′) and LckIntR02 (5′ATGATGTAGATGGGCTCCT3′). Sequencing was performed with BigDye 3.1 sequence kit and analyzed in ABI PRISM 310 genetic analyzer, with the ABI PRISM Sequencing Analysis 3.3 MT Navigator 1.0.2. (Perkin Elmer, Foster City, CA, USA) and Chromas 1.45 software. Other sequencing was done by MACROGEN Inc. Overlapping sequences were aligned using ClustalX 1.83 software and analyzed by GeneDoc software (multiple sequence alignment editor, version 2.5.000). The sequence submitted to GenBank (accession number: *AY821852*) was the consensus sequence from the three clones. Human, *Saimiri sciureus,* and *Aotus nancymaae* (accession numbers: *NP_005347*, *CAC38871*, and *AAV70114*, resp.) protein sequences were compared by using the same software. Sequences used were found in the GenBank protein databases.

2.4. Peptide FITC-Labeling and Fluorescence Microscopy. hTip-CSKH and scrambled CSKH peptides were labeled with fluorescein isothiocyanate (FITC). Shortly, 4.75 mL of

a 0.0125 mM solution of peptide was incubated 24 h in 0.1 M carbonate-bicarbonate buffer with 250 μL of a 2.5 mM FITC solution in DMSO. Dialysis was performed during 48 h against 0.1 M ammonium chloride in 1% DMSO (membrane of exclusion limit of 3.5 kDa; Spectrum Laboratories Inc., Rancho Dominguez, CA, USA). 10^5 human PBMC resuspended in RPMI 1640 supplemented with 10% FCS, 10 mM HEPES, and 1 mM sodium pyruvate (complete medium) for 1 h at 37°C were incubated with 40 μM of FITC-labeled hTip-CSKH or CSKH(Scr). Cells were washed in PBS and resuspended in 20 μL of media (150 mM NaCl, 50% glycerol) and mounted in a glass microscope slide with a coverslip and observed in a Nikon C-1plus fluorescence microscope. Digital photographs were taken with a Sony DSC-P73 digital camera.

2.5. Lymphocyte Proliferation Assays. A total of 5×10^4 PBMC/well were cultured for 1 h at 37°C and 5% CO_2 in complete medium in the absence or presence of different peptide concentrations (as indicated in each figure) in 96-well flat-bottomed microplates (Linbro, Aliso Viejo, CA, USA). In some experiments, PBMC were also stimulated with 2 μg/mL PHA-P or 25 ng/mL PMA for 48 h or 72 h with or without addition of peptides. Afterwards, 0.5 μCi/well [methyl-3H]-thymidine (ICN Biomedicals, Inc., Irvine, CA, USA) was added to cultures for the last 18 h. Cells were then harvested (PHD Harvester, Cambridge Tech) in glass fiber strips (Cambridge Technology, Watertown, MA, USA) and assayed for [methyl-3H]-thymidine incorporation by liquid scintillation counting β-scintillation system Beckman LS 6500 (Beckman Instruments, Fullertown, CA, USA).

Peptides-treated or peptides-untreated Jurkat cells (5×10^4) were stimulated with 2 μg/mL ionomycin or 2 μg/mL PHA-P and processed as described above for primary cells. The stimulation index percentage (SIP) was defined as being the ratio of mean [methyl-3H]-thymidine (counts per minute) incorporated in the presence of a peptide to that incorporated in the absence of peptide (×100).

2.6. Protein Tyrosine Kinase Immunostaining. PBMC from humans were preincubated (or not) for 1 h with 60 μM hTip-CSKH and further stimulated with PHA-P (5 μg/mL) for 15, 30 or 60 min. Stimulation was stopped by ice-cooling the cultures; these cells were then washed twice in ice-cold PBS and cell extracts were prepared by a 20-minute incubation in lysis buffer (20 mM Tris-Cl pH 8.0, 276 mM NaCl, 10% glycerol, 1% NP40, 1 mM PMSF, 10 μg/mL aprotinin, 10 μg/mL leupeptin, 1 mM Na3VO4, 10 mM NaF, and 2 mM EDTA). Extracts were centrifuged for 15 min at 10,000 g and 4°C; supernatants were recovered and subjected to 10% SDS-PAGE as described elsewhere. Proteins were then transferred to PVDF membranes (Immobilon-P, Millipore Corp., Bedford, MA, USA). Immunodetection was performed with anti-Lck (clone MOL171) antiphosphotyrosine (Clone PY20) (Pharmingen, San Diego, CA, USA). In other sets of experiments, human PBMC were stimulated with PHA-P or hTip-CSKH and cell extracts prepared as described above. Proteins were then transferred to PVDF membranes and immunodetection was performed with anti-Fyn (AHO0482, Invitrogen) and anti-β-Actin (sc-47778, Santa Cruz Biotechnology). For data analysis, p56Fyn and p59Fyn bands were normalized to β-actin.

2.7. Downstream Signaling after hTip-CSKH Stimulation. For ERK 1/2 phosphorylation, human PBMC were stimulated for 2 h with the different peptides or with PHA-PMA as described above. Cells extracts were prepared as above and assayed by WB with anti-p-ERK1/2 (sc-7383, Santa Cruz Biotechnology) and anti-ERK1/2 (sc-7383, Santa Cruz Biotechnology). Erk phosphorylation was normalized to total ERK1/2.

2.8. Biochemical Isolation of Detergent Resistant Membranes (DRMs). 6.5×10^7 human PBMC were treated with 40 μM of hTip-CSKH in serum-free RMPI-1640 during 1 hour at 37°C. The cells were washed in medium and the membranes were extracted during 20 min in 200 μL of ice-cold lysis buffer containing Tris 25 mM pH 7.4, 150 mM NaCl, 2 mM EDTA, 0.5% Triton-X100, 1 ug/mL leupeptin, 1 ug/mL pepstatin, 4 ug/mL aprotinin, 1 mM PMSF, 1 mM Na3VO4, and 50 mM NaF. For sucrose density gradients, cell extracts were mixed with 250 μL of 80% sucrose in TNE buffer (Tris 25 mM pH 7.4, 150 mM NaCl, and 2 mM EDTA) and overlayed with 730 μL of 35% sucrose and 320 μL 5% sucrose and centrifuged at 200,000 g during 5 h, 4°C (Beckman Optima, rotor TLS-55). Eight fractions of equal volume were recovered from the top of the gradient, diluted with 1 mL of TNE, and detergent resistant membranes in each fraction were precipitated by ultracentrifugation at 100,000 g during 45 min, 4°C. The pellets were extracted in 20 μL of Laemmli buffer: half used for WB and Flotillin-2 detection and the other half for SDS-PAGE in Tris-Tricine buffer for peptide identification as described [42]. To facilitate the identification of the peptides in this system, erythrocyte membranes were prepared in parallel and incubated with the different peptides used. Peptides were identified by sample separation in Tris-Tricine SDS-PAGE.

2.9. PBMC Surface Marker Characterization after hTip-CSKH Treatment. PBMC were incubated for 24 h in the absence or presence of 60 μM hTip-CSKH peptide, PBS washed, suspended in 0.5% BSA-PBS solution, and further incubated for 20 min at RT with the respective monoclonal antibody. Anti-CD3 PE-conjugated antibody (clone UCTH1) was purchased from Sigma (Sigma-Aldrich Co., St. Louis, MO, USA); and anti-TCR α/β FITC-conjugated antibodies were purchased from Pharmingen (San Diego, CA, USA). All incubations with fluorochrome-tagged antibodies were done in the dark. Then, cells were washed with 2 mL of PBS and centrifuged. After a final wash, cells were suspended in 0.5 mL PBS and immediately read in a FACScan flow cytometer (Beckton Dickinson, BD Biosciences, San Jose, CA, USA).

2.10. Statistical Analysis. Paired statistical analyses were performed using Student two-tailed t-test. Paired two-tailed t-test analyses were performed for the data comparing values obtained from nontreated and hTip-CSKH or hTip-treated cells at the same time points.

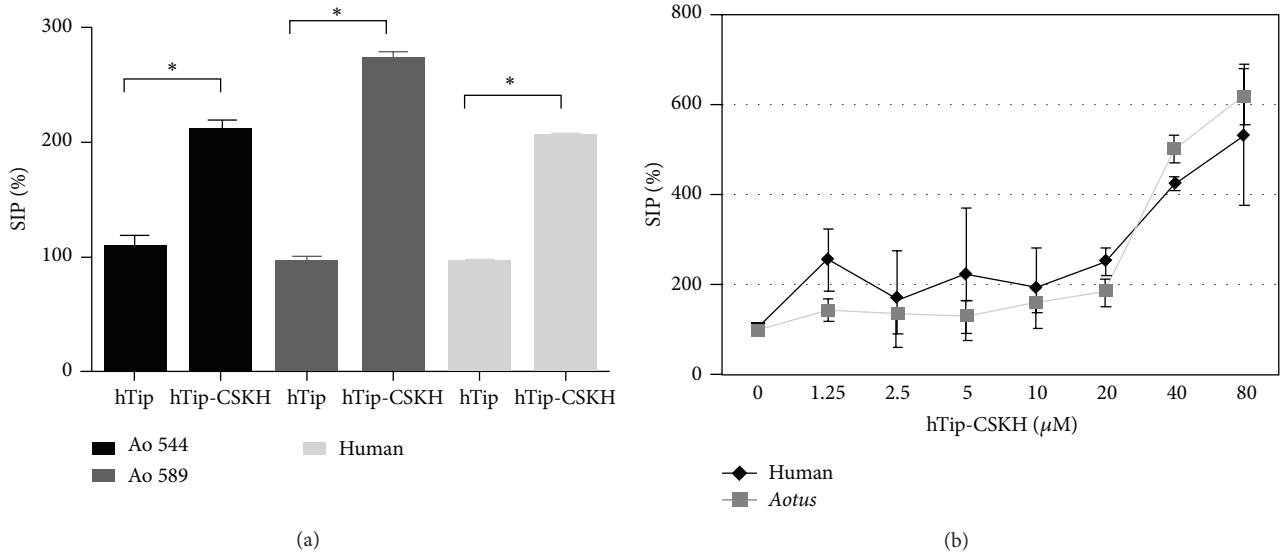

Figure 1: hTip-CSKH induced cell proliferation in human and *Aotus* cells. (a) PBMC from two *Aotus nancymaae* and one human donor were treated with 40 μM hTip or hTip-CSKH peptides and assayed for [3H]-thymidine incorporation after 48-hour treatment. (b) Human and *Aotus* PBMC exposed to several hTip-CSKH concentrations were assessed for [3H]-thymidine incorporation after 72-hour treatment. Stimulation index percentage (SIP) is shown (see Section 2). Student's t-test statistically significant values ($p < 0.05$) are marked with asterisk (*).

3. Results

3.1. High Identity in Lck and Similarity in T-Cell Proliferation in Response to hTip-CSKH between Aotus and Humans. The *Aotus* primate experimental model has proved to be useful for basic immunology and vaccination studies. The establishment of similarities is essential for physiological studies involving immune modulation, although some differences in T-cell response have been found [43]. Previously, we found that *Aotus* Lck was more related to *Saimiri sciureus* than to human Lck. Nevertheless, high identity (>98%) was also observed between human and *Aotus* Lck protein sequences (Supplementary Figure 1, see Supplementary Material available online at http://dx.doi.org/10.1155/2015/395371). Functionally important sequences for molecular docking (i.e., CENCH motif for CD4/CD8 coreceptors binding and SH2 phosphotyrosine binding domain) or catalysis (ATP binding region, 364D and 273K residues) were highly conserved. Differences between human and *Aotus* Lck sequences rely only on 12 residues.

Cell proliferation in *Aotus* and humans has different requirements: while *Aotus* PBMC respond poorly to PHA-P, they readily respond to favin stimulation [43]. On the other hand, it is well known that human lymphocytes require at least two different signals (signals 1 and 2) for proliferation [44]. These signals can be simulated *in vitro* by the combination of calcium influx (signal 1) and PKC activation (signal 2) or PHA-P stimulation (both signals). Interestingly, incubation of *Aotus* or human PBMC with hTip-CSKH (40 μM) for 48 h induced increased proliferation (2-3 times) (Figure 1(a)). The increased proliferation was dependent on the cargo sequence since proliferation of PBMC treated with hTip alone or the chimeric CSKH scrambled peptide (hTip-CSKHsc) was as low as that of control cells without peptide (not shown). Some variability in *Aotus* response to hTip-CSKH compared to humans was observed, but this is probably due to what we have previously described for this experimental model [43]. The hTip-CSKH effect is then similar to PHA-P, that is, inducing proliferation by its own, although to a lesser extent. The result observed with hTip-CSKH was stronger and dose-dependent in both human and *Aotus* PBMC when proliferation was assayed after 72-hour incubation and with different peptides concentrations (Figure 1(b)). Increased proliferation was initially observed between 20 and 40 μM but, remarkably, a sixfold proliferation induction was observed at 80 μM hTip-CSKH and 72-hour incubation in both human and *Aotus* T-cells without losing cell viability.

3.2. hTip-CSKH Induces Proliferation in Human T-Cells Independently of Signal 2. As indicated, proliferation induced by the polyclonal T-cell activator PHA-P in *Aotus* PBMC is lower compared to humans. Also human PBMC proliferation induced by hTip-CSKH was lower (40% or more dependent on the conditions) than that usually induced by PHA-P, suggesting different mechanisms of induction and/or different strength of activation. To address this issue initially, we examined hTip-CSKH proliferative effect on previously PHA-P-stimulated *Aotus* T-cells. In spite of the variability reported previously and observed above, there was a statistically significant increase in proliferation induced by hTip-CSKH (Figure 2) in 5 *Aotus* PBMC samples that have been previously activated by PHA-P. As expected, this increase was low (11–22%) but statistically significant. Control hTip peptide treatment did not increase proliferation, confirming

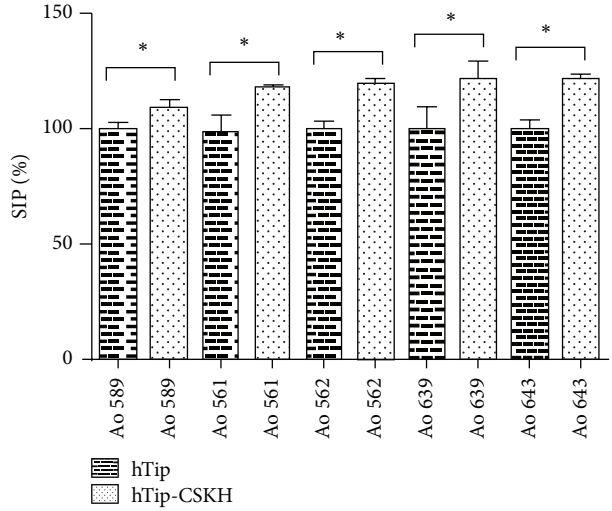

Figure 2: hTip-CSKH even induced a slight increase in proliferation in PHA-P-stimulated *Aotus nancymaae* PBMC. Five *Aotus nancymaae* PBMC samples were treated with hTip and hTip-CSKH peptides (40 μM); after 1-hour incubation, 2 μg/mL PHA-P was added to the culture. [3H]-thymidine incorporation was assessed after 72 h of culture. Student's t-test statistically significant values ($p < 0.05$) are marked with asterisk ($*$).

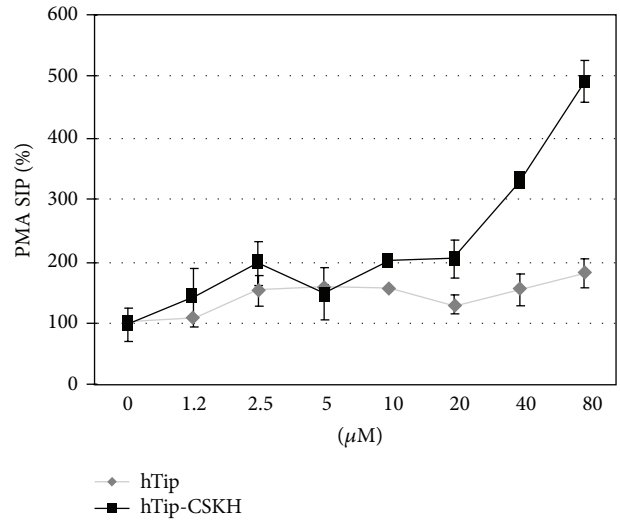

Figure 3: hTip-CSKH induced similar 5-fold increased proliferation in PMA-stimulated PBMC. Human PBMC exposed to different hTip-CSKH or hTip concentrations for 1 h were stimulated with 25 ng/mL PMA. Cells were assessed for [3H]-thymidine incorporation after 72 h. Stimulation index percentage (SIP) is shown.

that the proliferative effect is therefore cargo specific. Our results show that T-cells that have been previously stimulated by the strong activator PHA-P can still be further activated by the chimeric peptide hTip-CSKH, suggesting either that stimulation with PHA-P is not maximal in this condition and hTip-CSKH delivers a synergic proliferation signal or that hTip-CSKH signals through other pathway(s).

To further explore this topic, we used the classical protein kinase C (PKC) activator phorbol-12-myristate-13-acetate (PMA) which induces signal 2 [44], bypassing cell surface receptors stimulation. We hypothesized that PKC activation will act as a complementary signal to hTip-CSKH. As expected, a relatively low cell proliferation was obtained when human PBMC were treated only with PMA. Addition of hTip-CSKH induced a dose-dependent increase in proliferation (starting at 20–40 μM) with a maximum fivefold increase at 80 μM when compared to PMA-treated cells; the control peptide hTip did not produce the same effect (Figure 3). The onset of cell proliferation and maximal response to hTip-CSKH was very similar to that obtained without PMA (compare Figures 1(b) and 3). Therefore, hTip-CSKH seems to be able to efficiently replace signal 2 on its own. *Aotus* PBMC were not used in these PMA experiments, since we have previously shown that under certain circumstances (and for unknown reasons) these cells can respond to either signal 1 or signal 2 [43].

3.3. hTip-CSKH Effect on the T-Cell Line Jurkat. Jurkat T-cells were very interesting to further test hTip-CSKH effect, since TCR activation in this cell line causes growth inhibition, suggesting that these cells have different activation requirements [45]. Jurkat cells do not respond to PHA-P stimulation but respond adequately to calcium influx. Figure 4(a) shows that Jurkat cells had a proliferation rate about two- to threefold higher in the presence of ionomycin than unstimulated cells. As it has been previously reported, PHA-P-stimulated cells showed a slight reduction in the proliferation rate (Figure 4(a)). Interestingly, hTip-CSKH treatment of Jurkat cells also showed a slight diminution in proliferation, similar to what we have seen before with PHA-P (compare Figures 4(a) and 4(b), 3rd column with NS controls). Control hTip peptide had no effect (Figure 4(b), 2nd column). Ionomycin-stimulated Jurkat cell treated with hTip-CSKH showed a strong reduction in proliferation rate while control hTip-treated cells showed no effect (Figure 4(b)). Together, these results have shown that if T-cells are able to proliferate in response to PHA-P (signals 1 and 2 induction), as in normal human and *Aotus* T-cells, then h-Tip-CSKH will also induce proliferation. In contrast, if stimulation through signal 1 inhibits proliferation (as in Jurkat cells), then hTip-CSKH will also be inhibitory. This would give support to our previous suggestion that signaling by hTip-CSKH peptide is strongly enough (and probably includes both signals) to induce proliferation on its own.

3.4. hTip-CSKH Can Be Identified in Detergent Resistant Membranes (DRMs). It has been previously reported that the transmembrane domain (amino acid residues 229–250) of Tip is required for its association with lipid rafts [35]. We then explored biochemically hTip-CSKH localization at the plasma membrane, specifically its association with DRM. Since DRMs localize into the low-density fractions in sucrose gradients, they have usually been associated with lipid rafts [37]. First, we tested an electrophoresis system (SDS-PAGE in Tris-Tricine buffer) having high-resolution

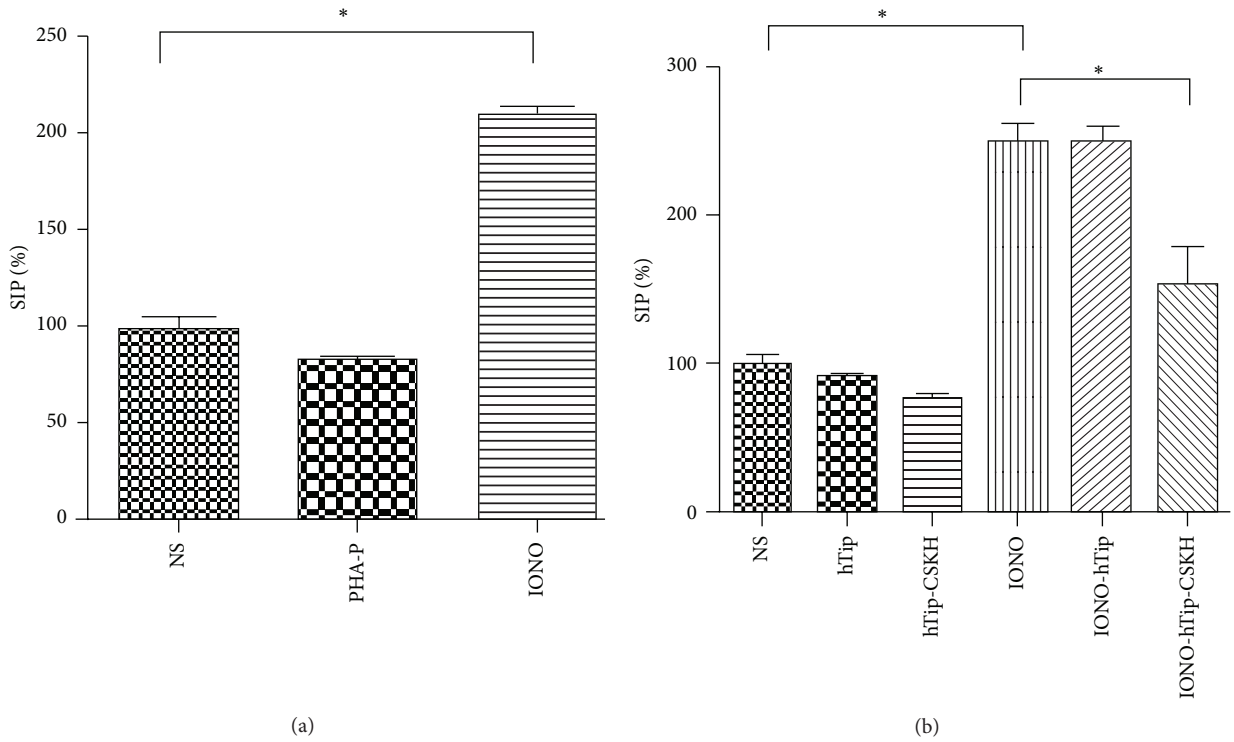

Figure 4: hTip-CSKH induced a decreased cell proliferation in Jurkat cells. (a) Jurkat cells were treated with PHA-P or ionomycin and assayed for [3H]-thymidine incorporation after 48-hour treatment. (b) Jurkat cells were treated with hTip, hTip-CSKH for 1 h, and then ionomycin-stimulated and assayed for [3H]-thymidine incorporation. Jurkat cells treated with each peptide alone or nontreated peptides were added as controls. Stimulation index percentage (SIP) is shown (see Section 2). NS: nonstimulated; Iono: ionomycin. Student's t-test statistically significant values ($p < 0.05$) are marked with asterisk (∗).

power for peptides identification compared to classical SDS-PAGE. 10 μg of each of hTip-CSKH, hTip, hTip-CSKHsc, or CSKH peptides was mixed with 10 μL of an erythrocyte cell membranes extract. As it can be seen in Figure 5(a), hTip-CSKH, hTip-CSKHsc, and CSKH could be identified as diffuse and fast migrating bands below the 6,9 kDa MW standard (arrow). hTip could not be resolved probably because of its high hydrophobicity. We next prepare a Triton X-100 extract of hTip-CSKH-treated PBMC and fractionated it by sucrose density gradient centrifugation. Eight fractions were collected and assayed for hTip-CSKH (by Tris-Tricine SDS-PAGE) and Flotillin-2 (by SDS-PAGE and WB) presence. Flotillin-2, a marker of lipid rafts, was distributed mainly in fractions 1–3 and 6–8 (Figure 5(b), lower panel). A band corresponding to the hTip-CSKH MW was detected in fractions 6 and 7 (Figure 5(b), upper panel, arrow), showing hTip-CSKH localization in membrane rafts. The existence of a novel type of membrane raft-like microdomains (heavy DRM), containing a number of membrane signaling molecules, including LAT and Lck, was recently demonstrated [46]. The above evidence suggests that almost all of the chimeric hTip-CSKH is present in these novel heavy rafts, where it could interact with the Lck protein. Additionally, incubation of human PBMC with the FITC-labeled hTip-CSKH during 1 h and analysis by fluorescence microscopy showed a homogeneous surface peripheral localization and no intracytoplasmatic accumulation (Supplementary Figure 2). This shows that hTip-CSKH interacts with the cytoplasmic membrane and is localized in lipid rafts.

3.5. hTip-CSKH Targets Lck and Induces Its Early Activation. The heavy lipid rafts are part of a TCR signaling platform involved in the early coordination of T-cell signaling events, namely, the activation of nonreceptor protein tyrosine kinases [46]. We have analyzed the hTip-CSKH effect on the lymphocyte-specific protein tyrosine kinase Lck, key molecule during T-cell activation, and hypothetical target of the hTip-CSKH chimeric peptide used here. Antibodies directed against human Lck and phosphotyrosine residues were used for assessing human Lck phosphorylation during time-course experiments, following T-cell short stimulation with PHA-P in the presence or absence of hTip-CSKH. Cell extracts were prepared after 0, 15, 30, and 60 min of stimulation; WB detection was simultaneously performed for Lck and phosphotyrosine residues. Defined bands of about 56 kDa and 59 kDa were evident in both blots (Figure 6(a)). When analyzing Lck staining at time point 0 (Figure 6(a), top panel), the p56Lck band appeared more intense than the p59Lck band in cells with PHA-P without hTip-CSKH. After 15 min of T-cell stimulation, a progressive increase in p59Lck band staining and tyrosine phosphorylation was noted and this lasted for the rest of the period tested (Figure 6, top left

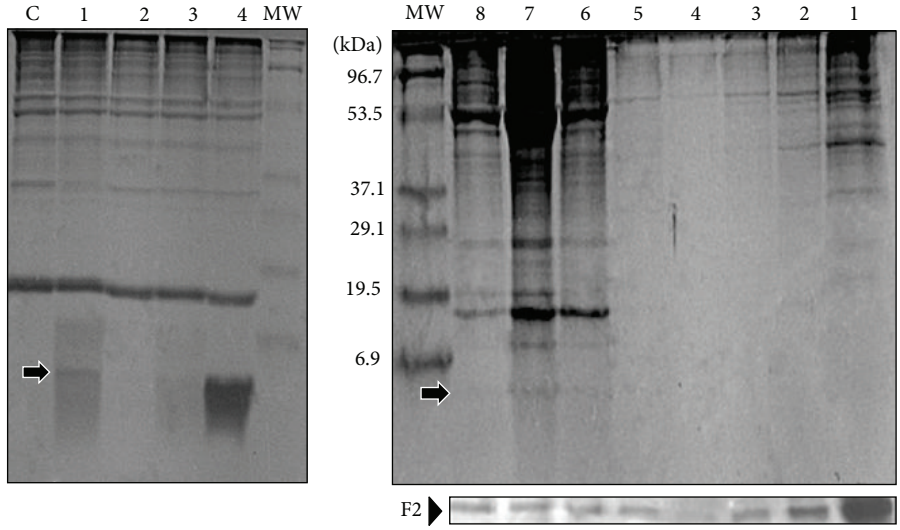

Figure 5: Tris-Tricine electrophoretic identification of hTip-CSKH or control peptides. (a) 10 μg of the indicated peptides (1 = hTip-CSKH; 2 = hTip; 3 = hTip-CSKH-Scr; 4 = CSKH) was mixed with 10 μL of a protein extract of red blood cells membranes. The gel was stained with Coomassie Brilliant Blue. The size of each molecular weight marker (MWM) is indicated in the right and the control (c) membranes without peptides in the left. The arrow indicates the band corresponding to hTip-CSKH molecular weight. (b) The membrane extract from hTip-CSKH-treated human PBMC was resolved by ultracentrifugation in a sucrose density gradient. Eight fractions were recovered as indicated in each line. Half of each fraction was used for Tris-Tricine electrophoresis for hTip-CSKH identification (the arrow marks the band corresponding to hTip-CSKH molecular weight). The remaining amount of the fraction was used for WB blot in order to know its Flotillin 2 content (bottom) and to differentiate between light (lanes 1–3) and heavy (lanes 5–8) fractions. The size of each molecular weight marker (MWM) is indicated in the left.

panel). This occurred simultaneously with reduced p56Lck band intensity, suggesting that a more intense p59Lck band depended on the contribution of p56Lck band during PHA-P stimulation. On the contrary, in hTip-CSKH-treated cells, the ratio between p59Lck and p56Lck bands became inverted immediately after stimulation and lasted for the period tested (Figure 6). This rapid increase in Lck phosphorylation after hTip-CSKH and PHA-P stimulation is consistent with the observed increase in proliferation induced by hTip-CSKH in T-cells that have previously been activated with PHA-P (Figure 2). As it would be expected, hTip-CSKH induced on its own Lck phosphorylation and increased tyrosine phosphorylation (Figure 6(c)) in full agreement with the proliferation experiments in Figure 1.

As it has been reported that Fyn is structurally related to Lck and has at least in part a redundant role during T-cell activation [47], we tested hTip-CSKH effect on this protein tyrosine kinase. Since Fyn activation depends on Lck activation [48] and the latter seems to be still maximal after 1 h of PHA-P or hTip-CSKH stimulation (Figure 6), we tested hTip-CSKH effect on Fyn after 2 h of peptide treatment. As it can be seen in Figure 7(a), PHA-P stimulation induces both the reduction in the intensity of the 59 kDa Fyn protein (by about 22%) and the appearance of a low MW band (56 kDa). hTip-CSKH had a similar effect (20% reduction) on the 59 kDa Fyn protein while the second band appeared diffused and poorly resolved. Thus, hTip-CSKH induces a different effect on Fyn when compared to PHA-P stimulation, suggesting a specificity towards Lck. Additionally, it can be concluded that the increase seen in the Lck band of 59 kDa (Figure 6) is not due to an increase in the Fyn band since, on the contrary, hTip-CSKH induces a reduction in the Fyn 59 kDa band. It might also be considered that although hTip-CSKH induced early activation signals and later proliferation, the signal induced must, of course, be different from the PHA-P signal and far from being complete.

3.6. Downstream Signaling Events Induced by hTip-CSKH. To further evaluate hTip-CSKH induced signal strength, we studied Erk phosphorylation, an important step in TCR-induced proliferation [49]. The ERK phosphorylation level achieved during human PBMC stimulation with both PHA-P and PMA was 5.5-fold when compared to control unstimulated cells (Supplementary Figure 3). hTip-CSKH produced 2.5-fold induction in ERK2 phosphorylation; the other peptides tested had minimal or no effect, as evaluated by densitometry. We observed that hTip peptide treatment induced a 1.5-fold increase in ERK1/2 phosphorylation but we considered this effect to be not relevant as it was not enough to induce T-cell proliferation as it was shown above. We conclude then that hTip-CSKH was able to activate signals that are known to occur downstream of Lck.

3.7. hTip-CSKH Does Not Downregulate Cell Surface Markers. HVS infection induced a reduction in TCR, CD4, CD3, and CD2 expression. It was shown that this downregulation was

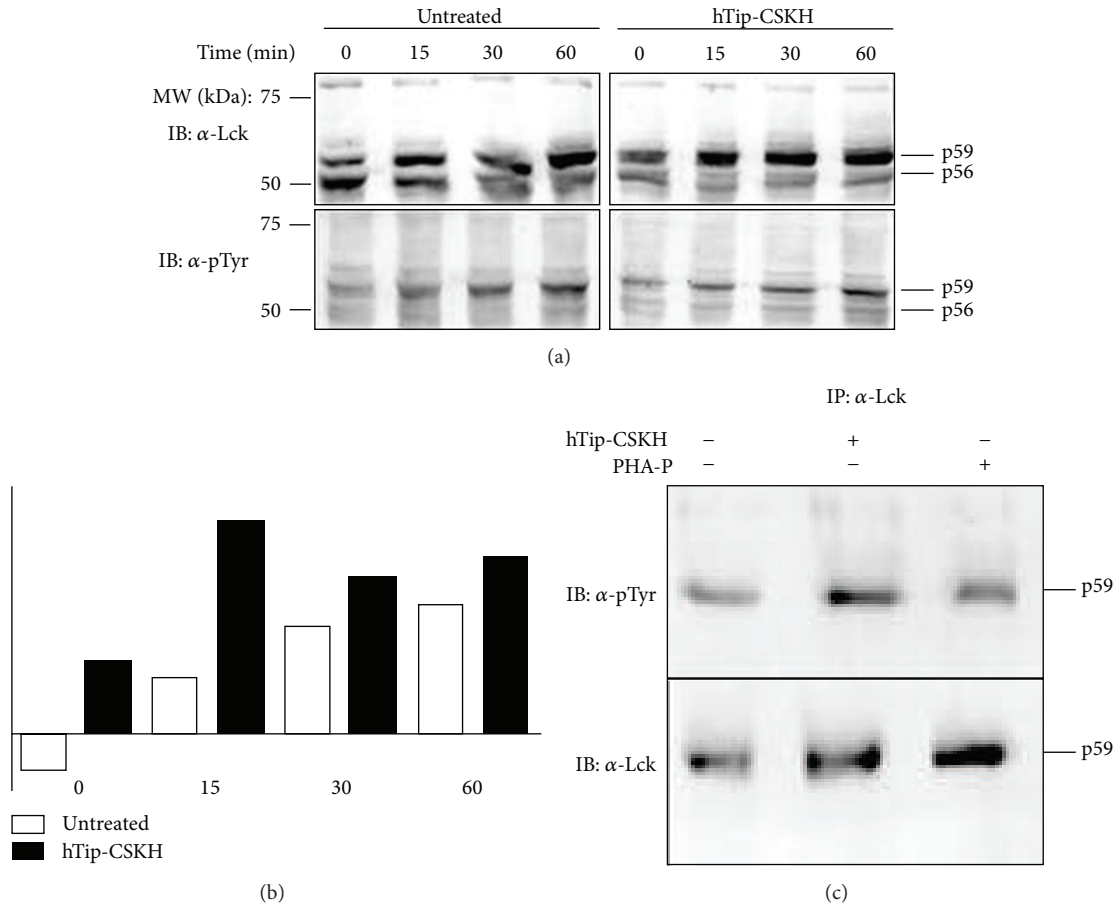

Figure 6: Time-course assay for Lck in human PBMC after cell stimulation. (a) PBMC either untreated (lanes 1–4) or treated (lanes 5–8) for 1 h with hTip-CSKH were stimulated with PHA-P for 0, 15, 30, and 60 min and then were lysed. Extracts were subjected to SDS-PAGE and proteins transferred to PVDF membranes. WB was performed with Lck (upper panels) and P-Y (lower panels) monoclonal antibodies. Two bands were clearly defined which correspond to the low molecular weight (p56) and the high molecular weight band (p59), respectively. (b) Quantification of p56 and p59 bands showed an increase of the p59/p56 ratio. White bars represent nontreated cells and black bars hTip-CSKH-treated cells p59/p56 ratio at different time points. (c) Lck immunoprecipitation of PBMC extracts after stimulation with PHA-P or hTip-CSKH for 30 min. WB was performed with monoclonal antibodies against pTyr and Lck as indicated.

partially dependent on Tip interactions with the cellular protein Tap (Tip-associated protein) and mapped to an amino-terminal portion of Tip, different from the Lck binding domain [50]. Therefore, 24-hour hTip-CSKH-treated human PBMC were evaluated for surface marker expression. We observed that CD3 and TCR expression was identical in hTip-CSKH-treated and untreated cells (Supplementary Figure 4), suggesting that the effect of Tip on cell surface receptor downregulation and proliferation could be dissociated by using hTip-CSKH.

4. Discussion

HVS infection transforms both non-human primates and human T-cells to TCR-independent proliferation [18–20]. Tip binding to Lck and subsequent Lck activation are partially responsible for this effect [24, 32]. We have previously performed the characterization of Lck in *Aotus nancymaae* and compared them to human Lck. The high identity (98%) found when comparing both species suggests that Lck functionality in *Aotus* T-cells is very similar to humans and that synthetic peptides designed for human Lck binding and modulation could also do so in *Aotus* Lck.

The HVS Tip carboxyl-terminal hydrophobic (hTip) sequence was selected in this study as a cargo vehicle since it has been demonstrated that Tip is constitutively present in lipid rafts [23, 35] and there is experimental evidence connecting hTip with Tip localization in lipid rafts [40]. Additionally, Tip binds specifically to Lck through SH3B and CSKH motifs. Given that a Tip mutant without the SH3B domain was able to transform T-cells [21], we focused on the other Tip motif (CSKH) responsible for Lck binding and activity. It has previously been shown that both motifs can bind Lck independently [32]. Thus, a chimeric peptide formed by hTip and Tip's CSKH motif was synthesized to study its ability to modify T-cell physiology by targeting Lck.

Our results showed a clear increase (2-3 times) in thymidine incorporation in human and *Aotus* PBMC treated with the chimeric hTip-CSKH peptide for 48 h. When longer stimulation periods were used (e.g., 72 h), a 5- to 6-fold increase

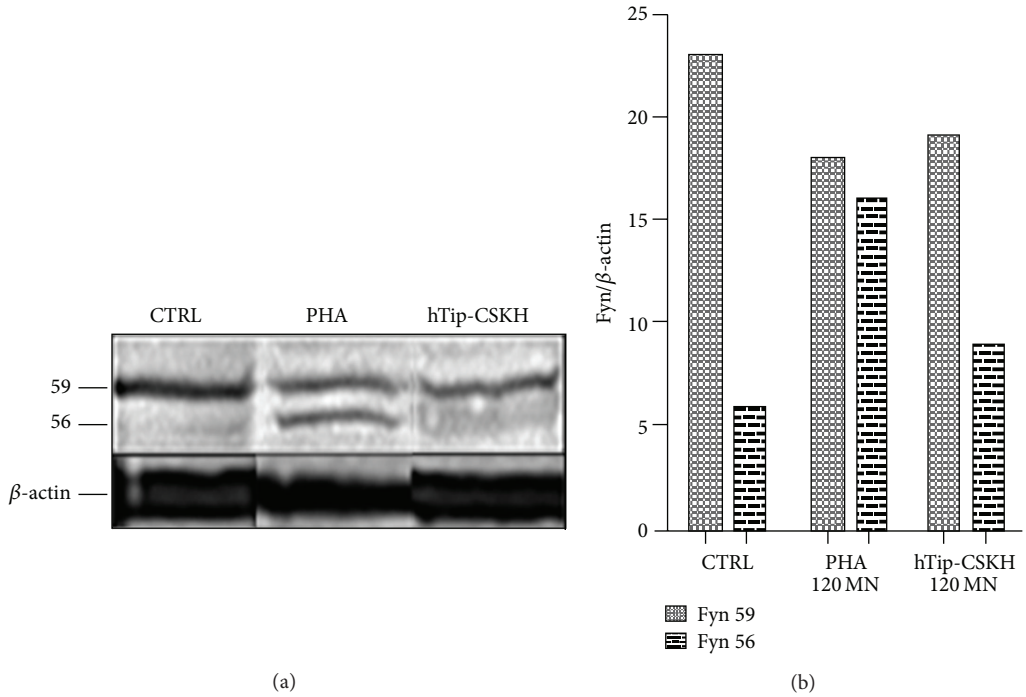

Figure 7: Fyn detection in stimulated human PBMC. (a) PBMC were treated with PHA-P and hTip-CSKH during 2 h, lysed, and the protein extract resolved by SDS-PAGE. Western blot was performed with an anti-Fyn specific antibody. PHA-P was used as positive control, which induces the appearance of a second band of 56 kDa. (b) Quantification of the Fyn p59 and p56 bands. The intensity of each Fyn band was normalized to the loading control β-actin.

in proliferation was observed. Taking into consideration that PHA-P induces multiple receptors engagement (with a strong intracellular signaling input), the fact that hTip-CSKH by its own can increase proliferation is remarkable since hypothetically only one specific pathway is being targeted by the use of a unique Lck binding motif (CSKH). Interestingly, after T-cell PHA-P stimulation, hTip-CSKH could further increase proliferation (11–22%), suggesting either a strong hTip-CSKH effect or additional hTip-CSKH stimulation through other mechanisms. This effect was cargo and sequence specific, since control peptides (hTip, hTip-CSKHsc, or CSKH) did not have any effect on proliferation.

Human T-cells require the simultaneous induction of at least two different signaling pathways for full activation, one through the TCR (signal 1) and the second through costimulatory molecules (signal 2). These signals can be mimicked by mitogenic stimulation (PHA-P) or the use of calcium ionophores (signal 1) plus PK-C activation (signal 2) [51]. hTip-CSKH-treated or hTip-treated cells were stimulated with the PK-C activator PMA to test whether signal 2 could further improve hTip-CSKH effect. A 5-fold increase in proliferation was observed with hTip-CSKH, suggesting either that the chimeric peptide is strong enough to induce both signals, as with PHA-P stimulation, or that, under very strong and atypical signal 1 stimulation, signal 2 is not anymore required.

Further evidence of this assumption was obtained by studying hTip-CSKH effect on the T-cell leukemia cell line Jurkat. These cells do not proliferate in response to TCR activation by mitogens (PHA-P) or to anti-CD3 antibodies; even an opposite effect, driving cells to an apoptotic state, has been shown [45]. Tip expression in these cells has also been used as a model for Lck modulation [52]. We have also shown here that hTip-CSKH induces a slight decrease in proliferation, equivalent to PHA-P treatment. This inhibition was more evident and statistically significant when ionomycin-stimulated (signal 1) Jurkat cells were used. It is possible that an apoptosis process is taking place, as in the case of PHA-stimulated Jurkat cells [45]. Thus, if stimulation via the TCR signaling pathway causes cells to proliferate, then hTip-CSKH treatment has a proliferation inducing effect too. On the contrary, if the TCR signaling pathway induces an inhibitory proliferative effect, as what happens in Jurkat cells, hTip-CSKH will also cause this outcome. Although very similar responses to PHA-P stimulation were observed in primary (stimulation) or transformed T-cells (inhibitory) with hTip-CSKH, clearly, an atypical T-cell stimulation by hTip-CSKH will hardly match completely with a classical activation model.

After PBMC hTip-CSKH stimulation and DRM extraction, we could identify the chimeric peptide in fractions containing "heavy" lipid rafts having high content of LAT, Lck, and Ras signaling molecules [46]. Recently, it was shown that an amphipathic helical sequence of 14 amino acids, enriched in charged and hydrophobic amino acids and contiguous to the Tip TM sequence, could increase Tip localization to

lipid rafts [40]. Our cargo CSKH sequence has about the same length of this sequence (16 aa) and is also enriched in charged and hydrophobic amino acids, suggesting a similar effect in lipid rafts localization. This membrane microdomain localization was essential to support our initial considerations regarding the use of this hTip sequence and its capacity to deliver a cargo sequence with the capacity to modulate Lck. In fact, we have shown here that hTip-CSKH induces a rapid increase in the appearance of the p59Lck band with a concomitant reduction in p56Lck. These changes are due to Lck phosphorylation and have been previously observed after TCR stimulation [53–55]. This effect was similar in PBMC stimulated only with PHA-P, although the activation kinetics in the presence of the chimeric peptide was extremely rapid. This suggests that hTip-CSKH induces a strong and rapid Lck activation and is responsible on its own for the induced proliferation observed. This is in agreement with the strong proliferation effect of hTip-CSKH shown above.

As Fyn can replace Lck, under certain circumstances, and there is a close sequence and structural identity between both tyrosine kinases, it was interesting to study hTip-CSKH effect on Fyn. Here, a reduction in the p59Fyn band was determined excluding its participation in the observed effect on Lck phosphorylation. The other changes observed in Fyn, especially the appearance of a diffuse p56Fyn band, deserve further experimentation. Nevertheless, these results are in agreement with those that have shown that Tip effect is specific for Lck, not for Fyn or Lyn [25], and consistent with their described differences in protein association and subcompartmental localization [48]. Interestingly, in the TCR signaling models, Fyn activation is dependent on Lck and this process is coordinated spatially in lipid rafts. How this could affect Fyn activation is not known. Since both kinases, Lck and Fyn, have been shown to play a role in the different models of T-cell anergy [56], it would be interesting to explore the hTip-CSKH capacity to revert this process in T-cell.

One of the protein kinases responsible for Lck phosphorylation in Ser residues is ERK, which was activated here too after hTip-CSKH stimulation. As shown before, Lck phosphorylation on Y394 and Y505 is crucial for modulating its activity [57]. Some authors have shown that, after activation, Lck autophosphorylates its Y394 residue further increasing its catalytic activity [58]. We therefore assessed Lck tyrosine phosphorylation and found that p59Lck was more phosphorylated than p56Lck. Taken together, our results have shown that hTip-CSKH induces enhanced T-cell proliferation by targeting and activating Lck. More biochemical and structural work in this field is needed to completely elucidate the mechanism of Lck activation by hTip-CSKH.

By using the hTip-CSKH peptide, the above-described effects on Lck and lymphocyte proliferation could be molecularly separated from the effects caused by other Tip domains. It has been shown that Tip amino-terminal region is particularly involved in cell surface molecules downregulation through Tip binding to a cytosolic p80 protein [23]. We have shown here that surface expression of CD3 and TCR$\alpha\beta$ was not altered after hTip-CSKH treatment. It was therefore possible to separate the effects induced by Tip CSKH motif from those obtained when the whole Tip molecule was used.

Targeting proteins involved in signal transduction, like protein tyrosine kinases [11, 59] or protein tyrosine phosphatases [60, 61], is considered to be a viable strategy for therapeutic intervention. The use of defined motifs for blocking or inducing a particular function in these signaling molecules is a valuable approach for the fine modulation of cellular processes. We have shown here that the information contained in discrete protein sequences (i.e., CSKH) could be sufficient to modulate complex biological responses, provided that they are duly delivered to specific subcellular compartments. To our knowledge, this is the first report that uses a chimeric peptide to modulate T-cell signaling in lipid rafts. This would undoubtedly be a valuable tool for therapeutic intervention to target molecules whose dynamics depends on lipid rafts.

5. Conclusions

We have developed a novel chimeric peptide to modulate Lck signaling in cell membrane lipid rafts. In fact, hTip-CSKH induced on its own strong cell proliferation in normal lymphocytes as a consequence of the specific activation of the lipid rafts-anchored Lck. Interestingly, hTip-CSKH was inhibitory to Jurkat cells, in total agreement with the different signaling pathways and activation requirements of this leukemic cell line. We propose that hTip could be an effective vehicle for delivering a cargo sequence to lipid rafts, and its use could be extended for other molecules responsible for cancer cell growth.

Disclosure

The current address for Ana María Perdomo-Arciniegas is Colombian Cord Blood Bank, Hemocentro Distrital, District Secretary of Health, Bogotá, Colombia, and that for Luis Alberto Pérez-Quintero is Neuroimmunology Laboratory, Centre de Recherche du Centre Hospitalier de l'Universite de Montréal (CRCHUM), Montréal, QC, Canada.

Conflict of Interests

The authors declare that there is no conflict of interests regarding the publication of this paper.

Acknowledgments

The authors are especially grateful to Dr. Manuel E. Patarroyo for his support and to staff members of the FIDIC for *Aotus* blood samples; also to Mr. Jason Garry for grammatical correction of the paper and Jeremy Tabery in Nonlinear Dynamics Ltd. for the shareware version of TotalLab software. They also want to thank MACROGEN Inc. for DNA sequencing. This study was partially financed by the División de Investigación Bogotá (DIB) and the Faculty of Medicine to Jean-Paul Vernot, Universidad Nacional de Colombia.

References

[1] E. N. Kersh, A. S. Shaw, and P. M. Allen, "Fidelity of T cell activation through multistep T cell receptor ζ phosphorylation," *Science*, vol. 281, no. 5376, pp. 572–575, 1998.

[2] T. Mustelin and K. Taskén, "Positive and negative regulation of T-cell activation through kinases and phosphatases," *Biochemical Journal*, vol. 371, no. 1, pp. 15–27, 2003.

[3] S. J. Anderson, S. D. Levin, and R. M. Perlmutter, "Involvement of the protein tyrosine kinase p56lck in T cell signaling and thymocyte development," *Advances in Immunology*, vol. 56, pp. 151–178, 1994.

[4] R. Zamoyska, A. Basson, A. Filby, G. Legname, M. Lovatt, and B. Seddon, "The influence of the src-family kinases, Lck and Fyn, on T cell differentiation, survival and activation," *Immunological Reviews*, vol. 191, pp. 107–118, 2003.

[5] A. Veillette, I. D. Horak, E. M. Horak, M. A. Bookman, and J. B. Bolen, "Alterations of the lymphocyte-specific protein tyrosine kinase (p56(lck)) during T-cell activation," *Molecular and Cellular Biology*, vol. 8, no. 10, pp. 4353–4361, 1988.

[6] C. E. Rudd, J. M. Trevillyan, J. D. Dasgupta, L. L. Wong, and S. F. Schlossman, "The CD4 receptor is complexed in detergent lysates to a protein-tyrosine kinase (pp58) from human T lymphocytes," *Proceedings of the National Academy of Sciences of the United States of America*, vol. 85, no. 14, pp. 5190–5194, 1988.

[7] H. L. Ostergaard, D. A. Shackelford, T. R. Hurley et al., "Expression of CD45 alters phosphorylation of the lck-encoded tyrosine protein kinase in murine lymphoma T-cell lines," *Proceedings of the National Academy of Sciences of the United States of America*, vol. 86, no. 22, pp. 8959–8963, 1989.

[8] L. M. L. Chow, M. Fournel, D. Davidson, and A. Veillette, "Negative regulation of T-cell receptor signalling by tyrosine protein kinase p50csk," *Nature*, vol. 365, no. 6442, pp. 156–160, 1993.

[9] D. B. Straus and A. Weiss, "Genetic evidence for the involvement of the lck tyrosine kinase in signal transduction through the T cell antigen receptor," *Cell*, vol. 70, no. 4, pp. 585–593, 1992.

[10] W. S. F. Wong and K. P. Leong, "Tyrosine kinase inhibitors: a new approach for asthma," *Biochimica et Biophysica Acta—Proteins and Proteomics*, vol. 1697, no. 1-2, pp. 53–69, 2004.

[11] K. C. Lee, I. Ouwehand, A. L. Giannini, N. S. Thomas, N. J. Dibb, and M. J. Bijlmakers, "Lck is a key target of imatinib and dasatinib in T-cell activation," *Leukemia*, vol. 24, no. 4, pp. 896–900, 2010.

[12] K. De Keersmaecker, M. Porcu, L. Cox et al., "NUP214-ABL1-mediated cell proliferation in T-cell acute lymphoblastic leukemia is dependent on the LCK kinase and various interacting proteins," *Haematologica*, vol. 99, no. 1, pp. 85–93, 2014.

[13] N. Isakov and B. Biesinger, "Lck protein tyrosine kinase is a key regulator of T-cell activation and a target for signal intervention by *Herpesvirus saimiri* and other viral gene products," *European Journal of Biochemistry*, vol. 267, no. 12, pp. 3413–3421, 2000.

[14] T. Morio, T. Chatila, and R. S. Geha, "HIV glycoprotein gp120 inhibits TCR-CD3-mediated activation of fyn and lck," *International Immunology*, vol. 9, no. 1, pp. 53–64, 1997.

[15] R. Swart, I. K. Ruf, J. Sample, and R. Longnecker, "Latent membrane protein 2A-mediated effects on the phosphatidylinositol 3-kinase/Akt pathway," *Journal of Virology*, vol. 74, no. 22, pp. 10838–10845, 2000.

[16] N.-H. Cho, P. Feng, S.-H. Lee et al., "Inhibition of T cell receptor signal transduction by tyrosine kinase-interacting protein of *Herpesvirus saimiri*," *Journal of Experimental Medicine*, vol. 200, no. 5, pp. 681–687, 2004.

[17] L. V. Meléndez, R. D. Hunt, M. D. Daniel, B. J. Blake, and F. G. Garcia, "Acute lymphocytic leukemia in owl monkeys inoculated with *Herpesvirus saimiri*," *Science*, vol. 171, no. 3976, pp. 1161–1163, 1971.

[18] B. Biesinger, I. Muller-Fleckenstein, B. Simmer et al., "Stable growth transformation of human T lymphocytes by *Herpesvirus saimiri*," *Proceedings of the National Academy of Sciences of the United States of America*, vol. 89, no. 7, pp. 3116–3119, 1992.

[19] E. Meinl, B. A. 't Hart, R. E. Bontrop et al., "Activation of a myelin basic protein-specific human T cell clone by antigen-presenting cells from rhesus monkeys," *International Immunology*, vol. 7, no. 9, pp. 1489–1495, 1995.

[20] J.-P. Vernot, L. A. Pérez-Quintero, A. M. Perdomo-Arciniegas, S. Quijano, and M. E. Patarroyo, "*Herpesvirus saimiri* immortalization of *Aotus* T lymphocytes specific for an immunogenically modified peptide of *Plasmodium falciparum* merozoite surface antigen 2," *Immunology & Cell Biology*, vol. 83, no. 1, pp. 67–74, 2005.

[21] S. M. Duboise, J. Guo, S. Czajak, R. C. Desrosiers, and J. U. Jung, "STP and Tip are essential for *Herpesvirus saimiri* oncogenicity," *Journal of Virology*, vol. 72, no. 2, pp. 1308–1313, 1998.

[22] L.-E. Wehner, N. Schröder, K. Kamino, U. Friedrich, B. Biesinger, and U. Rüther, "*Herpesvirus saimiri* Tip gene causes T-cell lymphomas in transgenic mice," *DNA and Cell Biology*, vol. 20, no. 2, pp. 81–88, 2001.

[23] J. Park, N.-H. Cho, J.-K. Choi, P. Feng, J. Choe, and J. U. Jung, "Distinct roles of cellular Lck and p80 proteins in herpesvirus saimiri Tip function on lipid rafts," *Journal of Virology*, vol. 77, no. 16, pp. 9041–9051, 2003.

[24] B. Biesinger, A. Y. Tsygankov, H. Fickenscher et al., "The product of the *Herpesvirus saimiri* open reading frame 1 (Tip) interacts with T cell-specific kinase p56lck in transformed cells," *Journal of Biological Chemistry*, vol. 270, no. 9, pp. 4729–4734, 1995.

[25] N. Wiese, A. Y. Tsygankov, U. Klauenberg, J. B. Bolen, B. Fleischer, and B. M. Bröker, "Selective activation of T cell kinase p56lck by *Herpesvirus saimiri* protein tip," *Journal of Biological Chemistry*, vol. 271, no. 2, pp. 847–852, 1996.

[26] P. Kjellen, K. Amdjadi, T. C. Lund, P. G. Medveczky, and B. M. Sefton, "The *Herpesvirus saimiri* Tip484 and Tip488 proteins both stimulate Lck tyrosine protein kinase activity in vivo and in vitro," *Virology*, vol. 297, no. 2, pp. 281–288, 2002.

[27] T. Lund, M. M. Medveczky, and P. G. Medveczky, "*Herpesvirus saimiri* tip-484 membrane protein markedly increases p56lck activity in T cells," *Journal of Virology*, vol. 71, no. 1, pp. 378–382, 1997.

[28] J. U. Jung, S. M. Lang, T. Jun, T. M. Roberts, A. Veillette, and R. C. Desrosiers, "Downregulation of Lck-mediated signal transduction by Tip of *Herpesvirus saimiri*," *Journal of Virology*, vol. 69, no. 12, pp. 7814–7822, 1995.

[29] J. Favero and V. Lafont, "Effector pathways regulating T cell activation," *Biochemical Pharmacology*, vol. 56, no. 12, pp. 1539–1547, 1998.

[30] J. U. Jung, S. M. Lang, U. Friedrich et al., "Identification of Lck-binding elements in Tip of *Herpesvirus saimiri*," *Journal of Biological Chemistry*, vol. 270, no. 35, pp. 20660–20667, 1995.

[31] T. C. Lund, P. C. Prator, M. M. Medveczky, and P. G. Medveczky, "The Lck binding domain of *Herpesvirus saimiri* Tip-484 constitutively activates Lck and STAT3 in T cells," *Journal of Virology*, vol. 73, no. 2, pp. 1689–1694, 1999.

[32] D. A. Hartley, K. Amdjadi, T. R. Hurley, T. C. Lund, P. G. Medveczky, and B. M. Sefton, "Activation of the Lck tyrosine protein kinase by the *Herpesvirus saimiri* Tip protein involves two binding interactions," *Virology*, vol. 276, no. 2, pp. 339–348, 2000.

[33] E. Heck, U. Friedrich, M. U. Gack et al., "Growth transformation of human T cells by herpesvirus saimiri requires multiple Tip-Lck interaction motifs," *Journal of Virology*, vol. 80, no. 20, pp. 9934–9942, 2006.

[34] S. M. Duboise, H. Lee, J. Guo et al., "Mutation of the Lck-binding motif of tip enhances lymphoid cell activation by *Herpesvirus saimiri*," *Journal of Virology*, vol. 72, no. 4, pp. 2607–2614, 1998.

[35] N.-H. Cho, D. Kingston, H. Chang et al., "Association of *Herpesvirus saimiri* Tip with lipid raft is essential for down-regulation of T-cell receptor and CD4 coreceptor," *Journal of Virology*, vol. 80, no. 1, pp. 108–118, 2006.

[36] S. K. Bromley, W. R. Burack, K. G. Johnsonn et al., "The immunological synapse," *Annual Review of Immunology*, vol. 19, pp. 375–396, 2001.

[37] P. S. Kabouridis, "Lipid rafts in T cell receptor signalling (review)," *Molecular Membrane Biology*, vol. 23, no. 1, pp. 49–57, 2006.

[38] J. J. Merlo and A. Y. Tsygankov, "*Herpesvirus saimiri* oncoproteins Tip and StpC synergistically stimulate NF-κB activity and interleukin-2 gene expression," *Virology*, vol. 279, no. 1, pp. 325–338, 2001.

[39] D. Filipp, O. Ballek, and J. Manning, "Lck, membrane microdomains, and TCR triggering machinery: defining the new rules of engagement," *Frontiers in Immunology*, vol. 3, article 155, 2012.

[40] C.-K. Min, S.-Y. Bang, B.-A. Cho et al., "Role of amphipathic helix of a herpesviral protein in membrane deformation and T cell receptor downregulation," *PLoS Pathogens*, vol. 4, no. 11, Article ID e1000209, 2008.

[41] R. A. Houghten, "General method for the rapid solid-phase synthesis of large numbers of peptides: specificity of antigen-antibody interaction at the level of individual amino acids," *Proceedings of the National Academy of Sciences of the United States of America*, vol. 82, no. 15, pp. 5131–5135, 1985.

[42] R. C. Judd, "Electrophoresis of peptides," *Methods in Molecular Biology*, vol. 32, pp. 49–57, 1994.

[43] A. Pinzoń-Charry, J. P. Vernot, R. Rodríguez, and M. E. Patarroyo, "Proliferative response of peripheral blood lymphocytes to mitogens in the owl monkey Aotus nancymae," *Journal of Medical Primatology*, vol. 32, no. 1, pp. 31–38, 2003.

[44] M. Croft and C. Dubey, "Accessory molecule and costimulation requirements for CD4 T cell response," *Critical Reviews in Immunology*, vol. 17, no. 1, pp. 89–118, 1997.

[45] G. J. J. C. Boonen, B. A. Van Oirschot, A. Van Diepen et al., "Cyclin D3 regulates proliferation and apoptosis of leukemic T cell lines," *Journal of Biological Chemistry*, vol. 274, no. 49, pp. 34676–34682, 1999.

[46] P. Otáhal, P. Angelisová, M. Hrdinka et al., "A new type of membrane raft-like microdomains and their possible involvement in TCR signaling," *Journal of Immunology*, vol. 184, no. 7, pp. 3689–3696, 2010.

[47] D. Filipp and M. Julius, "Lipid rafts: resolution of the 'fyn problem'?" *Molecular Immunology*, vol. 41, no. 6-7, pp. 645–656, 2004.

[48] D. Filipp, B. Moemeni, A. Ferzoco et al., "Lck-dependent Fyn activation requires C terminus-dependent targeting of kinase-active Lck to lipid rafts," *The Journal of Biological Chemistry*, vol. 283, no. 39, pp. 26409–26422, 2008.

[49] J. E. Ferrell Jr. and R. R. Bhatt, "Mechanistic studies of the dual phosphorylation of mitogen-activated protein kinase," *The Journal of Biological Chemistry*, vol. 272, no. 30, pp. 19008–19016, 1997.

[50] D.-W. Yoon, H. Lee, W. Seol, M. DeMaria, M. Rosenzweig, and J. U. Jung, "Tap: a novel cellular protein that interacts with tip of *Herpesvirus saimiri* and induces lymphocyte aggregation," *Immunity*, vol. 6, no. 5, pp. 571–582, 1997.

[51] A. G. Baxter and P. D. Hodgkin, "Activation rules: the two-signal theories of immune activation," *Nature Reviews Immunology*, vol. 2, no. 6, pp. 439–446, 2002.

[52] J. Guo, M. Duboise, H. Lee et al., "Enhanced downregulation of Lck-mediated signal transduction by a Y114 mutation of herpesvirus saimiri Tip," *Journal of Virology*, vol. 71, no. 9, pp. 7092–7096, 1997.

[53] S. C. Meuer, J. C. Hodgdon, R. E. Hussey, J. P. Protentis, S. F. Schlossman, and E. L. Reinherz, "Antigen-like effects of monoclonal antibodies directed at receptors on human T cell clones," *Journal of Experimental Medicine*, vol. 158, no. 3, pp. 988–993, 1983.

[54] J. E. Casnellie, "Sites of *in vivo* phosphorylation of the T cell tyrosine protein kinase in LSTRA cells and their alteration by tumor-promoting phorbol esters," *Journal of Biological Chemistry*, vol. 262, no. 20, pp. 9859–9864, 1987.

[55] J. D. Marth, D. B. Lewis, C. B. Wilson, M. E. Gearn, E. G. Krebs, and R. M. Perlmutter, "Regulation of pp56lck during T-cell activation: functional implications for the src-like protein tyrosine kinases," *The EMBO Journal*, vol. 6, no. 9, pp. 2727–2734, 1987.

[56] S. Choi and R. H. Schwartz, "Molecular mechanisms for adaptive tolerance and other T cell anergy models," *Seminars in Immunology*, vol. 19, no. 3, pp. 140–152, 2007.

[57] A. D. Holdorf, K.-H. Lee, W. R. Burack, P. M. Allen, and A. S. Shaw, "Regulation of Lck activity by CD4 and CD28 in the immunological synapse," *Nature Immunology*, vol. 3, no. 3, pp. 259–264, 2002.

[58] A. Veillette and M. Fournel, "The CD4 associated tyrosine protein kinase p56lck is positively regulated through its site of autophosphorylation," *Oncogene*, vol. 5, no. 10, pp. 1455–1462, 1990.

[59] M. E. M. Noble, J. A. Endicott, and L. N. Johnson, "Protein kinase inhibitors: insights into drug design from structure," *Science*, vol. 303, no. 5665, pp. 1800–1805, 2004.

[60] Z.-Y. Zhang, B. Zhou, and L. Xie, "Modulation of protein kinase signaling by protein phosphatases and inhibitors," *Pharmacology & Therapeutics*, vol. 93, no. 2-3, pp. 307–317, 2002.

[61] R. J. He, Z. H. Yu, R. Y. Zhang, and Z. Y. Zhang, "Protein tyrosine phosphatases as potential therapeutic targets," *Acta Pharmacologica Sinica*, vol. 35, no. 10, pp. 1227–1246, 2014.

Hindawi Publishing Corporation
Journal of Immunology Research
Volume 2015, Article ID 541984, 8 pages
http://dx.doi.org/10.1155/2015/541984

Review Article

New Insights into the Function of the Immunoproteasome in Immune and Nonimmune Cells

Hiroaki Kimura,[1] Patrizio Caturegli,[2] Masafumi Takahashi,[1] and Koichi Suzuki[3]

[1]*Division of Inflammation Research, Center for Molecular Medicine, Jichi Medical University School of Medicine, 3311-1 Yakushiji, Shimotsuke, Tochigi 329-0498, Japan*
[2]*Department of Pathology, The Johns Hopkins School of Medicine, Ross 656, 720 Rutland Avenue, Baltimore, MD 20205, USA*
[3]*Department of Clinical Laboratory Science, Faculty of Medical Science, Teikyo University, 2-11-1 Kaga, Itabashi, Tokyo 173-8605, Japan*

Correspondence should be addressed to Hiroaki Kimura; balhiro33@jichi.ac.jp and Koichi Suzuki; koichis0923@med.teikyo-u.ac.jp

Received 10 July 2015; Accepted 10 September 2015

Academic Editor: Darren R. Flower

The immunoproteasome is a highly efficient proteolytic machinery derived from the constitutive proteasome and is abundantly expressed in immune cells. The immunoproteasome plays a critical role in the immune system because it degrades intracellular proteins, for example, those of viral origin, into small proteins. They are further digested into short peptides to be presented by major histocompatibility complex (MHC) class I molecules. In addition, the immunoproteasome influences inflammatory disease pathogenesis through its ability to regulate T cell polarization. The immunoproteasome is also expressed in nonimmune cell types during inflammation or neoplastic transformation, supporting a role in the pathogenesis of autoimmune diseases and neoplasms. Following the success of inhibitors of the constitutive proteasome, which is now an established treatment modality for multiple myeloma, compounds that selectively inhibit the immunoproteasome are currently under active investigation. This paper will review the functions of the immunoproteasome, highlighting areas where novel pharmacological treatments that regulate immunoproteasome activity could be developed.

1. Introduction

The immunoproteasome is a large proteolytic machine derived from the constitutive proteasome [1, 2] and plays a critical role in homeostasis and immunity. The constitutive proteasome is expressed ubiquitously in the body, where it degrades ubiquitinated proteins including transcriptional factors and proteins required for cell cycle progression [3, 4]. Since the primary role of the immunoproteasome is to process antigens for presentation on major histocompatibility complex (MHC) class I molecules to $CD8^+$ T lymphocytes [5], the immunoproteasome degrades various proteins, including viral proteins. Therefore, the immunoproteasome plays an important role during viral infection [6, 7]. The expression of the immunoproteasome is induced by interferon-γ (IFN-γ) and tumor necrosis factor-α (TNF-α) [8] under inflammatory conditions, such as infections, and autoimmune diseases when inflammatory cytokines are present [9]. Accordingly the immunoproteasome is controlled by factors that impact the immune system [10–13]. Interestingly, various roles for the immunoproteasome in nonimmune cells have been reported recently [14–16], suggesting that there could still be unknown roles for the immunoproteasome.

This review summarizes the roles of the immunoproteasome and recent efforts to develop novel therapeutic approaches by regulating immunoproteasome activity.

2. Structure and Activity of the Immunoproteasome

The immunoproteasome is a large proteolytic machinery derived from the constitutive proteasome (also known as the 26S proteasome) and is expressed abundantly in immune cells, such as antigen-presenting cells [17–19]. The constitutive proteasome is expressed in the cytosol and nucleus of most cells, where it degrades ubiquitinated proteins to

Table 1: Human immunoproteasome subunits.

Subunit	Proteolytic activity	Molecular weight	Chromosome	Alternative name
iβ1	Chymotrypsin-like	23.3 kD	6p21.3	PSMB9, LMP2
iβ2	Undefined	28.9 kD	16q22.1	PSMB10, LMP10, and MECL-1
iβ5	Chymotrypsin-like	30.4 kD	6p21.3	PSMB8, LMP7
PA28α	N/A	28.7 kD	14q11.2	
PA28β	N/A	27.4 kD	14q11.2	

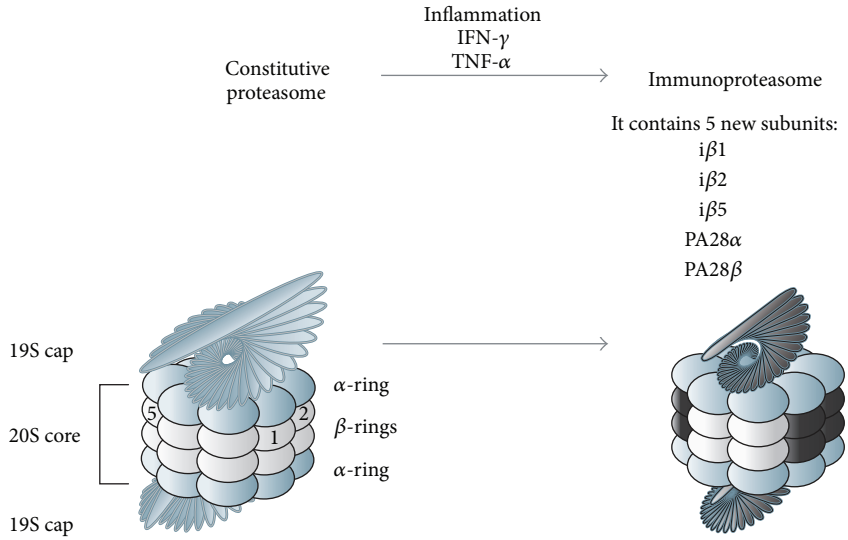

Figure 1: Structure of the constitutive proteasome and the immunoproteasome. The constitutive proteasome is composed of two pairs of inner β-rings, two pairs of outer α-rings, and two caps (19S regulatory complexes). Inflammatory cytokines induce the expression of the five subunits (iβ1 [LMP2], iβ2 [LMP10], iβ5 [LMP7], PA28α, and PA28β), which assemble on the proteasome core to create the immunoproteasome. When the induced subunits replace the β subunits and 19S regulatory complex, the resulting multiprotein complex is called the immunoproteasome.

maintain cell viability and homeostasis [4, 20]. For example, the constitutive proteasome degrades long-lived proteins, including proteins used for cell cycle progression and gene transcription. It is a large barrel-shaped protein complex [21, 22] composed of a catalytic 20S core proteasome and two 19S regulatory complex components located at both ends of the 20S core proteasome (Figure 1, left panel). The 20S core proteasome has two pairs of outer α rings consisting of seven α subunits and two pairs of inner β rings consisting of seven β subunits. The three β subunits (β1, β2, and β5) have proteolytic activities, including caspase-like activity for β1, trypsin-like activity for β2, and chymotrypsin-like activity for β5 [23]. The 20S core proteasome is usually capped at both ends by the 19S regulatory complex [21, 22]. The 19S regulatory complex recognizes ubiquitinated proteins and transfers them into the core of the proteasome where they are degraded by proteolysis.

When a cell is exposed to inflammatory stimuli, such as IFN-γ and TNF-α, five of the proteasome subunits are substituted with more efficient subunits: β1 is replaced with iβ1 (also known as large multifunctional peptidase 2 (LMP2) or proteasome subunit beta type 9 (PSMB9)), β2 is replaced with iβ2 (also known as LMP10, multicatalytic endopeptidase complex-like-1 (MECL-1), or PSMB10), β5 is replaced with iβ5 (also known as LMP7 or PSMB8), and the 19S regulatory complex is replaced with the 11S regulator composed of Proteasome Activator α (PA28α) and PA28β (Figure 1, right panel and Table 1) [24–29]. This modified proteasome is called the immunoproteasome and it performs its proteolytic functions more efficiently than the constitutive proteasome [1]. For example, it degrades viral proteins for antigen presentation [7] and also processes ubiquitinated proteins, as does the constitutive proteasome [30]. Expression of the immunoproteasome subunits can be induced in nonimmune cells stimulated by IFN-γ [13, 16, 31]. Therefore, the immunoproteasome plays multiple roles, and the function of the immunoproteasome is not restricted to the immune system.

3. Roles of the Immunoproteasome during Infection

The best characterized role of the immunoproteasome is the processing of proteins in order to present antigenic peptides on MHC class I molecules (Figure 2) [32]. Deficiency of the immunoproteasome in mice reduces $CD8^+$ T cell activation in hepatitis B virus (HBV) infection, lymphocytic choriomeningitis virus (LCMV) infection, and influenza virus infection [7, 33, 34], although not in coxsackie virus B3 (CVB3) infection [35]. The immunoproteasome is also

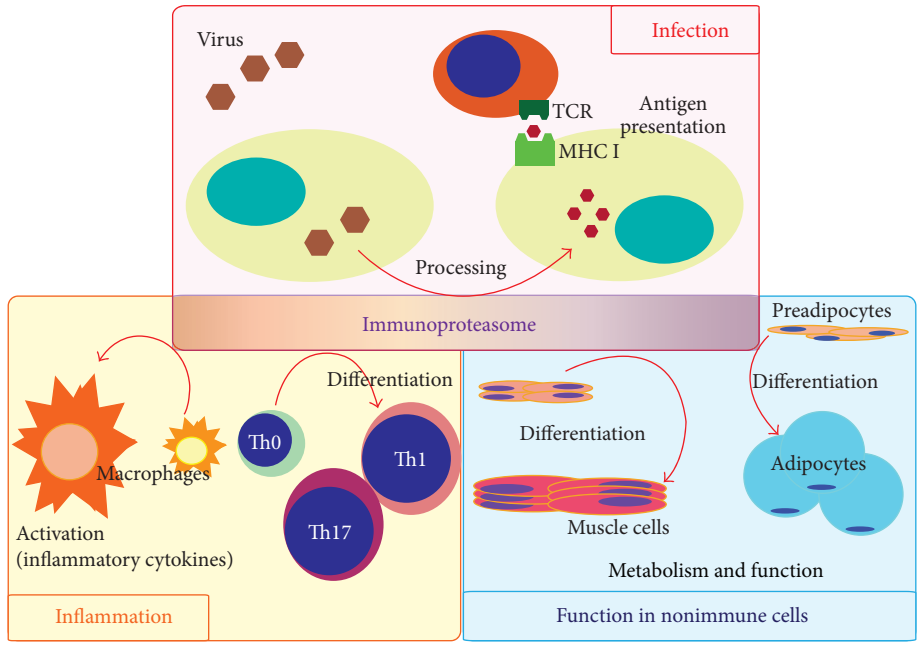

Figure 2: The immunoproteasome as a potential therapeutic target. The immunoproteasome plays an important role in immune responses, including processing viral proteins for antigen presentation, T cell differentiation, and macrophage activation. Recent studies have identified that the immunoproteasome is present in nonimmune cells, where it regulates cell differentiation and function.

important for activating the immune system against viral infection. For example, LMP2 deficiency reduced inflammatory cytokine (IL-1β, IL-6, and TNF-α) production during influenza viral infection [36]. Inflammatory cytokines, such as type I and type II IFNs and TNF-α, induce the expression of the subunits that assemble into the immunoproteasome [37, 38]. Hepatitis C viral (HCV) infection or poly(I : C)-stimulation (mimicking viral infection) induces the expression of type I IFN (IFN-β) and the immunoproteasome subunits in hepatocytes [38]. Suppression of IFN-β inhibits expression of the immunoproteasome, and type I IFN (IFN-α) treatment induces immunoproteasome expression in hepatocytes. Furthermore, Keller et al. showed that murine gammaherpesvirus-68 (MHV-68) infection induced expression of the immunoproteasome subunits in alveolar macrophages in the lung [16]. Thus, viral infection, IFN production, and expression of the immunoproteasome are strongly linked.

It should be noted that immunity against viral infections is not completely dependent on the immunoproteasome because there are some antiviral immune responses independent of the immunoproteasome [39]. In fact, mice lacking all of the immunoproteasome activities, generated by treating LMP2/LMP10 double-deficient mice with a LMP7-selective inhibitor, were still able to induce IFN-γ-producing cytotoxic $CD8^+$ T cells upon LCMV infection [39].

4. Roles of the Immunoproteasome in Inflammatory Diseases

The immunoproteasome is involved in the pathogenesis of numerous inflammatory diseases, such as autoimmune diseases, by influencing T cell polarization, signaling through the nuclear factor-κB (NF-κB) pathway, and the production of inflammatory cytokines by macrophage [40–45]. For example, Kalim et al. reported that LMP7 deficiency suppressed the differentiation of naïve $CD4^+$ T cells to Th1 and Th17 cells and instead promoted their differentiation to regulatory T cells (Figure 2) [46]. Maldonado et al. reported that deficiency of the immunoproteasome influenced NF-κB signaling [47]. The constitutive proteasome is involved in NF-κB signaling by degrading ubiquitinated I-κB. It remains to be defined how the constitutive proteasome and the immunoproteasome regulate NF-κB. Reis et al. reported that upregulated LMP7 expression in mouse macrophages due to LPS stimulation was suppressed by treatment with immunoproteasome inhibitors, including an LMP7 inhibitor (Figure 2) [48].

The immunoproteasome is essential for processing antigenic epitopes that are presented on MHC class I molecules to activate $CD8^+$ T lymphocytes. The immunoproteasome is also involved in the regulation of NF-κB, which is essential for the transcription of many genes that encode inflammatory cytokines. Therefore, the activity of the immunoproteasome is essential in various inflammatory scenarios that result in pathological conditions. Thus, attempts were made to inhibit the immunoproteasome to identify potential treatments for inflammatory diseases. ONX-0914 (also known as PR-957) is a selective LMP7 inhibitor, which has been used as a treatment for autoimmune diseases in animal models. Muchamuel et al. reported that ONX-0914 attenuated experimental arthritis by blocking inflammatory cytokine expression [10]. As we mentioned, this LMP7 inhibitor blocked antigen presentation by MHC class I, suppressed

the proliferation and activation of $CD8^+$ T cells and Th17 cells, and lowered the production of inflammatory cytokines. The inhibitory effects probably contribute to the attenuation of disease progression in experimental arthritis.

Basler et al. showed that treatment with ONX-0914 significantly attenuated the clinical symptoms of experimental colitis and encephalomyelitis in mice [11, 12]. Expression of the immunoproteasome subunits (LMP2, LMP7, and LMP10) was upregulated in colitis lesions, which was induced in mice deficient in each of the immunoproteasome subunits. Colon lesions were significantly ameliorated in each of the deficient mouse strains compared to wild-type controls, and the amelioration was associated with suppressed inflammatory cytokine expression (TNF-α, IL-1β, IFN-γ, IL-6, IL-23, and IL17). Then, they examined the effect of ONX-0914 in experimental colitis and showed that treatment with ONX-0914 significantly improved colitis lesions. Although deficiency of the individual immunoproteasome subunits (i.e., LMP2, LMP7, or MECL-1) did not improve disease in a mouse model of experimental encephalomyelitis, treatment with ONX-0914 significantly attenuated disease progression and prevented a second exacerbation [12]. The authors mentioned that this discrepancy between immunoproteasome subunit-deficient mice and inhibitor-treated mice could be explained by the fact that endogenous chymotrypsin-like activity in monocytic cells contributes to pathogenesis and ONX-0914 inhibits chymotrypsin-like activity [12]. Deficiency of a single subunit is not able to suppress all chymotrypsin-like activity in the immunoproteasome because both LMP2 and LMP7 have chymotrypsin-like activity [49, 50]. Overall, these studies suggest that ONX-0914 has potential for treating autoimmune diseases.

The immunoproteasome is involved in the pathogenesis of chronic thyroiditis [13]. Transgenic mice that express IFN-γ specifically in the thyroid develop chronic thyroiditis and hypothyroidism [51, 52]. In this mouse model, LMP2 deficiency significantly improved inflammatory thyroid morphology and function [13]. Nagayama et al. reported that treatment with ONX-0914 improved Th1-type autoimmune thyroid disease (Hashimoto's thyroiditis), but not Th2-type autoimmune thyroid disease (Graves' disease), using mouse models [53]. Treatment with ONX-0914 suppressed IFN-γ and IL-17 expression in the thyroid, which supports Basler's results.

LMP7 deficiency or treatment with ONX-0914 (a selective inhibitor of LMP7) seems to suppress inflammatory diseases with Th1 and Th17 cell-mediated inflammation. One report showed that LMP7 deficiency reduced Th2 responses in an asthma model [54]. LMP7 deficiency suppressed expression of the Th2 cytokines IL-4, IL-5, and IL-13 and infiltration of immune cells into the lung. The detailed mechanism of how LMP7 deficiency influences T cell polarization is still undefined. Because either Th1 or Th2 polarization is normally involved in the pathogenesis of many inflammatory diseases, it is necessary to know how the immunoproteasome influences T cell polarization in various inflammatory disease contexts in order to translate these findings to clinical studies.

Table 2: Human PSMB8 (LMP7 gene) alleles.

Mutation	Influenced cytokines	Reference
Thr 75 Met	IL-6, IL-8, and IFN-γ	[58–60]
Cys 135 termination	Unknown	[60]
Gly 197 Val	IL-6	[15]
Gly 201 Val	IL-6, IL-10	[57]

5. Roles of the Immunoproteasome in Nonimmune Cells

Recent studies have examined the role of the immunoproteasome in nonimmune cells. Cui et al. reported that the immunoproteasome regulated skeletal muscle differentiation (Figure 2) [14]. They found that inhibiting the immunoproteasome by short hairpin RNA suppressed muscle differentiation using the mouse myoblast cell line C2C12 and human skeletal muscle myoblasts. Proapoptotic proteins and apoptotic cells were upregulated by the treatment, which indicates that the immunoproteasome also regulates the degradation of proteins associated with apoptosis, as does the constitutive proteasome. They speculated that the immunoproteasome influences transcriptional factors associating with muscle differentiation. Zu et al. reported that the immunoproteasome regulated cardiac muscle mass in diabetic mice [55]. Streptozotocin (STZ) is commonly used to induce diabetic conditions in the experimental animal model. They showed that LMP2 expression was decreased in the hearts of STZ-injected mice. On the other hand, the expression of phosphatase and tensin homologue deleted on chromosome ten (PTEN) was upregulated, which impaired muscle regeneration [56]. LMP2 deficiency itself also leads to loss of cardiac muscle mass, which decreased cardiac function [55].

LMP7 has been associated with human disease, although no association has been found with the other immunoproteasome subunits (LMP2, LMP10, PA28α, and PA28β). LMP7 mutation causes disease with autoinflammation and lipodystrophy [15, 57–59], and the number of cases is increasing [60, 61]. As we described above, LMP7 plays a critical role in the immune system and is involved in cytokine expression. LMP7 mutation in humans causes abnormalities in cytokine expression, as listed in Table 2. Kitamura et al. showed that IL-6 expression was significantly higher in the skin lesions or sera of patients with LMP7 mutation [15], similar to other reports [57, 60]. In particular, an association of LMP7 and lipodystrophy is interesting. Reduction of LMP7 expression by siRNA suppressed adipogenesis in 3T3-L1 cells (Figure 2) [15]. LMP7 might be involved in lipid metabolic disorders because LMP7 is also associated with insulin-dependent diabetes mellitus [62], and inflammation is involved in the pathophysiology of metabolic diseases [63, 64]. To date, the role of the immunoproteasome in metabolic disorders and the endocrine system is poorly understood. We showed previously that overexpression of LMP2 was involved in the pathogenesis of chronic thyroid inflammation and hypothyroidism as described above [13]. In that study, we found that LMP2 was expressed in oxyphilic thyrocytes in

humans and mice, and deletion of LMP2 in mice dramatically improved thyroid function and thyrocyte morphology [13]. These findings suggest an association between the immunoproteasome and endocrine metabolic function.

The lung is a vulnerable site for pathogens that induce chronic inflammation. Therefore, the immunoproteasome may play an important role in the lung. In fact, Keller et al. reported that immunoproteasome expression was detected in the lung parenchymal cells, for example, alveolar type I and II cells, fibroblasts, and bronchial epithelial cells at basal levels [16]. Viral infection and subsequent IFN secretion upregulated immunoproteasome expression in the lung. It is still not clear why those cells in the lung constitutively express LMP7 without infection or inflammation.

Considering the involvement of the immunoproteasome in cell differentiation and function, the immunoproteasome is important in nonimmune cells, too. Expression of the immunoproteasome in nonimmune cells during normal conditions has been found, although its role is not fully understood. Therefore, the role of the immunoproteasome in nonimmune cells should be addressed using mice deficient in the various immunoproteasome subunits, by knockdown of the immunoproteasome genes and with immunoproteasome inhibitors.

6. Immunoproteasome Inhibitors and Their Clinical Relevance for Inflammatory Diseases and Neoplasms

ONX-0914 is, thus far, the best characterized immunoproteasome inhibitor. As shown in the previous section, ONX-0914 specifically inhibits LMP7 (iβ5), and it has been used in animal models and *in vitro* studies of inflammatory diseases [10–12, 46, 53, 65]. Although selective inhibitors for LMP2 were not available when we reported that LMP2 deficiency suppressed thyroid inflammation and improved thyroid function [13], we expect that such inhibitors will be used to treat patients with chronic thyroiditis in the future. More studies are needed to analyze the mechanisms underlying the action of LMP2 on thyroid function.

Recently, immunoproteasome inhibitors have been investigated for application in clinical settings to treat hematopoietic neoplasms. Bortezomib is an inhibitor of β5, a component of the constitutive proteasome, and has been used to treat multiple myeloma and mantle cell lymphoma [66]. Since the proteasome is responsible for the degradation of proteins involved in cell cycle progression, inhibition of proteasome function by bortezomib results in an accumulation of undigested proteins that leads to cell death.

Alternative treatments that overcome bortezomib-resistant malignancies have been characterized [66]. ONX-0912 is an inhibitor of both LMP7 (iβ5) and β5 and is effective for bortezomib-resistant myelomas [66, 67]. UK-101 and IPSI-001 selectively inhibit LMP2 and exhibit antitumor activity against malignant myelomas [68, 69]. Carfilzomib is effective for the treatment of myelomas and small cell lung cancers [70, 71]. Proteasome subunits LMP7 (iβ5), LMP2 (iβ1), and β5 have chymotrypsin-like activity. Since carfilzomib is a potent inhibitor of chymotrypsin-like activity [70], it appears likely that chymotrypsin-like activity is important for maintaining the proliferation of hematologic tumor cells. Precise differences in the chymotrypsin-like activity among the three subunits should be defined in order to understand how malignant cells acquire resistance to those proteasome inhibitors.

7. Conclusion

Regulating immunoproteasome expression and activity is a powerful tool for controlling cell function, which includes cell metabolism, differentiation, and immune regulation. So far, inhibitors of the immunoproteasome are widely available and applicable to the treatment of many inflammatory diseases and hematopoietic malignancies. In the near future, colitis and rheumatoid arthritis could be candidates for developing new treatments that target the immunoproteasome. In addition, metabolic diseases could provide additional candidates because the immunoproteasome is involved in both adipogenesis and inflammation of adipose tissue. As described in this review, most basic studies on the roles of the immunoproteasome in disease models have been achieved using mice (summarized in Figure 2). Since immunoproteasome enzymatic activity differs between species [72], findings from such basic studies should be carefully interpreted when considering the development of new therapeutic applications.

Conflict of Interests

The authors declare that there is no conflict of interests regarding the publication of this paper.

Acknowledgments

This work was supported by grants from the Japan Society for the Promotion of Science (JSPS) through the Grant-in-Aid for Scientific Research (C) and grants from Astellas Foundation for Research on Metabolic Disorders, Daiwa Securities Health Foundation, and Pancreas Research Foundation of Japan.

References

[1] K. Tanaka, "Role of proteasomes modified by interferon-gamma in antigen processing," *Journal of Leukocyte Biology*, vol. 56, no. 5, pp. 571–575, 1994.

[2] P.-M. Kloetzel and F. Ossendorp, "Proteasome and peptidase function in MHC-class-I-mediated antigen presentation," *Current Opinion in Immunology*, vol. 16, no. 1, pp. 76–81, 2004.

[3] K. Tanaka, "The proteasome: overview of structure and functions," *Proceedings of the Japan Academy. Series B: Physical and Biological Sciences*, vol. 85, no. 1, pp. 12–36, 2009.

[4] A. Ichihara and K. Tanaka, "Roles of proteasomes in cell growth," *Molecular Biology Reports*, vol. 21, no. 1, pp. 49–52, 1995.

[5] H. J. Fehling, W. Swat, C. Laplace et al., "MHC class I expression in mice lacking the proteasome subunit LMP-7," *Science*, vol. 265, no. 5176, pp. 1234–1237, 1994.

[6] A. J. A. M. Sijts, S. Standera, R. E. M. Toes et al., "MHC class I antigen processing of an adenovirus CTL epitope is linked to the levels of immunoproteasomes in infected cells," *The Journal of Immunology*, vol. 164, no. 9, pp. 4500–4506, 2000.

[7] W. Chen, C. C. Norbury, Y. Cho, J. W. Yewdell, and J. R. Bennink, "Immunoproteasomes shape immunodominance hierarchies of antiviral $CD8^+$ T cells at the levels of T cell repertoire and presentation of viral antigens," *The Journal of Experimental Medicine*, vol. 193, no. 11, pp. 1319–1326, 2001.

[8] P.-M. Kloetzel, "Antigen processing by the proteasome," *Nature Reviews Molecular Cell Biology*, vol. 2, no. 3, pp. 179–187, 2001.

[9] I. Shachar and N. Karin, "The dual roles of inflammatory cytokines and chemokines in the regulation of autoimmune diseases and their clinical implications," *Journal of Leukocyte Biology*, vol. 93, no. 1, pp. 51–61, 2013.

[10] T. Muchamuel, M. Basler, M. A. Aujay et al., "A selective inhibitor of the immunoproteasome subunit LMP7 blocks cytokine production and attenuates progression of experimental arthritis," *Nature Medicine*, vol. 15, no. 7, pp. 781–787, 2009.

[11] M. Basler, M. Dajee, C. Moll, M. Groettrup, and C. J. Kirk, "Prevention of experimental colitis by a selective inhibitor of the immunoproteasome," *Journal of Immunology*, vol. 185, no. 1, pp. 634–641, 2010.

[12] M. Basler, S. Mundt, T. Muchamuel et al., "Inhibition of the immunoproteasome ameliorates experimental autoimmune encephalomyelitis," *EMBO Molecular Medicine*, vol. 6, no. 2, pp. 226–238, 2014.

[13] H. J. Kimura, C. Y. Chen, S.-C. Tzou et al., "Immunoproteasome overexpression underlies the pathogenesis of thyroid oncocytes and primary hypothyroidism: studies in humans and mice," *PLoS ONE*, vol. 4, no. 11, article e7857, 2009.

[14] Z. Cui, S. M. Hwang, and A. V. Gomes, "Identification of the immunoproteasome as a novel regulator of skeletal muscle differentiation," *Molecular and Cellular Biology*, vol. 34, no. 1, pp. 96–109, 2014.

[15] A. Kitamura, Y. Maekawa, H. Uehara et al., "A mutation in the immunoproteasome subunit PSMB8 causes autoinflammation and lipodystrophy in humans," *The Journal of Clinical Investigation*, vol. 121, no. 10, pp. 4150–4160, 2011.

[16] I. E. Keller, O. Vosyka, S. Takenaka et al., "Regulation of immunoproteasome function in the lung," *Scientific Reports*, vol. 5, Article ID 10230, 2015.

[17] J. Haorah, D. Heilman, C. Diekmann et al., "Alcohol and HIV decrease proteasome and immunoproteasome function in macrophages: implications for impaired immune function during disease," *Cellular Immunology*, vol. 229, no. 2, pp. 139–148, 2004.

[18] T. Frisan, V. Levitsky, and M. G. Masucci, "Variations in proteasome subunit composition and enzymatic activity in B-lymphoma lines and normal B cells," *International Journal of Cancer*, vol. 88, no. 6, pp. 881–888, 2000.

[19] P. Leone, M. Di Tacchio, S. Berardi et al., "Dendritic cell maturation in HCV infection: altered regulation of MHC class i antigen processing-presenting machinery," *Journal of Hepatology*, vol. 61, no. 2, pp. 242–251, 2014.

[20] K. Tanaka, "Molecular biology of proteasomes," *Molecular Biology Reports*, vol. 21, no. 1, pp. 21–26, 1995.

[21] M. Unno, T. Mizushima, Y. Morimoto et al., "The structure of the mammalian 20S proteasome at 2.75 Å resolution," *Structure*, vol. 10, no. 5, pp. 609–618, 2002.

[22] M. Groll, L. Ditzel, J. Löwe et al., "Structure of 20S proteasome from yeast at 2.4 Å resolution," *Nature*, vol. 386, no. 6624, pp. 463–471, 1997.

[23] G. N. DeMartino and C. A. Slaughter, "The proteasome, a novel protease regulated by multiple mechanisms," *Journal of Biological Chemistry*, vol. 274, no. 32, pp. 22123–22126, 1999.

[24] V. Ortiz-Navarrete, A. Seelig, M. Gernold, S. Frentzel, P. M. Kloetzel, and G. J. Hämmerling, "Subunit of the '20S' proteasome (multicatalytic proteinase) encoded by the major histocompatibility complex," *Nature*, vol. 353, no. 6345, pp. 662–664, 1991.

[25] R. Glynne, S. H. Powis, S. Beck, A. Kelly, L.-A. Kerr, and J. Trowsdale, "A proteasome-related gene between the two ABC transporter loci in the class II region of the human MHC," *Nature*, vol. 353, no. 6342, pp. 357–360, 1991.

[26] A. Kelly, S. H. Powis, R. Glynne, E. Radley, S. Beck, and J. Trowsdale, "Second proteasome-related gene in the human MHC class II region," *Nature*, vol. 353, no. 6345, pp. 667–668, 1991.

[27] C. Realini, W. Dubiel, G. Pratt, K. Ferrell, and M. Rechsteiner, "Molecular cloning and expression of a γ-interferon-inducible activator of the multicatalytic protease," *The Journal of Biological Chemistry*, vol. 269, no. 32, pp. 20727–20732, 1994.

[28] J. Y. Ahn, N. Tanahashi, K. Akiyama et al., "Primary structures of two homologous subunits of PA28, a γ-interferon-inducible protein activator of the 20S proteasome," *FEBS Letters*, vol. 366, no. 1, pp. 37–42, 1995.

[29] N. Tanahashi, K.-Y. Yokota, J. Y. Ahn et al., "Molecular properties of the proteasome activator PA28 family proteins and γ-interferon regulation," *Genes to Cells*, vol. 2, no. 3, pp. 195–211, 1997.

[30] J. A. Nathan, V. Spinnenhirn, G. Schmidtke, M. Basler, M. Groettrup, and A. L. Goldberg, "Immuno- and constitutive proteasomes do not differ in their abilities to degrade ubiquitinated proteins," *Cell*, vol. 152, no. 5, pp. 1184–1194, 2013.

[31] M. E. Arellano-Garcia, K. Misuno, S. D. Tran, and S. Hu, "Interferon-γ induces immunoproteasomes and the presentation of MHC I-associated peptides on human salivary gland cells," *PLoS ONE*, vol. 9, no. 8, Article ID e102878, 2014.

[32] P. M. Kloetzel, "Generation of major histocompatibility complex class I antigens: functional interplay between proteasomes and TPPII," *Nature Immunology*, vol. 5, no. 7, pp. 661–669, 2004.

[33] M. D. Robek, M. L. Garcia, B. S. Boyd, and F. V. Chisari, "Role of immunoproteasome catalytic subunits in the immune response to hepatitis B virus," *Journal of Virology*, vol. 81, no. 2, pp. 483–491, 2007.

[34] E. Z. Kincaid, J. W. Che, I. York et al., "Mice completely lacking immunoproteasomes show major changes in antigen presentation," *Nature Immunology*, vol. 13, no. 2, pp. 129–135, 2012.

[35] E. Opitz, A. Koch, K. Klingel et al., "Impairment of immunoproteasome function by beta5i/lmp7 subunit deficiency results in severe enterovirus myocarditis," *PLoS Pathogens*, vol. 7, no. 9, Article ID e1002233, 2011.

[36] S. E. Hensley, D. Zanker, B. P. Dolan et al., "Unexpected role for the immunoproteasome subunit LMP2 in antiviral humoral and innate immune responses," *Journal of Immunology*, vol. 184, no. 8, pp. 4115–4122, 2010.

[37] F. Novelli and J.-L. Casanova, "The role of IL-12, IL-23 and IFN-γ in immunity to viruses," *Cytokine and Growth Factor Reviews*, vol. 15, no. 5, pp. 367–377, 2004.

[38] E.-C. Shin, U. Seifert, T. Kato et al., "Virus-induced type I IFN stimulates generation of immunoproteasomes at the site of infection," *The Journal of Clinical Investigation*, vol. 116, no. 11, pp. 3006–3014, 2006.

[39] M. Basler, U. Beck, C. J. Kirk, and M. Groettrup, "The antiviral immune response in mice devoid of immunoproteasome activity," *Journal of Immunology*, vol. 187, no. 11, pp. 5548–5557, 2011.

[40] I. Gutcher and B. Becher, "APC-derived cytokines and T cell polarization in autoimmune inflammation," *Journal of Clinical Investigation*, vol. 117, no. 5, pp. 1119–1127, 2007.

[41] C. B. Schmidt-Weber, M. Akdis, and C. A. Akdis, "TH17 cells in the big picture of immunology," *The Journal of Allergy and Clinical Immunology*, vol. 120, no. 2, pp. 247–254, 2007.

[42] P. J. Barnes and M. Karin, "Nuclear factor-κB—a pivotal transcription factor in chronic inflammatory diseases," *The New England Journal of Medicine*, vol. 336, no. 15, pp. 1066–1071, 1997.

[43] P. P. Tak and G. S. Firestein, "NF-kappaB: a key role in inflammatory diseases," *The Journal of Clinical Investigation*, vol. 107, no. 1, pp. 7–11, 2001.

[44] P. Libby, "Inflammation in atherosclerosis," *Arteriosclerosis, Thrombosis, and Vascular Biology*, vol. 32, no. 9, pp. 2045–2051, 2012.

[45] J.-L. Davignon, M. Hayder, M. Baron et al., "Targeting monocytes/macrophages in the treatment of rheumatoid arthritis," *Rheumatology*, vol. 52, no. 4, Article ID kes304, pp. 590–598, 2013.

[46] K. W. Kalim, M. Basler, C. J. Kirk, and M. Groettrup, "Immunoproteasome subunit LMP7 deficiency and inhibition suppresses Th1 and Th17 but enhances regulatory T cell differentiation," *Journal of Immunology*, vol. 189, no. 8, pp. 4182–4193, 2012.

[47] M. Maldonado, R. J. Kapphahn, M. R. Terluk et al., "Immunoproteasome deficiency modifies the alternative pathway of NFkappaB signaling," *PLoS ONE*, vol. 8, no. 2, Article ID e56187, 2013.

[48] J. Reis, X. Q. Guan, A. F. Kisselev et al., "LPS-induced formation of immunoproteasomes: TNF-α and nitric oxide production are regulated by altered composition of proteasome-active sites," *Cell Biochemistry and Biophysics*, vol. 60, no. 1-2, pp. 77–88, 2011.

[49] Y. K. Ho, P. Bargagna-Mohan, M. Wehenkel, R. Mohan, and K.-B. Kim, "LMP2-specific inhibitors: chemical genetic tools for proteasome biology," *Chemistry and Biology*, vol. 14, no. 4, pp. 419–430, 2007.

[50] J. Reidlinger, A. M. Pike, P. J. Savory, R. Z. Murray, and A. J. Rivett, "Catalytic properties of 26 S and 20 S proteasomes and radiolabeling of MB1, LMP7, and C7 subunits associated with trypsin-like and chymotrypsin-like activities," *The Journal of Biological Chemistry*, vol. 272, no. 40, pp. 24899–24905, 1997.

[51] P. Caturegli, M. Hejazi, K. Suzuki et al., "Hypothyroidism in transgenic mice expressing IFN-gamma in the thyroid," *Proceedings of the National Academy of Sciences of the United States of America*, vol. 97, no. 4, pp. 1719–1724, 2000.

[52] H. Kimura, M. Kimura, W. H. Westra, N. R. Rose, and P. Caturegli, "Increased thyroidal fat and goitrous hypothyroidism induced by interferon-gamma," *International Journal of Experimental Pathology*, vol. 86, no. 2, pp. 97–106, 2005.

[53] Y. Nagayama, M. Nakahara, M. Shimamura, I. Horie, K. Arima, and N. Abiru, "Prophylactic and therapeutic efficacies of a selective inhibitor of the immunoproteasome for Hashimoto's thyroiditis, but not for Graves' hyperthyroidism, in mice," *Clinical & Experimental Immunology*, vol. 168, no. 3, pp. 268–273, 2012.

[54] A. Volkov, S. Hagner, S. Löser et al., "Beta5i subunit deficiency of the immunoproteasome leads to reduced Th2 response in OVA induced acute asthma," *PLoS ONE*, vol. 8, no. 4, Article ID e60565, 2013.

[55] L. Zu, D. Bedja, K. Fox-Talbot et al., "Evidence for a role of immunoproteasomes in regulating cardiac muscle mass in diabetic mice," *Journal of Molecular and Cellular Cardiology*, vol. 49, no. 1, pp. 5–15, 2010.

[56] Z. Hu, H. Wang, I. H. Lee et al., "PTEN inhibition improves muscle regeneration in mice fed a high-fat diet," *Diabetes*, vol. 59, no. 6, pp. 1312–1320, 2010.

[57] K. Arima, A. Kinoshita, H. Mishima et al., "Proteasome assembly defect due to a proteasome subunit beta type 8 (PSMB8) mutation causes the autoinflammatory disorder, Nakajo-Nishimura syndrome," *Proceedings of the National Academy of Sciences of the United States of America*, vol. 108, no. 36, pp. 14914–14919, 2011.

[58] A. K. Agarwal, C. Xing, G. N. DeMartino et al., "PSMB8 encoding the beta5i proteasome subunit is mutated in joint contractures, muscle atrophy, microcytic anemia, and panniculitis-induced lipodystrophy syndrome," *The American Journal of Human Genetics*, vol. 87, no. 6, pp. 866–872, 2010.

[59] A. Garg, M. D. Hernandez, A. B. Sousa et al., "An autosomal recessive syndrome of joint contractures, muscular atrophy, microcytic anemia, and panniculitis-associated lipodystrophy," *Journal of Clinical Endocrinology and Metabolism*, vol. 95, no. 9, pp. E58–E63, 2010.

[60] Y. Liu, Y. Ramot, A. Torrelo et al., "Mutations in proteasome subunit β type 8 cause chronic atypical neutrophilic dermatosis with lipodystrophy and elevated temperature with evidence of genetic and phenotypic heterogeneity," *Arthritis and Rheumatism*, vol. 64, no. 3, pp. 895–907, 2012.

[61] K. Kunimoto, A. Kimura, K. Uede et al., "A new infant case of nakajo-nishimura syndrome with a genetic mutation in the immunoproteasome subunit: an overlapping entity with JMP and CANDLE syndrome related to PSMB8 mutations," *Dermatology*, vol. 227, no. 1, pp. 26–30, 2013.

[62] G. Y. Deng, A. Muir, N. K. Maclaren, and J.-X. She, "Association of LMP2 and LMP7 genes within the major histocompatibility complex with insulin-dependent diabetes mellitus: population and family studies," *The American Journal of Human Genetics*, vol. 56, no. 2, pp. 528–534, 1995.

[63] N. Rasouli and P. A. Kern, "Adipocytokines and the metabolic complications of obesity," *Journal of Clinical Endocrinology and Metabolism*, vol. 93, no. 11, pp. s64–s73, 2008.

[64] H. Sell, C. Habich, and J. Eckel, "Adaptive immunity in obesity and insulin resistance," *Nature Reviews Endocrinology*, vol. 8, no. 12, pp. 709–716, 2012.

[65] M. Mishto, M. L. Raza, D. de Biase et al., "The immunoproteasome beta5i subunit is a key contributor to ictogenesis in a rat model of chronic epilepsy," *Brain, Behavior, and Immunity*, vol. 49, pp. 188–196, 2015.

[66] A. M. Ruschak, M. Slassi, L. E. Kay, and A. D. Schimmer, "Novel proteasome inhibitors to overcome bortezomib resistance," *Journal of the National Cancer Institute*, vol. 103, no. 13, pp. 1007–1017, 2011.

[67] D. Chauhan, A. V. Singh, M. Aujay et al., "A novel orally active proteasome inhibitor ONX 0912 triggers *in vitro* and *in vivo* cytotoxicity in multiple myeloma," *Blood*, vol. 116, no. 23, pp. 4906–4915, 2010.

[68] M. Wehenkel, J.-O. Ban, Y.-K. Ho, K. C. Carmony, J. T. Hong, and K. B. Kim, "A selective inhibitor of the immunoproteasome

subunit LMP2 induces apoptosis in PC-3 cells and suppresses tumour growth in nude mice," *British Journal of Cancer*, vol. 107, no. 1, pp. 53–62, 2012.

[69] D. J. Kuhn, S. A. Hunsucker, Q. Chen, P. M. Voorhees, M. Orlowski, and R. Z. Orlowski, "Targeted inhibition of the immunoproteasome is a potent strategy against models of multiple myeloma that overcomes resistance to conventional drugs and nonspecific proteasome inhibitors," *Blood*, vol. 113, no. 19, pp. 4667–4676, 2009.

[70] F. Parlati, S. J. Lee, M. Aujay et al., "Carfilzomib can induce tumor cell death through selective inhibition of the chymotrypsin-like activity of the proteasome," *Blood*, vol. 114, no. 16, pp. 3439–3447, 2009.

[71] A. F. Baker, N. T. Hanke, B. J. Sands, L. Carbajal, J. L. Anderl, and L. L. Garland, "Carfilzomib demonstrates broad anti-tumor activity in pre-clinical non-small cell and small cell lung cancer models," *Journal of Experimental & Clinical Cancer Research*, vol. 33, article 111, 2014.

[72] M. Raule, F. Cerruti, and P. Cascio, "Comparative study of the biochemical properties of proteasomes in domestic animals," *Veterinary Immunology and Immunopathology*, vol. 166, no. 1-2, pp. 43–49, 2015.